Development of optical sensors for detection and measurement of fluoride using organic dyes and some of their derivatives

Roopa Venkataraj

International School of Photonics
Cochin University of Science and Technology

Development of optical sensors for detection and measurement of fluoride using organic dyes and some of their derivatives

Ph. D Thesis submitted to

Cochin University of Science and Technology

In partial fulfilment of the requirements for the award of the Degree of

Doctor of Philosophy

Roopa Venkataraj

Reg. No. 4339

International School of Photonics
Faculty of Technology
Cochin University of Science and Technology
Cochin-682022, Kerala, India

August 2019

Development of optical sensors for detection and measurement of fluoride using organic dyes and some of their derivatives

Ph D thesis in the field of Photonics

Author:

Roopa Venkataraj
Research Fellow
International School of Photonics
Cochin University of Science & Technology
Cochin -682022, Kerala, India
roopa.venkataraj@gmail.com

Research Advisors:

Dr. M. Kailasnath
Professor
International School of Photonics
Cochin University of Science & Technology
Cochin -682022, Kerala, India
mkailasnath@gmail.com

Dr. V P N Nampoori
Emeritus Professor
International School of Photonics
Cochin University of Science & Technology
Cochin -682022, Kerala, India
nampoori@gmail.com

Cover images
Front: Fluorescence cone produced in acetonitrile and anisole containing Curcumin (with and without TBAF) using fiber probes, image of chemically tapered fiber tip
Back: Images of results of irradiation of Curcumin stained filter paper exposed to different NaF concentration

Dedicated to my family and teachers......

Certificate

This is to certify that the thesis entitled **"Development of optical sensors for detection and measurement of fluoride using organic dyes and some of their derivatives"** submitted by **Ms. Roopa Venkataraj**, is an authentic record of research work carried out by her under our guidance and supervision in partial fulfilment of the requirement of the degree of Doctor of Philosophy of Cochin University of Science and Technology, under the Faculty of Technology and the work presented in this thesis has not been included in any other thesis submitted previously for the award of any degree.

Cochin - 682022   **Prof. V P N Nampoori**   **Prof. M Kailasnath**
07-08-2019   *(Co-guide)*   *(Supervising guide)*

Certificate

This is to certify that the thesis entitled **"Development of optical sensors for detection and measurement of fluoride using organic dyes and some of their derivatives"** submitted by **Ms. Roopa Venkataraj**, has incorporated all the relevant corrections and modifications suggested by the audience during the pre-synopsis seminar and those recommended by the Doctoral Committee.

Cochin - 682022   **Prof. V P N Nampoori**   **Prof. M Kailasnath**
07-08-2019   *(Co-guide)*   *(Supervising guide)*

Declaration

I, Roopa Venkataraj, do hereby declare that the thesis entitled "**Development of optical sensors for detection and measurement of fluoride using organic dyes and some of their derivatives**", is a genuine record of research work done by me under the joint guidance and supervision of Dr. M Kailasnath, Professor and Dr. V P N Nampoori, Emeritus Professor, International School of Photonics, Cochin University of Science and Technology, Cochin-22, Kerala, India and it has not been included in any other thesis submitted previously for the award of any degree

Cochin- 682022   **Roopa Venkataraj**
07-08-2019

Acknowledgement

Roopa Venkataraj

Preface

Sensing is very important in different fields like engineering, medicine, transportation, environment and manufacturing processes. In the present world, the problem of pollution takes many forms causing huge damage to many ecosystems. Many chemical sensors have been reported for a variety of pollutants. Anion sensing is considered to be a huge challenge owing to difficulty of realizing suitable water based sensing mechanisms or receptors that support it. Fluoride pollution in water resources is an interesting situation owing to the fact that not just man-made activities and products but also natural sources like fluorite rocks contribute to the problem. The exposure to fluoride beyond a certain limit is found to cause severe damage to human health. Considering the fact that many existing sensors for fluoride work only in organic solvents, it becomes very important to find receptors that are selective to fluoride and devise efficient methods for fluoride detection.

The thesis describes the results of experiments carried out using synthetic organic dyes like Rhodamine 6G, Coumarin 540A and natural dye Curcumin towards the realization of simple, low cost optical sensors for the detection and measurement of fluoride, both in the organic and inorganic forms.

Chapter 1 gives an introduction to the field of anion sensing and the challenges associated with it. The use of fluoride in its different forms along with the activities that lead to excess fluoride in water resources are also described in the chapter. The harmful effects of fluoride pollution and the importance of fluoride detection are discussed. The chapter also gives a brief literature review on the existing classes of sensors for the detection of both organic and inorganic forms of fluoride with the pros and cons of each method. The advantages of optical sensing technology and the use of some materials like dyes and their derivatives, nanoparticles etc to enable colorimetric and spectrophotometric detection of fluoride are detailed. Some basic properties of the dyes used in the present work are also mentioned in the chapter along with the scope of the thesis.

In *Chapter 2* the fluoride sensing response of synthetic organic dye Rhodamine 6G (Rh6G) in the organic solvent acetonitrile is described. The mechanism of NH deprotonation

leading to colour changes of Rh6G solution along with the rapid decrease in absorption and fluorescence was confirmed using FTIR spectroscopy and protic solvent addition. The Forster resonance energy transfer (FRET) based sensing of fluoride was studied using Coumarin 540A (C540A) donor-Rh6G acceptor pair by making use of the selective sensitivity of the acceptor to fluoride, for different donor-acceptor concentrations. The change in fluorescence lifetime of Rh6G was also used to study the FRET in C540A-Rh6G pair and the FRET efficiency was found to be a good indicator for the concentration measurement of fluoride. A simple system consisting of C540A doped in poly-methylmethacrylate (PMMA) polymer film coated on a hollow glass capillary was also demonstrated as an effective sensing element towards the detection of fluoride. The effect of varying concentration of C540A dye in PMMA and the thickness of the coated layer on the fluorescence emission from the capillary was studied. The detection of fluoride using both C540A and Rh6G emissions from the capillary is also described in the chapter.

Chapter 3 describes the detection of fluoride using low cost natural dye Curcumin via OH deprotonation mechanism. The use of Curcumin for the realization of intensity based fiber optic sensors involving the absorption and fluorescence changes of Curcumin in the presence of fluoride in two different organic solvents have also been presented. Fluorescence sensor probes using un-cladded and chemically tapered silica fibers were fabricated and the fluoride detection using collection of diminishing fluorescence of Curcumin in the presence of increasing fluoride was studied and compared.

Chapter 4 presents the results of irradiation of Curcumin in organo-aqueous media using different light sources for the detection of fluoride. The result of irradiation of Curcumin in the presence of organic and inorganic fluorides (Tetrabutylammonium fluoride and Sodium fluoride) in mixture solvent has been discussed in this chapter. Simple experimental set-ups for the continuous monitoring of fluoride by irradiation of Curcumin using low cost sources and the detection of the absorption or fluorescence signal using low cost detectors are also discussed. The chapter also gives a description of the possibility of using Curcumin stained filter paper strips for sodium fluoride (NaF) detection by the irradiation technique.

Chapter 5 details the preparation of Curcumin-Aluminium (Cur:Al) dye metal complexes in varying molar ratio for the detection of inorganic form of fluoride (NaF), acetate (CH_3COONa) and phosphate (NaH_2PO_4). The chapter also gives a brief description about

the importance of phosphate and acetate and the methods that exist for their detection. Cur:Al complexes were found to work in higher volume of water content with a decrease in absorption and fluorescence intensity along with an observed blue shift of absorption upon addition of the anions. The use of different ratio complexes to achieve good sensitivity and higher dynamic range of detection is also discussed in this chapter. The preliminary result of a sensor set-up using a Cur:Al complex doped poly-methymetahcrylate optical fiber towards the detection of three anions is also described.

Chapter 6 lists the general conclusions of the works described in the thesis and proposes a few possible future works towards the detection and measurement of fluoride.

The publications related to the works presented in the thesis are included in the 'Appendix'.

List of Journal Publications

Roopa Venkataraj, Arindam Sarkar, C. P. Girijavallabhan, P. Radhakrishnan, V. P. N. Nampoori, and M. Kailasnath. "Fluorescence resonance energy-transfer-based fluoride ion sensor." *Applied optics 57*, No. 15, 4322-4330 (2018)

Roopa Venkataraj, C. P. Girijavallabhan, P. Radhakrishnan, V. P. N. Nampoori and M. Kailasnath. "Photochemical Degradation of Curcumin: a Mechanism for Aqueous Based Sensing of Fluoride." *Journal of fluorescence* 27, No. 6, 2169-2176 (2017)

Roopa Venkataraj, V P N Nampoori, P Radhakrishnan, and M Kailasnath, "Chemically Tapered Multimode Optical Fiber Probe for Fluoride Detection Based on Fluorescence Quenching of Curcumin", *IEEE Sensors Journal*, Vol. 15, No. 10, 5584-5591 (2015)

Roopa Venkataraj, P. Radhakrishnan and M. Kailasnath. "Curcumin based optical sensing of fluoride in organo-aqueous media using irradiation technique." In *AIP Conference Proceedings*, Vol. 1849, No. 1, pp. 020009. AIP Publishing (2017)

Arindam Sarkar, **Roopa Venkataraj**, V. P. N. Nampoori, and M. Kailasnath. "Silver nanoparticles filled hollow polymer fiber laser with enhanced photostability." Optics & Laser Technology 112, 255-260 (2019).

List of Conferences/Conference publications

Roopa Venkataraj, Arindam Sarkar, P Radhakrishnan, V P N Nampoori, M Kailasnath, "Optical sensing of fluoride ion using dye coated hollow glass capillary", Photonics 2018-International Conference on Fiber Optics and Photonics,12-15 Dec 2018, IIT Delhi, Paper No. FA1-C3, Proceedings of the Photonics-2018, ISBN: 978-93-88653-41-1

Roopa Venkataraj, Arindam Sarkar, P Radhakrishnan, M Kailasnath, "Capillary based optical sensor structure for detection of fluoride", National Laser Symposium (NLS-26), BARC, Mumbai, 20-23 Dec, 2017 Identifier: CP-09-20

Roopa Venkataraj, Arindam Sarkar, M Kailasnath, "Laser induced fluorescence from Curcumin doped silica xerogel", National Laser Symposium (NLS-25), KIIT, Bhubneshwar, 20-23 Dec, 2016, ISBN: 978-81-903321-7-0 NLS-25 Identifier: CP-6.38

Roopa Venkataraj and M Kailasnath, "Curcumin Doped Silica Xerogel for Sensing Applications", Roopa Venkataraj and M. Kailasnath. "Curcumin doped silica xerogel for sensing applications." In *Workshop on Recent Advances in Photonics (WRAP),* pp. 1-3. IEEE (2015)

Roopa Venkataraj, Arindam Sarkar, V P N Nampoori, P Radhakrishnan and M Kailasnath, "Development of Optical Fiber Sensors for Fluoride Ion", IC-IMPACTS Summer Institute: Optical Sensing Technologies for Infrastructure, Water and Mobile Health, University of Toronto, Canada, 14-19 Jun, 2015

Roopa Venkataraj, V. P. N. Nampoori, P. Radhakrishnan and M. Kailasnath. "A simple fluorescence based optical fiber sensor for fluoride ions." In *International Conference on Fibre Optics and Photonics*, pp. M4A-15. Optical Society of America (2014)

Roopa Venkataraj, Arindam Sarkar, V P N Nampoori, P Radhakrishnan, M Kailasnath, "Evanescent wave optical fiber sensor for fluoride ions in organic solvent", National Laser Symposium, NLS-23, S.V. University, Tirupati. 3-6 Dec 2014, ISBN: 9788190332156 NLS-23 Identifier: CP-11-06

Arindam Sarkar, **Roopa Venkataraj,** V P N Nampoori, M Kailasnath, "Spectral tuning and amplified laser emission in dye-silver nanoparticles filled hollow polymer optical fiber", Photonics 2018-International Conference on Fiber Optics and Photonics,12-15 Dec 2018, IIT Delhi, Paper no. TP-124, Proceedings of the Photonics-2018, ISBN: 978-93-88653-41-1

Arindam Sarkar, **Roopa Venkataraj**, V.P.N Nampoori, M.Kailasnath, "Influence of silver nanoparticles on hollow polymer optical fiber resonator", National Laser Symposium (NLS-26), BARC, Mumbai, 20-23 Dec, 2017

Contents

3 Natural dye Curcumin for fluoride detection 65

4 Irradiation technique for aqueous based sensing of fluoride using Curcumin 93

6   Conclusions and Future prospects   147

Appendix   153

List of Figures

List of Tables

List of Abbreviations

AFB	Alizarin Fluorine Blue
ATR	Attenuated Total Reflection
AuNP	Gold Nanoparticle
BPO	Benzoyl Peroxide
C540A	Coumarin 540A
Cur-Al	Curcumin-Aluminium
EPA	United States Environmental Protection Agency
EtOH	Ethanol
EWOFS	Evanescent Wave Optical Fiber Sensor
FBG	Fiber Bragg Grating
FRET	Forster (Fluorescence) Resonance Energy Transfer
FTIR	Fourier Transform Infrared
HF	Hydrofluoric Acid
ICT	Intra-molecular Charge Transfer
ISFET	Ion Selective Field Effect transistor
KBr	Potassium Bromide
LOD	Limit of Detection
LPG	Long Period Grating
MeOH	Methanol
MMA	Methylmethacrylate
NaA	Sodium Acetate
NaB	Sodium Bromide
NaC	Sodium Chloride
NaF	Sodium Fluoride
NaN	Sodium Nitrate
NaOH	Sodium Hydroxide

NaP	Sodium Di-Hydrogen Phosphate
NaS	Sodium Hydrogen Sulphate
OH	Hydroxyl
PCS	Plastic Clad Silica
PMMA	Poly-methymethacrylate
Rh6G	Rhodamine 6G
SDS	Sodium Dodecyl Sulphate
SRI	Surrounding refractive index
TBA	Tetrabutylammonium
TBAA	Tetrabutylammonium Acetate
TBAB	Tetrabutylammonium Bromide
TBAC	Tetrabutylammonium Chloride
TBAF	Tetrabutylammonium Fluoride
TBAI	Tetrabutylammonium Iodide
TBAN	Tetrabutylammonium Nitrate
TBAP	Tetrabutylammonium Di-Hydrogen Phosphate
TBAS	Tetrabutylammonium Sulphate
TCSPC	Time Correlated Single Photon Counting
TFBG	Tilted Fiber Bragg Grating
THF	Tetrahydrofuran

Chapter 1

Introduction

In this chapter, an overview of the challenges in anion sensing is presented with special reference to the problems associated with fluoride detection. The different sources of fluoride in the environment, the forms utilized by mankind and the harmful effects of fluoride pollution are outlined. Various methods used for the detection and measurement of fluoride are also presented with their pros and cons. Some basic properties of organic dyes used in fluoride sensing methods described in the later parts of thesis are also listed with their applications.

1.1 Anion sensors-Challenges

Sensing of chemical species in water resources have always been of integral importance to ensure quality control and prevention of a number of health conditions and diseases that would wreak havoc in almost all living systems. Anions play a pivotal role in the field of medicine and catalysis [1]. Anion sensing is considered to be an interesting challenge by many researchers all over the world [1-4]. A variety of reasons are reported for the difficulty in realizing anion sensors when compared to cation sensors [5]. Anions have a larger size (larger ionic radius) and hence a lower charge to radius ratio. This means that the electrostatic binding interaction with a receptor would be weak and also the binding site of receptor should be large enough to accommodate the large sized anion. Secondly, the anions have differing geometries including linear, spherical, triagonal planar, tetragonal etc which makes it a huge challenge to design a receptor accordingly [1, 5].

Anions are also prone to losing their negative charge in acidic environments, thereby further restricting the use of receptors to a certain pH range. The selection of solvents too can affect proper detection of anions. Solvents with hydroxyl (OH) groups can bond with the anions thereby making it difficult for the sensing receptors to bond with the anions and generate a response [1, 6]. Fluoride ion detection in particular seems to be a true challenge amongst the clique of varied anions that find their way from various natural as well as industrial sources into the ground water resources. The high affinity of fluoride ion towards water molecules makes it difficult to selectively perform aqueous based measurements [7, 8].

1.2 Fluoride ion and its uses

Fluorine element belongs to Group 7A in the periodic table and has a deficiency of one electron from achieving the stable inert configuration. This makes fluorine highly electronegative and reactive. Fluorine further reacts to form hydrofluoric acid (HF) and sodium fluoride (NaF) in water [9]. Fluoride is reported to be beneficial for the prevention of tooth decay [10]. The bacteria present in the mouth produces acid via fermentation. Fluoride inhibits the growth of bacteria and prevents acid induced demineralization of the enamel [9]. HF is used in the production of aluminium fluoride and fluorocarbons and it is also used in etching glass. Other inorganic fluorides like sulphur hexafluoride is used as an electrical insulator in transformers. Fluorides are also used to manufacture the fluoro-

polymer Teflon that finds use in cooking utensils, paints and even cosmetic surgery. Some medications are also reported to contain fluorides [11, 12].

.

1.3 Sources of fluoride and fluoride pollution

There are both natural and artificial sources of fluoride. In the soil, fluoride is found in fluorite (CaF_2) [13] rocks, which is an accessory mineral to granitic rocks. Cryolite (Na_3AlFPO_6) and fluorapatite ($Ca_3(PO)_2$ $Ca(FCl)_2$) rocks also contain fluoride [11]. Around 20-3600 ppm of fluoride concentration was reported to be found in granite rocks. The concentration of fluoride in the soil is depth dependent. Even though the leaching of fluoride from soils is small, the content of fluoride in soil was found to be around 300 ppm. Application of fertilizers was also reported to cause fluoride pollution in ground water resources [9]. The fluoride content in soil and the water used for irrigation can also affect the concentration of fluoride in most food items, with even high level of fluoride reported in tea leaves [11].

The artificial sources of fluoride include various industries that make use of fluoride in its varied forms. Fluorides are found in products such as toothpaste (Na_2PO_3F or NaF), dietary supplements (as NaF), glass-etching or chrome-cleaning agents (NH_4HF_2 or HF), insecticides, rodenticides (NaF), and also in drinking water (NaF) [14]. The discharge of waste from HF, toothpaste, semiconductor, glass, ceramic and phosphate fertilizer manufacturing industries, aluminium smelters etc all contribute to excess fluoride in water resources [9, 15]. The presence of both natural and man-made sources of fluoride contributing to fluoride pollution is a huge cause for concern. Many adverse effects of fluoride pollution have been reported. Many parts of India and China are worst affected by excess fluoride ion concentration in ground water resources [15]. There have been reports of dental and skeletal fluorosis, both being incurable conditions [16], recorded for very low concentrations of fluoride ion. This led to the WHO declaration of 1 ppm as the permissible limit for fluoride ion in ground water resources in India whereas 1.5 ppm is the maximum acceptable concentration the world over [9]. The U.S environmental protection agency has declared 4 ppm as the permissible limit of fluoride in drinking water [17]. Dental fluorosis manifests itself as mottling of teeth [10] whereas skeletal fluorosis causes weakening of the bones even leading to fractures, joint pain and fatigue [9, 10, 15]. The other major diseases or conditions that have been reported to be caused by excessive fluoride intake include irritable bowel syndrome [15], infertility, osteoporosis, arthritis, cancer, Alzheimers, weak

immune system, deformed red blood cells and even neurological problems [10, 11, 16]. It was also reported that fluoride tends to accumulate in the aquatic species like fish, crab, shrimp etc [13]

1.4 Current sensors and techniques for fluoride detection and measurement

There are a wide variety of sensors for the detection of fluoride. They can be classified into the following major methods:

1.4.1   Ion-selective electrodes

The ion selective electrode for fluoride works on the principle of development of a potential across a membrane that is impervious to all other ions except fluoride ions [6]. The schematic of an ion selective electrode is as shown in Fig. 1.1. Crystalline lanthanum fluoride (LaF_3) membrane is mostly used as the sensing membrane. The potential usually in mV, measured with respect to a reference Ag/AgCl electrode is proportional to the concentration of fluoride in solution. A typical graph of the variation in potential with concentration is as shown in Fig. 1.2. In some cases europium is added to LaF_3 membranes to increase the conductivity [18]. Polycrystalline LaF_3 layers have also been shown to possess fluoride sensitivity identical to that of a LaF_3 single-crystal electrode. This vapour deposited LaF_3 membrane on Si-SiO_2 –Si_3N_4 structures was reported to be similar to the gate area of an ion selective field effect transistor (ISFET). Concentrations of fluoride ranging from 10^{-5} M to 0.1 M could be detected from the shift of the C-V curve on the voltage axis and the limit of detection was around 10^{-6} M [18].
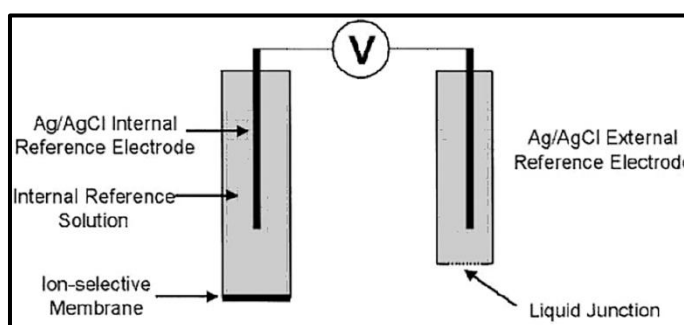
Figure 1.1 Schematic of an ion-selective electrode [5]
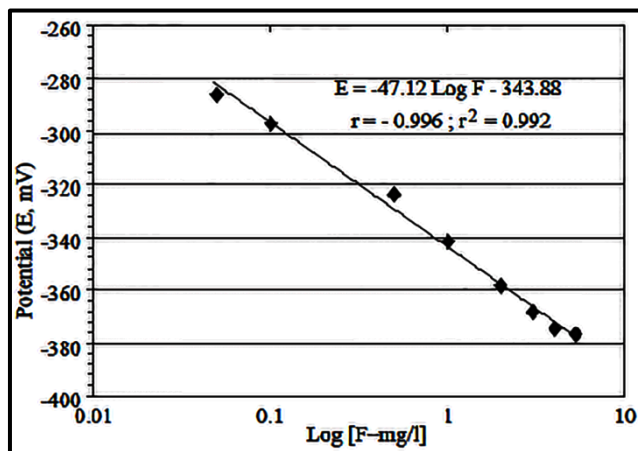
Figure 1.2 Example curve of variation in potential with fluoride concentration in the potentiometric method [19]

There are different variations of the ion selective electrode used for the detection of fluoride. S Liawruangrath et al [20] used an asparagus plant based bio-electrode which could detect fluoride concentrations above 0.5 ppm with a linear response of upto 14 ppm. Here the asparagus tissue was incorporated into a ferrocene modified carbon paste electrode and reduction in response of the electrode towards H_2O_2 in the presence of fluoride was used to estimate the concentration of fluoride. But the sensor has interference problems with other species and also suffers from variation of sensitivity with time. Zr(IV) porphyrins have also been used in PVC membrane to function as neutral anion carriers. This porphyrin along with cationic additives in polymer membrane shows faster response towards fluoride with high selectivity [8].

The organotin compound bis(chlorodiphenylstannyl)methane doped in PVC membrane showed enhanced Lewis acidity leading to high selectivity for fluoride [21]. Another study used poly-(borosiloxane), a soft polymer with Lewis acid sites having strong affinity towards fluoride, to achieve detection limits as low as 10^{-10} M [22]. Spiropyran assembled on single walled carbon nanotube modified carbon electrode was used to generate an electrochemical response towards fluoride via breakage of Si-O bond leading to a limit of detection of almost 8×10^{-8} M [23].

The method of ion selective electrodes requires complex procedures for sample preparation and temperature stability [24, 25]. It is costly [26] and needs the use of special agents to ensure no interference from other metal ions as well as to maintain the pH between 5.3-5.8. The stringent pH condition is imposed to prevent the formation of

lanthanum hydroxide in the basic pH condition [22, 27]. The method has a detection range of 10^{-9} M to 10^{-6} M [22] and can lead to errors at higher concentration range [25]. It was also reported that at low fluoride concentration the response of the electrode is slow and drifting of the electrode potential due to different reasons necessitates the frequent calibration of the electrode for optimal performance [28].

1.4.2 Ion-chromatography

Ion chromatography is considered to be a method that is sensitive enough to detect many ions [25, 29]. The ion chromatograph system for anion analysis consists of a number of sections like solvent (eluent) reservoir, separator and suppressor columns, provisions for sample injection, pump, conductivity cell, a meter and recorder. The eluent which is an electrolyte is used to extract the anions to be detected from the anion-ion exchange resin at the separator column. The rate at which the ions pass through depends on the affinity of the anion with the ion exchange resin. At the suppressor column, the electrolyte (base like sodium hydroxide or sodium carbonate) is removed by an acid resin and the anion is converted to its acid which is detected further by the conductivity cell. The suppressor column is used to ensure that the high conductance of the eluent does not affect the measurements of the anion [29]. The basic steps in each section are as shown in Fig. 1.3 and a typical chromatogram of anions is as shown in Fig. 1.4.
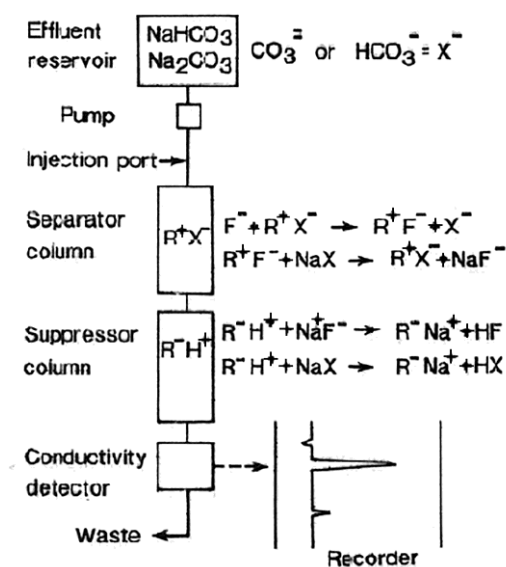
Figure 1.3 Steps in ion chromatography for anion detection [29]

[7]
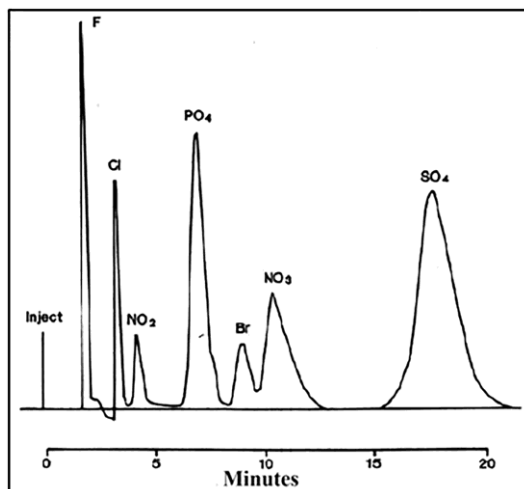
Figure 1.4 Ion-chromatogram of anions [29]

There are also modifications of the method to use detectors like spectrophotometers or fluorescence spectrometers instead of the conductivity cell to achieve higher sensitivity [25, 30]. In this method, formation of complex of aluminium and fluoride in the presence of excess aluminium was used for detection. The ion chromatography method being time consuming, bulky and expensive, is not considered as the most attractive option for fluoride ion sensing [19, 26].

1.4.3   Colorimetric and spectrophotometric methods

Ion selective electrodes and ion chromatography are considered as the standard methods for fluoride detection by the WHO. But both of these techniques require technical expertise, complicated equipment and stringent conditions for operation [17]. Electrochemical methods also have the disadvantage of having mostly a liquid electrolyte [24] whereas optical sensing techniques do not need the use of electrodes which are prone to electrical interference [31]. Optical sensing methods involve the study of changes in absorbance, fluorescence, chemi-luminescence, refractive index, photo-thermal effects and scattering in response to analyte [32]. Of all the different methods that have been used for detection of fluoride ions, the class of spectrophotometric and/colorimetric methods have a large number of advantages including low concentration measurement, easy to use etc [31, 33]. Fast straightforward detection with naked eye is offered by colorimetric methods, which obviously are low cost owing to the absence of bulky spectrophotometric instruments [34-36]. Exact concentration of the analyte is difficult to estimate with

colorimetric methods, but the presence of analyte above a certain concentration level can be surmised [5]. Colorimetric sensors also may have problems distinguishing between different anions having similar basicity or surface charge density [37].

Fluorescence based sensors are highly attractive owing to the high sensitivity [17] and high specificity offered by the choice of excitation and emission wavelengths. It also offers the possibility of monitoring different signals including emission intensity, emission wavelength and lifetime [35, 38]. The sensors based on visible wavelength excitation and emission are reported to have low background emissions and scattering [35]. Many optical sensors for fluoride ion employ either colorimetric, fluorescence or mostly a combination of both to effectively detect the fluoride species in organic media [39-41], mixtures of organic solvents [42], organic-aqueous solvent mixtures [43, 44] and very few in aqueous solvents [45, 46] or buffer solutions [47]. Most fluorescence probes involve a 'two in one unit' with a receptor that interacts with fluoride and a flurophore that signals the presence of this interaction [17]. The hydrogen bonding nature of fluoride is exploited by many chemosensors via the formation of O-H---F-, N-H---F-, C-H---F- and (C-H)+---F- bonds [34, 48]. The review by Massimo Cametti et al describes explicitly many different methods and mechanisms for sensing the elusive fluoride ion. Groups like amide, urea, thiourea, imidazolium, pyrrole are used as receptors for fluoride [48].

H Wada et al [49] developed a spectrophotometric method for the detection of fluoride ion which used Cerium or Lanthanum (La)/Alizarin complexone in a flow injection system. Lanthanum/alizarin complexone (1:l) in 70% acetone was used in conjunction with a 500 cm reaction coil at 60°C to determine 0.03-1.2 mg/L fluoride. Only aluminium seriously interfered with the method and this method is temperature dependent. Another such experiment using stopped flow reagent injection method using La (III) AFB complex in 15% (v/v) acetone, was devised by M E Leon Gonzalez et al [50]. The spectrophotometric alizarin fluorine blue (AFB) method was improved by developing a ternary complex in the presence of sodium dodecyl sulphate (SDS). The detection range for the method was 0.08-1.2 mg/L. Phosphate, nitrate, aluminium, iron, nickel and zinc ions caused interferences in the detection. A drawback of the method was that it required maintaining pH at 4.6.

A lot of fluorescence based methods for fluoride detection involve the use of organic dyes and their derivatives. Most of these sensors work in organic solvents. A coumarin derivative 7-(Diethylamino)-2-oxo-2H-chromene-3-carbaldehyde was used to detect

fluoride in acetonitrile via interaction of NH with F^- that led to NH deprotonation and an intramolecular charge transfer (ICT) with a red shifted absorption peak [51]. A bis (coumarin) methylene probe responded to fluoride via OH deprotonation in acetonitrile solvent leading to charge delocalization in the phenyl ring. This caused a corresponding colour change to yellow from the initial colourless state and an increase in fluorescence [34].

Shan Jiao et al [52] demonstrated a ratiometric probe for fluoride using fluorescein-coumarin probe in organo-aqueous mixture solvent by studying the ratio of intensities at two different wavelengths. The authors suggest that the ratiometric detection is far superior compared to monitoring either the decrease or increase in fluorescence. In most probes the single emission intensity can be affected by the concentration, instrumental and environment conditions. F^- triggered Si-O cleavage in the compound leads to a change in fluorescence emission from blue to green with a limit of detection (LOD) of 0.025 μmol/L and a linear detection range of 0-20 μmol/L.

Ratiometric sensing was also carried out using coumarin-bodipy compound by Xiaowei Cao et al [53] which brought huge red shift in the absorption spectrum, decrease in fluorescence emission at 606 nm and the appearance of a new band at 472 nm. Jianguang Wang et al prepared OH containing bodipy dyes for fluoride detection using O-H-F hydrogen bonding interaction. They studied the presence of methoxy groups and different positions of the OH group to get high selectivity towards fluoride for certain bodipy dyes [54]. Another interesting work involves the use of extracted natural dye Curcumin to detect fluoride and iron in mixture solvent [55] via OH deprotonation.

Aluminium (Al) has been reported to have a very high attraction towards fluoride ion. An optical sensor based on a poly (vinyl chloride) film containing aluminum (III) - octaethylporphyrin and a pH indicator was reported by I H A Badr et al [56]. Fluoride interacted with the Al (III) center of the porphyrin structure leading to changes in the absorption bands of both the porphyrin and the pH indicator. The authors attributed this to the change in the protonation state of the pH indicator when aluminium interacts with fluoride. Here also the pH condition of 3.6 was imposed to reduce interference from OH^- ions. The detection range of fluoride was 0.1 μM-1.6 mM using this method [56].

N-aryl imidazolium based probe for naked eye and dual channel (absorption and fluorescence) detection of F^- was described by Subodh Kumar et al [35]. The colour of the solution changed from yellow to orange in the presence of fluoride ions owing to the

generation of negative charge on nitrogen on addition of fluoride ions. Shyamaprosad Goswami et al [57] designed and synthesized nine 2, 3, 5-triphenylimidazole derivatives having nitro and/or OH groups at their phenyl groups as receptors for the colorimetric detection of F ion. Among these, the receptor having a nitro group at the para position of the 2-phenyl group with respect to the imidazole moiety showed colorimetric responses (yellow to red) towards F⁻ anion in acetonitrile-water (9:1 v : v). The nitro group acted as a signaling unit and OH and NH of imidazole acted as binding sites respectively. The intense red colour resulted because of the charge transfer interaction between fluoride bound NH of imidazole and the electron deficient nitro group at para position. There was a blue shifting of the emission peak from 550 nm to 477 nm and an increase in this emission with increase in fluoride. However the red colour change was also observed for acetate anion when added in very higher concentration.

Among the various recognition strategies that are available, researchers have focused a great deal of attention on Lewis acidic boron compounds. Three organoboron compounds were investigated as fluorescence sensors for fluoride by Zhi Qiang Liu and group [41]. In the presence of fluoride ion, the strong B-F interaction (Lewis acid-base interaction) interrupts the extended π-conjugation, thereby causing a dramatic change in the photo-physical properties, including two photon excited fluorescence leading to high sensitivity and selectivity. The colour changed from green yellow to colourless in Tetrahydrofuran (THF) solvent and there was also a blue shifting of emission band from 520 nm to 411 nm.

Organic–inorganic materials have also been widely studied for fluoride sensing. Eunjeong Kim et al [58] described an Anthraquinone-based fluorescent receptor which was immobilized on mesoporous silica (AFMS) or on silica particles (AFSP) via a sol–gel reaction. The addition of fluoride ions to a suspension of AFMS resulted in a large decrease in the fluorescence intensity of the anthraquinone of AFMS owing to the binding of fluoride to two urea N–H protons of receptor in AFMS. In the case of AFSP, the sensitivity for fluoride ions was 10 times lower than that of AFMS due to the immobilization of smaller amounts of receptor on the silica particles. A linear response of AFMS upon the addition of fluoride ions was observed between 0.50 µM and 10.0 µM, with a detection limit of 0.50 µM. The pore diameters of mesoporous silica are large enough to allow rapid anion diffusion resulting in sensing response times of less than 10 seconds.

Bin Liu et al [59] described the fluoride sensitivity of derivative 1, 4 benzoylamido-N-butyl- 1, 8-naphthalimide. In the presence of fluoride, the extent of intra-molecular charge

transfer (ICT) from the amide anion to the electron withdrawing imide moiety is enhanced, facilitated by an intermolecular proton transfer from the amide to fluoride. This enhancement in ICT (effectively fluorescence quenching) leads to an intensity-reduced and wavelength-shifted fluorescence as a function of fluoride concentration. Fluoride concentrations in the range of 20–100 mM can be detected. The colourless-to-yellow colour change and red shifted emission from 468 nm to 583 nm were reported to be due to the deprotonation of the 4-amido moiety of the naphthalimide fluorophore. Since the amide group also interacts with other strong bases, such as OH^-, the compound would also be likely to have a pH-dependent response.

A fluoride-responsive organogelator based on oxalamide-derived Anthraquinone was described by Zoran Dzolic et al [60]. This was the first example of a fluoride responsive gel system which allows naked-eye detection of fluoride by colour change or gel-to-sol transition owing to the presence of amidic NH in the structure. P Rajamalli et al [61] reported poly(aryl ether) dendrons with an anthracene moiety attached to the core through a acylhydrazone undergoing a gel-to-sol transition, accompanied by a color change from deep yellow to bright red, in the presence of fluoride ions. Fluoride ion concentration as low as 0.1 equivalent could be detected by this method.

Another such colorimetric fluoride sensor was reported by Yuping Zhang et al [62] with a cyano substituted amide gelator which could turn yellow owing to N-H deprotonation. The cyano-substituted aromatic amide with strong intermolecular hydrogen bonding and π–π stacking can easily form the organogel. The two NH groups of the amide act as anion acceptors and the cyano-substituted aromatic groups function as the chromophore that converts the interaction between hydrogen atom and anion to optical signals. A reversible organogel based on anthracene based uracil gelator was studied by Ling Bao Xing et al [63]. The aromatic anthracene unit serves as a signaling chromophore, and the amidic N−H in the uracil unit serves as the recognition site for its hydrogen-bonding ability.

Nanoparticles have also been reported for the detection of fluoride using colour changes, quenching or enhancement of fluorescence. S Wantanabe et al [46] reported thioglucose-capped gold nanoparticle which underwent aggregation in the presence of F- leading to a colour change from red to blue in aqueous solution with a detection range of 20–40 mM. However, the selectivity and sensitivity of this sensor were poor. A similar method was implemented by Jiun-An Gu et al [64] with a gold agglomeration probe

(AuNP) comprising of a dual silyl-protected dithiol-modified flexible linker. Fluoride ions remove silyl groups from phenol causing release of a dithiol which in turn caused aggregation of the AuNPs. The colour change from pink-red to violet-blue was observed with LOD of 120 µM in the dynamic concentration range from 120 µM to 1.5 mM. The method was reported to be simple, fast and could detect inorganic fluoride salts in polar solvents without the interference by the oxygen-containing anions.

Sunlight induced gold nanoparticles [65] were also demonstrated for sequential detection of Al^{3+} and F^-. Here poly-acrylic acid functionalized gold nanoparticles aggregated in the presence of Al^{3+} (red to blue colour) whereas the addition of F^- caused a dispersal of the aggregated nanoparticles (blue to red colour) as F^- removes Al^{3+}. The time for detection of change in peak absorbance was 10 minutes. Ag doped CdS/ZnS core/shell nanoparticles [66] functionalized using L-cystein responds to F^- by the formation of $N-H-F^-$ bond with amide group of L-cystein leading to an enhancement in fluorescence. The LOD for the method was reported to be 99.7 µg/L.

Another method reports the use of 7-nitro-2, 1, 3-benzoxadiazole (NBD) dye covalently attached to mesoporous silica nanoparticles. Even though this system has reduced fluorescence emission, upon addition of fluoride, there is an enhancement in fluorescence owing to the cleavage of Si-O bond leading to the free movement of fluorophore in the solution [67]. The method requires longer times (~40 minutes) to ensure the movement of NBD molecules from the mesoporous silica surface and has a detection range of 10^{-5} M-10^{-3} M at an operating pH between 2.3 to 3.5. Fast response time for fluoride detection was reported with the use of fluorescent carbon dots via quenching of fluorescence using an organic receptor like 4-mercaptophenyboronic acid. The method reports an LOD of 1.1×10^{-4} M and a linear detection range of 0-26.7 mM concentration. But phosphate ion was reported to cause interference in the detection. [68].

Most of the nanoparticle based fluoride detection schemes involve aqueous medium [46, 65, 66, 68] and mixture solvent [67] which is a huge advantage. But some of them exhibit pH dependent response [67] or narrow detection ranges [46] or longer response times [65, 67].

1.4.4 Other methods

An acoustic wave sensor for fluoride ion was reported by N.I.P. Valente et al using a sensitive coating on a piezoelectric crystal and the frequency decrease upon addition of

fluoride was studied [26]. The method could linearly detect fluoride concentrations till 80 ppm, but it has a detection limit of 3.7 ppm which is above the permissible limit of fluoride ion in water. Moreover it requires the use of gold coated quartz crystals which would render it costly. The authors also reported leaching of sensing agent affecting its stability.

Another method involves the use of inorganic cage structures to trap fluoride ion (Fig. 1.5a) at the central empty space, this not just helps in fluoride detection but also in the removal of fluoride from the solvent. Different D4R zinc phosphate molecular clusters were reported to complex F- (both organic and inorganic fluoride) in both the solution and solid state forming anionic, neutral or cationic products. The reaction of one such cluster is as shown in Fig. 1.5b. NMR spectroscopy was used to study the inclusion of fluoride in the host by observed chemical shifts of the host in the presence of fluoride [14].
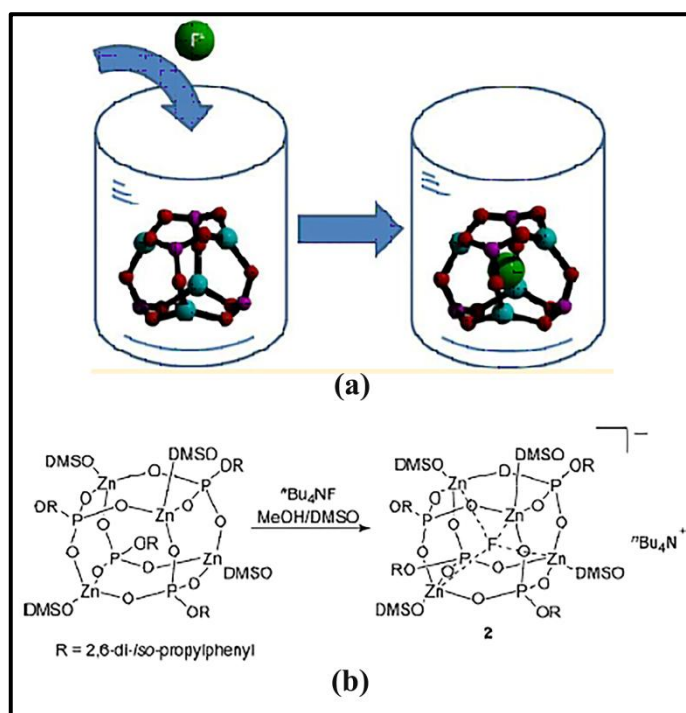
Figure 1.5 (a) Schematic of fluoride ion entrapment in cage structure (b) Chemical structure of D4R zinc phosphate heterocubane before and after fluoride additon [14]

1.4.5 Optical fiber sensors

Fiber optic sensors are deployed for a wide variety of sensing applications. The numerous advantages of fiber optic sensors include its high sensitivity, small size, light weight, immunity to electromagnetic interference and also the possibility of carrying out

remote and distributed sensing of multiple parameters even in hazardous environments [69, 70]. Optical fiber sensors can broadly be divided into two types- intrinsic sensors and extrinsic sensors. In the intrinsic sensor, the sensing region is intrinsic to the fiber i.e. the optical fiber is itself the sensing element, whereas in the extrinsic fiber senor the sensing region is external to the fiber and the fiber collects the light that is modulated by the measureand [70]. There are also classifications of the optical fiber sensor based on the type of signal viz. the intensity, wavelength, polarization and phase change of light upon interaction of measureand with light [69]. Intensity based fiber optic sensors record the change in intensity of light with respect to measureand. Different methods can be used to study the variation in intensity of light with respect to the measureand including evanescent field interaction, scattering of light, displacement of fiber and reflection. The intensity based fiber optic sensors are very low cost, easy to use and simple [71].
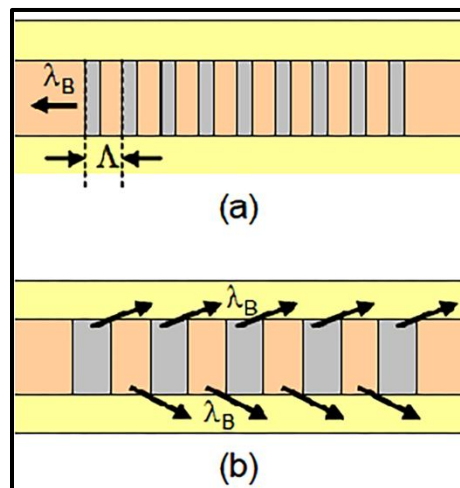
Figure 1.6 Schematic of (a) FBG and (b) LPG [72]

Wavelength modulation based sensors involve the fiber gratings like long period grating (LPG) and fiber bragg grating (FBG). FBG's and LPG's have a grating pitch of a few nanometers and a few hundred micrometers respectively. FBG reflects a particular wavelength depending upon the grating pitch whereas in LPG the particular wavelength is coupled into the cladding as depicted in Fig. 1.6. Interferometric sensors which involve phase modulation are reported to have a high level of sensitivity while FBG's and LPG's depend on the shift of central wavelength and loss peaks in transmission respectively. Here

the advantage is that the output is not affected by the fluctuations in light source intensity [69, 70]

Evanescent wave fiber optic sensors depend on the decaying exponential electromagnetic field called the evanescent wave originating at the core-cladding interface which can interact with the species surrounding the core region. When the evanescent wave is absorbed by the species, it leads to attenuated total internal reflection causing a decrease in the optical power transmitted by the optical fiber [73]. The evanescent wave fiber optic sensors can be implemented in a wide variety of methods including the simple un-cladded straight fiber [74], U shaped optical fiber sensors [75], D shaped fibers [76], side polished fibers [77], tapered fibers [72], hollow fibers [72], micro-bending [78] and LPG [72]. Some of the above mentioned configurations are shown in Fig 1.7.
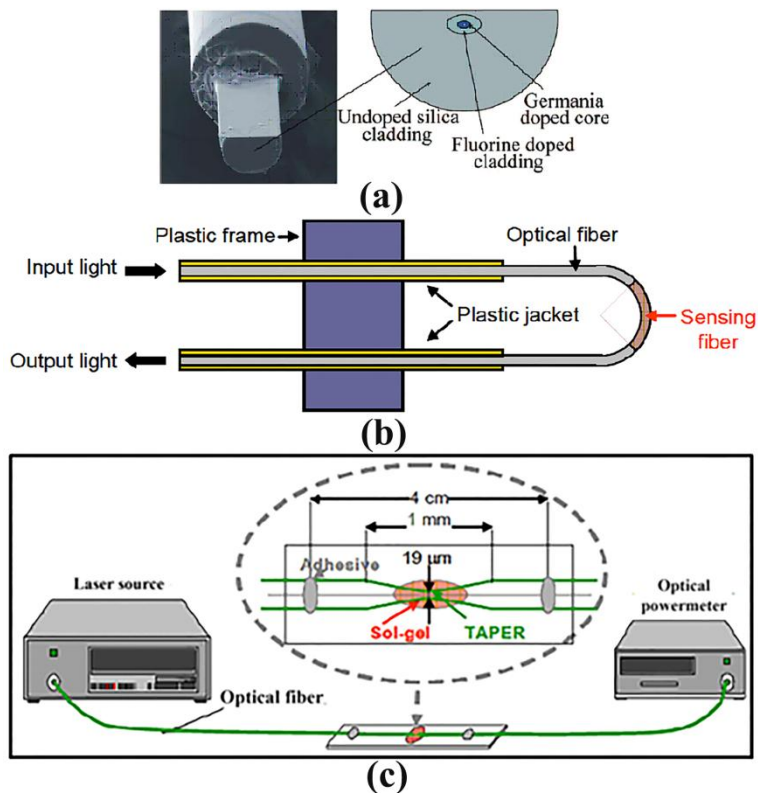
Figure 1.7 (a) D shaped fiber [76] (b) Schematic of a U shaped optical fiber probe [72] (c) Tapered fiber and simple evanescent wave interrogation set-up [72]

Different types of fibers have been reported for sensing applications including silica core-silica clad fiber, silica core-plastic clad fibers and polymer fibers. The evanescent wave

in plastic-clad silica fibers can easily be accessed by removing the plastic cladding using chemicals like acetone whereas the silica cladding requires the use of HF which is toxic [72]. Polymer fibers or plastic fibers have higher transmission losses than glass fibers, but they have comparatively lower manufacturing cost. The other advantages of polymer fibers include biocompatibility[79], high flexibility, high elastic strain limits etc which make them attractive for sensing applications [80] especially in structural health monitoring, medicine, chemical sensors and biosensors [80, 81]. Dye doped polymer fibers can especially be advantageous as light sources for sensing fibers and a variety of dopants can be used to get the required source wavelength [79].

Only a few optical fiber sensors have been reported for the detection of fluoride. R Narayanaswamy et al reported an alizarin fluorine blue (cerium (III) - alizarin complexone) binary complex immobilized on amberlite XAD-2 polymer beads for reflectance based measurements in a flow cell system. The flow cell system packed with the beads was interrogated by an optical fiber system consisting of a number of polymer fibers both for excitation and collection of light reflected from the beads. The Ce metal cation of this complex forms a ternary complex with fluoride leading to a colour change from wine red of the binary complex to blue of the ternary complex. The response time recorded was 12 minutes with the detection range of 0.16 mM to 0.95 mM [82]

Two other works reported from the same group use the Calcein blue complex with Zirconium to detect fluoride [83, 84]. A flow cell (Fig. 1.8) packed with calcein blue-zirconium complex adsorbed on amberlite XAD-4 polymer beads and a system consisting of a single silica fiber for excitation of beads surrounded by six fibers for collection of fluorescence from the beads was realized by the group [83]. The fluorescence intensity of calcein blue decreased upon zirconium complexation. But upon addition of fluoride, the formation of a ternary complex caused an enhancement in fluorescence. The response time was found to be around 2 minutes and the detection range was linear in the 0.11-0.42 mM (i.e. 2-8 ppm) range with a limit of detection of 5.3×10^{-5} M. Other ions like iron, tin, barium, aluminium, phosphate and acetate were reported to cause interferences in the detection.

A slight improvement in the detection limit (2.63×10^{-5} M) was observed with the use of a porous polytetrafluoroethylene membrane [84] to house the polymer beads instead of the flow cell. The authors attributed this improvement to the reduction in noise in this configuration compared to the flow cell based sensor system.
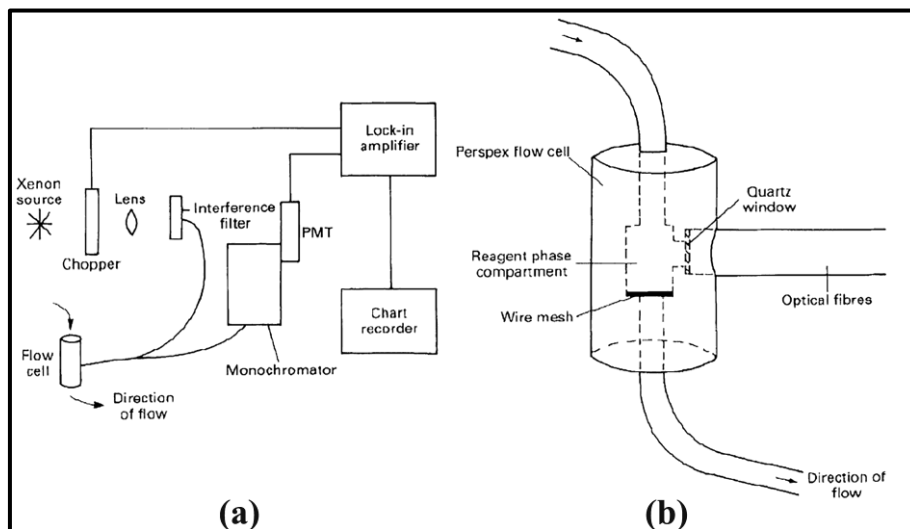
Figure 1.8 (a) Flow cell system for fiber optic fluorimetric determination of fluoride (b) Enlarged view of the flow cell system [83]
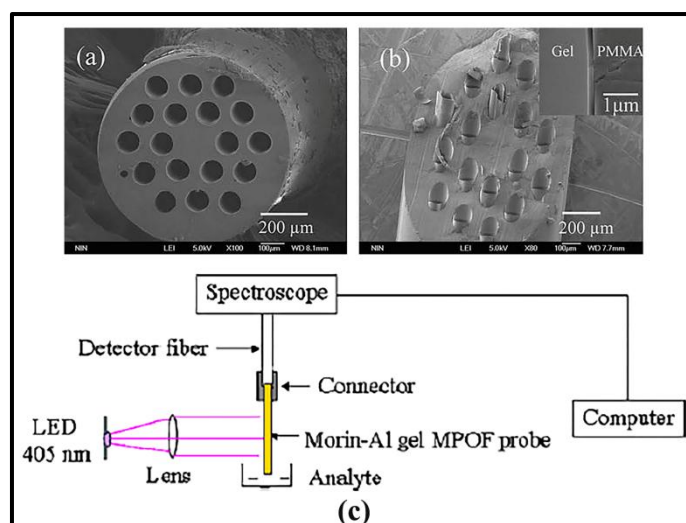
Figure 1.9 SEM image of (a) Microstructured fiber end face and (b) cross section of end face after sol gel coating inside the hole (c) experimental set up for interrogation of sol gel coated fiber [45]

All the above methods work in the acidic pH range of 2.2 [83, 84] and 4.1 [82]. A microstructured polymer optical fiber with the hole coated with a thin layer of morin-Al doped sol gel film was reported by Yang et al [45]. The coated fiber and the experimental set up used by the group are as shown in Fig. 1.9. Morin is non fluorescent and upon complexation with Al^{3+} gives strong fluorescence. When F^- is added Al^{3+} is removed from

the morin structure and there is a quenching of fluorescence. Authors reported a detection range of 5-50 mM with the use of a simple set up for interrogation as shown in the figure. PO_4^{3-} ions were also reported to have a similar effect on morin-Al structure. Here also stringent pH condition of less than 4.6 was imposed to ensure that OH^- ions do not interact with Al^{3+} in the gel.

Aji Balan Pillai [85] compared the fluoride detection capability of a simple LED-photodiode based set-up with that of a system consisting of U shaped evanescent wave fiber optic sensors employing polymer fibers. The set-up with LED excitation source is as shown in Fig. 1.10. Zirconyl-SPADNS reagent was used in both the cases for the formation of colourless ZrF_6^{2-} and the concentration of this complex was proportional to the fluoride concentration. The reaction rate was reported to be pH dependent and it was found that LED and optical fiber based sensor set ups exhibited sensitivity of 8 mV/ppm and 4.22 mV/ppm respectively. The advantages of these methods include aqueous based sensing capability. But such a sensor can operate only in acidic pH ranges, whereas for practical applications it should function in basic pH too as pH of water in ground water resources would mostly be basic.
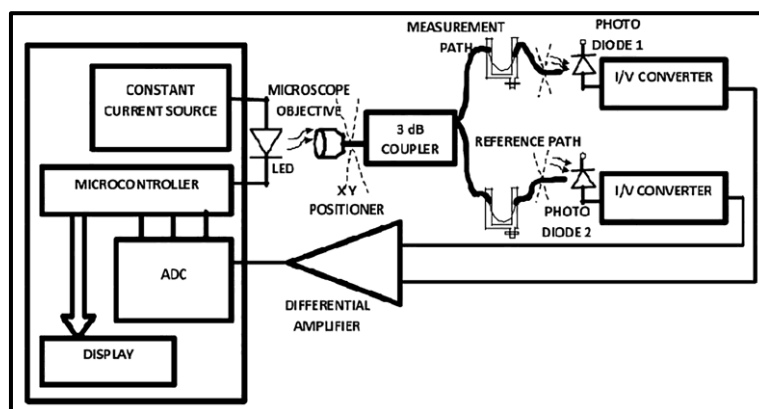
Figure 1.10 Schematic of the experimental set-up of the evanescent wave optical fiber sensor with LED light source [85]

A tilted fiber bragg grating (TFBG) was demonstrated for the detection of organic form of F^-, CH_3COO^- and Cl^- in organic solution by L B Melo et al [86]. TFBG consists of modulation of refractive index tilted with respect to the fiber axis. The transmission spectrum from such a fiber consists of multiple dips owing to the coupling between forward propagating core mode and forward or backward propagating cladding modes.

The experimental set-up used by the group and the TFBG spectrum are as shown in Fig. 1.11. The resonance wavelength and intensity of the dips varies with the changes in the surrounding refractive index (SRI). The variation in anion concentration changes the SRI leading to corresponding changes in the transmission spectrum which is demodulated to calculate the concentration.
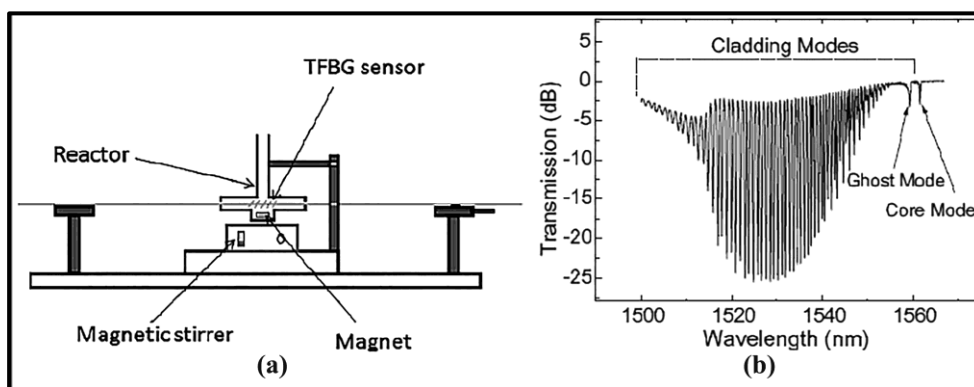
Figure 1.11(a) Experimental set-up of TBFG sensor and (b) Transmission of TBFG [86]

1.5 Organic dyes for chemical sensing applications

Organic dyes find a lot of applications including fluorescence enhancement [87], imaging [88], fluorescent labeling [89], lasing [90-93], sensing [94-96], dye sensitized solar cells [97] and even lighting applications [98]. Organic dyes have complex structures involving many conjugated bonds and such structures can especially be easily used for chemical sensor applications. Most of them also show inherent sensitivity to solvent environment [99, 100]. Rhodamine, coumarin, bodipy dyes and their derivatives as well as combinations of dyes have been reported for chemical sensing [94, 95, 101-104].

Coumarin 540A and Rhodamine 6G dyes are reported for lasing and FRET applications [87, 90, 93, 105] whereas Curcumin, a natural dye is reported to have a wide variety of medicinal applications [106-108]. A brief description of the dyes used in the present work is discussed below:

1.5.1   Coumarin 540A (C540A)

Coumarin 540A belongs to the class of benzo-α-pyrones (Fig. 1.12) [95] and has been reported for use with polymer films for lasing, as a donor for FRET systems and also as a standard for the determination of fluorescence quantum yields [87, 90, 109]. Some of the

coumarin derivatives are reported to be found in plants. Coumarin dyes have a variety of structures and are sensitive to local environment pH, viscosity and polarity and this is reflected in the change in fluorescence properties. These properties make them ideal candidates for sensing applications [95]. Coumarins and their derivatives have been reported for sensing Cu(II), Ni(II), CN⁻, nucleotides etc [110-112].
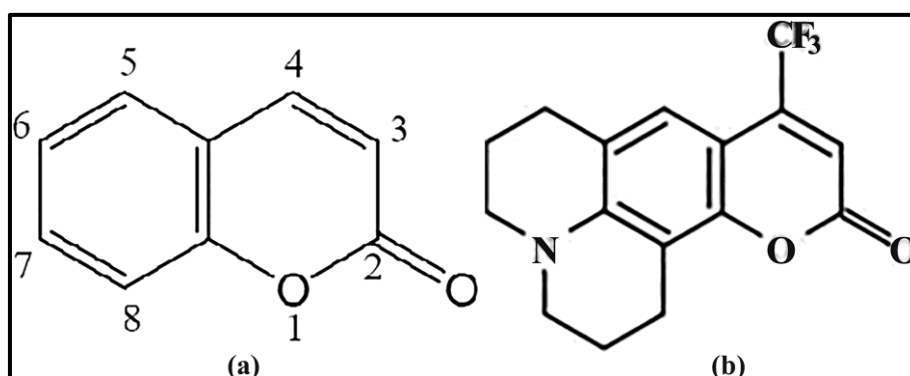
Figure 1.12 (a) Benzo-pyrone structure [95] and (b) C540A structure [105]

1.5.2   Rhodamine 6G (Rh6G)

Rhodamine 6G belongs to the class of xanthene dyes [113]. The basic xanthene structure and that of Rh6G dye are as shown in Fig. 1.13. Rhodamine dyes have very high absorption coefficient and broad visible fluorescence emission. They are also highly photo-stable and possess high quantum yield. Due to their excellent optical properties they find use in lasing applications, imaging and also as molecular probes [93, 94, 113].

   The absorption, fluorescence emission and fluorescence lifetime of Rh6G have been reported to vary with solvent environment as well as in solid matrices [114, 115] making them highly sensitive to parameters irrespective of the host. Rhodamine dyes exist in fluorescent amide form and the non-fluorescent ring closed spirolactum form [116]. Rhodamine derivatives are generally non fluorescent and have been used for sensing Hg(II), Cu(II), Fe(III), Cr(III), thiols, Cu^{2+} and Ce^{4+} [113, 117].
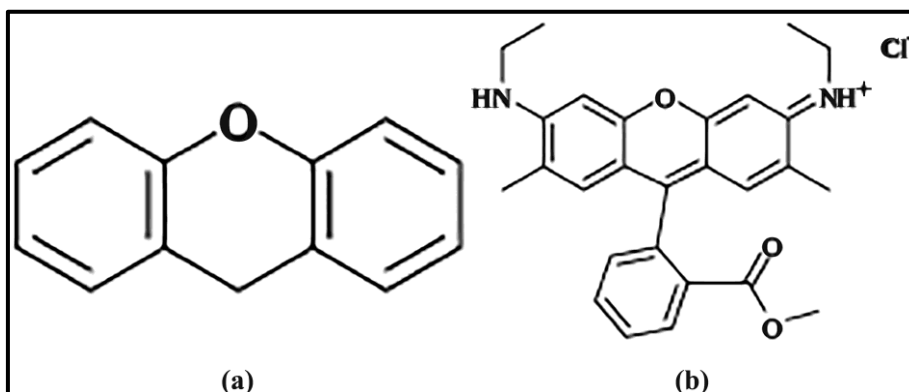
Figure 1.13 Structure of (a) xanthene and (b) Rh6G [113]

1.5.3   Curcumin

Curcumin is considered to be a miracle molecule derived from the roots of turmeric plant. Curcumin has a diferuloylmethane structure [118]. Commercial Curcumin consists of curcumin (major component), bis-demethoxycurcumin and demethoxycurcumin [107]. Curcumin being a non-toxic dye [119] finds a large number of applications in the field of medicine. Curcumin is reported to have anti-viral, anti-cancer, anti-Alzheimers, anti-bacterial and anti-inflammatory properties. It is also used in the treatment of wounds, skin infections, liver problems, heart diseases, high blood cholesterol, arthritis etc [106-108]. Metal complexes of Curcumin are also associated with medicinal capabilities including anti-Alzheimer, anti-cancer and neuroprotective properties [107]. Curcumin has also been reported for its use in sensing F^- and Fe [55], dye sensitized solar cells [120] and for preparation of nanoparticles [118].

Curcumin has limited solubility in water but has good solubility in most organic solvents. The β-diketone structure leads to keto-enol tautomer forms of Curcumin via intra-molecular hydrogen atom transfer as shown in Fig 1.14. The enol form of Curcumin is more stable and is most likely the form found in organic solvents [108]. The molecule also shows solvent, temperature and pH dependent fluorescence properties [108, 119, 121, 122]. Curcumin is also reported to undergo degradation in alkaline conditions [120, 122] even as it is partially soluble in this condition [108, 119].
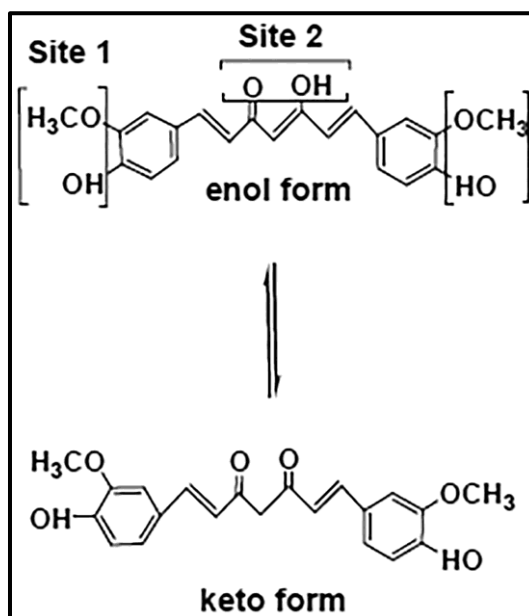
Figure 1.14 Keto-enol forms of Curcumin [118]

1.6 Summary

The chapter describes the property of fluoride ion, its available forms, sources of fluoride in nature and the adverse effects of fluoride pollution. The challenges in the detection of fluoride and the major methods for fluoride detection like the ion selective electrodes, ion chromatography, colorimetric, spectrophotometric and optical fiber based methods are described in detail. The structure, properties and some applications of the organic dyes used in the present work are also described briefly.

1.7 Scope of the thesis

Fluoride sensing is a formidable problem. With the many pathways of fluoride pollution prevalent, it is of utmost importance to devise simple, sensitive, selective, low cost optical probes and measurement techniques for the detection of fluoride. The thesis describes the use of both synthetic and natural dyes for the detection of fluoride using optical sensing techniques. It also proposes improvement in methodology using mechanisms like fluorescence resonance energy transfer, optical fiber probes for fluorescence collection and irradiation technique to enable detection in aqueous based solvents. Further, it describes the use of dye-metal complexes to enable the extremely sensitive detection of fluoride,

phosphate and acetate. Some of the methods described in the thesis like optical fiber probes and filter paper based sensing strategies can easily be adapted for deployment in practical applications for monitoring fluoride in water resources.

1.8 References

[1] Paul D. Beer, and Philip A. Gale. "Anion recognition and sensing: the state of the art and future perspectives." Angewandte Chemie International Edition 40, no. 3 (2001): 486-516.

[2] Hidekazu Miyaji, and Jonathan L. Sessler. "Off-the-Shelf Colorimetric Anion Sensors." Angewandte Chemie International Edition 40, no. 1 (2001): 154-157.

[3] Xuan Zhang, Lin Guo, Fang-Ying Wu, and Yun-Bao Jiang. "Development of fluorescent sensing of anions under excited-state intermolecular proton transfer signaling mechanism." Organic letters 5, no. 15 (2003): 2667-2670.

[4] Ramón Martínez-Máñez, and Félix Sancenón. "New advances in fluorogenic anion chemosensors." Journal of fluorescence 15, no. 3 (2005): 267-285.

[5] Frank Davis, Stuart D. Collyer, and Seamus PJ Higson. "The construction and operation of anion sensors: current status and future perspectives." In Anion Sensing, pp. 97-124. Springer, Berlin, Heidelberg, 2005.

[6] Bela G Liptak. Instrument Engineers' Handbook, Volume One: Process Measurement and Analysis. CRC press, 2003, pp 1353-1357.

[7] Soon Young Kim and Jong-In Hong. "Chromogenic and fluorescent chemodosimeter for detection of fluoride in aqueous solution." Organic letters 9, no. 16 (2007): 3109-3112.

[8] Łukasz Górski, Mark E. Meyerhoff, and Elżbieta Malinowska. "Polymeric membrane electrodes with enhanced fluoride selectivity using Zr (IV)-porphyrins functioning as neutral carriers." Talanta 63, no. 1 (2004): 101-107.

[9] Sulaiman Ayoob and Ashok Kumar Gupta. "Fluoride in drinking water: a review on the status and stress effects." Critical Reviews in Environmental Science and Technology 36, no. 6 (2006): 433-487.

[10] Vaishali Tomar, and Dinesh Kumar. "A critical study on efficiency of different materials for fluoride removal from aqueous media." Chemistry Central Journal 7, no. 1 (2013): 51.

[11] Sneha Jagtap, Mahesh Kumar Yenkie, Nitin Labhsetwar, and Sadhana Rayalu. "Fluoride in drinking water and defluoridation of water." Chemical reviews 112, no. 4 (2012): 2454-2466.

[12] https://www.news-medical.net/health/Fluoride-Uses.aspx

[13] Jamie E. Lefler, and Michelle M. Ivey. "Ion chromatography detection of fluoride in calcium carbonate." Journal of chromatographic science 49, no. 8 (2011): 582-588.

[14] Alok Ch Kalita, and Ramaswamy Murugavel. "Fluoride ion sensing and caging by a preformed molecular D4R zinc phosphate heterocubane." Inorganic chemistry 53, no. 7 (2014): 3345-3353.

[15] Mohammad Hadi Dehghani, Gholam Ali Haghighat, Kaan Yetilmezsoy, Gordon McKay, Behzad Heibati, Inderjeet Tyagi, Shilpi Agarwal, and Vinod Kumar Gupta. "Adsorptive removal of fluoride from aqueous solution using single-and multi-walled carbon nanotubes." Journal of Molecular Liquids 216 (2016): 401-410.

[16] Surendra Roy and Gurcharan Dass. "Fluoride contamination in drinking water–a review." Resour. Environ 3, no. 3 (2013): 53-58.

[17] Lei Xiong, Jiao Feng, Rui Hu, Shuangqing Wang, Shayu Li, Yi Li, and Guoqiang Yang. "Sensing in 15 s for aqueous fluoride anion by water-insoluble fluorescent probe incorporating hydrogel." Analytical chemistry 85, no. 8 (2013): 4113-4119.

[18] W. Moritz, I. Meierhöfer, and L. Müller. "Fluoride-sensitive membrane for ISFETs." Sensors and Actuators 15, no. 3 (1988): 211-219

[19] Şerife Tokalioğlu, Şenol Kartal, and Uğur Şahin. "Determination of fluoride in various samples and some infusions using a fluoride selective electrode." Turkish Journal of Chemistry 28, no. 2 (2004): 203-212.

[20] S. Liawruangrath, W. Oungpipat, S. Watanesk, B. Liawruangrath, C. Dongduen, and P. Purachat. "Asparagus-based amperometric sensor for fluoride determination." Analytica chimica acta 448, no. 1-2 (2001): 37-46.

[21] Katerina Perdikaki, Ioannis Tsagkatakis, Nikolas A. Chaniotakis, Reiner Altmann, Klaus Jurkschat, and Gregor Reeske. "Selective fluoride recognition and potentiometric properties of ion-selective electrodes based on bis (halodiphenylstannyl) alkanes." Analytica Chimica Acta 467, no. 1-2 (2002): 197-204.

[22] Puneet, Puhup, Raman Vedarajan, and Noriyoshi Matsumi. "Alternating poly (borosiloxane) for solid state ultrasensitivity toward fluoride ions in aqueous media." ACS Sensors 1, no. 10 (2016): 1198-1202.

[23] Jia Tao, Peng Zhao, Yinhui Li, Wenjie Zhao, Yue Xiao, and Ronghua Yang. "Fabrication of an electrochemical sensor based on spiropyran for sensitive and selective detection of fluoride ion." Analytica chimica acta 918 (2016): 97-102.

[24] Abu Bakar Md Ismail, Koji Furuichi, Tatsuo Yoshinobu, and Hiroshi Iwasaki. "Light-addressable potentiometric fluoride (F−) sensor." Sensors and Actuators B: Chemical 86, no. 1 (2002): 94-97.

[25] Phil. Jones, "Development of a high-sensitivity ion chromatography method for the determination of trace fluoride in water utilizing the formation of the AlF2+ species." Analytica chimica acta 258, no. 1 (1992): 123-127.

[26] Nuno IP Valente, Paulino V. Muteto, Andreia SF Farinha, Augusto C. Tomé, João ABP Oliveira, and M. Teresa SR Gomes. "An acoustic wave sensor for the hydrophilic fluoride." Sensors and Actuators B: Chemical 157, no. 2 (2011): 594-599.

[27] Rakesh Ranjan, and Amita Ranjan. Fluoride toxicity in animals. Springer, 2015, pp 69-83.

[28] Erik. Kissa, "Determination of fluoride at low concentrations with the ion-selective electrode." Analytical Chemistry 55, no. 8 (1983): 1445-1448.

[29] Marvin J. Fishman, and Grace Pyen. Determination of selected anions in water by ion chromatography. No. 79-101. US Geological Survey, 1979.

[30] María Montes Bayón, Ana Rodríguez Garcia, J. Ignacio García Alonso, and Alfredo Sanz-Medel. "Indirect determination of trace amounts of fluoride in natural waters by ion chromatography: a comparison of on-line post-column fluorimetry and ICP-MS detectors." Analyst 124, no. 1 (1999): 27-31.

[31] W. Rudolf. Seitz, "Chemical sensors based on fiber optics." Analytical Chemistry 56, no. 1 (1984): 16A-34A.

[32] G. A. Ibañez, and G. M. Escandar. "Fluorescence and phosphorescence chemical sensors applied to water samples." In Smart Sensors for Real-Time Water Quality Monitoring, pp. 45-64. Springer, Berlin, Heidelberg, 2013.

[33] Yasuhiro Shiraishi, Hajime Maehara, Takahiro Sugii, Dongping Wang, and Takayuki Hirai. "A BODIPY–indole conjugate as a colorimetric and fluorometric probe for selective fluoride anion detection." Tetrahedron Letters 50, no. 29 (2009): 4293-4296.

[34] Ajit Kumar Mahapatra, Kalipada Maiti, Prithidipa Sahoo, and Prasanta Kumar Nandi. "A new colorimetric and fluorescent bis (coumarin) methylene probe for fluoride ion detection based on the proton transfer signaling mode." Journal of Luminescence 143 (2013): 349-354.

[35] Subodh Kumar, Vijay Luxami, and Ashwani Kumar. "Chromofluorescent probes for selective detection of fluoride and acetate ions." Organic letters 10, no. 24 (2008): 5549-5552.

[36] Eun Jin Cho, Byung Ju Ryu, Young Ju Lee, and Kye Chun Nam. "Visible colorimetric fluoride ion sensors." Organic letters 7, no. 13 (2005): 2607-2609.

[37] Pavel Anzenbacher, Manuel A. Palacios, Karolina Jursíková, and Manuel Marquez. "Simple electrooptical sensors for inorganic anions." Organic letters 7, no. 22 (2005): 5027-5030.

[38] Jason R. Epstein, and David R. Walt. "Fluorescence-based fibre optic arrays: a universal platform for sensing." Chemical Society Reviews 32, no. 4 (2003): 203-214.

[39] Ju-Ying Li, Xin-Qi Zhou, Yi Zhou, Yuan Fang, and Cheng Yao. "A highly specific tetrazole-based chemosensor for fluoride ion: A new sensing functional group based on intramolecular proton transfer." Spectrochimica Acta Part A: Molecular and Biomolecular Spectroscopy 102 (2013): 66-70.

[40] Eun Jin Jun, Zhaochao Xu, Minji Lee, and Juyoung Yoon. "A ratiometric fluorescent probe for fluoride ions with a tridentate receptor of boronic acid and imidazolium." Tetrahedron Letters 54, no. 22 (2013): 2755-2758.

[41] Zhi-Qiang Liu, Mei Shi, Fu-You Li, Qi Fang, Zhang-Hai Chen, Tao Yi, and Chun-Hui Huang. "Highly selective two-photon chemosensors for fluoride derived from organic boranes." Organic letters 7, no. 24 (2005): 5481-5484.

[42] Jin Yong Lee, Eun Jin Cho, Shaul Mukamel, and Kye Chun Nam. "Efficient fluoride-selective fluorescent host: Experiment and theory." The Journal of organic chemistry 69, no. 3 (2004): 943-950.

[43] Min Hyung Lee, Tomohiro Agou, Junji Kobayashi, Takayuki Kawashima, and François P. Gabbaï. "Fluoride ion complexation by a cationic borane in aqueous solution." Chemical Communications 11 (2007): 1133-1135.

[44] Ilke Simsek Turan, and Engin U. Akkaya. "Chemiluminescence sensing of fluoride ions using a self-immolative amplifier." Organic letters 16, no. 6 (2014): 1680-1683.

[45] Xinghua Yang, Jian Wang, and Lili Wang. "Sol–gel matrix modified microstructured optical fibre towards a fluoride sensitive optical probe." Optics Communications 282, no. 13 (2009): 2502-2505.

[46] Shigeru Watanabe, Hideki Seguchi, Katsuhira Yoshida, Kouichi Kifune, Tsugio Tadaki, and Hisayoshi Shiozaki. "Colorimetric detection of fluoride ion in an aqueous solution using a thioglucose-capped gold nanoparticle." Tetrahedron letters 46, no. 51 (2005): 8827-8829.

[47] Yong Sung Kim, Jae Jun Lee, Ye Won Choi, Ga Rim You, LeTuyen Nguyen, Insup Noh, and Cheal Kim. "Simultaneous bioimaging recognition of cation Al3+ and anion F− by a fluorogenic method." Dyes and Pigments 129 (2016): 43-53.

[48] Massimo Cametti, and Kari Rissanen. "Recognition and sensing of fluoride anion." Chemical Communications 20 (2009): 2809-2829.

[49] H. Wada, H. Mori, and G. Nakagawa. "Spectrophotometric determination of fluoride with lanthanum/alizarin complexone by flow injection analysis." Analytica Chimica Acta 172 (1985): 297-302.

[50] M. E. Leon-Gonzalez, M. J. Santos-Delgado, and L. M. Polo-Diez. "Flow-injection spectrophotometric determination of fluoride based on alizarin fluorine blue in the presence of sodium dodecyl sulphate." Analytica Chimica Acta 219 (1989): 329-333.

[51] Xiaoqing Zhuang, Weimin Liu, Jiasheng Wu, Hongyan Zhang, and Pengfei Wang. "A novel fluoride ion colorimetric chemosensor based on coumarin." Spectrochimica Acta Part A: Molecular and Biomolecular Spectroscopy 79, no. 5 (2011): 1352-1355.

[52] Shan Jiao, Xiaochun Wang, Yihan Sun, Lijun Zhang, Weihong Sun, Ying Sun, Xinghua Wang, Pinyi Ma, and Daqian Song. "A novel fluorescein-coumarin-based fluorescent probe

for fluoride ions and its applications in imaging of living cells and zebrafish in vivo." Sensors and Actuators B: Chemical 262 (2018): 188-194.

[53] Xiaowei Cao, Weiying Lin, Quanxing Yu, and Jiaoliang Wang. "Ratiometric sensing of fluoride anions based on a BODIPY-coumarin platform." Organic letters 13, no. 22 (2011): 6098-6101.

[54] Jianguang Wang, Yuanjun Hou, Chao Li, Baowen Zhang, and Xuesong Wang. "Selectivity tune of fluoride ion sensing for phenolic OH-containing BODIPY dyes." Sensors and Actuators B: Chemical 157, no. 2 (2011): 586-593.

[55] Mahesh P. Bhat, Pravin Patil, S. K. Nataraj, Tariq Altalhi, Ho-Young Jung, Dusan Losic, and Mahaveer D. Kurkuri. "Turmeric, naturally available colorimetric receptor for quantitative detection of fluoride and iron." Chemical Engineering Journal 303 (2016): 14-21.

[56] Ibrahim HA Badr, and Mark E. Meyerhoff. "Fluoride-selective optical sensor based on aluminum (III)− Octaethylporphyrin in thin polymeric film: further characterization and practical application." Analytical chemistry 77, no. 20 (2005): 6719-6728.

[57] Shyamaprosad Goswami, and Rinku Chakrabarty. "An imidazole based colorimetric sensor for fluoride anion." European Journal of Chemistry 2, no. 3 (2011): 410-415.

[58] Eunjeong Kim, Hyun Jung Kim, Doo Ri Bae, Soo Jin Lee, Eun Jin Cho, Moo Ryeong Seo, Jong Seung Kim, and Jong Hwa Jung. "Selective fluoride sensing using organic–inorganic hybrid nanomaterials containing anthraquinone." New Journal of Chemistry 32, no. 6 (2008): 1003-1007.

[59] Bin Liu, and He Tian. "A ratiometric fluorescent chemosensor for fluoride ions based on a proton transfer signaling mechanism." Journal of Materials Chemistry 15, no. 27-28 (2005): 2681-2686.

[60] Zoran Džolić, Massimo Cametti, Antonella Dalla Cort, Luigi Mandolini, and Mladen Žinić. "Fluoride-responsive organogelator based on oxalamide-derived anthraquinone." Chemical Communications 34 (2007): 3535-3537.

[61] P. Rajamalli and Edamana Prasad. "Low molecular weight fluorescent organogel for fluoride ion detection." Organic letters 13, no. 14 (2011): 3714-3717.

[62] Yuping Zhang, and Shimei Jiang. "Fluoride-responsive gelator and colorimetric sensor based on simple and easy-to-prepare cyano-substituted amide." Organic & biomolecular chemistry 10, no. 34 (2012): 6973-6979.

[63] Ling-Bao Xing, Bing Yang, Xiao-Jun Wang, Jiu-Ju Wang, Bin Chen, Qianhong Wu, Hui-Xing Peng, Li-Ping Zhang, Chen-Ho Tung, and Li-Zhu Wu. "Reversible sol-to-gel transformation of uracil gelators: specific colorimetric and fluorimetric sensor for fluoride ions." Langmuir 29, no. 9 (2013): 2843-2848.

[64] Jiun-An Gu, Yu-Jen Lin, Yu-Ming Chia, Hsin-Yi Lin, and Sheng-Tung Huang. "Colorimetric and bare-eye determination of fluoride using gold nanoparticle agglomeration probes." Microchimica Acta 180, no. 9-10 (2013): 801-806.

[65] Anshu Kumar, Madhuri Bhatt, Gaurav Vyas, Shreya Bhatt, and Parimal Paul. "Sunlight induced preparation of functionalized gold nanoparticles as recyclable colorimetric dual sensor for aluminum and fluoride in water." ACS applied materials & interfaces 9, no. 20 (2017): 17359-17368.

[66] Siddhartha Sankar Boxi, and Santanu Paria. "Fluorometric selective detection of fluoride ions in aqueous media using Ag doped CdS/ZnS core/shell nanoparticles." Dalton Transactions 45, no. 2 (2016): 811-819.

[67] Gaurav Jha, N. Anoop, Abdur Rahaman, and Moloy Sarkar. "Fluoride ion sensing in aqueous medium by employing nitrobenzoxadiazole-postgrafted mesoporous silica nanoparticles (MCM-41)." Physical Chemistry Chemical Physics 17, no. 5 (2015): 3525-3533.

[68] Mojtaba Shamsipur, Afsaneh Safavi, Zahra Mohammadpour, and Amin Reza Zolghadr. "Fluorescent carbon nanodots for optical detection of fluoride ion in aqueous media." Sensors and Actuators B: Chemical 221 (2015): 1554-1560.

[69] Wentai Lin, Chunxi Zhang, Lijing Li, and Sheng Liang. "Review on development and applications of fiber-optic sensors." In 2012 Symposium on Photonics and Optoelectronics, pp. 1-4. IEEE, 2012.

[70] K. T. V. Grattan, and T. Sun. "Fiber optic sensor technology: an overview." Sensors and Actuators A: Physical 82, no. 1-3 (2000): 40-61.

[71] Y. N. Ning, K. T. V. Grattan, W. M. Wang, and A. W. Palmer. "A systematic classification and identification of optical fibre sensors." Sensors and Actuators A: Physical 29, no. 1 (1991): 21-36.

[72] Cesar Elosua, Ignacio Matias, Candido Bariain, and Francisco Arregui. "Volatile organic compound optical fiber sensors: A review." Sensors 6, no. 11 (2006): 1440-1465.

[73] S. Thomas Lee, Jose Gin, V. P. N. Nampoori, C. P. G. Vallabhan, N. V. Unnikrishnan, and P. Radhakrishnan. "A sensitive fibre optic pH sensor using multiple sol-gel coatings." Journal of Optics A: Pure and Applied Optics 3, no. 5 (2001): 355.

[74] B D Gupta, SK. Khijwania,"Experimental studies on the response of the fiber optic evanescent field absorption sensor." Fiber & Integrated Optics 17, no. 1 (1998): 63-73.

[75] B. D. Gupta, and Navneet K. Sharma. "Fabrication and characterization of U-shaped fiber-optic pH probes." Sensors and Actuators B: Chemical 82, no. 1 (2002): 89-93.

[76] John D. Gordon, Tyson L. Lowder, Richard H. Selfridge, and Stephen M. Schultz. "Optical D-fiber-based volatile organic compound sensor." Applied optics 46, no. 32 (2007): 7805-7810.

[77] Navneet K. Sharma, and B. D. Gupta. "Fabrication and characterization of pH sensor based on side polished single mode optical fiber." Optics communications 216, no. 4-6 (2003): 299-303.

[78] S. Thomas Lee, V. P. N. Nampoori, C. P. G. Vallabhan, P. Radhakrishnan, and K. Geetha. "Microbent optical fibers as evanescent wave sensors." Society of Photo-Optical Instrumentation Engineers, 2002.

[79] H. Y. Tam, Chi-Fung Jeff Pun, Guiyao Zhou, Xin Cheng, and M. L. V. Tse. "Special structured polymer fibers for sensing applications." Optical Fiber Technology 16, no. 6 (2010): 357-366.

[80] Kara. Peters "Polymer optical fiber sensors—a review." Smart materials and structures 20, no. 1 (2010): 013002.

[81] Lúcia Bilro, Nélia Alberto, João L. Pinto, and Rogério Nogueira. "Optical sensors based on plastic fibers." Sensors 12, no. 9 (2012): 12184-12207.

[82] R. Narayanaswamy, D. A. Russell, and F. Sevilla III. "Optical-fibre sensing of fluoride ions in a flow-stream." Talanta 35, no. 2 (1988): 83-88.

[83] David A. Russell, and Ramaier Narayanaswamy. "Fibre optic fluorimetric determination of fluoride ions." Analyst 114, no. 3 (1989): 381-385.

[84] David A. Russell, and Ramaier Narayanaswamy. "An optical-fibre sensor for fluoride." Analytica chimica acta 220 (1989): 75-81.

[85] Aji Balan Pillai, Benjamin Varghese, and Kottarathil Naduvil Madhusoodanan. "Design and development of novel sensors for the determination of fluoride in water." Environmental science & technology 46, no. 1 (2011): 404-409.

[86] L. B. Melo, J. M. M. Rodrigues, A. S. F. Farinha, C. A. Marques, L. Bilro, N. Alberto, J. P. C. Tomé, and R. N. Nogueira. "Concentration sensor based on a tilted fiber Bragg grating for anions monitoring." Optical Fiber Technology 20, no. 4 (2014): 422-427.

[87] Chiranjib Banerjee, Niloy Kundu, Surajit Ghosh, Sarthak Mandal, Jagannath Kuchlyan, and Nilmoni Sarkar. "Fluorescence resonance energy transfer in microemulsions composed of tripled-chain surface active ionic liquids, RTILs, and biological solvent: an excitation wavelength dependence study." The Journal of Physical Chemistry B 117, no. 32 (2013): 9508-9517.

[88] Mindan Lu, Ning Kang, Chuan Chen, Liuqing Yang, Yang Li, Minghui Hong, Xiangang Luo, Lei Ren, and Xiumin Wang. "Plasmonic enhancement of cyanine dyes for near-infrared light-triggered photodynamic/photothermal therapy and fluorescent imaging." Nanotechnology 28, no. 44 (2017): 445710.

[89] Vadim P. Boyarskiy, Vladimir N. Belov, Rebecca Medda, Birka Hein, Mariano Bossi, and Stefan W. Hell. "Photostable, amino reactive and water-soluble fluorescent labels based on

sulfonated rhodamine with a rigidized xanthene fragment." Chemistry–A European Journal 14, no. 6 (2008): 1784-1792.

[90] A. Costela, I. Garcia-Moreno, J. Barroso, and R. Sastre. "Laser performance of Coumarin 540A dye molecules in polymeric host media with different viscosities: From liquid solution to solid polymer matrix." Journal of applied physics 83, no. 2 (1998): 650-660.

[91] W. L. Sha, C-H. Liu, and R. R. Alfano. "Spectral and temporal measurements of laser action of Rhodamine 640 dye in strongly scattering media." Optics letters 19, no. 23 (1994): 1922-1924.

[92] Luis Cerdán, Angel Costela, Gonzalo Durán-Sampedro, and Inmaculada García-Moreno. "Random lasing from sulforhodamine dye-doped polymer films with high surface roughness." Applied Physics B 108, no. 4 (2012): 839-850

[93] Virginia Martín, Jorge Bañuelos, Eduardo Enciso, Íñigo López Arbeloa, Ángel Costela, and Inmaculada García-Moreno. "Photophysical and lasing properties of rhodamine 6G confined in polymeric nanoparticles." The Journal of Physical Chemistry C 115, no. 10 (2011): 3926-3933.

[94] Ha Na Kim, Min Hee Lee, Hyun Jung Kim, Jong Seung Kim, and Juyoung Yoon. "A new trend in rhodamine-based chemosensors: application of spirolactam ring-opening to sensing ions." Chemical Society Reviews 37, no. 8 (2008): 1465-1472.

[95] Brian. Wagner, "The use of coumarins as environmentally-sensitive fluorescent probes of heterogeneous inclusion systems." Molecules 14, no. 1 (2009): 210-237.

[96] Fanyong Yan, Keqing Fan, Zhangjun Bai, Ruiqi Zhang, Fanlin Zu, Jinxia Xu, and Xiang Li. "Fluorescein applications as fluorescent probes for the detection of analytes." TrAC Trends in Analytical Chemistry 97 (2017): 15-35.

[97] Dongshe Zhang, Suzanne M. Lanier, Jonathan A. Downing, Jason L. Avent, June Lum, and Jeanne L. McHale. "Betalain pigments for dye-sensitized solar cells." Journal of photochemistry and photobiology A: Chemistry 195, no. 1 (2008): 72-80.

[98] Rafael Turra Alarcon, Caroline Gaglieri, Bruno Henrique Sacoman Torquato da Silva, Luiz Carlos da Silva Filho, and Gilbert Bannach. "New fluorescein dye derivatives and their use as an efficient photoiniator using blue light LED." Journal of Photochemistry and Photobiology A: Chemistry 343 (2017): 112-118.

[99] R. Giri, S. S. Rathi, M. K. Machwe, and V. V. S. Murti. "Effect of substituents on the fluorescence and absorption spectra of coumarins." Spectrochimica Acta Part A: Molecular Spectroscopy 44, no. 8 (1988): 805-807.

[100] Amit Nag, and Debabrata Goswami. "Solvent effect on two-photon absorption and fluorescence of rhodamine dyes." Journal of Photochemistry and Photobiology A: Chemistry 206, no. 2-3 (2009): 188-197.

[101] Ankush B. More, Soumyaditya Mula, Shrikant Thakare, Saikat Chakraborty, Alok K. Ray, Nagaiyan Sekar, and Subrata Chattopadhyay. "An acac-BODIPY dye as a reversible "ON-OFF-ON" fluorescent sensor for Cu2+ and S2-ions based on displacement approach." Journal of Luminescence 190 (2017): 476-484.

[102] Norman Scholz, Amol Jadhav, Milind Shreykar, Thomas Behnke, Nithiya Nirmalananthan, Ute Resch-Genger, and Nagaiyan Sekar. "Coumarin-Rhodamine Hybrids—Novel Probes for the Optical Measurement of Viscosity and Polarity." Journal of fluorescence 27, no. 6 (2017): 1949-1956.

[103] Bao-xing Shen, and Ying Qian. "Building Rhodamine-BODIPY fluorescent platform using Click reaction: Naked-eye visible and multi-channel chemodosimeter for detection of Fe3+ and Hg2+." Sensors and Actuators B: Chemical 260 (2018): 666-675.

[104] Kaibo Zheng, Hui Chen, Shirong Fang, and Ying Wang. "A ratiometric fluorescent probe based on a Bodipy-Coumarin conjugate for sensing of nitroxyl in living cells." Sensors and Actuators B: Chemical 233 (2016): 193-198.

[105] Ping He, Huili Wang, Lili Zhang, Jialing Wang, Yugang Jiang, Rongwei Fan, and Deying Chen. "Solid-state laser based on PMMA doped with Coumarin 540A." Optics & Laser Technology 44, no. 2 (2012): 341-343.

[106] F. Cavaleri, and W. Jia. "The true nature of curcumin's polypharmacology." J. Prev. Med 2, no. 5 (2017).

[107] Simon Wanninger, Volker Lorenz, Abdus Subhan, and Frank T. Edelmann. "Metal complexes of curcumin–synthetic strategies, structures and medicinal applications." Chemical Society Reviews 44, no. 15 (2015): 4986-5002.

[108] K. Indira. Priyadarsini, "Photophysics, photochemistry and photobiology of curcumin: Studies from organic solutions, bio-mimetics and living cells." Journal of Photochemistry and Photobiology C: Photochemistry Reviews 10, no. 2 (2009): 81-95

[109] Albert M. Brouwer, "Standards for photoluminescence quantum yield measurements in solution (IUPAC Technical Report)." Pure and Applied Chemistry 83, no. 12 (2011): 2213-2228.

[110] Tuğçe Aksungur, Burcu Aydıner, Nurgül Seferoğlu, Müjgan Özkütük, Leyla Arslan, Yasemin Reis, Leyla Açık, and Zeynel Seferoğlu. "Coumarin-indole conjugate donor-acceptor system: Synthesis, photophysical properties, anion sensing ability, theoretical and biological activity studies of two coumarin-indole based push-pull dyes." Journal of Molecular Structure 1147 (2017): 364-379.

[111] Hongqi Li, Li Cai, Jinxing Li, Yixin Hu, Pingping Zhou, and Jiming Zhang. "Novel coumarin fluorescent dyes: synthesis, structural characterization and recognition behavior towards Cu (II) and Ni (II)." Dyes and Pigments 91, no. 3 (2011): 309-316.

[112] Alexandre Bettoschi, Andrea Ceglie, Francesco Lopez, Valeria Meli, Sergio Murgia, Manuela Tamburro, Claudia Caltagirone, and Francesca Cuomo. "On the role of a coumarin derivative for sensing applications: Nucleotide identification using a micellar system." Journal of colloid and interface science 477 (2016): 8-15.

[113] Mariana Beija, Carlos AM Afonso, and Jose MG Martinho. "Synthesis and applications of Rhodamine derivatives as fluorescent probes." Chemical Society Reviews 38, no. 8 (2009): 2410-2433.

[114] Renata Reisfeld, Rivka Zusman, Yoram Cohen, and Marek Eyal. "The spectroscopic behaviour of rhodamine 6G in polar and non-polar solvents and in thin glass and PMMA films." Chemical physics letters 147, no. 2-3 (1988): 142-147.

[115] Douglas Magde, Gail E. Rojas, and Paul G. Seybold. "Solvent dependence of the fluorescence lifetimes of xanthene dyes." Photochemistry and Photobiology 70, no. 5 (1999): 737-744.

[116]Perumal Sakthivel, Karuppannan Sekar, Gandhi Sivaraman, and Subramanian Singaravadivel. "Rhodamine diaminomaleonitrile conjugate as a novel colorimetric fluorescent sensor for recognition of Cd 2+ ion." Journal of fluorescence 27, no. 3 (2017): 1109-1115

[117] Jaemyeng Jeong, Boddu Ananda Rao, and Young-A. Son. "Dual sensing performance of a rhodamine-derived scaffold for the determination of Cu2+ and Ce4+ in aqueous media." Sensors and Actuators B: Chemical 220 (2015): 1254-1265.

[118] Kavirayani. Priyadarsini, "The chemistry of curcumin: from extraction to therapeutic agent." Molecules 19, no. 12 (2014): 20091-20112.

[119] Pil Hun. Bong, "Spectral and photophysical behaviors of curcumin and curcuminoids." Bulletin of the Korean Chemical Society 21, no. 1 (2000): 81-86.

[120] Hee-Je Kim, Dong-Jo Kim, S. N. Karthick, K. V. Hemalatha, C. Justin Raj, Sunseong Ok, and Youngson Choe. "Curcumin dye extracted from Curcuma longa L. used as sensitizers for efficient dye-sensitized solar cells." International Journal of electrochemical science 8, no. 6 (2013): 8320-8328

[121] Yuval Erez, Itay Presiado, Rinat Gepshtein, and Dan Huppert. "Temperature dependence of the fluorescence properties of curcumin." The Journal of Physical Chemistry A 115, no. 40 (2011): 10962-10971.

[122] Ying-Jan Wang, Min-Hsiung Pan, Ann-Lii Cheng, Liang-In Lin, Yuan-Soon Ho, Chang-Yao Hsieh, and Jen-Kun Lin. "Stability of curcumin in buffer solutions and characterization of its degradation products." Journal of pharmaceutical and biomedical analysis 15, no. 12 (1997): 1867-1876.

Chapter 2

Coumarin 540A - Rhodamine 6G dye mixture for FRET based fluoride detection

The chapter describes the strong and sensitive response of the organic dye Rh6G towards fluoride in organic media. The increase in the dynamic range of fluoride detection of the C540A-Rh6G FRET pair when compared to Rh6G is discussed. The fabrication of a simple C540A dye doped PMMA coated hollow glass capillary for the detection of fluoride and its sensing response under laser and UV LED excitation are also discussed. The effects of coating thickness and doping concentration of C540A on the fluorescence emission from the capillary and the resulting change in optical response of the capillary towards fluoride are described in detail.

2.1 Introduction

Organic dyes like Rhodamine 6G (Rh6G) and Coumarin 540a (C540A) find a number of applications as fluorescent labels, gain media for laser action and optical probes or sensors [1-3]. High sensitivity, selectivity, possibility of monitoring both the intensity and wavelength of emission are some of the advantages of fluorescence based detection techniques [4, 5]. The use of organic dyes for fluorescence based sensing applications would enable the realization of simple, highly sensitive and low cost sensing systems. Forster resonance energy transfer (FRET) phenomena between the donor and the acceptor depends on a variety of factors including the refractive index of the environment, the distance between donor-acceptor pair, their relative dipole angular orientation and their optical properties [6]. Consequently, the FRET based detection scheme boasts of high sensitivity and accuracy of detection. It offers a range of options viz. measurement of both donor and acceptor fluorescence intensities, peak emission wavelengths and ratio of intensities to accomplish sensing [4, 7].

The present chapter describes the fluoride sensing mechanism of Rh6G in an organic medium. The use of C540A-Rh6G FRET pair to extend the range of detection is also described. The use of different concentrations of dye mixtures and their corresponding sensing responses are described in detail. A simple system consisting of C540A doped PMMA, coated on hollow glass capillary for the detection of tetrabutylammonium fluoride (TBAF) in the presence of Rh6G is also described. The tailoring of fluorescence emission from the capillary by changing the concentrations of C540A dye as well as by increasing the number of layers of coating is also discussed.

2.2 Experimental methods

The solutions of both Rh6G (Acros Organic) and C540A (Exciton) dyes in acetonitrile (CH_3CN) were prepared with concentrations in the range of 10^{-6}, 10^{-5} and 10^{-4} M. The solutions with dye mixture were prepared by diluting appropriate volumes of stock solutions of Rh6G and C540A. The stock solutions of anions in acetonitrile were prepared by dissolving the tetrabutylammonium (TBA) salts. The required volumes of the anion stock solutions were added to individual dye solutions or dye mixture solutions for the analysis. The absorption and fluorescence spectra were recorded using Jasco V-570 spectrophotometer and Cary Eclipse (Varian) fluorescence spectrometer respectively. The excitation and emission slit width for recording fluorescence was fixed at 2.5 nm.

Fourier transform infrared (FTIR) spectrum was recorded using Jasco 4100 spectrometer in the 400-4000 cm^{-1} range using the KBr pellet method. The samples of Rh6G in acetonitrile with and without fluoride were dropped onto KBr pellet and left to dry before recording the spectrum.

Horiba (Jobin Yvon) DeltaPro time correlated single photon counting (TCSPC) lifetime measurement system was used to record the fluorescence decay curves of the dye samples. The excitation source was a NanoLED (N-370) with peak emission wavelength of 370±10 nm and pulse duration of 1.4 ns. A long pass filter (500 nm) was used to separate the fluorescence emission of the samples from the excitation wavelength. Horiba DAS6 decay analysis software was used to fit the decay curves and to calculate the lifetime values using the method of least squares.

2.3 Results and Discussion

2.3.1   Rh6G for fluoride detection

Rh6G solution exhibits a strong response towards TBAF leading to a drastic change in colour from pink to dull brownish orange (Fig.2.1) especially in the presence of high concentration TBAF. Along with the colorimetric changes, there is a decrease in peak absorption intensity along with a blue shift of the absorption peak from 525 nm to around 480 nm as shown in Fig. 2.2 a. The peak fluorescence intensity of Rh6G around 550 nm also decreases with increase in TBAF concentration as shown in Fig. 2.2 b.

In the case of un-esterified rhodamines like Rhodamine B, the increase in pH of solution can lead to a change in the structure of the molecule into the zwitterionic form and cause a blue shift (<10 nm) of absorption and fluorescence spectra. But Rh6G has an esterified structure and hence the change in basicity of the solution induced by TBAF would not lead to changes in the structure. The zwitterion form undergoes reversible changes to the lactone form leading to a single absorption peak in the ultra-violet (UV) region [8-10]. Therefore, the colorimetric and spectral changes observed in Rh6G could be due to the deprotonation of the amide group of Rh6G [11].

Figure 2.1 Colour changes of Rh6G in CH_3CN in the presence of 2×10^{-4} M anions (from left to right: Nil, TBAC, TBAB, TBAI, TBAN, TBAS, TBAP, TBAA, TBAF added to Rh6G in CH_3CN with C-Chloride, B-Bromide, I-Iodide, N-Nitrate, S-Hydrogen sulphate, P-Di-hydrogen phosphate, A-Acetate, F-Fluoride)
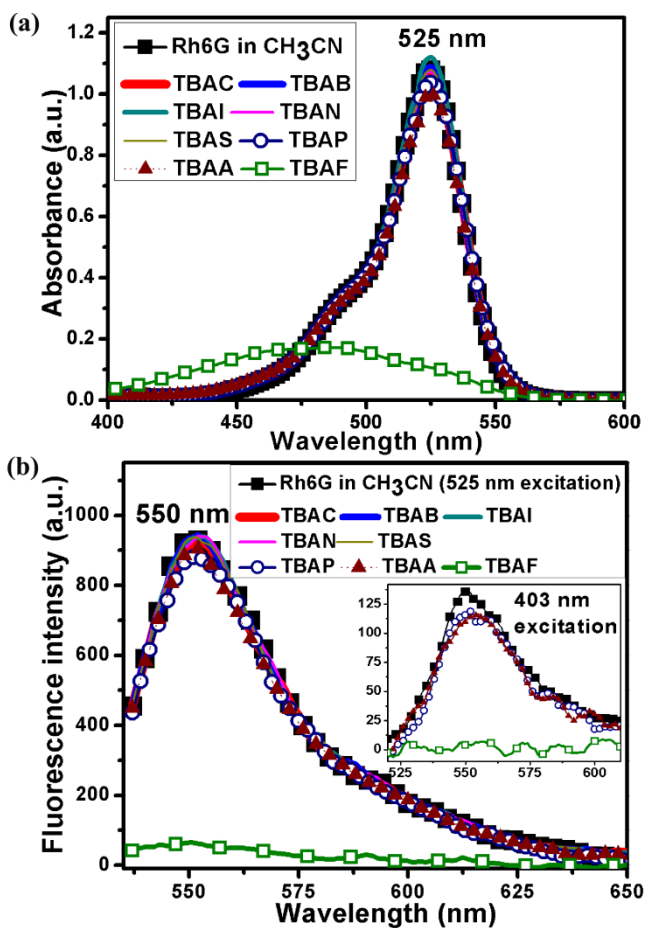
Figure 2.2 Variation in (a) absorbance and (b) fluorescence of Rh6G in CH_3CN in the presence of 2×10^{-4} M anions. Inset of Fig. 2.2b shows the fluorescence of Rh6G in the presence of TBAP, TBAA and TBAF with 403 nm excitation

The variation in the normalized peak absorbance and peak fluorescence of Rh6G in the presence of varying TBAF is as shown in Fig. 2.3a. The peak intensity values of the samples are normalized with respect to the intensity values of the reference Rh6G sample containing no fluoride. It can be observed that there is a fast decrease of fluorescence upon TBAF addition. There is also fluorescence decrease with increase in TBAF under 405 nm and 365 nm excitation wavelengths, though the fluorescence level is very low as shown in Fig. 2.3b.
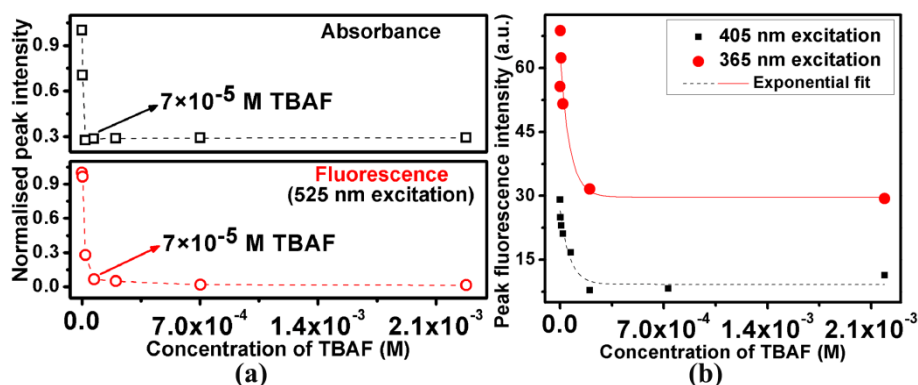
Figure 2.3 (a) Variation in the normalised peak absorbance and peak fluorescence intensity of Rh6G with increasing TBAF (b) Decrease in peak fluorescence intensity of Rh6G with increase in TBAF under 405 nm and 365 nm excitation
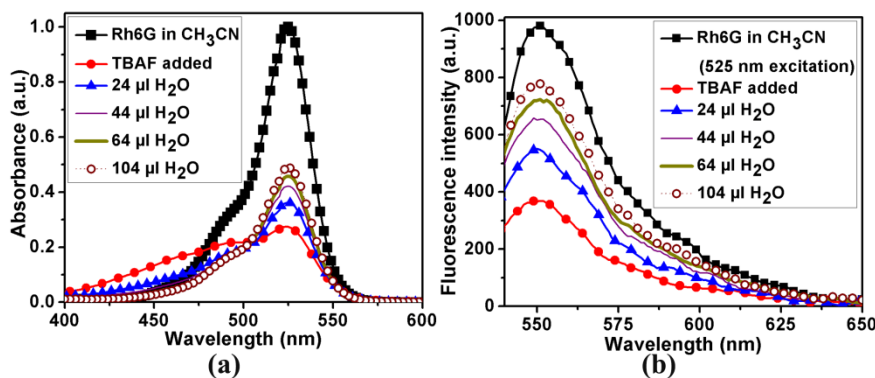
Figure 2.4 Recovery of (a) absorbance and (b) fluorescence peak intensities of Rh6G in CH$_3$CN in the presence of high concentration TBAF upon addition of water

The presence of hydrogen bonding in an interaction between molecules can be studied by the addition of protic solvents like water (H$_2$O), ethanol, methanol etc. It was observed that on addition of even micro-liter volumes of water, the initial value of absorption intensity of Rh6G which had decreased upon addition of high concentration TBAF tends to

increase. The fluorescence intensity which decreased in the presence of fluoride was also found to increase gradually towards the initial value in the presence of water as shown in Fig. 2.4. The colour of solution was also changed back to pink upon addition of the protic solvent. These changes could be due to the disruption of the bond between Rh6G and TBAF.

The structural change of Rh6G on addition of TBAF was confirmed using FTIR spectroscopy. The FTIR spectrum of Rh6G is as shown in Fig. 2.5. There is a clear increase in transmittance in 3431 cm^{-1} band (N-H stretching of Rh6G) pointing to the quantitative conversion of amide group of Rh6G to the deprotonated form [12].
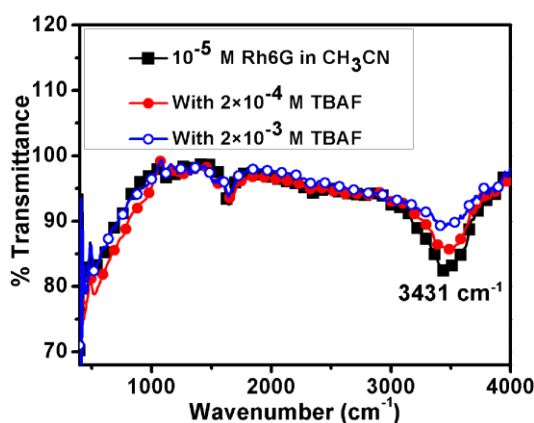
Figure 2.5 Changes in FTIR spectrum of Rh6G in the presence of high concentration TBAF

2.3.2   C540A-Rh6G FRET donor-acceptor pair for fluoride detection

Rh6G dye was found to be sensitive for the detection of fluoride especially in the lower concentration range. But the fast and drastic change of absorbance and fluorescence of Rh6G would limit its use in the higher concentration range. Hence, the mixture of C540A-Rh6G FRET pair was investigated for the detection of fluoride. FRET depends on the concentrations of donor and acceptor molecules, distance between them, the relative dipole angular momentum, the spectral overlap between them and the refractive index of the solvent [6, 13]. The absorption and fluorescence peak of 10^{-5} M C540A was found to be around 420 nm and 513 nm respectively. From Fig. 2.6a it is clear that there is huge spectral overlap of the acceptor Rh6G absorption with the donor C540A fluorescence emission. The fluorescence of donor C540A was quenched whereas the fluorescence of the acceptor Rh6G was increased (Fig. 2.6b), indicating the FRET interaction between the dyes. It was also observed that Rh6G had negligible fluorescence when excited with the donor absorption

wavelength. Similarly C540A had negligible fluorescence when excited with the acceptor absorption wavelength.
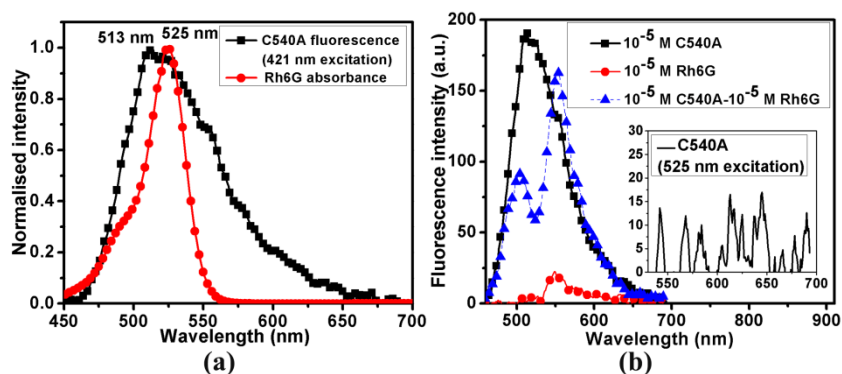
Figure 2.6 (a) Overlap of fluorescence of 10^{-5} M C540A with the absorbance of 10^{-5} M Rh6G (b) Quenching of donor C540A fluorescence in the presence of Rh6G acceptor (421 nm excitation). Inset of Fig 2.6b shows the low values of fluorescence of C540A donor when excited with acceptor absorption wavelength (525 nm)

C540A dye does not respond to fluoride and this is illustrated in Fig. 2.7. There is no change in the absorbance and fluorescence of C540A in the presence of even high concentration TBAF. Hence by using the C540A-Rh6G FRET pair, the change in absorption and fluorescence characteristics of both dyes can be studied as a function of TBAF concentration. The changes in optical properties can be brought about by changes in the FRET interaction between the dyes, even though only one of the dyes directly interacts with TBAF.
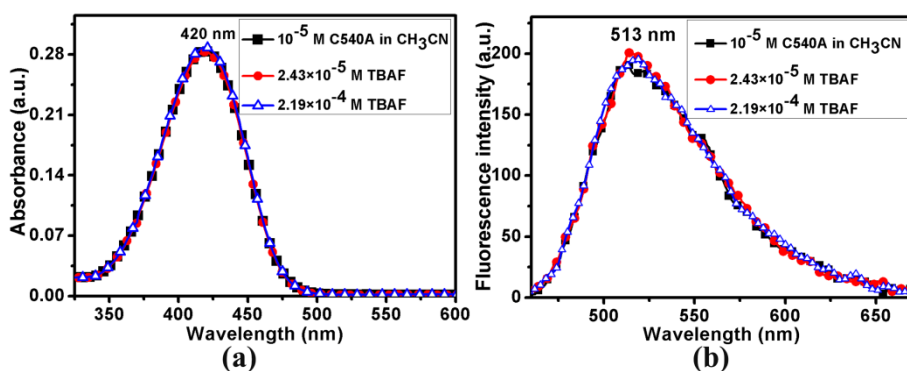
Figure 2.7 (a) Absorbance and (b) fluorescence of C540A in CH_3CN in the presence of TBAF

Since FRET efficiency depends on concentration [6, 13], two different combinations of the dye concentrations were initially studied namely 10^{-5} M C540A-10^{-5} M Rh6G and 10^{-4} M C540A-10^{-5} M Rh6G. A higher donor to acceptor ratio can increase FRET efficiency when the donor lifetime is appreciably higher than acceptor lifetime [14, 15]. The FRET efficiency E is described by the equation [13]:

$$E = 1 - \frac{I_{DA}}{I_D}$$
-(2.1)

where I_{DA} and I_D are respectively the fluorescence intensities of the donor in the presence and absence of the acceptor. The FRET efficiency for 10^{-5} M C540A-10^{-5} M Rh6G and 10^{-4} M C540A-10^{-5} M Rh6G were calculated to be 0.52 and 0.44 respectively.

FRET phenomena can also be studied using the lifetimes of the donor, acceptor and the donor-acceptor system. The fluorescence decay of the acceptor, the dye mixture pair and that of the pair in the presence of TBAF are as shown in Fig. 2.8. The donor lifetime is expected to decrease while the lifetime of sensitized emission of the acceptor is expected to increase [14]. Many factors need to be considered to estimate the lifetime changes in the donor-acceptor system. The observation of decrease in donor lifetime is very difficult due to longer lifetime of unquenched donor emission which would also be present along with the FRET component [16]. The excitation energy transfer due to donor-donor interaction [17] is not expected to take place in the present C540A-Rh6G system owing to the negligible spectral overlap of C540A absorption and fluorescence when compared to the C540A fluorescence-Rh6G absorption spectral overlap. Since the possibility of direct excitation of acceptor would be negligible, emission of fluorescence from Rh6G acceptor when excited with 370 nm would also be very small.

The fluorescence decay of C540A was found to be single exponential in nature with a lifetime of 5.68 ns, in agreement with the value reported in literature [18]. The lifetime of Rh6G was also single exponential with a value of 5.36 ns. Considering the above mentioned factors and the fact that the lifetime values of both the dyes are comparable, the time resolved fluorescence decay of the dye mixture pair can be fitted as bi-exponential. The C540A-Rh6G dye mixture system exhibited lifetime values of 3.28 ns and 6.17 ns with pre-exponential factors -0.13 × 10^{-2} (-1.39 relative amplitude) and 4.9 × 10^{-2} (101.39 relative amplitude) respectively. The presence of negative pre-exponential factors can be attributed to the energy transfer process [16, 19]. The lifetime values of the system changed to 4.88 ns

and 6.18 ns with pre-exponential factors of 2.85×10^{-2} (50.66 relative amplitude) and 2.19×10^{-2} (49.34 relative amplitude) respectively in the presence of TBAF. The presence of positive pre-exponential factors could be due to the disruption of efficient FRET between C540A and Rh6G in the presence of high concentration TBAF.
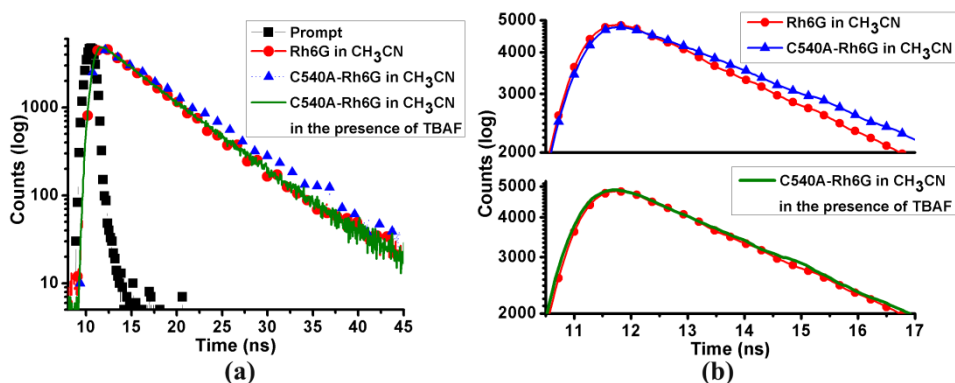
Figure 2.8 (a) Changes in the lifetime of C540A-Rh6G dye mixture pair in comparison to Rh6G alone (b) Expanded views of graphs in (a)
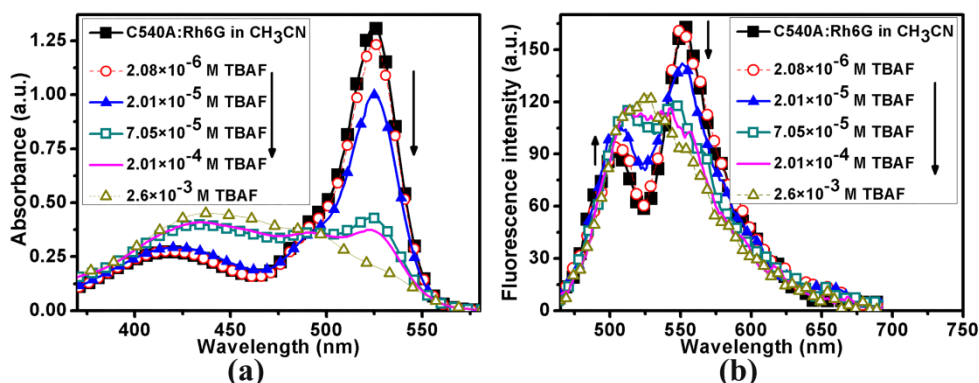
Figure 2.9 (a) Decrease in peak absorbance and (b) variation in fluorescence of the 10^{-5} M C540A - 10^{-5} M Rh6G dye mixture in CH_3CN with increasing TBAF concentration

Figure 2.9 shows the variation in absorption and fluorescence of the dye mixture in the presence of increasing TBAF concentration. Two peaks of absorption corresponding to C540A (420 nm) and Rh6G (525 nm) were observed in the spectrum. The peak absorption in Rh6G absorption range decreases with increase in TBAF as described above. But there is an apparent increase in absorption in the 440-480 nm range. This could be the combined absorption of C540A which does not react with TBAF and the de-protonated form of Rh6G. The fluorescence spectrum clearly shows a decrease in Rh6G fluorescence and a

corresponding increase in C540A fluorescence with increase in TBAF. The increase in TBAF and the subsequent conversion of Rh6G to its de-protonated form lead to reduced spectral overlap between the two dyes and hence a reduction in the FRET efficiency. This leads to the recovery of fluorescence of C540A dye molecules in the presence of TBAF.

The effect of addition of water to the dye mixture also gave similar results as that in the case of Rh6G alone. There was a retrace of the absorption and fluorescence spectra of the dye mixture containing TBAF upon addition of water. The decrease in FRET efficiency and the consequent increase in donor emission were observed only in the case of TBAF and not in the case of other anions as shown in Fig. 2.10 indicating the high selectivity of the dye mixture pair towards TBAF detection.
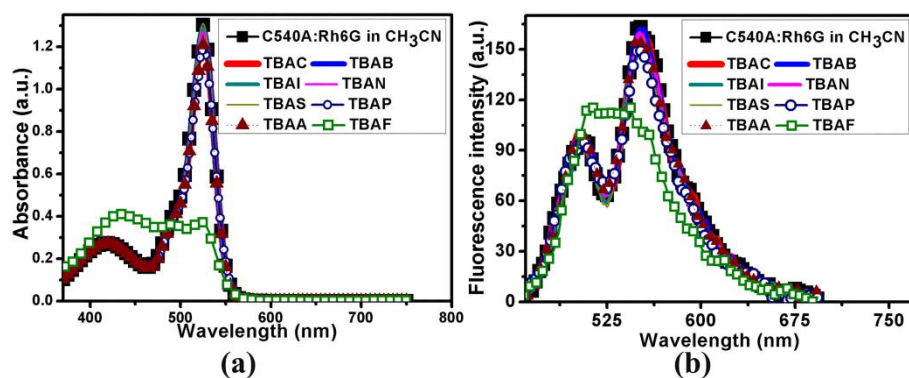
Figure 2.10 Selectivity of C540A-Rh6G in CH$_3$CN towards TBAF as evidenced from the (a) absorbance and (b) fluorescence of the dye mixture pair

The change in normalized peak fluorescence intensity as well as peak fluorescence intensity of the Rh6G dye alone and C540A-Rh6G pair were compared (Fig. 2.11a). It was found that the response of both the dye alone and dye mixture was linear in the 0-7×10^{-6} M range. Also, while there was almost an enhancement of peak fluorescence by a factor of 7 (Fig. 2.11b) in the case of dye mixture, Rh6G alone was very sensitive towards TBAF detection as is evident from the fast decrease in normalized intensity even in the acceptable concentration range of TBAF (< 2×10^{-5} M). C540A-Rh6G dye pair on the other hand, exhibits a gradual decrease and hence would be able to detect higher TBAF concentrations more effectively than Rh6G alone.

The limit of detection (LOD) was estimated using the method described in literature [20]. In this method, the LOD is estimated as that particular value of analyte (TBAF) which when added to the sensing agent (dye or dye mixture) gives a signal (peak fluorescence)

that is thrice the value of the error (standard deviation) added (or subtracted) to the signal of blank sample. Using this method, the LOD of TBAF using both Rh6G alone and C540-Rh6G dye mixture can be approximated to be 3×10^{-6} M (0.78 ppm TBAF). Hence the LOD using C540A-Rh6G is not only comparable to that using the single dye Rh6G, but the pair also has the added advantage of having a higher dynamic range of detection compared to Rh6G alone.
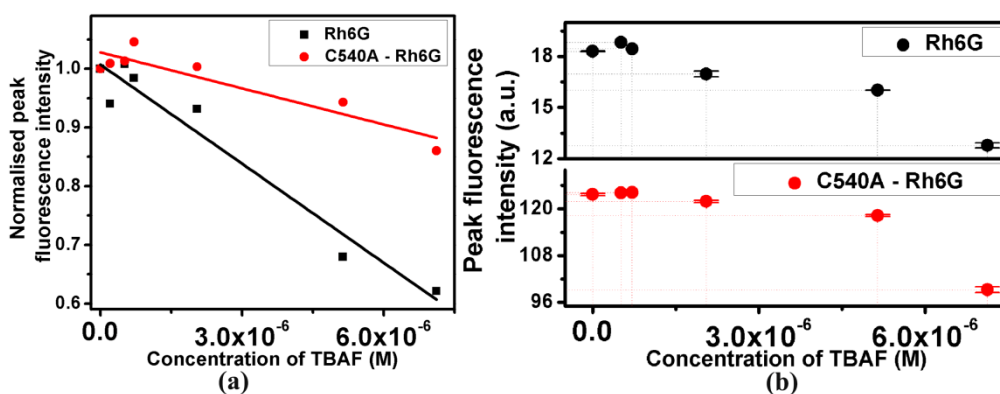
Figure 2.11 (a) Comparison of normalized peak fluorescence intensity of Rh6G with that of C540A-Rh6G FRET pair (b) Peak fluorescence intensity variation of Rh6G and C540-Rh6G in CH$_3$CN in the presence of lower TBAF concentration (0-7×10^{-6} M). Standard deviation was plotted as the error bar for each concentration

The variation in donor and acceptor absorption as well as fluorescence with increase in TBAF concentration for two different dye mixture pairs 10^{-5} M C540A-10^{-5} M Rh6G (denoted as A) and 10^{-4} M C540A-10^{-5} M Rh6G (denoted as B) are as shown in figures 2.12 and 2.13. The peak absorption and fluorescence wavelengths of 10^{-4} M C540A in acetonitrile are 417 nm and 516 nm respectively. As expected there was a decrease in the acceptor absorption. But there was a slight increase in absorption in the region of donor absorption (420 nm for A and 417 nm for B). This could be owing to the overlap of the C540A absorption spectrum with that of the Rh6G de-protonated form.

Similarly, a decrease in acceptor fluorescence intensity was observed with increase in TBAF for both the dye mixture pairs. But the level of donor and acceptor fluorescence intensity in case B was found to be higher than that of case A. This could be due to the inherent higher fluorescence intensity of 10^{-4} M C540A dye molecules.
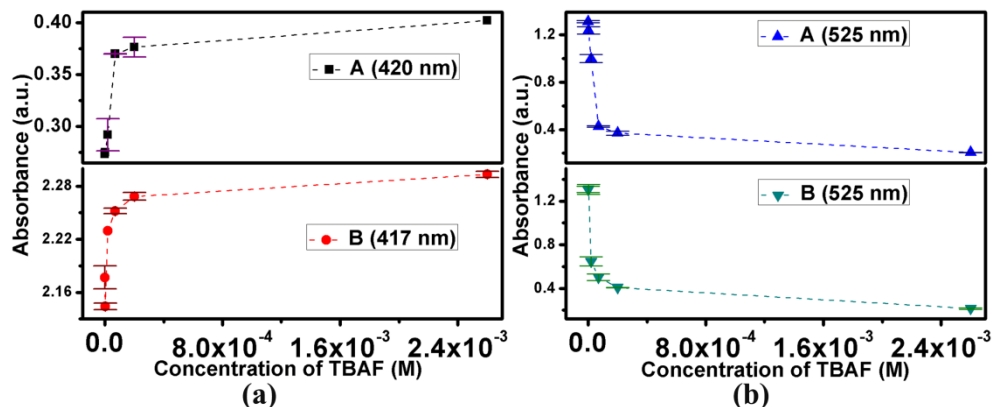
Figure 2.12 Variation in the (a) donor C540A and (b) acceptor Rh6G absorbance values in the dye mixture pairs in the presence of varying TBAF. A = 10^{-5} M C540A:10^{-5} M Rh6G and B = 10^{-4} M C540A:10^{-5} M Rh6G
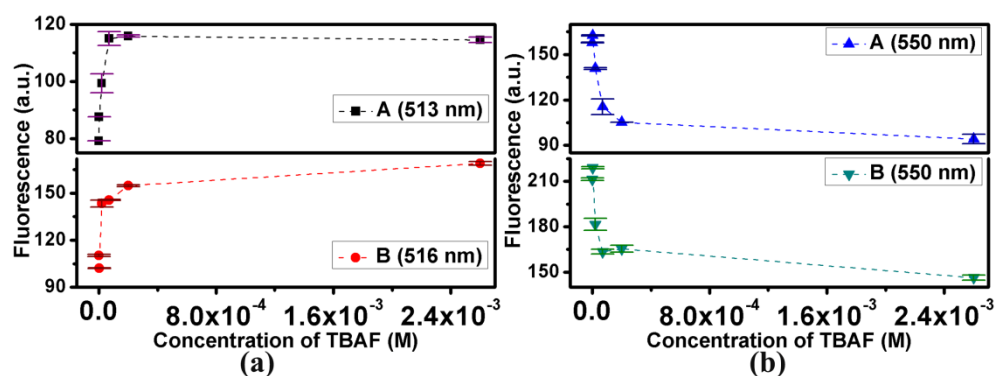
Figure 2.13 Variation in the (a) donor C540A and (b) acceptor Rh6G fluorescence values in the dye mixtures in the presence of varying TBAF. A = 10^{-5} M C540A:10^{-5} M Rh6G and B = 10^{-4} M C540A:10^{-5} M Rh6G

The variation in peak absorbance and fluorescence wavelength with TBAF concentration in the region of donor absorption and emission is as shown in Fig. 2.14. As there was a huge overlap of absorption spectrum of deprotonated Rh6G (blue shifted peak) with C540A absorption, there was a red shift of peak absorption wavelength in the donor absorption region with increase in TBAF (Fig. 2.14a). This apparent red shift of donor region peak absorption wavelength was not readily observable in the dye mixture pair with 10^{-4} M C540A (case B) because of the donor's much higher absorption when compared to that of deprotonated Rh6G. The peak fluorescence wavelengths in the case of both the dye mixtures show a red shift with increase in TBAF. This is due to the gradual recovery of

the fluorescence spectra of C540A caused by the reduced FRET efficiency between the C540A donor and Rh6G acceptor in the presence of TBAF.
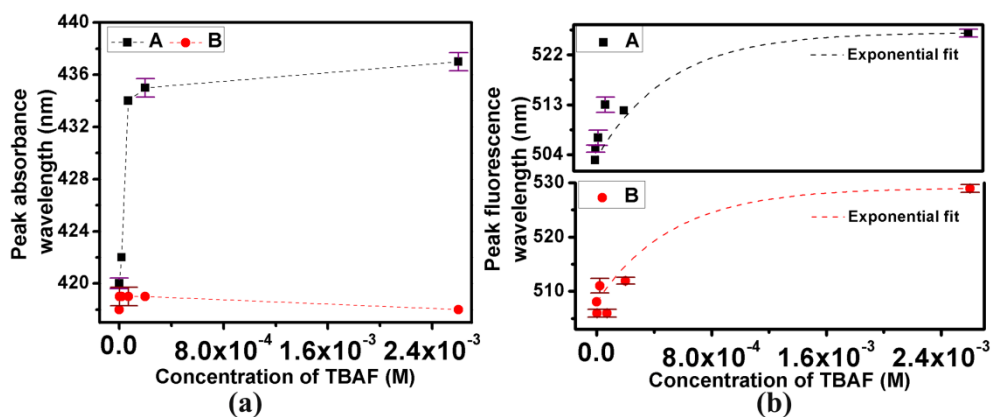
Figure 2.14 (a) Peak absorbance and (b) peak fluorescence wavelength shift of donor C540A in the dye mixture. A = 10^{-5} M C540A:10^{-5} M Rh6G and B = 10^{-4} M C540A:10^{-5} M Rh6G

C540A has very broad fluorescence spectrum and the recovery of fluorescence of C540A in the presence of high TBAF concentration can alter the recorded values of Rh6G acceptor fluorescence. So, recording the acceptor fluorescence alone would not be reliable as there could be donor fluorescence in the acceptor channel. But donor emission intensity and wavelength can very well be used to study the FRET phenomena as changes in FRET efficiency will cause changes in donor emission. Moreover, the FRET efficiency calculated using the quenching of donor fluorescence is more accurate than monitoring the acceptor fluorescence [14].

A slightly modified dye mixture pair involving a higher donor concentration and a lower acceptor concentration was prepared to test the sensitivity of FRET towards TBAF. The fluorescence decrease in this dye mixture pair when excited with acceptor absorption wavelength as well the variation in FRET efficiency E of the same pair when excited with the donor absorption wavelength is as shown in Fig. 2.15. It can be seen that as described in earlier sections of the chapter, there is a rapid fluorescence decay of the acceptor in the presence of TBAF (Fig. 2.15a). The FRET efficiency on the other hand shows a gradual decrease with increase in TBAF (Fig. 2.15b). Hence it can be said that the lower concentrations may be detected using the fluorescence of the acceptor alone but both the lower and higher TBAF concentrations can be detected using the FRET efficiency. Hence multiple parameters like peak intensity, peak wavelength of absorption and fluorescence of

donor as well as acceptor and the FRET efficiencies can be used to detect TBAF over a broad range.
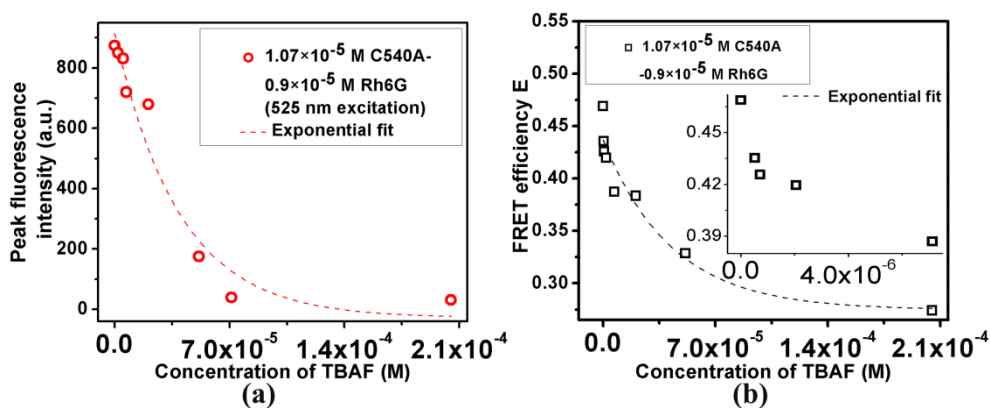
Figure 2.15 (a) Variation in peak fluorescence intensity of C540A-Rh6G when excited at peak absorption wavelength (525 nm) of the Rh6G acceptor (b) Variation in FRET efficiency of the same pair with increase in TBAF concentration. Inset of figure 2.15b shows the expanded view of the lower TBAF concentration

The variation of FRET efficiency E with increase in TBAF in the case of 10^{-5} M C540A-10^{-5} M Rh6G and 10^{-4} M C540A-10^{-5} M Rh6G is as shown in Fig. 2.16. The pair with higher donor (C540A) concentration exhibited lower values of FRET efficiency. This could be owing to the presence of large amount of un-quenched donor emission along with the sensitized emission of the acceptor [14, 15]. But this FRET pair too showed comparable resolution in values of E when compared to the lower donor concentration FRET pair and hence can also be used to detect TBAF. Fig. 2.16b shows the variation in FRET efficiency in the case of a FRET pair with lower donor C540A concentration and higher acceptor Rh6G concentration. The FRET efficiency is reported to increase in this condition as the probability of the donor emission to transfer energy to the acceptor is very high compared to the donor emitting the energy as fluorescence. Also, the competition of multiple donors to transfer energy to a single acceptor is absent when the acceptor concentration is higher than that of the donor [13]. The fluorescence level decreases rapidly with increase in fluoride as in the earlier cases (Fig. 2.16b inset). The value of efficiency was found to slightly increase in this case when compared to other dye pairs described in the chapter. Here too it was observed that there is a considerable decrease in the value of efficiency with increase in TBAF.
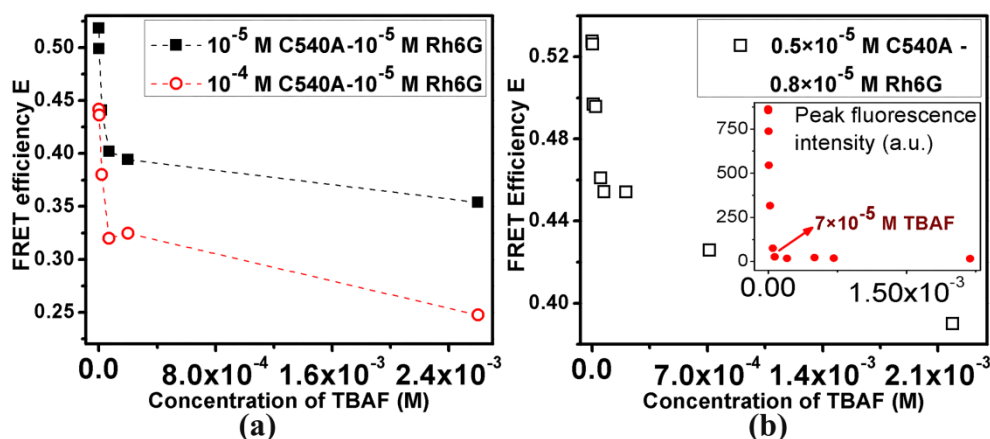
Figure 2.16 (a) Variation in FRET efficiency with increase in TBAF concentration for different C540A donor concentration in C540A-Rh6G FRET pairs (b) FRET efficiency variation in the case of a lower donor-higher acceptor concentration. Inset of Fig 2.16b shows the variation in peak fluorescence intensity of this FRET pair when excited at 525 nm

2.4 Hollow glass capillary based sensor set up for fluoride detection

Hollow glass capillaries coated with an internal layer of dielectric film or polymer film have been used to generate lasing action via random lasing or by the formation of whispering gallery modes [21, 22]. There have also been studies where a coating of quantum dots or dye doped polymer films inside the capillary hole can be used for sensing refractive index [23, 24]. In the present studies, the strong fluorescence emission from C540A dye doped polymer coating outside the hollow glass capillary is investigated as source of excitation for Rh6G solution inside capillary to enable detection of fluoride.

2.4.1 Preparation of C540A dye coated hollow glass capillary

C540A dye was directly doped into the solution of acetonitrile containing 20 % by weight PMMA granules (15,000 M. W, Himedia) [25]. A viscous solution was formed after stirring the mixture for about an hour using a magnetic stirrer. The capillary tubes of 1 mm diameter and 10 cm length were cleaned by rinsing repeatedly with water followed by isopropyl alcohol. A Teflon masking tape was used to mask around 1 cm of the capillary end that was to be dipped into the polymer solution, to ensure that there is no inner coating of polymer inside the hollow capillary. The cleaned capillaries were then dip coated at 0.95 mm/sec withdrawal rate to form a coating over a length of about 4 cm at one end of the

capillary tube on the outside as shown in Fig. 2.17a. A layer of C540A doped PMMA film was immediately formed upon withdrawal from the solution. Multiple layers were coated one above the other by immersion and dip coating the capillary repeatedly with 2 minutes drying time in between. C540A concentrations of 10^{-4} M, 10^{-3} M and 10^{-2} M were doped into PMMA and coated onto the capillary. About 0.3 ml was drop casted onto glass slides to form free standing C540A doped PMMA thick films as shown in Fig. 2.17c. The thickness of the drop casted PMMA and the capillary coating were estimated using a screw guage (0.001 mm resolution) with provision for read-out of diameters. The drop casted samples of un-doped PMMA, 10^{-4} M and 10^{-3} M C540A doped PMMA were about 0.4 mm thick whereas that of 10^{-2} M C540A doped PMMA was about 0.32 mm thick. The average thickness of the capillary coating increased with the number of layers and was found to be approximately around 0.03±0.013 mm, 0.12±0.04 mm and 0.35±0.15 mm respectively for two layer, five layer and ten layer coating.

2.4.2 Experimental set-up of capillary based sensor

The capillary was mounted on a holder and the light from a 100 mW 403 nm (Vortran Stradus) laser was focused onto the coated section as a 3 cm stripe using a plano-convex lens and cylindrical lens (Fig. 2.17b). The coating on the capillary was also excited with a single 368 nm UV LED (Epistar) by directly exposing it to the coating without using any coupling optics. The samples of Rh6G containing varying amounts of TBAF were introduced into the capillary by capillary action. The emission from the capillary end was collected in a direction transverse to that of the incident light and the spectra were recorded using a fiber probe connected to the SpectraSuite HR 4000 Ocean Optics spectrometer (190-1100 nm, 0.3 nm resolution).

The fluorescence of the drop casted samples recorded by the fluorescence spectrometer is as shown in Fig. 2.18. There was a clear shift in fluorescence peak with increase in C540A concentration in the PMMA matrix. This could mean that the higher concentration (10^{-2} M) C540A doped PMMA coating on capillary can provide better excitation for fluorescence from Rh6G solution taken inside the capillary.
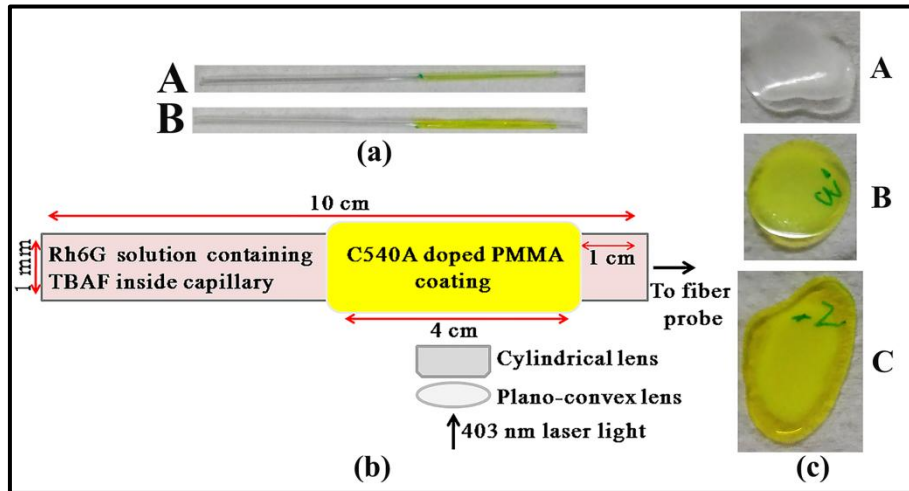
Figure 2.17 (a) Capillaries coated with C540A doped in PMMA, A = 5 layer coating with 10^{-3} M C540A, B = 10 layer coating with 10^{-2} M C540A (b) Schematic of the set-up for detection of fluoride using dye coated hollow glass capillary (c) Drop casted samples of (A) un-doped PMMA (B) 10^{-3} M C540A doped PMMA and (C) 10^{-2} M C540A doped PMMA
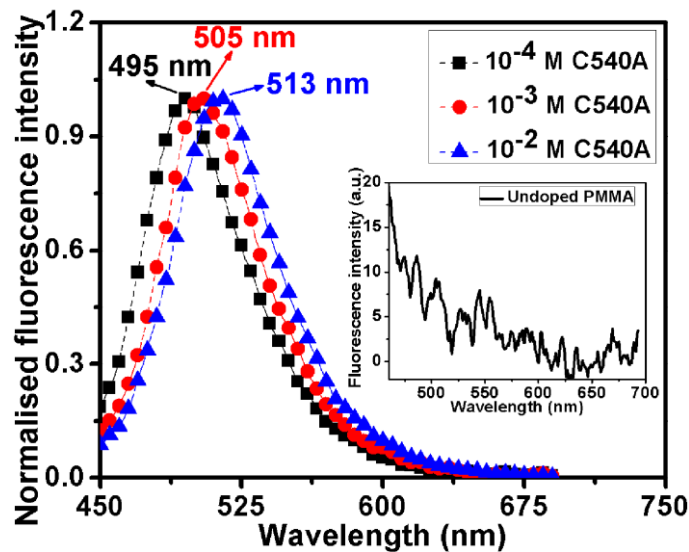
Figure 2.18 Normalised fluorescence intensity of drop casted samples of C540A doped PMMA with 405 nm excitation wavelength (excitation-emission slit width = 20 nm). Inset shows absence of fluorescence from un-doped PMMA.

2.4.3 Fluorescence from hollow glass capillary

The fluorescence emission from capillary upon different excitation conditions is as shown in Fig. 2.19. The emission in the case of an uncoated capillary when excited with 403 nm

laser wavelength (A) was found to be quite low whereas there was considerable emission in the case of 532 nm laser excitation (B) as depicted in the Fig. 2.19a. There was a strong fluorescence emission from the C540A coated PMMA capillaries upon excitation by both 403 nm laser and 368 nm UV LED. The emission (inside the capillary) visibly looked similar to that due to 532 nm laser excitation on the bare capillary. This would mean that even a simple UV LED source can be used to excite the fluorescence of Rh6G inside the capillary by using the requisite concentration of C540A in the PMMA coating.
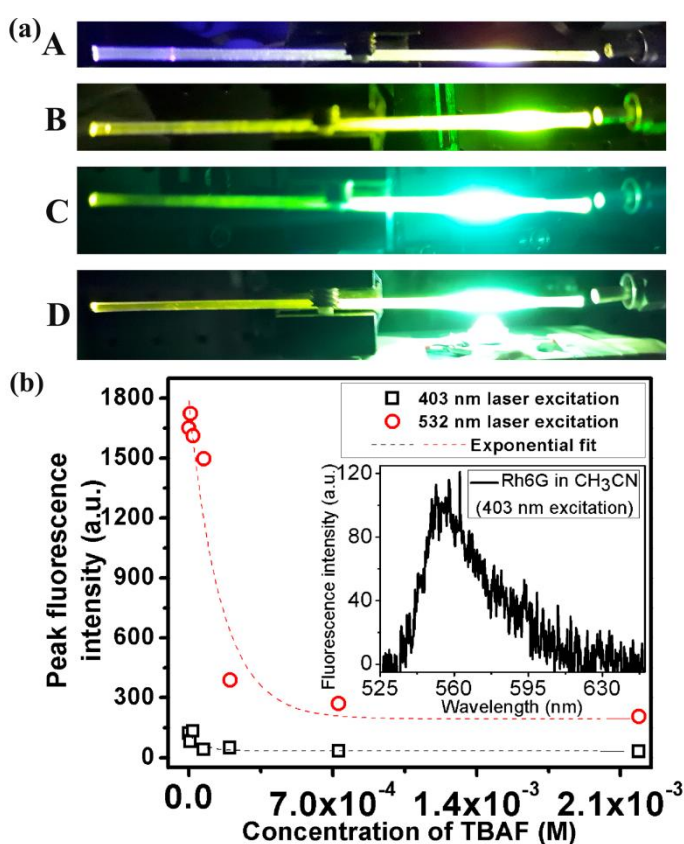
Figure 2.19 (a) Emission from capillaries containing Rh6G in CH_3CN with (A) Un-coated hollow glass capillary under 403 nm laser excitation (B) Un-coated hollow glass capillary under 532 nm laser excitation (C) C540A coated capillary under 403 nm excitation (D) C540A coated capillary under 368 nm UV-LED excitation (b) Variation of peak fluorescence intensity from un-coated capillary containing Rh6G in CH_3CN, under 403 nm and 532 nm laser excitation. Inset shows the low fluorescence recorded with 403 nm excitation.

The fluorescence peak intensities of the emissions recorded using an un-coated capillary under 403 nm and 532 nm laser excitations are as shown in Fig. 2.19b. The

emission using 403 nm was very less and it is difficult to distinguish between the different TBAF concentrations. The emission using 532 nm laser was considerably high, but there is a fast decrease in fluorescence recorded and it may be difficult to distinguish between individual high fluoride concentrations. Coating the capillary would enable the use of a different excitation wavelength than the absorption wavelength, the monitoring of two fluorescence wavelengths for detection and also allow the use of easily available low cost sources like LED's.

The fluorescence emitted from the capillary filled with Rh6G solution with an outside capillary coating of 10^{-2} M C540A doped PMMA for different thickness of coating is as shown in Fig. 2.20. The coating thickness for the two layer, five layer and ten layer were about 0.03±0.01 mm, 0.16±0.018 mm and 0.48±0.096 mm respectively. It was observed that there is an increase in emission with increase in coating thickness. Two peaks predominantly corresponding to C540A and Rh6G emission were observable in the emission spectrum from capillary and this emission spectrum can be divided into two regions viz. C540A region (< 525 nm) and Rh6G region (> 525 nm) as shown in the figure.
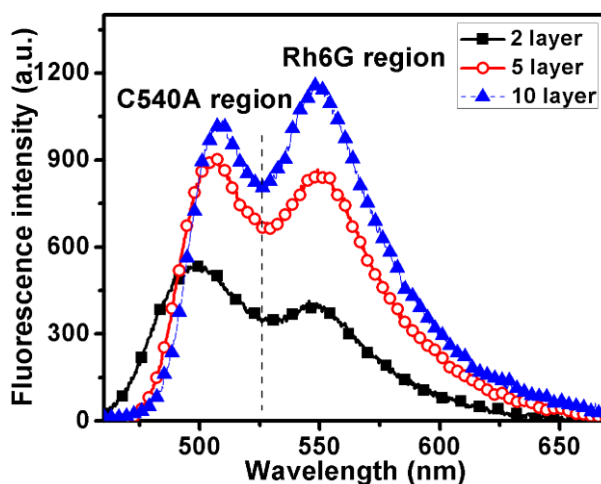
Figure 2.20 Fluorescence emission from capillary coated with 10^{-2} M C540A doped PMMA with different coating thickness and containing Rh6G in CH_3CN at 403 nm laser excitation. Two emission peaks corresponding to C540A and Rh6G are observed.

The coating with 10^{-4} M C540A doped PMMA gave only a feeble emission whereas the coating with 10^{-3} M and 10^{-2} M C540A doped PMMA coated capillaries gave significantly higher fluorescence emission. The fluorescence emission recorded from the capillary with different thickness of 10^{-2} M C540A in PMMA in response to TBAF is as shown in Fig. 2.21.

It can be seen that there is an increase in the fluorescence emission in C540A emission region and a decrease in the fluorescence emission in the Rh6G emission region. The decrease in Rh6G emission region was expected owing to the deprotonation of Rh6G. The fluorescence values for both the Rh6G and C540A emission were quite high for both the 5 layer and 10 layer capillary compared to the 2 layer coated capillary. The resolution between the readings was also found to be higher in these cases compared to the 2 layer coating. Therefore, coating thickness and the concentration of C540A in the coating can be tailored to get resolution in the fluorescence emission corresponding to different TBAF concentration, thereby increasing the sensitivity of detection.
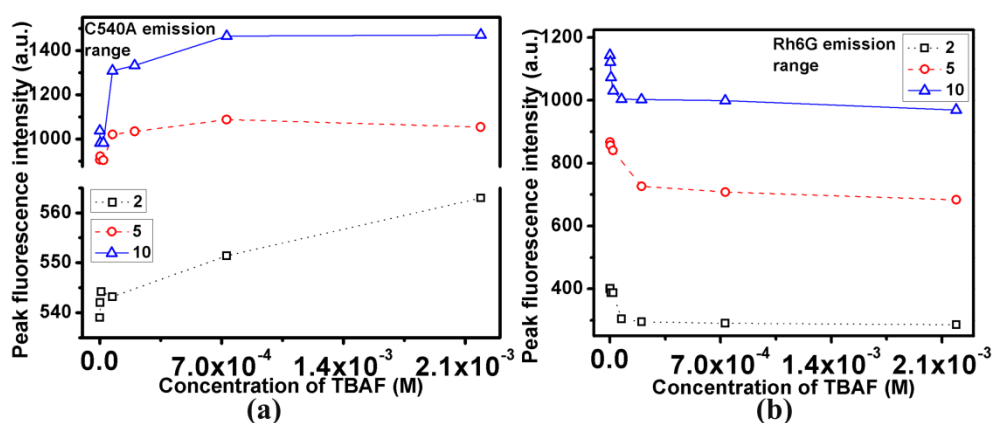
Figure 2.21 Fluorescence increase in the C540A emission range and corresponding fluorescence decrease in the Rh6G emission range from the 10^{-2} M C540A doped PMMA coated capillaries with different coating thickness in response to varying TBAF (Rh6G concentration in $CH_3CN = 1.2 \times 10^{-5}$ M)

The possible mechanism for detection is the excitation of fluorescence of Rh6G molecules in solution inside the capillary by the C540A molecules coated outside the capillary. C540A molecules emit fluorescence in all directions when laser or LED light is incident on the coated portion. A fraction of this emitted light is used to excite Rh6G molecules inside the capillary. Since the Rh6G absorption as well as fluorescence decreases with increase in TBAF, this affects the emission spectrum from the capillary too. This is especially discernible in the case of high TBAF concentration where there is a clear increase in emission from the C540A fluorescence with a corresponding decrease in Rh6G fluorescence. At high TBAF concentrations, most of Rh6G molecules would be in deprotonated form and would have lower absorption leading to only small fraction of

C540A emission used for excitation of fluorescence. Hence the optical interaction of the dyes without the dyes being in contact was enough to exhibit fluorescence changes that could be used for fluoride detection. The normalized values of peak fluorescence intensities with reference to the fluorescence intensities in the case of the blank sample (without TBAF) are as shown in Fig. 2.22. The normalized values point to the higher resolution of fluorescence values in the case of higher number of coatings (C540A range). It can also be observed that the Rh6G emission range can be used for lower concentration TBAF and C540A emission range for higher concentration TBAF in all cases.
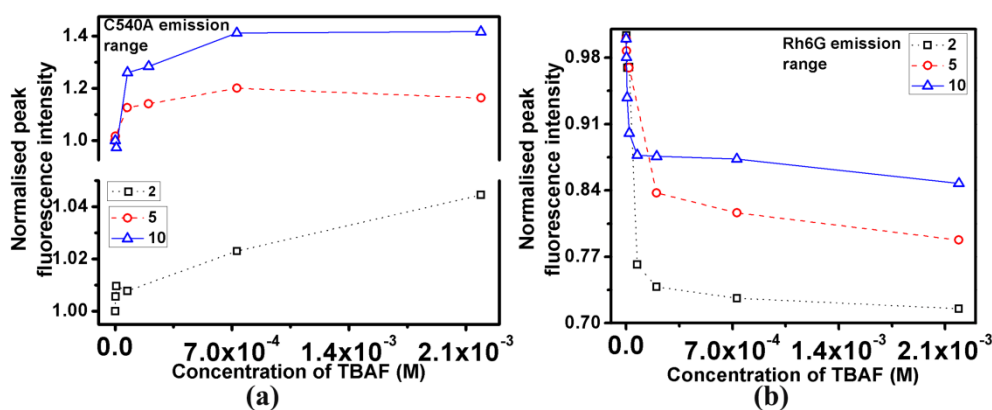
Figure 2.22 Variation in the normalized peak fluorescence intensity in the (a) C540A and (b) Rh6G emission regions in the 10^{-2} M C540A doped PMMA coated capillaries for different number of coating layers

Hence the emission regions of individual dyes can be used to detect different TBAF concentration i.e. Rh6G emission and C540A emission can individually be used to detect lower and higher TBAF concentrations respectively [25]. As in the case with C540A in solution, the broad fluorescence spectrum of C540A could overlap with the emission of the Rh6G molecules inside the capillary, especially at higher fluoride concentration. Therefore, the ratio of peak fluorescence intensities can be used to filter out the effect of overlap of C540A emission into the Rh6G emission region. Fig. 2.23a shows the variation in the ratio of the fluorescence emission in the C540A and Rh6G regions of capillary emission. It can be seen that there is an increase in the peak ratio values with increase in TBAF concentration as expected for all the cases. The peak ratio values are slightly lower for the 5 layer and 10 layer coated capillary, probably because of the extensive absorption of C540A radiation by the Rh6G molecules inside the capillary. Fig. 2.23b shows the observed red shift in peak

fluorescence wavelength in the C540A emission region for the different layer coated capillaries with increase in TBAF concentration. This further indicates the increase in C540A emission and the recovery of the broad nature of the C540A fluorescence when the concentration of TBAF is very high.
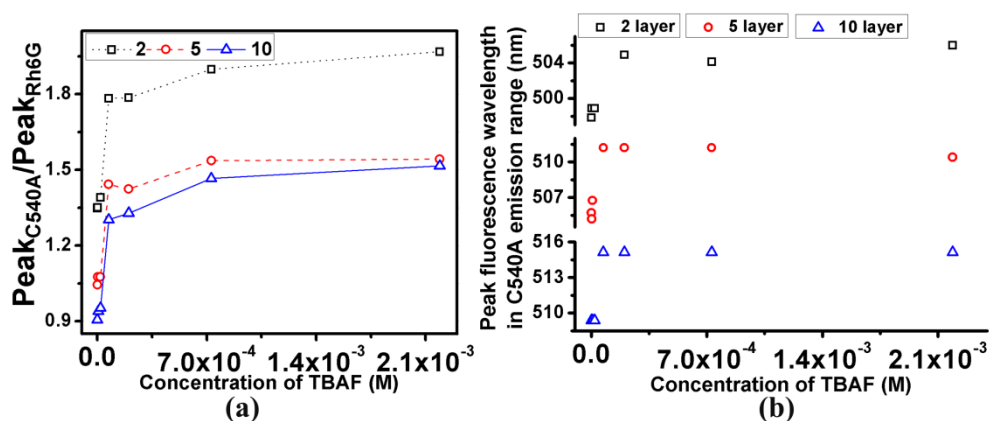
Figure 2.23 (a) Ratio of peak fluorescence intensities (Peak$_{C540A}$/Peak$_{Rh6G}$) for different number of coating layers of 10^{-2} M C540A doped PMMA coated capillaries with variation in TBAF concentration under 403 nm laser excitation (b) Red shift in peak fluorescence wavelength in the C540A emission region with increase in TBAF concentration

The use of a low cost LED for excitation of fluorescence would further increase the utility of the capillary system. A 368 nm UV LED was used to excite fluorescence from the capillary containing solutions of Rh6G. The variation in the normalized peak fluorescence intensities (Fig. 2.24) in this case reveal that a single UV LED can itself serve as an excellent source for fluorescence excitation. Here too there is a decrease in Rh6G fluorescence and a corresponding increase in the C540A emission.

The response of the 5 layer and 10 layer coated capillaries were found to be significantly better than the 2 layer coated capillary. The normalized peak fluorescence intensity values were also found to be considerably lower in the Rh6G emission region and this could be due to the lower concentration of Rh6G used in the solution when compared to the experiments with laser. The excellent resolution in this case could also be due to the dispersed excitation light of the LED which could easily illuminate a large area of the C540A coated section.
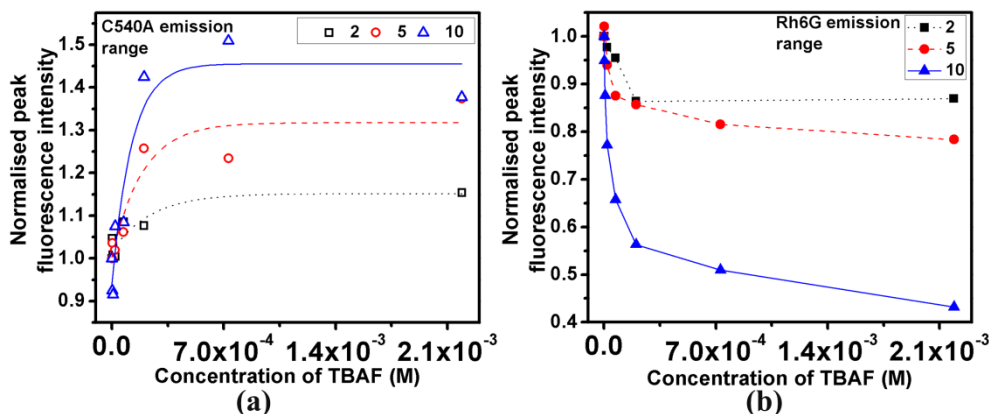
Figure 2.24 Variation in the normalized peak fluorescence intensity in the (a) C540A and (b) Rh6G emission regions in the 10^{-2} M C540A doped PMMA coated capillaries for different number of coating layers under 368 nm UV LED excitation (Rh6G concentration in CH_3CN = 0.92×10^{-5} M)
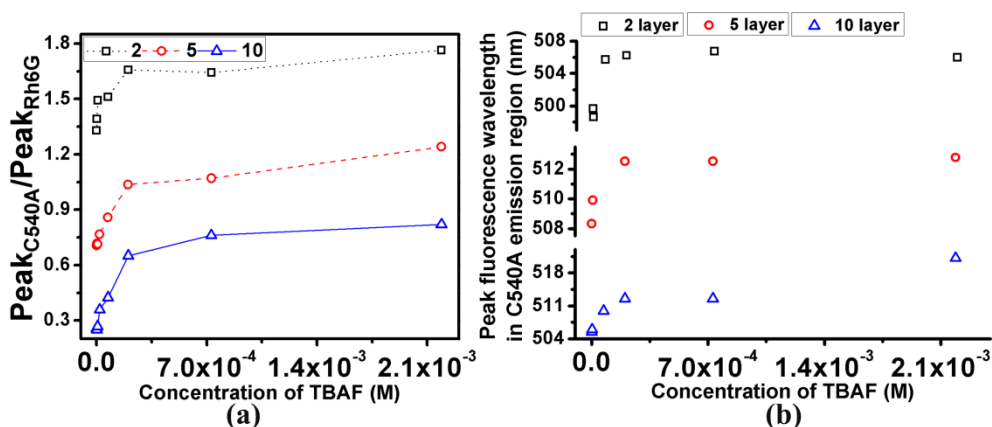
Figure 2.25 (a) Ratio of peak fluorescence intensities (Peak$_{C540A}$/Peak$_{Rh6G}$) for different number of coating layers of 10^{-2} M C540A doped PMMA coated capillaries with variation in TBAF concentration under 368 nm UV LED excitation (b) Red shift in peak fluorescence wavelength in the C540A emission region with increase in TBAF concentration

The plot of ratio of the peak fluorescence intensities as well as the peak fluorescence wavelength (Fig. 2.25) for UV LED excitation shows similar trend as that of laser excitation. The plots show the tendency of increase in C540A emission with TBAF. The red shift of peak fluorescence wavelength in the C540A emission region indicates that there is a recovery of fluorescence emission contribution from C540A.

The selectivity of the dye coated hollow glass capillary towards TBAF was studied using a 10^{-2} M and 10^{-3} M C540A doped PMMA (5 layer) coated capillary exposed to a

focused laser stripe of length 2 cm. The approximate coating thickness of the 10^{-2} M and 10^{-3} M C540A doped PMMA were 0.109 mm and 0.09 mm respectively. The fluorescence emissions recorded in these cases are as shown in Fig. 2.26. It was observed that in the case of Rh6G alone as well as in samples containing Rh6G with other common anions, the presence of both the peaks ascribed to Rh6G and C540A fluorescence were observed from the capillary. The addition of phosphate and acetate anions showed slight decrease in fluorescence in the region of Rh6G emission, but there was no increase in emission in the region of C540A fluorescence. It was also observed that in the presence of TBAF, there was only one dominant fluorescence peak in the spectrum near the region of C540A fluorescence emission. This suggests the possibility of distinguishing high concentration TBAF with just the number of peaks in the spectrum i.e one peak in the case of TBAF and two peaks for all other anions and the blank sample. The capillary based detection of TBAF is attractive as low cost sources and detectors can be used for detection. Also very small volume of samples is required for interrogation [25].
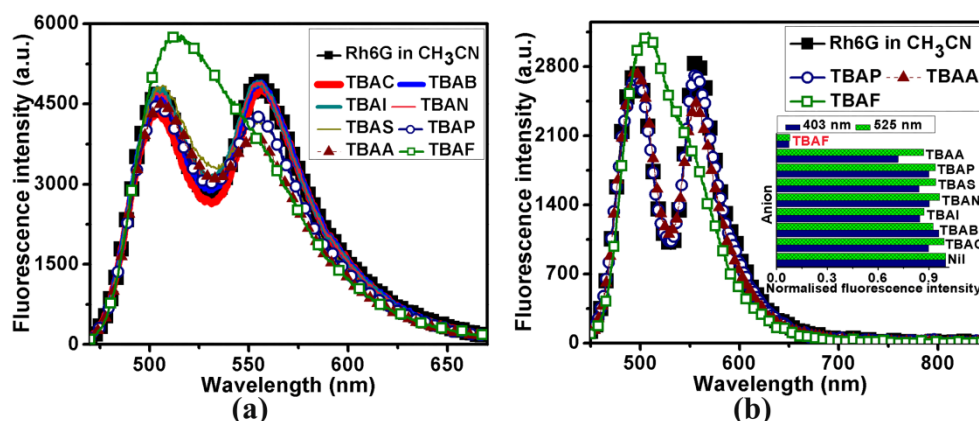
Figure 2.26 Fluorescence from capillaries coated with five layer PMMA doped with (a) 10^{-2} M C540A and (b) 10^{-3} M C540A in the presence of Rh6G solution having varied anions of 1.5×10^{-4} M-1.8×10^{-4} M concentration. (Rh6G concentration in CH_3CN = 1.2×10^{-5} M). Inset shows the fluorescence spectrometer response from Rh6G solution in the presence of varied anions under 403 nm and 525 nm excitation

2.5 Conclusions

The rapid and sensitive response of Rh6G dye towards fluoride is described. The dynamic range of TBAF detection was found to be limited with the use of Rh6G alone. The possibility of using the C540A-Rh6G FRET pair to detect broad range of TBAF was studied.

The increase in TBAF caused a reduction in FRET efficiency leading to an increase in donor C540A emission. A number of FRET pair combinations having different concentrations of donor and acceptor were investigated and it was found that all the pairs could detect TBAF effectively even though the FRET efficiencies varied with donor-acceptor concentration. Moreover, the absorption and fluorescence peak intensities as well as peak wavelengths of both the donor and acceptor can also be used along with FRET efficiency for accurate determination of TBAF

The use of C540A dye doped PMMA coated hollow glass capillary with Rh6G test solution inside for the detection of TBAF was also studied. The effect of C540A concentration in the coating as well as the number of coating layers on the response of the sensing element was investigated. The fluorescence emission from the capillary increased with increase in concentration as well as the number of coating layers. The results indicate that Rh6G emission and C540A emission can respectively be used to detect lower and higher TBAF concentrations whereas the ratio of peak intensities of the dyes can be used to estimate TBAF concentration over a broad range. The possibility of employing a low cost UV LED to excite fluorescence from the capillary system was also investigated. The capillary system for the detection of fluoride offers the advantages of using different coating thicknesses and dopant concentration leading to good resolution in fluorescence values corresponding to different TBAF concentrations. The method also required only micro-liter volumes of samples for interrogation.

2.6 References

[1] A Costela, I. Garcia-Moreno, J. Barroso, and R. Sastre. "Laser performance of Coumarin 540A dye molecules in polymeric host media with different viscosities: From liquid solution to solid polymer matrix." Journal of applied physics 83, no. 2 (1998): 650-660.

[2] Hong Zheng, Xin-Qi Zhan, Qing-Na Bian, and Xiao-Juan Zhang. "Advances in modifying fluorescein and rhodamine fluorophores as fluorescent chemosensors." Chemical communications 49, no. 5 (2013): 429-447.

[3] Vadim P. Boyarskiy, Vladimir N. Belov, Rebecca Medda, Birka Hein, Mariano Bossi, and Stefan W. Hell. "Photostable, amino reactive and water-soluble fluorescent labels based on sulfonated rhodamine with a rigidized xanthene fragment." Chemistry–A European Journal 14, no. 6 (2008): 1784-1792.

[4] X. Zhang, Y. Xiao, and X. Qian, "A ratiometric fluorescent probe based on FRET for imaging Hg2+ ions in living cells," Angew. Chem. 47, (2008): 8025–8029.

[5] S. Kumar, V. Luxami, and A. Kumar, "Chromofluorescent probes for selective detection of fluoride and acetate ions," Org. Lett. 10, (2008): 5549–5552.

[6] J. Saha, A. D. Roy, D. Dey, S. Chakraborty, D. Bhattacharjee, P. K. Paul, and S. A. Hussain, "Investigation of fluorescence resonance energy transfer between fluorescein and rhodamine 6G," Spectrochim. Acta A 149, (2015): 143–149.

[7] Y. Liu, Z. M. Zhao, J. Y. Miao, and B. X. Zhao, "A ratiometric fluorescent probe based on boron dipyrromethene and rhodamine Förster resonance energy transfer platform for hypochlorous acid and its application in living cells," Anal. Chim. Acta 921, (2016): 77–83.

[8] D. A. Hinckley, P. G. Seybold, and D. P. Borris, "Solvatochromism and thermochromism of rhodamine solutions," Spectrochim. Acta A 42, (1986): 741–746.

[9] M. Beija, C. A. M. Afonso, and J. M. G. Martinho, "Synthesis and applications of rhodamine derivatives as fluorescent probes," Chem. Soc. Rev. 38, (2009): 2410–2433.

[10] K. H. Drexhage, "Fluorescence efficiency of laser dyes," J. Res. Natl. Bur. Stand.A 80A, (1976): 421–428.

[11] Roopa Venkataraj, Arindam Sarkar, C. P. Girijavallabhan, P. Radhakrishnan, V. P. N. Nampoori, and M. Kailasnath. "Fluorescence resonance energy-transfer-based fluoride ion sensor." Applied optics 57, no. 15 (2018): 4322-4330.

[12] M. Majoube and M. Henry, "Fourier transform Raman and infrared and surface-enhanced Raman spectra for rhodamine 6G," Spectrochim. Acta A 47, (1991): 1459–1466.

[13] C. Berney and G. Danuser, "FRET or no FRET: a quantitative comparison," Biophys. J. 84, (2003): 3992–4010.

[14] F. S. Wouters, "Förster resonance energy transfer and fluorescence lifetime imaging," in Fluorescence Microscopy: From Principles to Biological Applications, U. Kubitscheck, ed., 2nd ed. (Wiley-Blackwell, 2017), pp. 430–444.

[15] O. A. Goryacheva, N. V. Beloglazova, A. M. Vostrikova, M. V. Pozharov, A. M. Sobolev, and I. Y. Goryacheva, "Lanthanide-to quantum dot Förster resonance energy transfer (FRET): application for immunoassay," Talanta 164, (2017): 377–385.

[16] A. Roy, N. Kundu, D. Banik, and N. Sarkar, "Comparative fluorescence resonance energy-transfer study in pluronic triblock copolymer micelle and niosome composed of biological component cholesterol: an investigation of effect of cholesterol and sucrose on the FRET parameters," J. Phys. Chem. B 120, (2015): 131–142.

[17] U. Tripathy, P. B. Bisht, and K. K. Pandey, "Study of excitation energy migration and transfer in 3,30-dimethyloxacarbocyanine iodide (DMOCI) and o-(6-diethylamino-3-diethylimino-3H-xanthen-9-yl) benzoic acid (RB) in thin films of polyvinyl alcohol," Chem. Phys. 299, (2004): 105–112.

[18] P. Verma and H. Pal, "Aggregation studies of dipolar coumarin-153 dye in polar solvents: a photophysical study," J. Phys. Chem. A 118, (2014): 6950–6964.

[19] A. Ghosh, C. K. De, T. Chatterjee, and P. K. Mandal, "What type of nanoscopic environment does a cationic fluorophore experience in room temperature ionic liquids," Phys. Chem. Chem. Phys. 17, (2015): 16587–16593.

[20] J. Shi, C. Chan, Y. Pang, W. Ye, F. Tian, J. Lyu, Y. Zhang, and M. Yang, "A fluorescence resonance energy transfer (FRET) biosensor based on graphene quantum dots (GQDs) and gold nanoparticles (AuNPs) for the detection of mecA gene sequence of Staphylococcus aureus," Biosens. Bioelectron. 67, (2015): 595–600.

[21] Wei Li Zhang, Meng Ya Zheng, Rui Ma, Chao Yang Gong, Zhao Ji Yang, Gang Ding Peng, and Yun Jiang Rao. "Fiber-type random laser based on a cylindrical waveguide with a disordered cladding layer." Scientific reports 6 (2016): 26473.

[22] Alexandre François, Nicolas Riesen, Kirsty Gardner, Tanya M. Monro, and Al Meldrum. "Lasing of whispering gallery modes in optofluidic microcapillaries." Optics express 24, no. 12 (2016): 12466-12477.

[23] CP Kyle Manchee, V. Zamora, J. W. Silverstone, J. G. C. Veinot, and A. Meldrum. "Refractometric sensing with fluorescent-core microcapillaries." Optics express 19, no. 22 (2011): 21540-21551.

[24] Kristopher J. Rowland, Alexandre François, Peter Hoffmann, and Tanya M. Monro. "Fluorescent polymer coated capillaries as optofluidic refractometric sensors." Optics express 21, no. 9 (2013): 11492-11505.

[25] Roopa Venkataraj, Arindam Sarkar, P Radhakrishnan, V P N Nampoori, M Kailasnath, "Optical sensing of fluoride ion using dye coated hollow glass capillary", Paper no. FA1-C3, Proceedings of Photonics 2018, ISBN-978-93-88653-41-1

Chapter 3

Natural dye Curcumin for fluoride detection

This chapter describes the use of natural dye Curcumin for the detection of organic fluoride in organic medium. The effect of protic solvents on the ability of Curcumin to sense fluoride and the nature of bonding of Curcumin with fluoride has been studied. The possibility of using straight and U shaped evanescent wave optical fiber sensors for fluoride detection using Curcumin is investigated. The dye fluorescence when dissolved in two organic solvents namely, acetonitrile and anisole, having smaller and larger refractive indices with respect to the core of the optical fiber are recorded. The results of probes consisting of combinations of chemically tapered and bare uncladded optical fibers are compared.

3.1 Introduction

Many organic dyes are employed for chemical sensing applications using different mechanisms to achieve sensing response. Numerous methods have been described in literature for the detection of fluoride ion. The most widely used sensing technique involves the study of changes in optical properties of sensing compounds in the presence of fluoride [1]. A few optical fiber sensors have been reported for the detection of fluoride using reflectance and fluorescence of reagents, microstructured fibers and tilted fiber bragg gratings [2-7]. But even with the wide variety of advantages offered by optical fiber sensors, the use of optical fibers for the detection of fluoride is sparsely investigated.

In this chapter, the prospects of using a natural dye like Curcumin for the detection of fluoride in an organic medium is described. The use of natural dyes would be very attractive owing to their low cost, easy availability, bio-compatibility and non-toxic nature. The effect of pH on the optical properties of Curcumin and the effect of addition of protic solvents on the sensing response are discussed. The implementation of absorption and fluorescence based fiber sensors with the use of Curcumin dye would further enable low cost, easy to use systems for fluoride detection. The results of the evanescent wave absorption based straight and U shaped optical fiber sensors for the detection of fluoride are compared. The fluorescence collection using combinations of bare uncladded and chemically tapered fibers in two solvents having different refractive indices are studied.

3.2 Theoretical section

3.2.1 Evanescent wave optical fiber sensor (EWOFS)

Evanescent wave optical fiber sensors employ attenuated total reflection (ATR) of light as it propagates along the extended length of the optical fiber. The schematic of evanescent field formed at the core-cladding interface is as shown in Fig. 3.1. A section of the cladding is removed and replaced by an absorbing medium that would then function as the cladding in the un-cladded (sensing) region. When the evanescent wave propagates in this region, it is absorbed by the medium. The fraction of power absorbed by the medium depends on the waveguide parameters, the free space wavelength and also on the properties of the absorbing medium. Hence the transmitted output power by a given length of the optical fiber is a direct measure of the variation in absorption of the medium. V Ruddy et al [8] have explicitly described the theoretical background of the evanescent wave and A Messica

et al [9] have studied the effect of coupling angle, fiber diameter and length on the evanescent multimode fiber sensor response theoretically as well as experimentally.
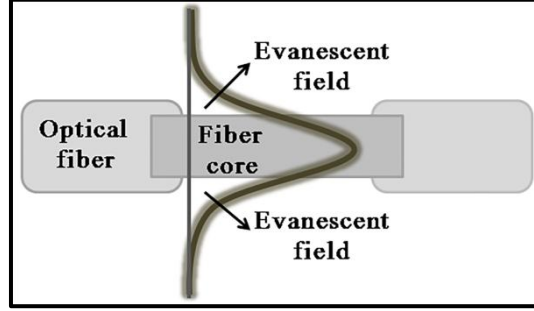
Figure 3.1 Evanescent field in an optical fiber sensor

The power transmitted *P(z)* by an optical fiber with un-cladded length along z direction in the presence of absorbing medium is given by[8, 10]:

$$P(z) = P(0)e^{-\gamma z} \tag{3.1}$$

where *P(0)* is the power transmitted by the same fiber without any absorbing species and γ is the evanescent absorption coefficient.

When all the modes are excited, the power transmitted by un-cladded length *L* in the optical fiber in terms of bulk absorption coefficient α of the medium is:

$$P(L) = P(0)e^{-p\alpha L} \tag{3.2}$$

where *p* is the fraction of power in the sensing region which depends on the V number and hence on waveguide parameters and the wavelength of incident light.

Hence the evanescent absorbance *A* is,

$$A = log\frac{P(0)}{P(L)} = \frac{p\alpha L}{2.303} \tag{3.3}$$

For a medium obeying Lambert-Beer law, the bulk absorption coefficient can be written in terms of concentration of absorbing species *C* and molar extinction coefficient ε_x as:

$$\alpha = \varepsilon_x C \tag{3.4}$$

Therefore, Eq. 3.3 becomes,

$$A = \frac{p\varepsilon_x CL}{2.303} \tag{3.5}$$

Hence it is very clear that the evanescent absorbance is directly proportional to concentration of the absorbing species and the length of the sensing region. From equations (3.1), (3.2) and (3.3), the evanescent absorption coefficient γ can be expressed as:

$$\gamma = \frac{2.303}{L} log \frac{P(0)}{P(L)} \tag{3.6}$$

For an absorbing medium with constant refractive index, the sensitivity of the optical fiber sensor is proportional to the evanescent absorption coefficient as Lγ/α [11].The bending of the fiber in the form of a U shape increases the penetration of the evanescent wave into the surrounding region, thereby increasing the fraction of power in the sensing region. This leads to a considerable increase in the evanescent absorption coefficient and consequently an increase in the sensitivity of the U shaped optical fiber sensor. The theoretical formulation of the U shaped probe has been extensively and clearly formulated by B D Gupta et al [11]. The effect of refractive index of the surrounding medium, bending angle and core diameter on sensitivity of the U shaped optical fiber sensor has also been studied and elucidated by the same group. It has been experimentally verified by them, that there is an increase in sensitivity of the optical fiber sensor with increase in the refractive index of the absorbing medium.

3.2.2   Tapered optical fiber probe

The evanescent wave travelling into the surrounding absorbing medium with concentration of absorbing species C is described by the expression [12]:

$$P = P_o e^{-\gamma CL} \tag{3.7}$$

where P and P_o are respectively the power transmitted by the optical fiber in the presence and absence of an absorbing medium. L is the length of the uncladded section of the optical fiber and γ is the evanescent absorption coefficient.

The penetration depth of the evanescent wave is given by the equation [13]:

$$d = \frac{\lambda}{2\pi \sqrt{n_c^2 sin^2\theta - n_{cl}^2}} \tag{3.8}$$

where n_c and n_{cl} are the refractive indices of the fiber core and cladding respectively. θ and λ are the incident angle normal to the interface and wavelength of light respectively.

The propagating modes in a multimode fiber have different penetration depths. This leads to a broad range of evanescent absorption coefficients associated with the large number of modes travelling along the optical fiber. So the coupling of evanescent power to the surrounding medium leads to the logarithmic nature of the detected transmitted power at the detector end [12].Tapering a fiber increases the coupling of evanescent wave into the external media and hence increases the sensitivity. The smaller the diameter and larger the length of the taper, higher is the coupling efficiency [14].

The exposure of evanescent wave into the surrounding medium excites fluorescence from the dye molecules which is coupled back by guided modes of the core. Fluorescence collection efficiency depends on many factors like refractive indices of the core, cladding, sensing medium/layer, geometry of the probe etc [14]. The number of modes (mode capacity) travelling in the fiber is given by the V parameter or the V number. In general, for a multimode fiber, the total number of modes is given by $V^2/2$. V number depends on the fiber radius r and the index as [15]:

$$V = 2\pi r \frac{\sqrt{n_c^2 - n_{cl}^2}}{\lambda} \tag{3.9}$$

When the optical fiber cladding has been replaced by an absorbing medium, $n_{cl} = n_{med}$. For the same wavelength λ, V is modified as V′ (say) as there is now a mode number mismatch, given by:

$$V' = 2\pi r \frac{\sqrt{n_c^2 - n_{med}^2}}{\lambda} \tag{3.10}$$

So as to ensure maximum fluorescence power coupling from un-cladded section immersed in absorbing medium to the cladded section, there should be V number matching between the two sections.

From (3.9) and (3.10), for V number matching, we need V≈V′, so considering a new parameter, called matching radius $r=R_m$, when the condition V≈V′ is satisfied, we can write,

$$V' = V = 2\pi R_m \frac{\sqrt{n_c^2 - n_{med}^2}}{\lambda} = 2\pi r \frac{\sqrt{n_c^2 - n_{cl}^2}}{\lambda} \tag{3.11}$$

[70]

Simplifying Eq. 3.11 we get [13, 15]:

$$R_m = r\frac{\sqrt{n_c^2 - n_{cl}^2}}{\sqrt{n_c^2 - n_{med}^2}} \qquad (3.12)$$

Significant loss in fluorescence signal acquisition can be prevented by modifying the core radius to a value smaller than the matching radius. This matching radius can be easily achieved by chemically tapering the multimode fibers.

The matching radius for a 200/229 µm optical fiber with n_c=1.462, n_{cl}=1.414 and acetonitrile as the sensing medium (n_{med} = 1.3431) is calculated to be 129 µm. For a medium with higher refractive index than the core refractive index like in anisole, it is not expected that there would be significant collection of excited fluorescence. The fluorescence signal collection approaches its least value as the index of surrounding medium reaches a value above the core index value [16]. But, the fluorescence rays generated in a medium with higher refractive index like anisole can be coupled back into the core of collection fiber provided they are incident at angles between [0, θ_{cr}]. The critical angle θ_{cr} is given by the equation [14]:

$$\theta_{cr} = \sin^{-1}\frac{n_c}{n_{med}} \qquad (3.13)$$

With n_{med} =1.516 for anisole, the value of θ_{cr} is calculated to be 0.42π radian=74.7 degrees.

3.3 Experimental methods

3.3.1 Preparation of anion samples

10^{-5} M of Curcumin dye (Acros Organics, 98% purity) was dissolved in AR grade acetonitrile (CH_3CN) and anisole ($CH_3OC_6H_5$). Tetrabutylammonium fluoride (TBAF, 75 % in water, Spectrochem Pvt. Ltd., Mumbai) was added to the stock solution of Curcumin to get fluoride samples of varying concentrations. Other anions samples were also prepared by adding tetrabutylammonium anions (Sigma Aldrich, Spectrochem India Pvt Ltd) of acetate (TBAA), dihydrogen phosphate (TBAP), hydrogen sulphate (TBAS), nitrate (TBAN), chloride (TBAC), bromide (TBAB) and iodide (TBAI) to measured volumes of Curcumin stock solution. The changes in the absorption and fluorescence spectra of

Curcumin were studied using Jasco V 570 UV-Vis spectrophotometer and Cary eclipse (Varian) fluorescence spectrometer.

3.3.2 Preparation of EWOFS

The straight optical fiber sensor was prepared by removing the cladding of around 14.5 cm length in the middle of a 200/229 µm plastic clad silica (PCS, Polymicro Technologies) of 97 cm length by immersing it in acetone for 2 hours. This optical fiber was then fixed inside a cylindrical vessel with provisions for easy removal of samples. A U shaped optical fiber couples a large fraction of light from the core to the outside medium when compared to the straight fiber. For preparing the U shaped optical fiber sensor, a 109 cm length was at first un-cladded (7 cm). The un-cladded section was then bent in the form a U shaped probe of approximately 1.5 cm radius. The optical fiber was fixed on microscopic glass slide using epoxy glue such that the U shaped portion is positioned outside the glass slide.

3.3.3 Tapered fiber probe fabrication

Tapered fiber probes can be fabricated by heat pulling, arc splicing and chemical methods**.** The chemical method involves treating the optical fiber surface with etchants like hydrofluoric acid (HF) to create a taper profile [17, 18]. The chemically tapered probes do not usually have the cladding and hence it is reported that they can be readily used for fluorescence collection applications [19]. The taper profile at the end of PCS optical fibers were fabricated using 48 % HF. For this purpose, optical fibers of about 60 cm length were uncladded (2 cm) at one end by immersion in acetone. The uncladded section was then placed and fixed on a specially constructed Teflon reaction chamber. About 20 µl of HF was added onto the fixed fiber such that the tip of the uncladded section was at the center of the HF drop.

This drop of HF moves along the length of the uncladded section and as it moves, it evaporates. This capillary effect is also called the Marangoni effect [18]. The result of such an etchant motion along the uncladded fiber surface creates a taper profile. The etchant was exposed to fiber surface for different time durations. The reaction time for getting a clear taper profile was found to be around 75 minutes. The reaction of the etchant with the fiber surface was stopped after the required time of exposure using a 5 N sodium hydroxide (NaOH) solution. The reaction chamber was then washed repeatedly with de-ionised water. The taper tips were then stored in 0.1 N NaOH until it is fixed on the microscopic

glass slide. The taper profile of the prepared optical fibers was observed under a GP-KR 222 CCD camera connected to a TV screen. The average taper length and taper diameter of the prepared fiber was found to be 3.3 mm and 36 μm respectively.

3.3.4   Experimental set-up for interrogation

The experimental set-up for the U shaped evanescent wave optical fiber sensor is shown in Fig 3.2. The light from the 403 nm laser was focused into one end of optical fiber using a convex lens (f=3.5 cm) and the transmitted light from the other end was detected by a Si biased photo-detector (DET 36 A/M, Thorlabs, 350-1100 nm). The detector was connected to an hp 34401a digital multimeter which was in turn interfaced to a personal computer having RS 232 data logger software. The U shaped sensor head was immersed in the beaker containing the samples of Curcumin in acetonitrile with varying concentrations of TBAF, using a 3D translational stage. The output voltage values corresponding to the transmitted light from the sensor head was recorded as a function of time. Hence fluctuations in output voltage values if any could also be monitored easily. The acquisition of transmitted output voltage values was carried out over a period of 60 seconds for each of the fluoride samples.
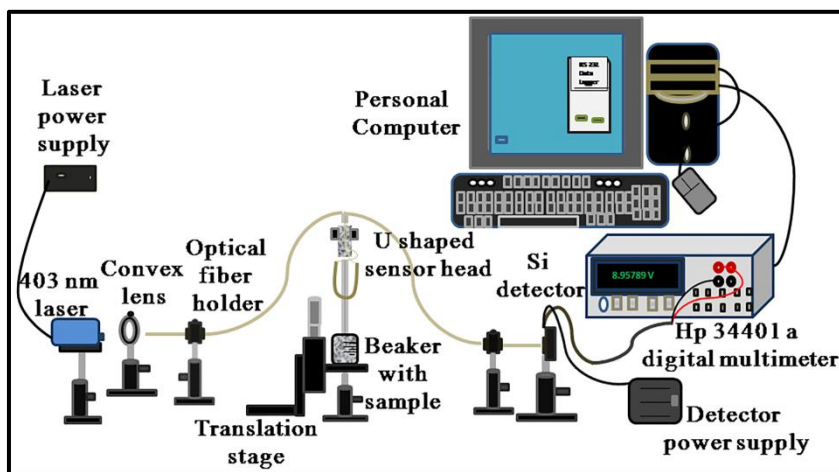
Figure 3.2 Experimental set-up for U shaped evanescent wave fiber optic sensor

The experimental set-up for the straight fiber sensor is also similar to the one shown in Fig. 3.2 except that the U shaped fiber was replaced by a straight fiber fixed in a cylindrical vessel with provisions for introducing the fluoride samples. The effect of refractive index of TBAF samples on the output of EWOFS was also studied and is described in later sections of this chapter.

The image of the chemically etched tapered section of the multimode fiber is shown in Fig. 3.3a. The experimental set-up for the collection of fluorescence from the single tapered fiber probe upon direct laser excitation of the samples is as shown in Fig. 3.3b. The laser was focused onto the fiber in the form of a stripe of 2 cm length using plano-convex and cylindrical lenses. The samples were taken in a 1 cm quartz cuvette and the laser light stripe is adjusted in such a way that it is directly incident on the tapered tip inside the solution.
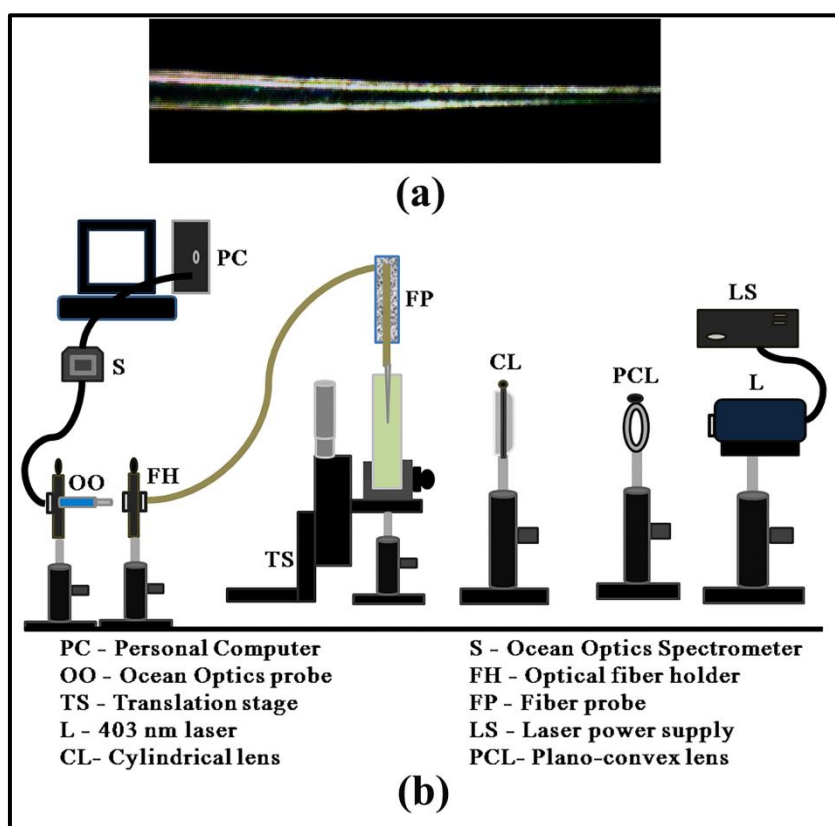
Figure 3.3 (a) Tapered tip at the end of multimode fiber using CCD camera (b) Experimental set-up for the collection of fluorescence from a single tapered fiber

The different sensor probes constructed with short length (0.7 cm) uncladded or tapered fibers for excitation and tapered or longer length (2 cm) uncladded fiber for collection of fluorescence are as shown in Fig. 3.4a. The laser path in the two different refractive index solvents is as shown in the Fig. 3.4b. The experimental set-up for studying the excitation and collection of fluorescence from Curcumin using the different sensor probes is shown in Fig. 3.5. The laser beam was focused onto the input fiber using a convex

lens. The fluorescence of Curcumin with varying fluoride concentrations in the case of single tapered probe and the two fiber probes were recorded using an HR 4000 SpectraSuite Ocean Optics spectrometer.
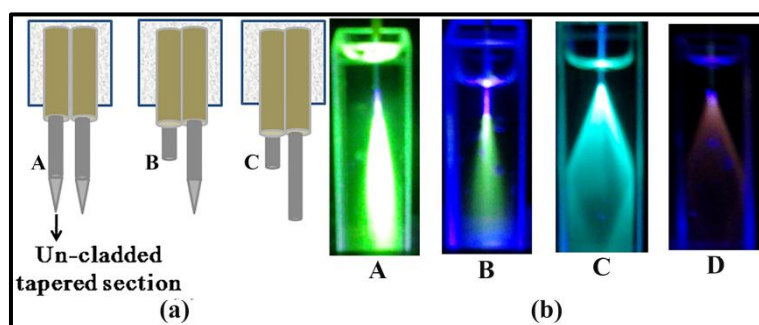
Figure 3.4 (a) Sensor probe configuration for the excitation and collection of fluorescence from Curcumin (b) Light path in CH_3CN (A, B) and $CH_3OC_6H_5$ (C, D) with A,C - Curcumin alone in the solvents and B, D- Curcumin in the presence of high concentration TBAF
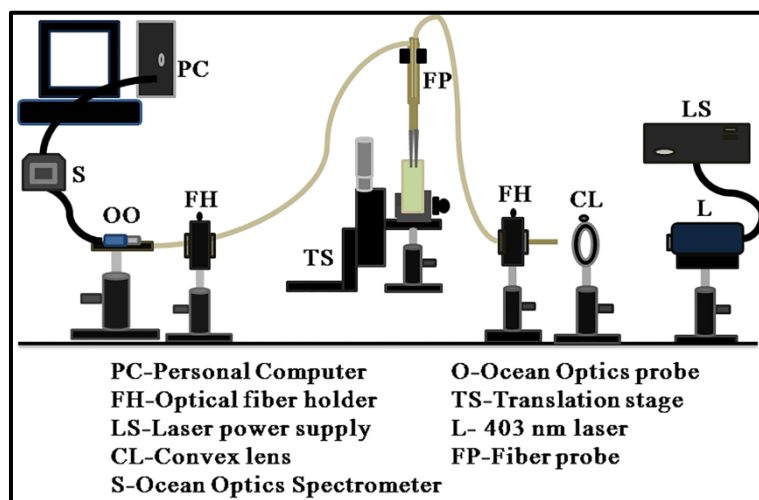
Figure 3.5 Experimental set-up for interrogation of the two-fiber sensor probes

3.4 Results and Discussion

3.4.1 Sensing response of Curcumin towards fluoride in organic medium

Curcumin has an absorption peak at 418 nm and 423 nm in acetonitrile and anisole respectively. This prominent absorption peak intensity decreases with the addition of TBAF, accompanied by an increase in the absorption band around 560 nm as shown in figures 3.6a and 3.7a.
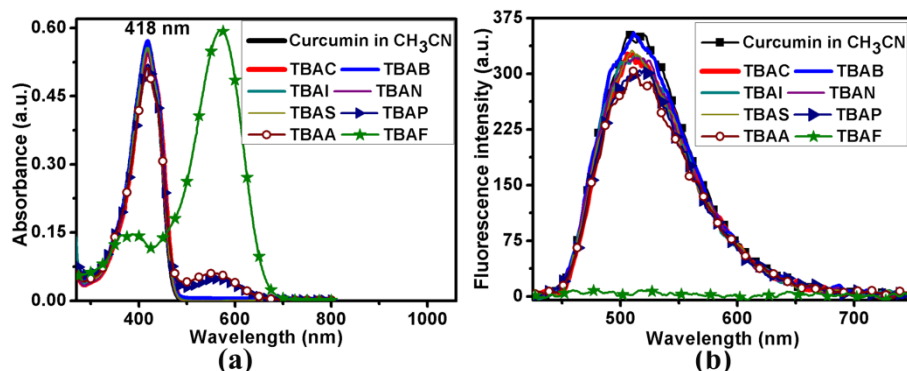
Figure 3.6 Variation in (a) absorbance and (b) fluorescence of Curcumin in CH₃CN in the presence of common anions (Exact concentrations of anions: TBAC=2.63 mM, TBAB, TBAI, TBAN, TBAS=0.2 mM, TBAP=0.193 mM, TBAA=0.184 mM and TBAF=0.22mM)
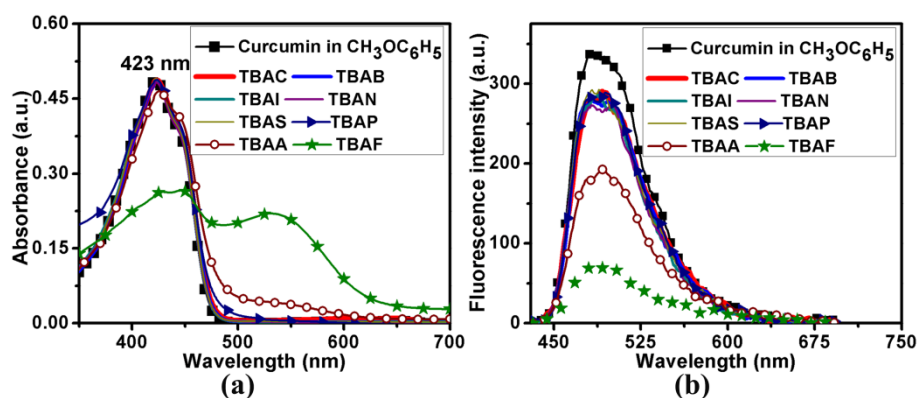
Figure 3.7 Variation in (a) absorbance and (b) fluorescence of Curcumin in CH₃OC₆H₅ in the presence of common anions (Exact concentrations of anions: TBAB=0.232 mM, TBAI=0.177 mM, TBAN, TBAP,TBAA=0.22 mM, TBAC, TBAS, TBAF=0.2 mM)

These changes in the absorption of Curcumin in both the solvents can be attributed to the deprotonation of OH in the phenol group of Curcumin [20, 21]. At low concentration of TBAF, the complex of TBAF with curcumin formed via bonding of F⁻ at the OH site of Curcumin, is prevalent. This complex exists in equilibrium with the deprotonated state at lower TBAF concentration. The reaction then shifts towards the formation of large number of deprotonated Curcumin when concentration of TBAF is very high. Consequently, a decrease in fluorescence of Curcumin is also observed with increase in TBAF and this could be due to overlap of the absorption spectrum of deprotonated form of Curcumin with the fluorescence spectrum of the free Curcumin [20] (Fig. 3.6b and 3.7b).

[76]

It was also observed that there was a change in initial yellow colour of the solution to a deep purple and reddish brown in the case of acetonitrile and anisole respectively at high TBAF concentration as shown in Fig. 3.8. The optical and colourimetric changes of Curcumin were observed only in the case of TBAF and not in the case of other anions. The gradual colour change in solutions of Curcumin in the presence of increasing concentration of fluoride is as shown in Fig. 3.9.
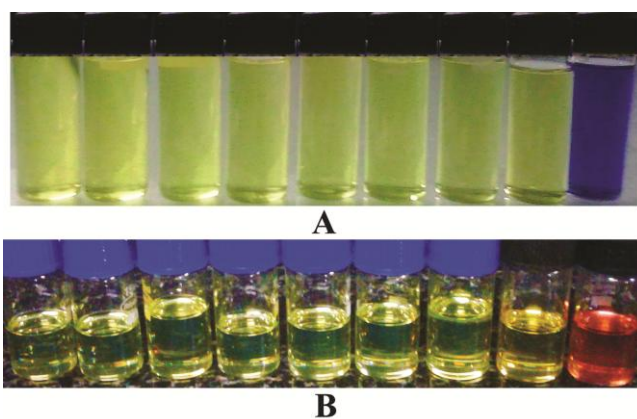
Figure 3.8 Colour changes of Curcumin in (A) CH_3CN and (B) $CH_3OC_6H_5$ in the presence of (from extreme right to left) 2×10^{-4} M of TBAF, TBAA, TBAP, TBAS, TBAN, TBAI, TBAB and TBAC. Sample at the extreme left depicts Curcumin in the solution without any anion
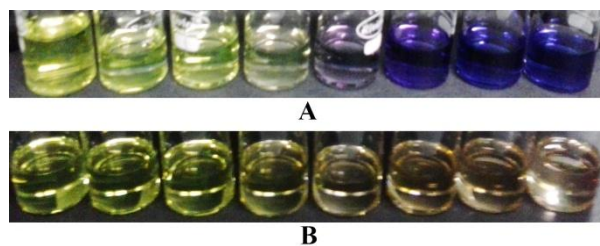
Figure 3.9 Colour changes of Curcumin in (A) CH_3CN and (B) $CH_3OC_6H_5$ in the presence of (from left to right) 0, 2×10^{-6}, 7×10^{-6}, 2×10^{-5}, 7×10^{-5}, 2×10^{-4}, 7×10^{-4}, 2×10^{-3} M TBAF

The decrease in normalized peak absorbance values in the 400-500 nm wavelength range and the corresponding increase in absorbance in 500-600 nm range is shown in Fig. 3.10. Also, the decrease in normalized peak fluorescence intensity of Curcumin with increase in TBAF is as shown in Fig. 3.11. The graphs indicate a complexation and conversion of Curcumin to its deprotonated form in the presence of TBAF.
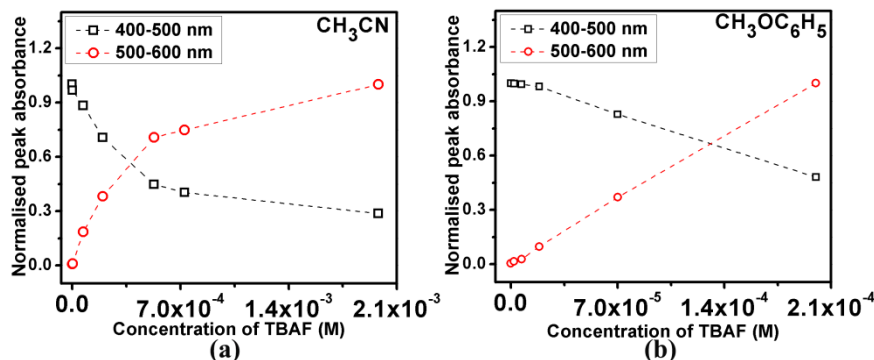
Figure 3.10 Variation in normalized peak absorbance values of Curcumin with increase in TBAF in (a) CH₃CN and (b) CH₃OC₆H₅ in the 400-500 nm and 500-600 nm wavelength ranges. Normalization is carried out with respect to maximum values in the respective wavelength ranges.
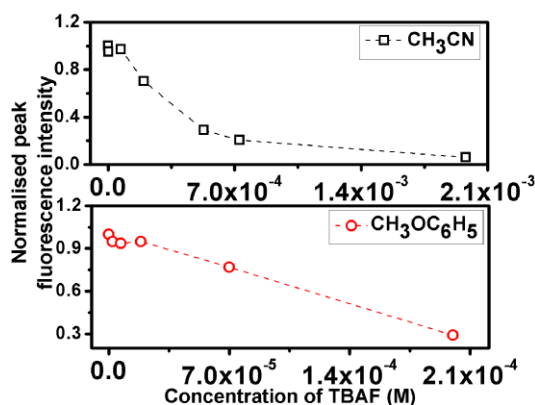
Figure 3.11 Decrease in normalised peak fluorescence intensity of Curcumin with increase in TBAF in CH₃CN and CH₃OC₆H₅

3.4.2   Effect of pH and addition of protic solvents

The effect of pH on the optical properties of Curcumin was verified by the addition of buffer solutions and addition of NaOH. It was observed that there is a red shift in the absorption spectrum with increase in pH. This could be due to the removal of the proton from the acidic phenol group [22, 23]. The solution of Curcumin in 0.5 M NaOH was reported to have maximum absorption at 463 nm with a shoulder at 360 nm [24]. The same effect was observed in acetonitrile-water solvent mixture in the presence of NaOH as shown in Fig 3.12b. It was reported that the variation of pH in the range 9-11 caused a red shift in absorption spectrum of Curcumin to around 522 nm. But further increase in pH

leads to a blue shift from 522 to 485 nm due to the simultaneous deprotonation of both the phenol groups [20].
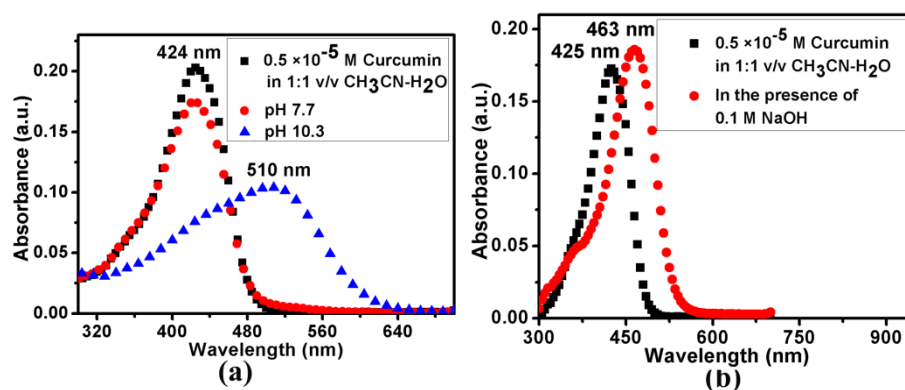
Figure 3.12 Shift in the peak absorption wavelength of Curcumin in mixture solvent of 1:1 v/v CH₃CN:H₂O in the presence of (a) pH buffer 7 and 10 and (b) NaOH

The complex between Curcumin and TBAF is very sensitive to the solvent environment around it. The presence of protic solvents like ethanol (EtOH) and water (H₂O) can lead to the disruption of the complex owing to the competitive binding of the molecules with Curcumin [20]. The effect of addition of protic solvents is as shown in Fig. 3.13. It was observed that the absorption curves retraced back to their original state (i.e without TBAF) when even microliter volumes of protic solvents were added. A faster recovery of absorption spectra was observed in the case of strong protic solvent like ethylene glycol (EG). This recovery of absorption spectrum leads to the gradual shifting of peak absorption wavelength from 560 nm of the deprotonated state to 418 nm of Curcumin as shown in Fig. 3.13c. The colour of the solution changed from purple to yellow, indicating the reversal of the state of Curcumin from the complexed form to the free form.

Therefore, the presence of even a small volume of protic solvents can lead to a huge change in absorption spectra and hence the detection of fluoride using Curcumin is very difficult in aqueous medium or even mixtures of aqueous and organic solvents. But the volume of protic solvents required for different concentration of TBAF is different and therefore, the volume of protic solvent required for retrace of absorption spectrum can also in turn be used to estimate the concentration of TBAF in the solution.

[79]
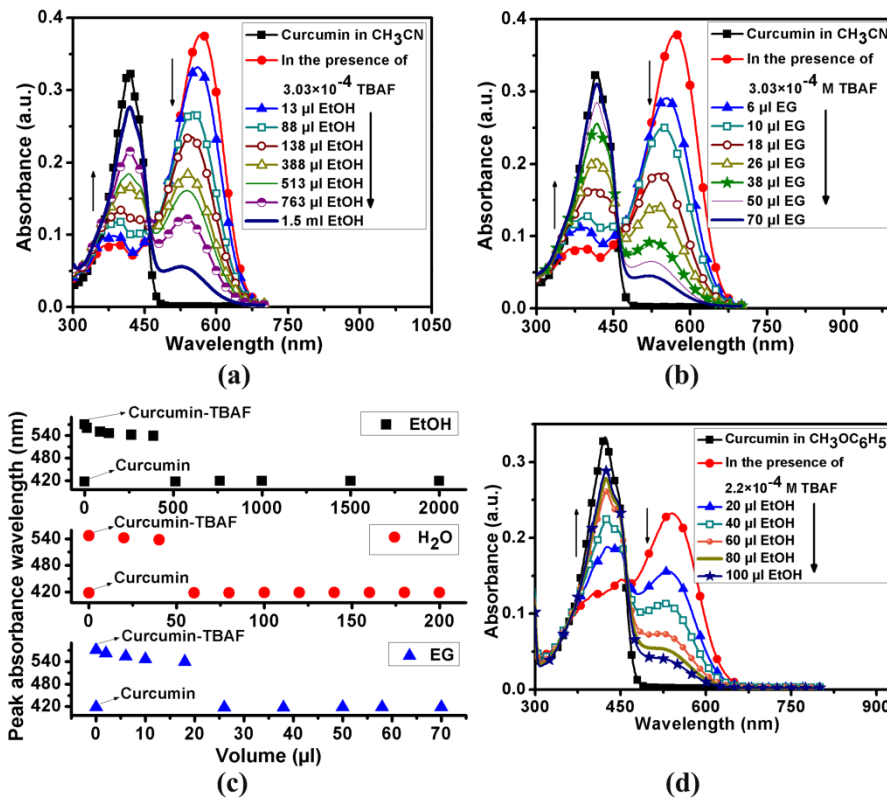
Figure 3.13 Recovery of the peak absorbance of Curcumin in CH_3CN in the presence of high concentration TBAF upon addition of protic solvents (a) EtOH and (b) EG (c) The shift in peak absorption wavelength of Curcumin upon addtition of protic solvents (d) Recovery of peak absorbance of Curcumin in $CH_3OC_6H_5$ on addition of EtOH

3.4.3 Straight and U shaped EWOFS

The variation in the detected output voltage corresponding to different TBAF concentrations in acetonitrile is as shown in Fig. 3.14. It was seen that there is an increase in transmittance of incident light or output voltage recorded by the detector with increase in TBAF. This is in accordance with the decrease in the initial peak absorbance of Curcumin at 418 nm with increase in fluoride. Since the change in output voltage of the straight fiber is very low, the distinction between TBAF concentrations would be difficult using this configuration (Fig. 3.14b). On the other hand, with the U shaped optical fiber sensor of only half the length of the straight fiber sensor, a considerable change in output voltage was recorded. This is in accordance with the increased sensitivity of the U shaped optical fiber sensor to the surrounding environment [11].
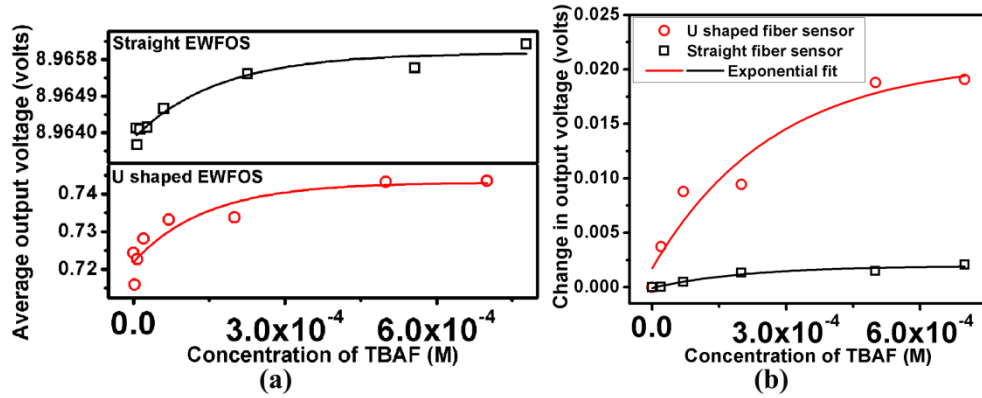
Figure 3.14 (a) Variation in transmittance and (b) Change in the output voltage of the straight and U shaped optical fiber sensor with increase in TBAF concentration

3.4.4   Effect of index of refraction on EWOFS response

The increase in refractive index of surrounding medium leads to an increase in sensitivity of the fiber sensor [11]. To study the influence of any refractive index change with increase in TBAF concentration a 400/431 µm PCS fiber was uncladded and fixed in the cylindrical vessel. Light from a superluminescent white LED was directly fed to one end of the fiber without the use of any bulk optics. The samples of acetonitrile containing varying amounts of TBAF were introduced into the cell. The light from the output end was recorded by a spectrometer (HR 4000 Spectra Suite Ocean Optics).

As depicted in Fig. 3.15, there is no change in transmittance at both the bands of the LED centered at 450 nm and 532 nm with increase in fluoride ion concentration. Since there was no absorbing species in the medium, the increase in fluoride concentration alone does not seem to bring about major changes in the transmittance. This could also mean that there are no significant refractive index changes on increasing fluoride concentration. The refractive index measurements of the TBAF samples in acetonitrile using the Abbe's refractometer also indicated only a 0.001 RIU change at the higher TBAF concentrations. A rough approximation of the refractive index of solutions of Curcumin with different TBAF concentrations by the hollow prism method using a 10 mW 633 nm He-Ne laser also showed that the change in refractive index was even lesser than 0.001 RIU.
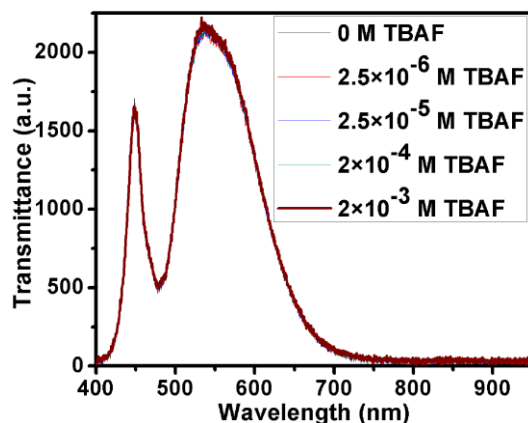
Figure 3.15 Transmitted spectrum of the evanescent wave straight optical fiber sensor for varying concentration of TBAF in CH₃CN

3.4.5   Fluorescence quantum yield of Curcumin

For comparing the characteristics of the fluorescence probes, an estimation of the quantum yield of Curcumin in both the solvents is necessary. Fluorescence emission in general, depends on a variety of factors like solvent polarity and viscosity, solvent relaxations, excited state reactions, conformational changes etc [25]. The fluorescence quantum yield is also dependent on various factors including solvent polarity and refractive index [26].

The quantum yield using the single point method is given by the equation [27]:

$$Q = Q_R \frac{I}{I_R} \frac{A_R}{A} \frac{n^2}{n_R^2} \qquad (3.14)$$

In the comparative method, the equation for quantum yield is given by [25, 27]:

$$Q = Q_R \frac{m}{m_R} \frac{n^2}{n_R^2} \qquad (3.15)$$

where I, A, n, m are the integrated fluorescence intensity, absorbance, refractive index and slope of A versus I graph respectively. The subscript 'R' denotes the standard reference for quantum yield.

Curcumin exhibits very low quantum yield (< 0.2) in many protic solvents with the maximum value reported to be observed in acetonitrile [28]. Coumarin 540A (C540A) dissolved in ethanol was selected as the standard for estimating the quantum yield of Curcumin in anisole [29, 30]. The quantum yield of Curcumin in acetonitrile was also

estimated for comparison of quantum yield in the solvents. Two different excitation wavelengths were used for analysis viz. 403 nm, which is the laser source excitation wavelength and 422 nm, which is near to the peak absorption wavelength of Curcumin in acetonitrile and anisole.

Table 3.1 Fluorescence quantum yield of Curcumin in acetonitrile using single point method

$\lambda_{excitation}$	Curcumin in CH$_3$CN		C540A in EtOH		Q
	A	I	A$_R$	I$_R$	
403 nm	0.06859	6399.71	0.0683	23938.03	0.098
	0.04998	4925.582	0.04893	18369.53	0.097
	0.04256	4622.638	0.04053	13824.4	0.118
	0.01839	2834.76	0.01996	10500.13	0.108
422 nm	0.09007	8602.767	0.08737	28091.64	0.1097
	0.06027	5748.154	0.06354	21729.6	0.103
	0.05306	5373.962	0.05282	18556.86	0.106
	0.036	4043.504	0.03509	14236.18	0.102

Table 3.2 Fluorescence quantum yield of Curcumin in anisole using single point method

$\lambda_{excitation}$	Curcumin in CH$_3$OC$_6$H$_5$		C540A in EtOH		Q
	A	I	A$_R$	I$_R$	
403 nm	0.05031	4735.787	0.04893	18369.53	0.1197
	0.04201	3984.164	0.04053	13824.48	0.133
	0.03128	2901.12	0.03453	13824.48	0.111
	0.02739	2936.564	0.02545	12070.99	0.108
422 nm	0.0672	6374.622	0.06354	21729.6	0.133
	0.05619	5139.011	0.05282	18556.86	0.125
	0.04314	4637.294	0.04536	16059.11	0.145
	0.03788	3930.295	0.03509	14236.18	0.122

Here Q$_R$ for C540A in EtOH = 0.38 [29]. n$_R$ = 1.3725 at 403 nm and 1.3706 at 422 nm [31, 32]. The n values for acetonitrile are 1.3531 and 1.3513 at 403 nm and 422 nm respectively [32, 33]. The experimentally verified value of n for anisole at 434 nm is 1.5382 [34]. Using the above values, the quantum yields of Curcumin in the two solvents were estimated

using both the single point and the comparative method. The values of quantum yield calculated using the single point method (Eq. 3.14) are tabulated in Table 3.1 and Table 3.2.

The values of slopes for the three cases of Curcumin in acetonitrile, Curcumin in anisole and C540A in EtOH were calculated from the linear fit of plot between integrated fluorescence intensity and absorbance [Fig. 3.16]. Using equation 3.15 (comparative method) the quantum yields of Curcumin in acetonitrile was found to be 0.093 and 0.1 for 403 nm and 422 nm excitation respectively, which is in good agreement with values reported in literature [28]. The quantum yield of Curcumin in anisole was calculated to be 0.111 and 0.125 for 403 nm and 422 nm excitation respectively. Hence it was found that the quantum yield of Curcumin in anisole was approximately 1.2-1.3 times higher than that in acetonitrile.
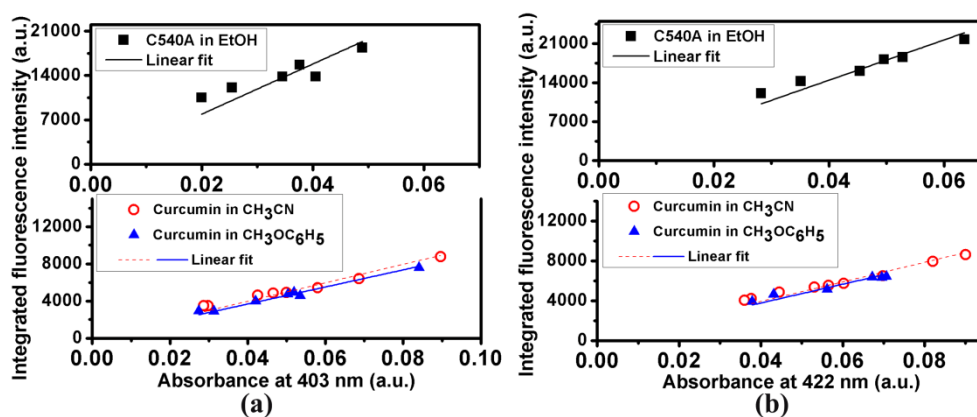
Figure 3.16 Plot of integrated fluorescence intensity versus absorbance of Curcumin in CH_3CN and $CH_3OC_6H_5$ when compared to the C540A dye in EtOH solvent for (a) 403 nm excitation and (b) 422 nm excitation

3.4.6   Fluorescence collection by a single tapered probe

The evanescent wave absorption based fiber sensors are extremely simple to construct and use. Fluorescence based sensors are reported to be very attractive owing to the possibility of monitoring a variety of parameters including excitation wavelength, emission wavelength, intensity and fluorescence lifetime [35]. The fluorescence spectra collected by a single tapered fiber probe is as shown in Fig. 3.17. The fluorescence recorded by the tapered fiber tip is found to be considerably good even in the case of higher index solvent like anisole.
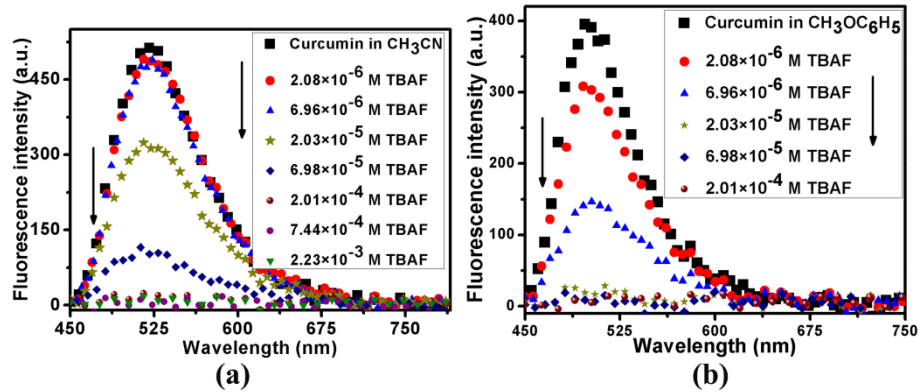
Figure 3.17 Fluorescence spectra collected by a single tapered probe immersed in (a) CH_3CN and (b) $CH_3OC_6H_5$

3.4.7   Fluorescence collection by two fiber probes

In comparison to the single tapered probe, a two fiber probe would enable remote sensing capability. Initially the response of a probe consisting of two uncladded fibers was recorded. The laser was directly coupled into the uncladded excitation fiber. The collection of fluorescence of Curcumin by the uncladded collection fiber was found to be very small in both the solvents as shown in Fig. 3.18.
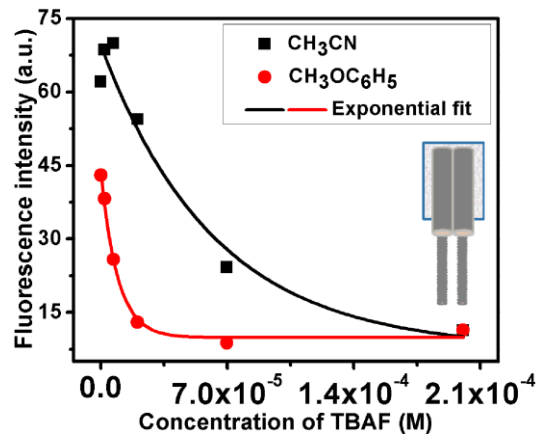
Figure 3.18 Fluorescence values recorded in CH_3CN and $CH_3OC_6H_5$ by a probe consisting of two uncladded fibers placed side by side. Inset shows the structure of the probe

Tapered fibers are reported to couple a large fraction of light into the external medium and also have the capacity to collect fluorescence from the medium [13, 36]. The probe A consisting of two tapered fibers for excitation and collection of fluorescence is inefficient in both the solvents as shown in Fig 3.19. This could be owing to the poor collection of fluorescence via the evanescent wave. There could also be collection of fluorescence along

the direction of fiber axis. Since this collection would also be very small, the overall efficiency of fluorescence collection of such a system was very small.
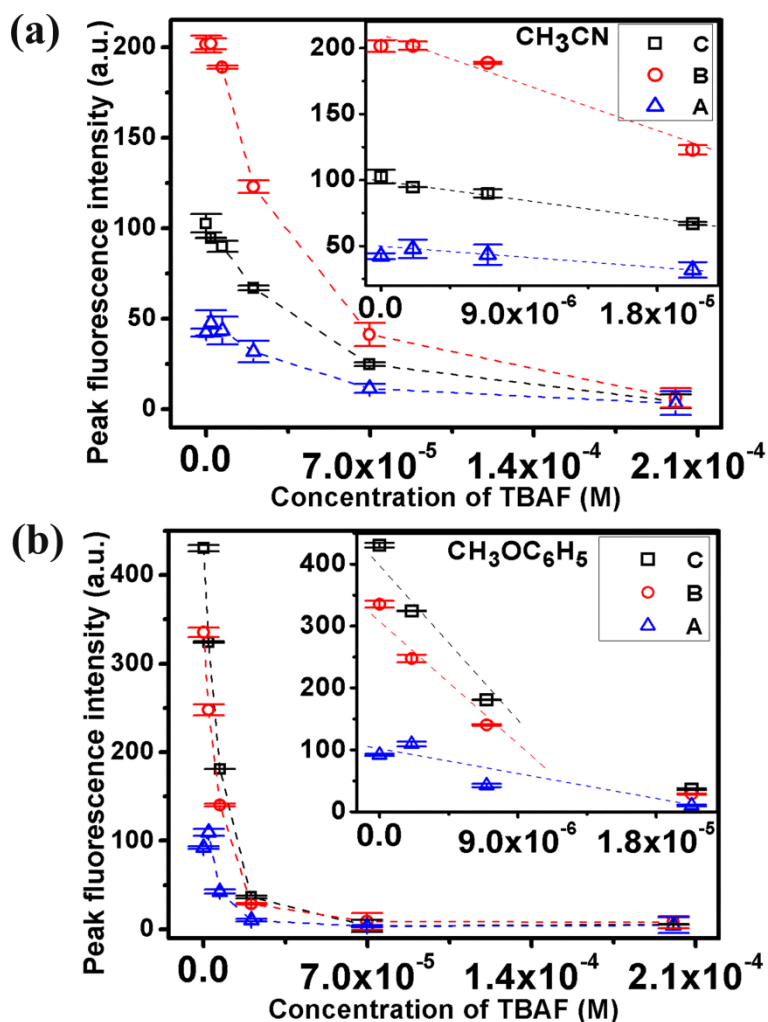
Figure 3.19 Fluorescence collected by the different probe configurations of Fig. 3.4a in (a) CH_3CN and (b) $CH_3OC_6H_5$. Insets of (a) and (b) show the expanded graphs corresponding to lower TBAF concentration

The uncladded bare fiber when immersed in solvent produces a fluorescence cone inside the medium. Especially in the case of higher index solvent anisole, the fluorescence cone is dispersed and appears to be reflecting off the walls off the cuvette as shown in Fig. 3.4b. Hence a shorter length uncladded fiber was used for excitation of fluorescence in the case of probes B and C as shown in Fig. 3.4a. In these cases, there is axial excitation of fluorescence and also excitation of fluorescence due to the evanescent wave propagating in

the uncladded region. The axial excitation of fluorescence leads to the formation of fluorescence cone inside the medium which in turn leads to a wide range of angles of incidence on the collection fiber [37]. The critical angle condition would then be easily satisfied. This would especially be the case for higher refractive index solvent anisole. It can be seen from Fig. 3.19 that there is considerable resolution in fluorescence values in the solvent anisole. This could be owing to the higher quantum yield of Curcumin in anisole. The wide range of absorption coefficients corresponding to the different modes of a multimode fiber and the varied fluorescence collection efficiency corresponding to these modes could have also led to the higher resolution in fluorescence values even at high fluoride concentration. Both the systems containing short length uncladded fiber for fluorescence excitation and tapered fiber (Probe B) or uncladded fiber (Probe C) for fluorescence collection recorded higher values compared to the two tapered fiber system.

The fluorescence values corresponding to high fluoride concentration is near zero in the case of anisole. This could be due to the 1:1 binding nature of Curcumin with fluoride [20]. From Fig. 3.19 it can be seen that the linear detection range of TBAF in anisole is around 2×10^{-5} M (5.2 ppm TBAF) and slightly higher than this value in acetonitrile. But fluorescence values corresponding to 7×10^{-5} M (18 ppm) in anisole and 2×10^{-4} M (52 ppm) in acetonitrile can be recorded using the probes B and C. The LOD is calculated using the method described in literature [38]. From Fig. 3.19, the LOD using the probes B and C are approximately 2×10^{-6} M (0.52 ppm TBAF, 0.038 ppm F) in anisole and 6×10^{-6} M (1.6 ppm TBAF, 0.11 ppm F) in acetonitrile. Hence it is clear that the combination involving two dissimilar length bare uncladded fibers can also serve as an efficient excitation-collection system for fluorescence in a similar manner to the uncladded-tapered fiber combination.

3.5 Conclusions

Natural dye Curcumin was used to detect fluoride over a broad range of concentration in two organic solvents viz. acetonitrile and anisole. The addition of protic solvents led to the recovery of the absorption spectrum of Curcumin, indicating the hydrogen bonding nature of interaction of Curcumin with fluoride. It also points to the difficulty of using Curcumin for aqueous based sensing. The use of evanescent wave straight and U shaped optical fiber sensors in the detection of fluoride using Curcumin was also investigated. The variation in output voltage corresponding to the transmitted optical power by the U shaped fiber sensor was better than that of the straight fiber sensor. Fluorescence probes were assembled

using combinations of uncladded and chemically tapered optical fibers. Such combination of probes collected significant fluorescence from both the higher and lower refractive index solvents compared to the case when a probe consisting of only uncladded fiber or tapered fiber is used. The use of such fluorescence probes with natural dye Curcumin proves to be sensitive enough to distinguish between broad ranges of fluoride concentrations. Furthermore, the probes could also be extended to study chemical reactions and its byproducts, in solvents of even higher refractive index compared to the fiber core.

3.6 References

[1] Ying Zhou, Jun Feng Zhang, and Juyoung Yoon. "Fluorescence and colorimetric chemosensors for fluoride-ion detection." Chemical reviews 114, no. 10 (2014): 5511-5571.

[2] Xinghua Yang, Jian Wang, and Lili Wang. "Sol–gel matrix modified microstructured optical fibre towards a fluoride sensitive optical probe." Optics Communications 282, no. 13 (2009): 2502-2505.

[3] L. B. Melo, J. M. M. Rodrigues, A. S. F. Farinha, C. A. Marques, L. Bilro, N. Alberto, J. P. C. Tomé, and R. N. Nogueira. "Concentration sensor based on a tilted fiber Bragg grating for anions monitoring." Optical Fiber Technology 20, no. 4 (2014): 422-427.

[4] David A. Russell, and Ramaier Narayanaswamy. "An optical-fibre sensor for fluoride." Analytica chimica acta 220 (1989): 75-81.

[5] David A. Russell, and Ramaier Narayanaswamy. "Fibre optic fluorimetric determination of fluoride ions." Analyst 114, no. 3 (1989): 381-385.

[6] R. Narayanaswamy, D. A. Russell, and F. Sevilla III. "Optical-fibre sensing of fluoride ions in a flow-stream." Talanta 35, no. 2 (1988): 83-88.

[7] Aji Balan Pillai, Benjamin Varghese, and Kottarathil Naduvil Madhusoodanan. "Design and development of novel sensors for the determination of fluoride in water." Environmental science & technology 46, no. 1 (2011): 404-409.

[8] V. Ruddy, B. D. MacCraith, and J. A. Murphy. "Evanescent wave absorption spectroscopy using multimode fibers." Journal of Applied Physics 67, no. 10 (1990): 6070-6074.

[9] A. Messica,, A. Greenstein, and A. Katzir. "Theory of fiber-optic, evanescent-wave spectroscopy and sensors." Applied optics 35, no. 13 (1996): 2274-2284.

[10] P. Suresh Kumar, C. P. G. Vallabhan, V. P. N. Nampoori, VN Sivasankara Pillai, and P. Radhakrishnan. "A fibre optic evanescent wave sensor used for the detection of trace nitrites in water." Journal of Optics A: Pure and Applied Optics 4, no. 3 (2002): 247-250

[11] B. D. Gupta, H. Dodeja, and A. K. Tomar. "Fibre-optic evanescent field absorption sensor based on a U-shaped probe." Optical and Quantum Electronics 28, no. 11 (1996): 1629-1639

[12] P. Suresh Kumar, S. Thomas Lee, C. P. G. Vallabhan, V. P. N. Nampoori, and Periasamy Radhakrishnan. "Design and development of an LED based fiber optic evanescent wave sensor for simultaneous detection of chromium and nitrite traces in water." Optics communications 214, no. 1-6 (2002): 25-30.

[13] Joel P. Golden, George P. Anderson, S. Y. Rabbany, and F. S. Ligler. "An evanescent wave biosensor. II. Fluorescent signal acquisition from tapered fiber optic probes." IEEE Transactions on Biomedical Engineering 41, no. 6 (1994): 585-591.

[14] Yinquan Yuan, and Liyun Ding. "Theoretical investigation for excitation light and fluorescence signal of fiber optical sensor using tapered fiber tip." Optics express 19, no. 22 (2011): 21515-21523.

[15] George P. Anderson, Joel P. Golden, and Frances S. Ligler. "An evanescent wave biosensor. I. Fluorescent signal acquisition from step-etched fiber optic probes." IEEE Transactions on Biomedical Engineering 41, no. 6 (1994): 578-584.

[16] Elena Sinchenko, WE Keith Gibbs, Alexander P. Mazzolini, and Paul R. Stoddart. "The effect of the cladding refractive index on an optical fiber evanescent-wave sensor." Journal of Lightwave Technology 31, no. 20 (2013): 3251-3257.

[17] Hong S. Haddock, P. M. Shankar, and R. Mutharasan. "Fabrication of biconical tapered optical fibers using hydrofluoric acid." Materials Science and Engineering: B 97, no. 1 (2003): 87-93.

[18] Eric J. Zhang, Wesley D. Sacher, and Joyce KS Poon. "Hydrofluoric acid flow etching of low-loss subwavelength-diameter biconical fiber tapers." Optics express 18, no. 21 (2010): 22593-22598.

[19] Hani J Kbashi. "Fabrication of submicron-diameter and taper fibers using chemical etching." Journal of Materials Science & Technology 28, no. 4 (2012): 308-312.

[20] Fang-Ying Wu, Mei-Zhen Sun, Yan-Ling Xiang, Yu-Mei Wu, and Du-Qiu Tong. "Curcumin as a colorimetric and fluorescent chemosensor for selective recognition of fluoride ion." Journal of Luminescence 130, no. 2 (2010): 304-308.

[21] Mahesh P. Bhat, Pravin Patil, S. K. Nataraj, Tariq Altalhi, Ho-Young Jung, Dusan Losic, and Mahaveer D. Kurkuri. "Turmeric, naturally available colorimetric receptor for quantitative detection of fluoride and iron." Chemical Engineering Journal 303 (2016): 14-21.

[22] Ying-Jan Wang, Min-Hsiung Pan, Ann-Lii Cheng, Liang-In Lin, Yuan-Soon Ho, Chang-Yao Hsieh, and Jen-Kun Lin. "Stability of curcumin in buffer solutions and

characterization of its degradation products." Journal of pharmaceutical and biomedical analysis 15, no. 12 (1997): 1867-1876.

[23] Suresh D.Kumavat, Yogesh S.Chaudhari, Priyanka Borole, Preetesh Mishra, Khusbu Shenghani, Pallavi Duvvuri. "Degradation studies of curcumin." Int. J. Pharm. Rev. Res 3, no. 2 (2013): 50-55.

[24] Bernabé-Pineda, Margarita, Mari ́a Teresa Rami ́rez-Silva, Mario Romero-Romo, Enrique González-Vergara, and Alberto Rojas-Hernández. "Determination of acidity constants of curcumin in aqueous solution and apparent rate constant of its decomposition." Spectrochimica Acta Part A: Molecular and Biomolecular Spectroscopy 60, no. 5 (2004): 1091-1097.

[25] J. R. Lakowicz, "Solvent and environmental effects.", Principles of fluorescence spectroscopy, Springer, Boston, MA, (2006):205-235. DOI- https://doi.org/10.1007/978-0-387-46312-4_6 Online ISBN 978-0-387-46312-4

[26] C. V. Bindhu, S. S. Harilal, V. P. N. Nampoori, and C. P. G. Vallabhan. "Solvent effect on absolute fluorescence quantum yield of rhodamine 6G determined using transient thermal lens technique." Modern physics letters B 13, no. 16 (1999): 563-576.

[27] Williams, Alun T. Rhys, Stephen A. Winfield, and James N. Miller. "Relative fluorescence quantum yields using a computer-controlled luminescence spectrometer." Analyst 108, no. 1290 (1983): 1067-1071.

[28] K. Indira. Priyadarsini, "Photophysics, photochemistry and photobiology of curcumin: Studies from organic solutions, bio-mimetics and living cells." Journal of Photochemistry and Photobiology C: Photochemistry Reviews 10, no. 2 (2009): 81-95.

[29] Albert M. Brouwer, "Standards for photoluminescence quantum yield measurements in solution (IUPAC Technical Report)." Pure and Applied Chemistry 83, no. 12 (2011): 2213-2228.

[30] Christian Würth, Markus Grabolle, Jutta Pauli, Monika Spieles, and Ute Resch-Genger. "Relative and absolute determination of fluorescence quantum yields of transparent samples." Nature protocols 8, no. 8 (2013): 1535

[31] Elisa Sani, and Aldo Dell'Oro. "Spectral optical constants of ethanol and isopropanol from ultraviolet to far infrared." Optical Materials 60 (2016): 137-141.

[32] M. N. Polyanskiy, "Refractive index database," https://refractiveindex.info. Accessed on 2019-04-07.

[33] I. Kozma, P. Krok, and E. Riedle, "Direct measurement of the group-velocity mismatch and derivation of the refractive-index dispersion for a variety of solvents in the ultraviolet," J. Opt. Soc. Am. B 22, (2005): 1479-1485.

[34] http://www.op.titech.ac.jp/polymer/lab/sando/DFT_refindex/Anisole.pdf

[35] Jason R. Epstein, and David R. Walt. "Fluorescence-based fibre optic arrays: a universal platform for sensing." Chemical Society Reviews 32, no. 4 (2003): 203-214.

[36] Kwang-Taek Kim, Ki-Bum Hong, and Jae-Hee Park. "Transmission and sensing characteristics of the biconically tapered cladded multimode fibers." Journal of the Optical Society of Korea 13, no. 2 (2009): 234-239.

[37] Roopa Venkataraj, Vadakkedathu Parameswaran Narayana Nampoori, Padmanabhan Radhakrishnan, and Madanan Kailasnath. "Chemically tapered multimode optical fiber probe for fluoride detection based on fluorescence quenching of curcumin." IEEE Sensors Journal 15, no. 10 (2015): 5584-5591.

[38] J. Shi, C. Chan, Y. Pang, W. Ye, F. Tian, J. Lyu, Y. Zhang, and M. Yang, "A fluorescence resonance energy transfer (FRET) biosensor based on graphene quantum dots (GQDs) and gold nanoparticles (AuNPs) for the detection of mecA gene sequence of Staphylococcus aureus," Biosens. Bioelectron. 67, (2015): 595–600.

Chapter 4

Irradiation technique for aqueous based sensing of fluoride using Curcumin

The chapter describes the simple technique of irradiation of Curcumin using UV and visible light sources for sensing fluoride in organo-aqueous mixture solvent. Irradiation of Curcumin in the presence of fluoride facilitates its accelerated photochemical degradation leading to changes in its optical properties. The corresponding changes in optical properties with irradiation can be used to quantify fluoride in the mixture solvent. The chapter also describes the effect of irradiation time and solvent ratio on the photochemical degradation of the dye. The chapter also demonstrates the use of a simple experimental set up with low cost LED source for continuous monitoring of fluoride.

4.1 Introduction

Irradiation is the process of exposure of substances to radiation from a variety of sources. Ultra-violet (UV) and Visible light irradiation have been used for the photo-catalytic splitting of water to generate hydrogen in new generation clean energy fuel cells [1, 2]. Photo-catalysts have also been used for the breakdown of dyes, contaminants and for the conversion of atmospheric CO_2 to formate ions under visible light irradiation [3-6]. Some harmful chemicals have been reported to directly undergo degradation when exposed to UV radiation [7] and a similar principle is applied for the purification of drinking water [8]. Visible light irradiation has found applications in the treatment of acne [9] and limiting growth of bacteria that causes periodontal disease [10]. Visible light has also been used to aid nanoparticle synthesis [11] and a study indicates that nanoparticles exposed to radiation have better therapeutic properties [12].

In this chapter, the irradiation technique is described for the detection and quantification of fluoride in organo-aqueous media using Curcumin. The effect of irradiation time and type of solvent on the degradation rate of Curcumin has been discussed. The photo-degradation mechanisms involved as a result of the irradiation process and the effect of fluoride in enhancing the degradation are described in detail in the chapter

4.2 Experimental methods

4.2.1 Preparation of anion samples

10^{-5} M of Curcumin dye (Acros Organics) was dissolved in AR grade 90:10 v/v acetonitrile (CH_3CN): water (H_2O) mixture solvent. Tetrabutylammonium fluoride (TBAF, Spectrochem Pvt. Ltd., Mumbai) was added to the stock solution to get fluoride samples of varying concentrations. Separate aliquots of stock solution of Curcumin were also prepared with the addition of common tetrabutylammonium anions (Sigma Aldrich, Spectrochem India Pvt Ltd) of acetate (TBAA), dihydrogen phosphate (TBAP), hydrogen sulphate (TBAS), nitrate (TBAN), chloride (TBAC), bromide (TBAB) and iodide (TBAI).

4.2.2 Experimental set-up for irradiation

The beam of light from a 100 mW semiconductor laser (403 nm, Vortran Stradus) was converted into a 3 cm stripe by using a combination of plano-convex lens and a cylindrical lens as shown in Fig. 4.1. The peak emission wavelength from this laser source is close to

the absorption peak of Curcumin in mixture solvent. About 3.5 ml of the samples were taken in a 1 cm × 1 cm quartz cuvette and the irradiation process was carried out for varying time durations. A handheld UV lamp (365 nm) was also used to irradiate 10 ml of the samples taken in glass bottles. To study the effect of combined visible and UV light irradiation, samples of about 10 ml in volume were exposed to a 125 W mercury vapour (Hg) lamp (GE) that irradiates at the wavelengths of 364 nm, 403 nm, 435 nm, 545 nm, 576 nm and 619 nm.
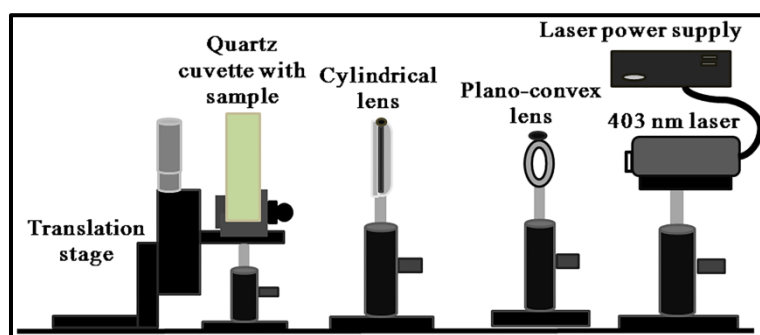
Figure 4.1 Experimental set-up for 403 nm laser irradiation process

4.2.3   Studies on variation in optical properties and structure of Curcumin upon irradiation

In order to study the changes in the optical characteristics of Curcumin upon irradiation, Jasco V-570 absorption spectrophotometer and Varian (Cary Eclipse) fluorescence spectrophotometer were used. The excitation and emission slit widths for the fluorescence measurements were fixed at 5 and 10 nm respectively. The fluorescence lifetime of the samples was recorded using Horiba (Jobin Yvon) DeltaPro lifetime measurement system.

The structural changes in the Curcumin molecule upon photochemical degradation were studied using the method of FTIR spectroscopy and Raman scattering. FTIR spectrum was recorded using Thermo Nicolet Avatar 370 FTIR spectrometer in the 400-4000 cm^{-1} range using the KBr pellet method. In this method, samples in the mixture solvent were dropped onto KBr pellet and left to dry before recording the spectrum. The samples that were irradiated for 45 minutes with 403 nm laser were used for fluorescence lifetime measurements.

Raman spectrum was recorded using WITec Alpha300RA confocal Raman microscope coupled with a 532 nm DPSS laser (70 mW) and UHTS 300 spectrograph. The samples for

Raman study were prepared by irradiating 10^{-2} M Curcumin in 70:30 v/v acetonitrile-water mixture solvent for 9 hours.

4.3 Results and Discussion

4.3.1   Response of un-irradiated Curcumin to fluoride in mixture solvent

Curcumin, with phenolic OH groups in the chemical structure responds to fluoride via complexation and subsequent deprotonation of hydrogen from the OH group [13]. In an organic solvent environment, Curcumin shows deep colour changes and the presence of the new peak can be ascribed to the complex between Curcumin and fluoride. But in the presence of even a small volume of protic solvents, the complex is disrupted and this is reflected in the optical characteristics too. In the case of organic-aqueous medium also, irrespective of the small volume used, Curcumin exhibits no significant colorimetric and optical changes. Figure 4.2 shows that there is no change in absorption and fluorescence of Curcumin in the mixture solvent of acetonitrile (CH_3CN) and water (H_2O). This is expected to happen, because of the competitive binding of water molecules and fluoride for bonding sites in Curcumin [13].
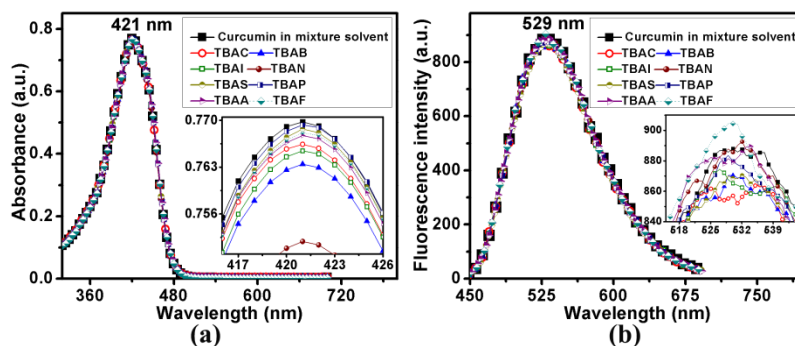
Figure 4.2 No significant changes in the (a) absorption and (b) fluorescence intensity of 10^{-5} M Curcumin in mixture solvent in the presence of common anions

However, for practical applications, the detection of fluoride in aqueous medium or even a mixture solvent is highly desirable. The optical properties of Curcumin are highly sensitive to solvent environment. Changes in temperature, polarity, pH can give rise to considerable changes in optical characteristics [14-17]. It has also been reported that the photo-stability of Curcumin is highly affected by many solvent environment parameters, a key paramenter being the solution pH. Curcumin is easily soluble in basic solvents whereas it is highly stable in acidic solvents [18, 19]. We studied the fluoride induced basicity

changes in solvent environment and the enhanced photo-degradation of Curcumin under irradiation and propose the degradation to be an indicator of fluoride content in the solution.

4.3.2 Effect of irradiation of Curcumin in the presence of fluoride

The degradation products of Curcumin have negligible absorption in the region of Curcumin absorption (400 nm-425 nm) and hence the change in absorption in this wavelength region as well as the fluorescence can serve as an effective indicator of degradation [20]. Figure 4.3 illustrates the changes in the absorption and fluorescence peaks of Curcumin under laser irradiation with varying fluoride concentration.
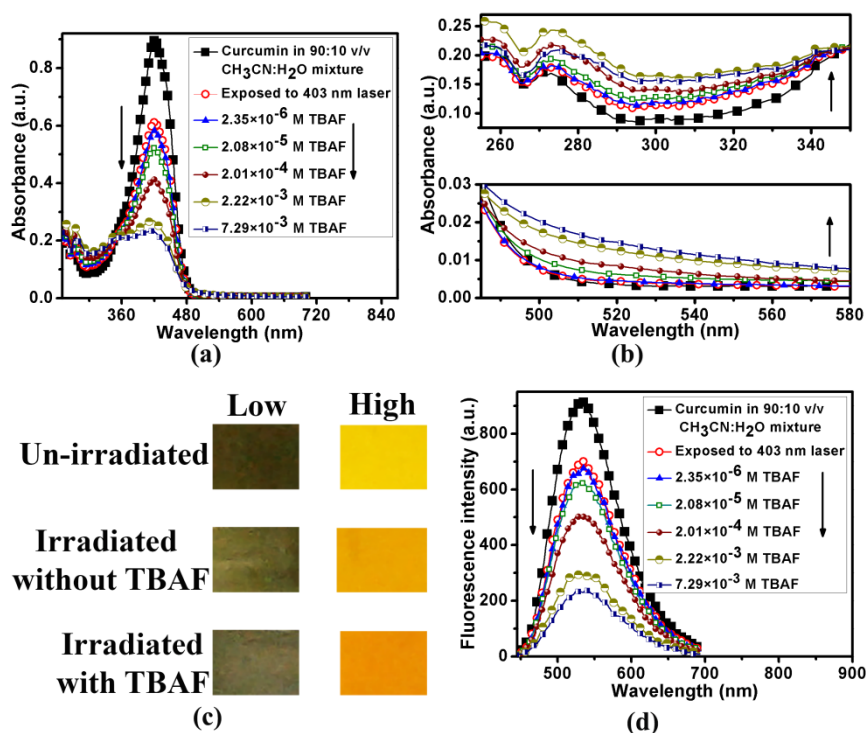
Figure 4.3 (a) Variation in absorbance corresponding to different TBAF concentration upon irradiation with laser for 45 minutes (b) Expanded views of 250-350 nm and 480-600 nm wavelength regions (c) Colour changes in solution upon irradiation with and without TBAF in the case of 10^{-5} M (low) and 10^{-2} M (high) Curcumin in mixture solvent (d) Fluorescence peak intensity changes upon laser irradiation

There is a gradual decrease in peak absorbance at 421 nm along with a slight increase in absorbance in the 250-350 nm as well as in the 480-600 nm wavelength range of the

absorption spectra. The expanded views of the two regions are as shown in Fig. 4.3b. The presence of two isobestic points in the spectra around 349 nm and 495 nm along with the aforementioned changes in peak intensity about them, points to the degradation of Curcumin and subsequent formation of its degradation products.

There are several pathways of alkaline degradation of Curcumin. Many reports suggest that the degradation products are formed via the deprotonation of phenolic OH group of Curcumin or the breakage in the heptadienedione linkage [14, 19, 21]. Curcumin exhibits keto and enol tautomeric forms in solution (structures depicted in Chapter 1). At pH below 7, Curcumin exists in the keto form and is a hydrogen atom donor whereas at pH above 8 the enol form is an electron donor [21, 22]. Curcumin is stable at acidic pH due to conjugated structure, and at higher pH, deprotonation causes a disruption of the structure [21]. Studies indicate that the degradation products formed include trans-6-(4′-hydroxy-3′-methoxy phenyl)-2,4-dioxo-5-hexanal, ferulic aldehyde, ferulic acid, feruloyl methane, vanillin and vanilic acid [19, 23, 24]. There are reports proposing that trans-6-(4′-hydroxy-3′-methoxy phenyl)-2,4-dioxo-5-hexanal is the main product of Curcumin degradation which is further broken down to Vanilin, ferulic acid, and feruloylmethane [20]. Others indicate that ferulic acid and feruloylmethane are formed initially and upon hydrolysis of feruloylmethane, vanillin and acetone are formed [21]. Separate studies in recent times reported the formation of bicyclopentadione and 7-norcyclopentadione via auto-oxidation at basic pH [25, 26].

The changes reflected in the absorption spectra shown in Fig. 4.3a indicate photo-degradation of Curcumin via multiple mechanisms upon irradiation in the mixture solvent. The increase in absorbance in the UV region may be ascribed to formation of lower molecular weight degradation products owing to breakage in the heptadienedione linkage of Curcumin [27]. The degradation products of Curcumin are reported to be yellow or brownish yellow [21, 28, 29] and hence only fading of the initial colour of the solution can be observed in the case of lower concentration of Curcumin (10^{-5} M) as depicted in Fig. 4.3c. The small increase in the absorbance above 480 nm may be due to the deprotonation of the hydroxyl group [14] or due to the polymerization of smaller chain degradation products into larger molecules [24]. Deprotonation of the hydroxyl group of Curcumin causes a deep red coloration [28] of the solution in aprotic solvents. Irradiation of higher concentration of Curcumin (10^{-2} M) in the presence of TBAF causes a deep orange colouration (Fig. 4.3c) which could be due to the deprotonation being the major mechanism of degradation. There

is also a huge decrease in fluorescence of Curcumin upon irradiation in mixture solvent in the presence of increasing fluoride indicating the conversion of fluorescent Curcumin to its degradation products. The increase of TBAF concentration increases the basicity of the solution [30]. The increase in basicity of the solvent environment of Curcumin with increase in fluoride concentration could lead to the enhanced degradation rate of Curcumin upon irradiation.

The changes in peak absorbance and fluorescence intensities with fluoride in terms of the difference in intensities (I-U) of each sample after irradiation I and before irradiation U is as shown in Fig. 4.4. The plot of peak absorption and fluorescence intensities versus the logarithm of TBAF concentration was found to be linear (not shown here). Also, the plot of change in peak absorbance and fluorescence with the logarithm of TBAF concentration as shown in the inset of Fig. 4.4 was also linear throughout the entire range of TBAF concentration. This offers the possibility of developing a simple irradiation technique for direct readout of fluoride concentration in practical applications.
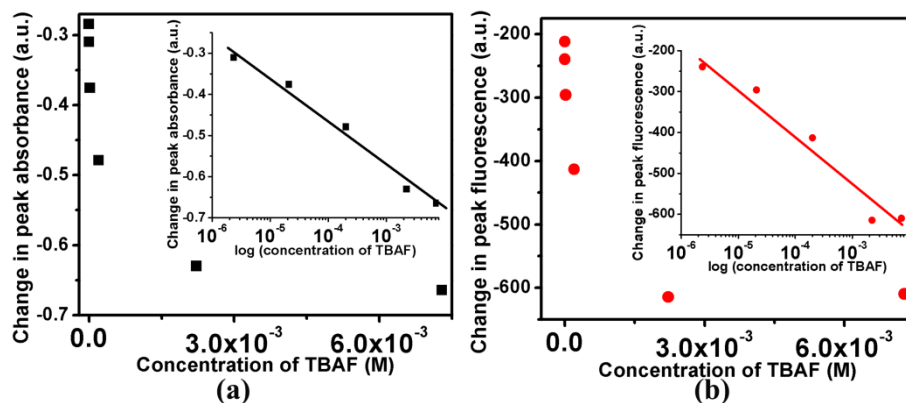
Figure 4.4 Change in (a) peak absorbance and (b) peak fluorescence after irradiation plotted as a function of TBAF concentration. Insets show the plots of change in peak intensities with logarithm of TBAF concentration

UV irradiation is also reported to give similar results of degradation as with visible light irradiation [29]. Some studies suggest that shorter wavelength light sources can lead to efficient degradation of multiple curcuminoids present in Curcumin in comparison to longer wavelength sources [23]. It was found that irrespective of the source of irradiation, the change in peak absorbance increases with irradiation time as shown in Fig. 4.5. This could be owing to the enhanced conversion of Curcumin molecules to the degradation products in the presence of fluoride upon irradiation.
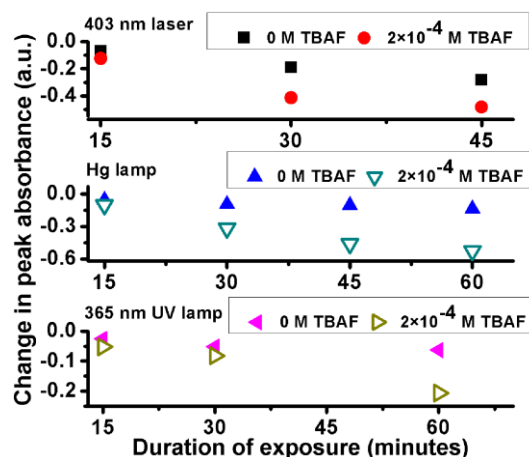
Figure 4.5 Change in peak absorbance values of 10^{-5} M Curcumin in 90:10 v/v CH_3CN:H_2O solvent with irradiation time when irradiated with different light sources
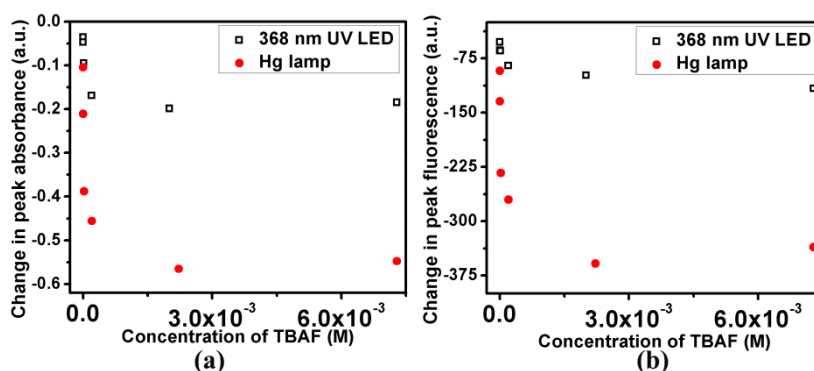
Figure 4.6 Change in (a) peak absorbance and (b) peak fluorescence with 45 minutes of irradiation using UV LED and Hg lamp

Figure 4.6 shows the change in peak absorbance and fluorescence of Curcumin when irradiated with Hg lamp and a single 368 nm UV LED source. In the case of irradiation using UV LED, the change in intensities with increase in TBAF is lesser compared to the case for Hg lamp and 403 nm laser radiation. But even so, the samples with permissible TBAF concentration and without TBAF show similar change in peak intensities whereas the toxic fluoride concentration shows an increased change in peak absorbance and fluorescence intensities. Hence a single UV LED source or an array of such LED's can be used as an efficient source for irradiation to distinguish between samples of different fluoride concentration.

4.3.3 Irradiation of Curcumin in different solvents

The effect of solvent type on irradiation and the consequent optical changes were studied by 403 nm laser irradiation of Curcumin in the presence of varying TBAF for 45 minutes. Curcumin exists in diketone form in non-polar solvents and enol form in both polar protic and aprotic solvents [31]. The enol form of Curcumin can form intermolecular hydrogen bond with solvent molecules and depending on the type of solvent, can actually provide extra stability to the dye or increase its chances to undergo photochemical degradation [32]. Acetonitrile and tetrahydrofuran are respectively polar aprotic and moderately polar aprotic solvents.

The results depicted in Fig. 4.7 show that the change in peak absorbance of acetonitrile decreases with increase in fluoride concentration. The same trend was observed in the case of tetrahydrofuran and non-polar solvent like anisole. This could be because of the conversion of Curcumin to deprotonated form in the presence of TBAF. Further irradiation does not lead to significant changes in peak absorbance values owing to lower number of Curcumin molecules present following deprotonation. However, in the solvent mixture of acetonitrile and tetrahydrofuran with water, the irradiation process shows the trend of increase in degradation rate with increase in TBAF concentration.

The effective dielectric constant ε of the mixture solvent is given by the equation [31]:

$$\varepsilon = \frac{[(\varepsilon_A \times A_v) + (\varepsilon_B \times B_v)]}{100}$$

-(4.1)

where ε_A and ε_B are respectively the dielectric constants of 'A' and 'B' solvents, A_v and B_v are volume percentages of the solvents.

The dielectric constants of water, tetrahydrofuran and acetonitrile at 20°C are 79.7, 7.6 and 37.5 respectively [33]. For 10 % volume of water in the mixture solvents, the effective dielectric constants for acetonitrile-water and tetrahydrofuran-water mixture solvents are increased to 41.72 and 14.81 respectively. The increase in dielectric constants of the solvent has been reported to enhance the degradation rate of Curcumin [32]. This can be clearly observed in the Fig 4.7 where Curcumin in acetonitrile-water mixture solvent shows comparatively higher degradation than in tetrahydrofuran-water mixture solvent. The

degradation is further enhanced with the addition of TBAF. Hence, irradiation technique using Curcumin works in different mixture solvents and can be used as a technique to detect fluoride in a wide variety of solvents.
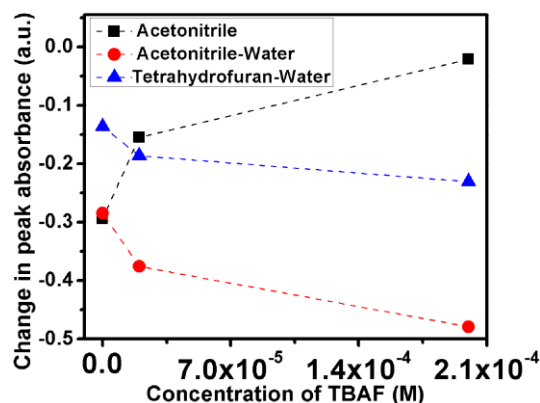
Figure 4.7 Change in peak absorbance with different fluoride concentration upon irradiation in different solvents and their mixtures with water

4.3.4   Structural studies using FTIR and Raman spectrum

The Fourier transform infrared (FTIR) spectra of the samples are as shown in Fig. 4.8a. The medium intensity band around 1640 cm^{-1} corresponds to the mixed C = O and C = C stretch in the benzene ring [34]. There is a clear increase in the transmittance in this band upon irradiation of Curcumin. The transmittance is still higher in the case of irradiation of Curcumin in the presence of fluoride.

The weak band at 1423 cm^{-1} corresponds to the in plane bending of aromatic (CCC, CCH), enolic (COH), CH in plane bending due to CH_2 [34]. Here also a huge increase in transmittance is observed in the case of irradiated Curcumin with fluoride in mixture solvent. The results of the FTIR analysis indicates a quantitative decrease in the Curcumin content as a result of irradiation in the presence of fluoride in mixture solvent pointing to the formation of degradation products of Curcumin.
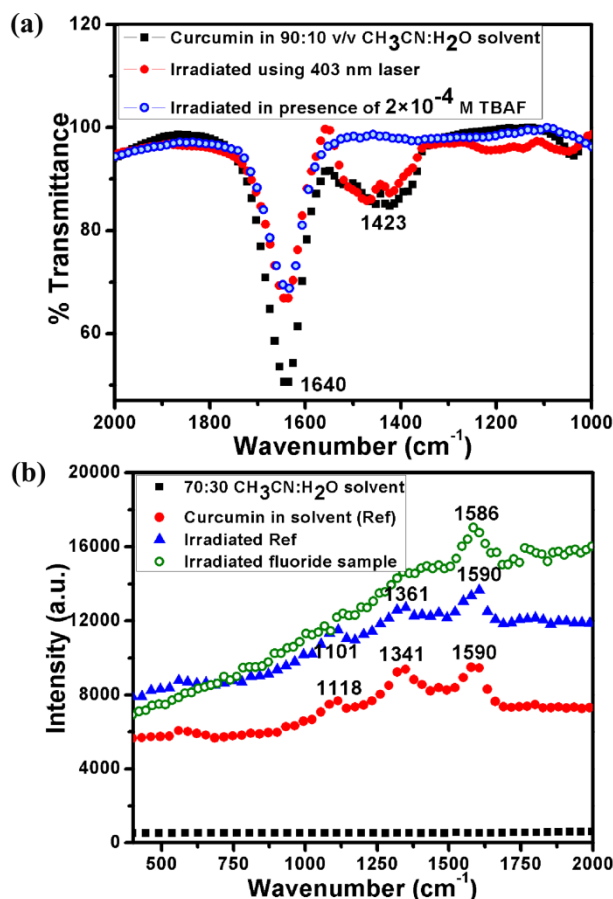
Figure 4.8 (a) FTIR spectral changes of 10^{-5} M Curcumin and (b) Variation in Raman peak intensites of 10^{-2} M Curcumin upon irradiation without and with TBAF

Raman spectrum of the un-irradiated Curcumin in mixture solvent was compared with that of irradiated Curcumin in the presence and absence of fluoride as shown in Fig. 4.8b. The band corresponding to aromatic C=C stretching at 1590 cm^{-1} is found to be slightly broadened in the case of irradiated Curcumin sample without TBAF. This band is shifted to 1586 cm^{-1} and also broadened in the case of the sample with TBAF. These changes indicate the presence of degradation products of Curcumin [24]. The region of bands around 1300-1400 cm^{-1} contains mixed vibrations. The band centered around 1341 cm^{-1} corresponds to the in plane bending of COH group in enol form, in plane bending of CCH in aromatic ring and C=C stretching. In plane bending of CCH, O-CH3 stretching vibrations and the in plane bending of CCH in the aromatic ring of enol form could be the reason for the presence of the band at 1118 cm^{-1} [35]. The reported degradation products of Curcumin i.e Vanillin exhibits a weak Raman band centered at 1375 cm^{-1} owing to the CC stretching and in CH plane bending [36] whereas Vanillic acid has two bands at 1118 cm^{-1}

owing to CO stretch of COOH and 1379 cm^{-1} owing to CH$_3$ bend and ring stretching respectively [37]. From the Raman spectrum it can be seen that both the bands at 1118 cm^{-1} and 1341 cm^{-1} show a large extent of broadening after irradiation in the presence of fluoride. Hence both these bands can involve a mixture of vibrations corresponding to both Curcumin and to a higher extent the degradation products.

4.3.5   Lifetime studies of photochemical degradation

The degradation products of Curcumin are non fluorescent. But even then, the decrease in relative amplitudes of lifetime components of Curcumin before and after irradiation can indicate a quantitative conversion of Curcumin to its degradation products. Curcumin exhibits a bi-exponential decay in many solvents including water and acetonitrile. The shorter fluorescence lifetime (~ 0.18 ns) is the major component while the longer fluorescence lifetime (~ 3 ns) is the minor component in all the samples as reported in literature [38]. A decrease in relative amplitude of the major component of lifetime from the initial 98 % to 97.3 % was noticed in the case of irradiated Curcumin sample without the presence of TBAF. This was further decreased to 91.8 % in the case of irradiated sample containing TBAF. The large decrease in relative amplitude corresponding to Curcumin indicates the enhanced photochemical degradation of Curcumin in mixture solvent in the presence of fluoride.

4.3.6   Effect of irradiation of Curcumin in the case of different anions

To study the selectivity of irradiation technique using Curcumin, the samples of Curcumin in mixture solvent with approximately 2×10^{-4} M of common anions were exposed to 403 nm laser and Hg lamp radiation for 45 minutes. Fig. 4.9 shows that in the case of both laser and Hg lamp irradiation, there is considerable decrease in absorption and fluorescence intensity with TBAF. The change in absorption and fluorescence intensity in the case of most anions is comparable to that for the blank sample. TBAF is highly basic in nature [30] and this could have caused extensive degradation of Curcumin in the vicinity of TBAF molecules. The phosphate and acetate anions are reported to have comparable basicity to TBAF and hence could possibly interfere with the response of TBAF [39]. But it was observed that the irradiation technique shows slightly higher selectivity towards TBAF compared to other anions.
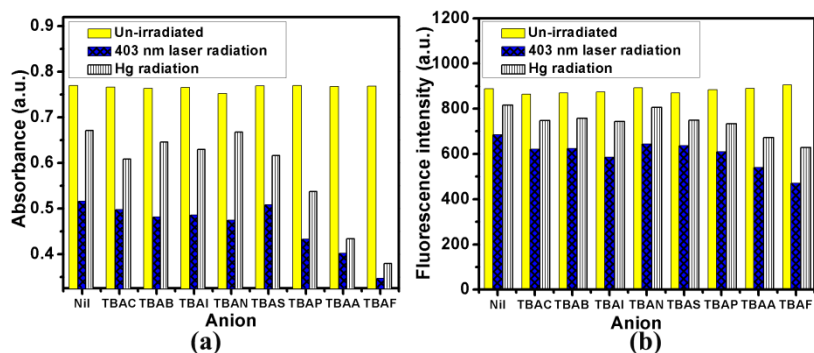
Figure 4.9 (a) Peak absorbance and (b) peak fluorescence intensity changes of Curcumin in mixture solvent upon irradiation in the presence of common anions

4.4 Sensing of fluoride in ambient light

The change in peak absorbance of Curcumin in mixture solvent kept in ambient light was also studied over a number of days (Fig. 4.10). Even though the change in colour of solution was not easily observable, there was a decrease in peak absorbance with increase in number of days of exposure to ambient light. Hence irradiation process in ambient light can also bring about changes in Curcumin over a long duration of time and this provides the possibility of using Curcumin in mixture solvent for detection of fluoride without the use of a separate irradiation source.
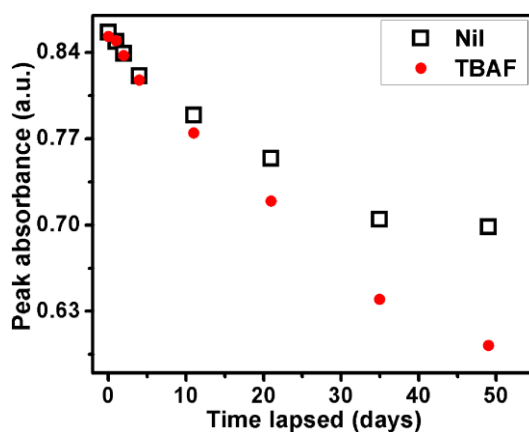
Figure 4.10 Decrease in peak absorbance of Curcumin in mixture solvent in the absence and presence of TBAF

4.5 Experimental set-up for continuous monitoring of fluoride ion via transmittance and fluorescence

The strong change in optical characteristics of Curcumin in mixture solvent upon irradiation can also be studied using simple experimental set-ups for continuous monitoring of optical changes with low cost sources and detectors. Figure 4.11 shows the experimental set-up where the samples in a cuvette are irradiated with laser focused to a spot using a bi-convex lens of focal length 3.5 cm.
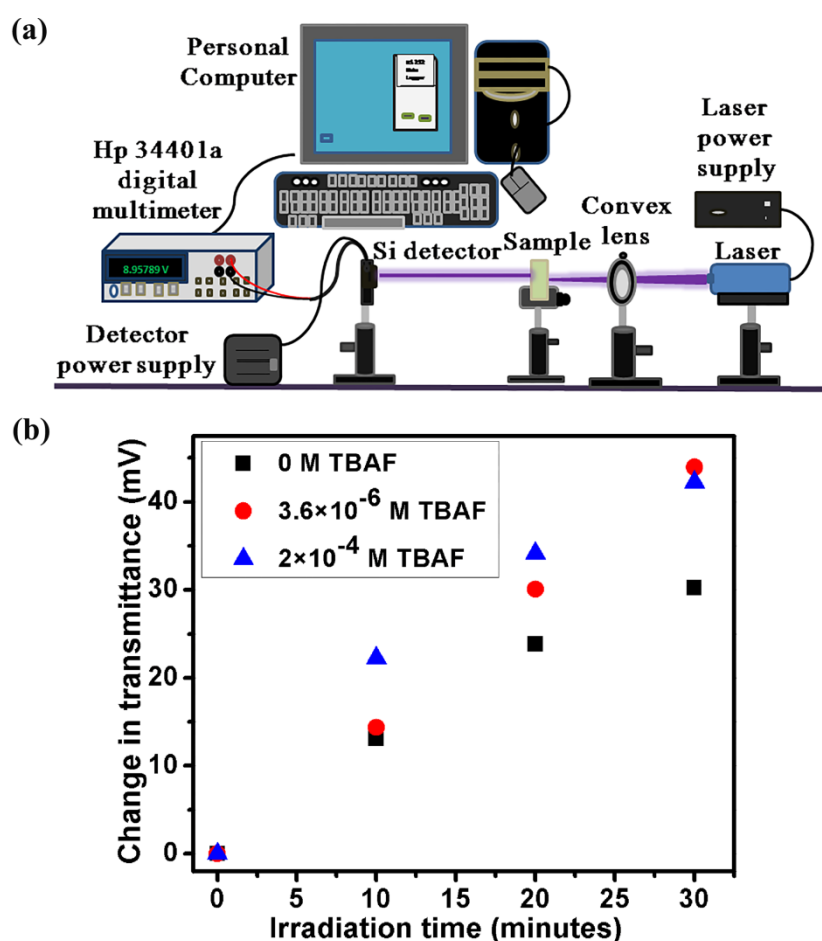
Figure 4.11 (a) Experimental set-up for continuous monitoring of transmittance of Curcumin in mixture solvent when exposed to 403 nm laser irradiation (b) Change in transmittance with respect to irradiation time corresponding to lower and higher TBAF concentration

The laser acts as the source for irradiation and also as the signal that quantifies the rate of degradation in the sample and consequently the concentration of TBAF leading to

enhanced degradation of Curcumin. From the result depicted in Fig.4.11b, it can be seen that there is an increase in the transmittance with increase in irradiation time in all the cases. But, a significant increase in transmittance was observed for the cases with Curucmin containing TBAF compared to that without TBAF.
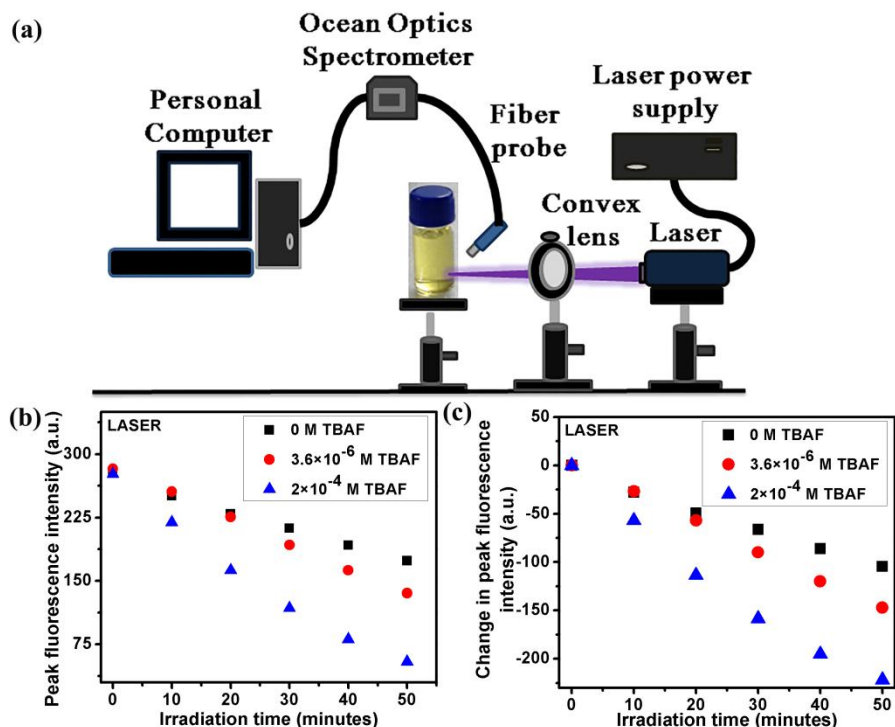
Figure 4.12 (a) Schematic of the experimental set-up for continuous monitoring of fluorescence of Curcumin in mixture solvent when exposed to 403 nm laser (b) Variation in fluorescence with respect to laser irradiation time for two TBAF concentrations (c) Change in peak fluorescence values plotted with respect to irradiation time

Figure 4.12a shows the experimental set-up for collection of fluorescence from sample taken in glass bottles irradiated with a 403 nm laser using a bi-convex lens of focal length 7.5 cm. The fluorescence is collected at a direction of 90° from incident laser path using an optical fiber cable connected to SpectraSuite HR 4000 Ocean Optics spectrometer. The results (Fig. 4.12b) show that there is a decrease in peak fluorescence intensity with irradiation time, where the decrease in fluorescence is considerably higher for TBAF samples. The decrease in fluorescence is also rapid and significantly higher in the case of toxic TBAF concentration. The experiment was also conducted using a single 368 nm UV LED (3 W, 14 nm FWHM) light directly incident on the samples taken in glass bottles and

collecting the fluorescence as described above. The glass bottles used in the experiment allows the transmission of the source UV light onto the samples inside. Figure 4.13 shows that in this case also, the change in peak fluorescence intensity increases with irradiation time and is considerably higher in the case of toxic TBAF concentration. The experiment points to the use of single LED source for continuous monitoring of fluoride in samples.
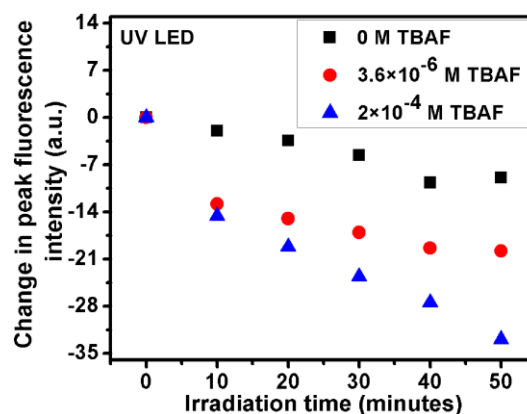
Figure 4.13 Change in fluorescence of Curcumin with irradiation time in the case of 368 nm UV LED irradiation

4.6 Colorimetric response of high concentration Curcumin to fluoride

The presence of even microliter volumes of protic solvents can lead to disruption of the bond between Curcumin and fluoride. Studies on the extraction of Curcumin for sensing fluoride in 90:10 v/v acetonitrile-water mixture solvent was reported [40]. The group reported change in colour of solution from yellow to brown upon the addition of TBAF. We tried to study the response of 10^{-2} M Curcumin to varying TBAF concentrations. As shown in Fig. 4.14a, there was a colour change from dark yellow to orange and then deep red with increasing TBAF concentration in the case of 90:10 v/v acetonitrile-water mixture solvent. But, this colour change was not observable in the case of 70:30 v/v acetonitrile-water mixture solvent (Fig. 4.14b). Also there is no considerable shift observed in the absorption peak in this case. In the case of the 90:10 v/v acetonitrile-water mixture solvent, the presence of higher concentration of Curcumin is able to provide binding sites for both water molecules and TBAF, which is not possible in the case of 70:30 v/v acetonitrile-water mixture solvent. This shows that in the presence of more than 10 percent water in the mixture solvent, it is difficult to get a colorimetric response from Curcumin, even when higher concentration of the dye is used. But irradiation technique works with higher water

percentage by simply modifying the irradiation time. Hence the TBAF concentration can be quantified using the absorption and fluorescence peak intensities upon irradiation.
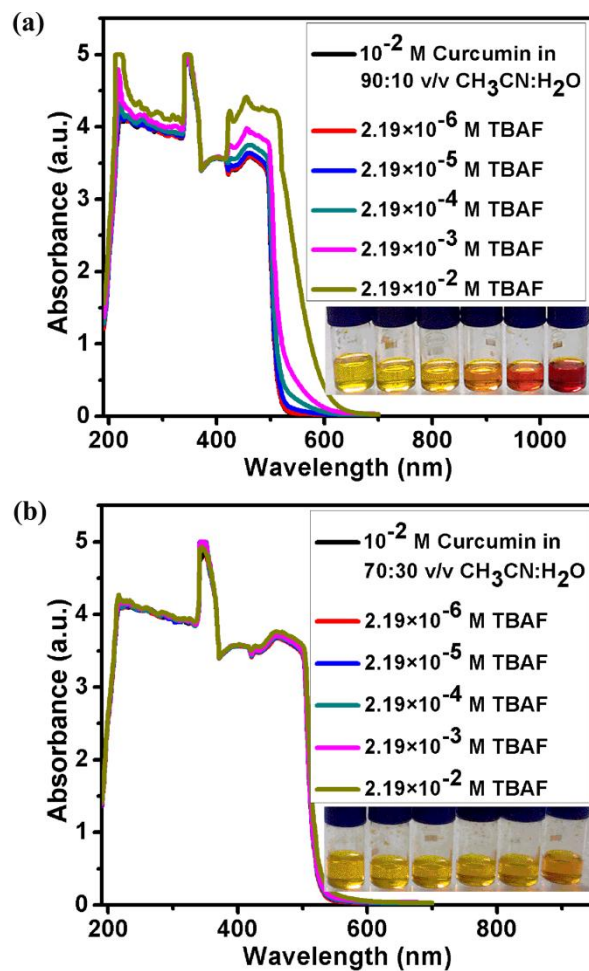
Figure 4.14 (a) Variation in absorbance of 10^{-2} M Curcumin in (a) 90:10 and (b) 70:30 v/v $CH_3CN:H_2O$ mixture solvent

4.7 Irradiation technique for detection of inorganic fluoride (NaF)

The detection of fluoride in both organic and inorganic form is highly desirable. The samples of Curcumin containing sodium fluoride (NaF) in mixture solvent was irradiated for 45 minutes using 403 nm laser radiation. The results shown in Fig.4.15 indicate that irradiation technique is effective for quantifying both inorganic and organic fluoride by using the decrease in absorbance and fluorescence of Curcumin upon irradiation.
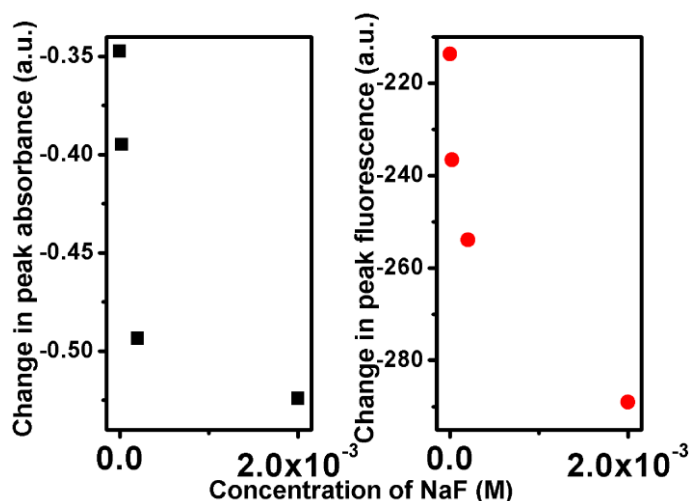
Figure 4.15 Decrease in peak absorbance and fluorescence of Curcumin with increase in NaF concentration upon irradiation in mixture solvent

4.8 Response of Curcumin to NaOH

The presence of OH^- ions can also cause degradation of Curcumin and hence it is necessary to study the effect of addition of strongly basic NaOH to the mixture solvent. From Fig. 4.16 it can be seen that in the presence of NaOH, there is change in colour of solution from dull yellow to deep red. This reddish tinge in colour of solution keeps fading with time until the colour of the solution becomes pale brown. With irradiation, the change in colour from deep red to pale brown was found to be very rapid. On the other hand, as discussed before there was no change in colour of solution in the case of fluoride samples. Also, the absorption spectrum showed decrease in absorption at 421 nm and the presence of a new peak around 510-520 nm in the case of samples with NaOH, whereas there was no shift in absorption and fluorescence peaks in the case of NaF. Both the colourimetric and optical changes in the case of NaOH can be ascribed to the rapid deprotonation of Curcumin in the presence of strong base NaOH [18]. Also, the OH deprotonation of Curcumin induced by NaOH was reported to involve both the phenolic OH groups of Curcumin whereas that in the presence of fluoride involves only a single OH group [13]. Hence it is fairly easy to distinguish between NaOH and NaF samples using the colour of solution and the corresponding optical spectra.
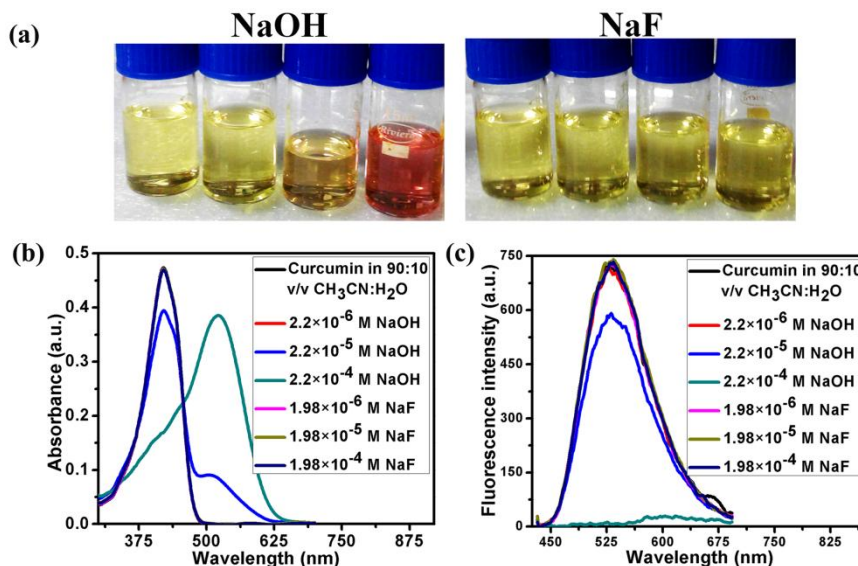
Figure 4.16 (a) Colourimetric changes of Curcumin in mixture solvent in the presence of (from left to right) 0, 2.2×10^{-6} M, 2.2×10^{-5} M and 2.2×10^{-4} M NaOH. There is no colour change in the case of fluoride samples (b) Absorption spectra and (c) Fluorescence spectra of 10^{-5} M Curcumin in the presence of NaOH and NaF

4.9 Curcumin stained filter paper strips for detection of NaF
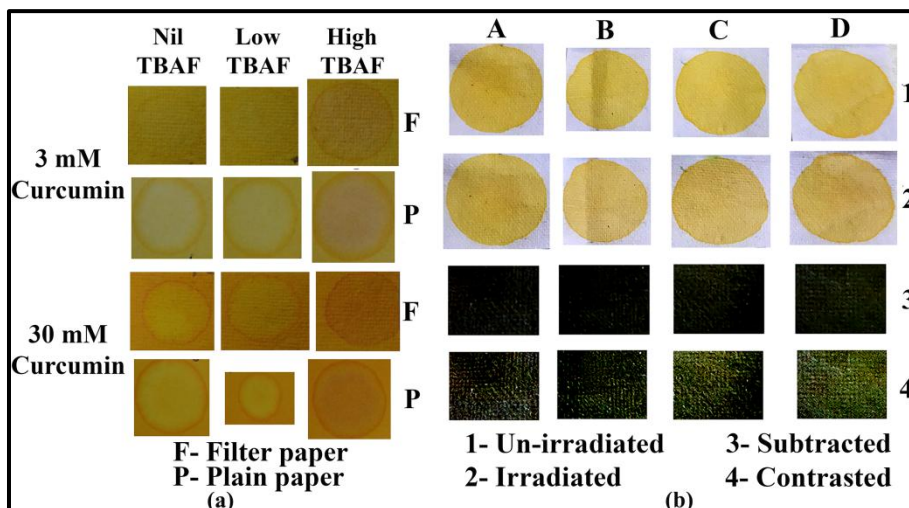
Figure 4.17 (a) Colour changes observed in filter paper and plain paper stained with 3 mM and 30 mM Curcumin on addition of low (2×10^{-6} M) and high (2×10^{-3}) TBAF concentrations (b) Change in colour of filter paper stained with 3 mM Curcumin in the presence of (A) 0 M (B) 2×10^{-6} M (C) 2×10^{-4} M and (D) 2×10^{-3} M NaF before and after UV irradiation

The irradiation technique is a versatile method for detection of fluoride but to further extend the method as an easy to use platform for sensing of fluoride, Curcumin was stained on filter paper. About 3 mM and 30 mM of Curcumin were separately dissolved in acetonitrile and the solutions were dropped onto the filter paper using a 1 mm hollow glass capillary to form spots. Filter paper and plain paper strips were also stained with the solutions by immersion into it. Samples of NaF were prepared in de-ionised water by dissolving appropriate quantities of NaF whereas TBAF was dissolved in acetonitrile. Addition of high concentration TBAF to filter and plain paper strips as shown in fig. 4.17a led to a purple colour of the strip portion as expected. But the addition of NaF samples dissolved in water did not lead to any significant colour changes. Equal volumes of the NaF samples were dropped onto the stained Curcumin spots on the filter paper. The spots were illuminated by handheld 365 nm UV lamp for 15 minutes. A mobile phone camera was used to record images of the spots before the addition of fluoride samples (row 1) and after irradiation of the spots (row 2) as shown in the Fig. 4.17b.

Fig. 4.17b (row 2) shows the clear colour change between the samples with no NaF from those with NaF. The central region of the spots, where major diffusion of liquid is expected was selected and for each concentration of NaF, the images before irradiation and after irradiation were subtracted using Image J software. As shown in row 3 there is almost near dark region in the resultant image of subtraction for 0 M NaF. But with increase in concentration of fluoride, the yellowish green tinge increases. The contrast of the images was increased for clarity as shown in row 4. This clearly shows the stark change in different concentrations of fluoride as identified by the yellow-green regions in the image. Hence the irradiation technique can easily be extended to fluoride detection with low cost materials, light sources, image capturing and processing software.

4.10 Conclusions

The irradiation technique involving exposure of Curcumin to UV, Visible and mixed UV-Visible radiation led to degradation of Curcumin. The degradation was studied using the changes in absorption, fluorescence spectra, FTIR and Raman spectroscopy. The photo-chemical degradation of Curcumin was enhanced upon the addition of TBAF owing to the increase in basicity of the mixture solvent environment in the presence of TBAF. The degradation was also found to increase with increase in exposure time in all cases of irradiation. Enhanced degradation rate was observed in the case of solvents with large

dielectric constant. Simple experimental set-ups were demonstrated for the continuous monitoring of TBAF using low cost light sources. The irradiation technique was further extended to low cost, easy to use filter paper strips to detect NaF with the help of mobile phone camera and image processing software.

4.11 References

[1] Zhigang Zou, Jinhua Ye, Kazuhiro Sayama, and Hironori Arakawa. "Direct splitting of water under visible light irradiation with an oxide semiconductor photocatalyst." Nature 414, no. 6864 (2001): 625-627.

[2] Jum Suk Jang, Hyun Gyu Kim, Upendra A. Joshi, Ji Wook Jang, and Jae Sung Lee. "Fabrication of CdS nanowires decorated with TiO2 nanoparticles for photocatalytic hydrogen production under visible light irradiation." International Journal of Hydrogen Energy 33, no. 21 (2008): 5975-5980.

[3] X. Z. Li, F. B. Li, C. L. Yang, and W. K. Ge. "Photocatalytic activity of WOx-TiO2 under visible light irradiation." Journal of Photochemistry and Photobiology A: Chemistry 141, no. 2-3 (2001): 209-217.

[4] Junwang Tang, Zhigang Zou, and Jinhua Ye. "Photocatalytic decomposition of organic contaminants by Bi 2 WO 6 under visible light irradiation." Catalysis Letters 92, no. 1-2 (2004): 53-56.

[5] Chen, Chuncheng, Wanhong Ma, and Jincai Zhao. "Semiconductor-mediated photodegradation of pollutants under visible-light irradiation." Chemical Society Reviews 39, no. 11 (2010): 4206-4219

[6] Nasrin Sadeghi, Shahram Sharifnia, and Trong-On Do. "Enhanced CO_2 photoreduction by a graphene–porphyrin metal–organic framework under visible light irradiation." Journal of Materials Chemistry A 6, no. 37 (2018): 18031-18035.

[7] Ilho Kim and Hiroaki Tanaka. "Photodegradation characteristics of PPCPs in water with UV treatment." Environment International 35, no. 5 (2009): 793-802.

[8] Getoff, Nikola. "Purification of drinking water by irradiation. A review." Journal of Chemical Sciences 105, no. 6 (1993): 373-391.

[9] P. Papageorgiou, A. Katsambas, and A. Chu. "Phototherapy with blue (415 nm) and red (660 nm) light in the treatment of acne vulgaris." British journal of Dermatology 142, no. 5 (2000): 973-978.

[10] M. Fukui, M. Yoshioka, K. Satomura, H. Nakanishi, and M. Nagayama. "Specific-wavelength visible light irradiation inhibits bacterial growth of Porphyromonas gingivalis." Journal of periodontal research 43, no. 2 (2008): 174-178.

[11] P. K. Sudeep,, and Prashant V. Kamat. "Photosensitized growth of silver nanoparticles under visible light irradiation: a mechanistic investigation." Chemistry of materials 17, no. 22 (2005): 5404-5410.

[12] Rita Mendes, Pedro Pedrosa, João C. Lima, Alexandra R. Fernandes, and Pedro V. Baptista. "Photothermal enhancement of chemotherapy in breast cancer by visible irradiation of Gold Nanoparticles." Scientific reports 7, no. 1 (2017): 10872

[13] Fang-Ying Wu, Mei-Zhen Sun, Yan-Ling Xiang, Yu-Mei Wu, and Du-Qiu Tong. "Curcumin as a colorimetric and fluorescent chemosensor for selective recognition of fluoride ion." Journal of Luminescence 130, no. 2 (2010): 304-308.

[14] K. Indira Priyadarsini, "Photophysics, photochemistry and photobiology of curcumin: Studies from organic solutions, bio-mimetics and living cells", Journal of Photochemistry and Photobiology C: Photochemistry Reviews 10 (2009): 81–95.

[15] Yuval Erez, Itay Presiado, Rinat Gepshtein, and Dan Huppert, "Temperature Dependence of the Fluorescence Properties of Curcumin", J. Phys. Chem. A, 115, (2011): 10962–10971.

[16] Pill-Hoon Bong, "Spectral and Photophysical Behaviors of Curcumin and Curcuminoids", Bull. Korean Chem. Soc., Vol. 21, no. 1, (2000): 81-86.

[17] Ramya Jagannathan, Priya Mary Abraham, and Pankaj Poddar. "Temperature-dependent spectroscopic evidences of curcumin in aqueous medium: a mechanistic study of its solubility and stability." The Journal of Physical Chemistry B 116, no. 50 (2012): 14533-14540.

[18] Ying-Jan Wang, Min-Hsiung Pan, Ann-Lii Cheng, Liang-In Lin, Yuan-Soon Ho, Chang-Yao Hsieh, and Jen-Kun Lin. "Stability of curcumin in buffer solutions and characterization of its degradation products." Journal of pharmaceutical and biomedical analysis 15, no. 12 (1997): 1867-1876.

[19] Hanne Hjorth Tønnesen, Jan Karlsen, and Gerard Beijersbergen van Henegouwen. "Studies on curcumin and curcuminoids VIII. Photochemical stability of curcumin." Zeitschrift für Lebensmittel-Untersuchung und Forschung 183, no. 2 (1986): 116-122.

[20] Mai Mouslmani, Kamal H. Bouhadir, and Digambara Patra. "Poly (9-(2-diallylaminoethyl) adenine HCl-co-sulfur dioxide) deposited on silica nanoparticles constructs hierarchically ordered nanocapsules: curcumin conjugated nanocapsules as a novel strategy to amplify guanine selectivity among nucleobases." Biosensors and Bioelectronics 68 (2015): 181-188.

[21] Suresh D. Kumavat, Yogesh S. Chaudhari, Priyanka Borole, Preetesh Mishra, Khusbu Shenghani, and Pallavi Duvvuri. "Degradation studies of curcumin." Int J Pharm Rev Res 3, no. 2 (2013): 50-55.

[22] Parth Malik, and Tapan K. Mukherjee. "Structure-function elucidation of antioxidative and prooxidative activities of the polyphenolic compound curcumin." Chinese Journal of Biology 2014 (2014).

[23] Francisco G. Rego-Filho, Maria T. de Araujo, Kleber T. de Oliveira, and Vanderlei S. Bagnato. "Validation of photodynamic action via photobleaching of a new curcumin-based composite with enhanced water solubility." Journal of fluorescence 24, no. 5 (2014): 1407-1413.

[24] Maria Vega Cañamares, Jose V. Garcia-Ramos, and Santiago Sanchez-Cortes. "Degradation of curcumin dye in aqueous solution and on Ag nanoparticles studied by ultraviolet–visible absorption and surface-enhanced Raman spectroscopy." Applied spectroscopy 60, no. 12 (2006): 1386-1391.

[25] Odaine N. Gordon, Paula B. Luis, Herman O. Sintim, and Claus Schneider. "Unraveling Curcumin Degradation-Autoxidation proceeds through Spiroepoxide and Vinylether intermediates en route to the main Bicyclopentadione." Journal of Biological Chemistry 290, no. 8 (2015): 4817-4828.

[26] Joseph, Akil I., Paula B. Luis, and Claus Schneider. "A Curcumin Degradation Product, 7-Norcyclopentadione, Formed by Aryl Migration and Loss of a Carbon from the Heptadienedione Chain." Journal of natural products 81, no. 12 (2018): 2756-2762.

[27] Jiahn-Haur Liao, Yi-Shiang Huang, Yu-Ching Lin, Fu-Yung Huang, Shih-Hsiung Wu, and Tzu-Hua Wu, "Anticataractogenesis Mechanisms of Curcumin and a Comparison of Its Degradation Products: An in Vitro Study." Journal of agricultural and food chemistry 64, no. 10 (2016): 2080-2086.

[28] Lisa C. Price, and R. W. Buescher. "Kinetics of alkaline degradation of the food pigments curcumin and curcuminoids." Journal of food science 62, no. 2 (1997): 267-269.

[29] Bo Hyun Lee, Hyun A. Choi, Mi-Ri Kim, and Jungil Hong. "Changes in chemical stability and bioactivities of curcumin by ultraviolet radiation." Food Science and Biotechnology 22, no. 1 (2013): 279-282.

[30] Qu, Yi, Sanyin Qu, Lin Yang, Jianli Hua, and Dahui Qu. "A red-emission diketopyrrolopyrrole-based fluoride ion chemosensor with high contrast ratio working in a dual mode: solvent-dependent ratiometric and "turn on" pathways," Sensors and Actuators B: Chemical 173 (2012): 225-233.

[31] Ornchuma Naksuriya, Mies J. van Steenbergen, Javier S. Torano, Siriporn Okonogi, and Wim E. Hennink. "A kinetic degradation study of curcumin in its free form and loaded in polymeric micelles." The AAPS journal 18, no. 3 (2016): 777-787.

[32] Luca Nardo, Roberta Paderno, Alessandra Andreoni, Már Másson, Tone Haukvik, and Hanne Hjorth TØnnesen. "Role of H-bond formation in the photoreactivity of curcumin." Journal of Spectroscopy 22, no. 2-3 (2008): 187-198.

[33] Ian M Smallwood, Handook of Organic solvent properties, Halsted Press, New York, 1996, pp. 217, 289, 301.

[34] P R Krishna Mohan, G. Sreelakshmi, C. V. Muraleedharan, and Roy Joseph, "Water soluble complexes of curcumin with cyclodextrins: Characterization by FT-Raman spectroscopy." Vibrational Spectroscopy 62 (2012): 77-84.

[35] Tsonko M. Kolev, Evelina A. Velcheva, Bistra A. Stamboliyska, and Michael Spiteller. "DFT and experimental studies of the structure and vibrational spectra of curcumin." International Journal of Quantum Chemistry 102, no. 6 (2005): 1069-1079.

[36] V. Balachandran, and K. Parimala. "Vanillin and isovanillin: Comparative vibrational spectroscopic studies, conformational stability and NLO properties by density functional theory calculations." Spectrochimica Acta Part A: Molecular and Biomolecular Spectroscopy 95 (2012): 354-368.

[37] E. Clavijo, J. R. Menéndez, and R. Aroca. "Vibrational and surface-enhanced Raman spectra of vanillic acid." Journal of Raman Spectroscopy: An International Journal for Original Work in all Aspects of Raman Spectroscopy, Including Higher Order Processes, and also Brillouin and Rayleigh Scattering 39, no. 9 (2008): 1178-1182.

[38] Digambara Patra, Christelle Barakat, "Synchronous fluorescence spectroscopic study of solvatochromic curcumin dye", Spectrochimica Acta Part A 79 (2011) 1034–1041.

[39] Soon Young Kim, and Jong-In Hong. "Chromogenic and fluorescent chemodosimeter for detection of fluoride in aqueous solution." Organic letters 9, no. 16 (2007): 3109-3112.

[40] Mahesh P. Bhat, Pravin Patil, S. K. Nataraj, Tariq Altalhi, Ho-Young Jung, Dusan Losic, and Mahaveer D. Kurkuri. "Turmeric, naturally available colorimetric receptor for quantitative detection of fluoride and iron." Chemical Engineering Journal 303 (2016): 14-21.

Chapter 5

Curcumin-Aluminium complexes for sensing fluoride, phosphate and acetate

In this chapter, the preparation of complexes of natural dye Curcumin with Aluminium and their sensing response towards inorganic salts of fluoride, phosphate and acetate in organo-aqueous medium have been described. Different ratios of Curcumin to Aluminium were prepared by varying the molar ratios of the precursors. The variations in optical characteristics of the dye-metal complexes in response to the three anions are discussed in the chapter. The limit of detection and range of detection of each complex towards the anions are estimated. The lower molar ratio of Curcumin-Aluminium complex had the lowest limit of detection whereas the complex with the higher molar ratio exhibited higher values for maximum measureable anion concentration. The response of a polymer fiber sensor doped with Curcumin-Aluminium complex towards the three anions has also been described in the chapter.

5.1 Introduction

The importance of fluoride ion, the sources, the main methods of detection and the harmful effects of fluoride have already been reviewed in Chapter 1. As discussed in the chapter, the permissible limits of fluoride in drinking water is around 1.5 ppm as per WHO (1 ppm in India) and 4 ppm as per United States Environmental Protection Agency [1, 2].

Acetate ion is one of the most important biological anions with huge relevance in biochemical, environmental, pharmaceutical science and industrial applications [3, 4]. Many sensors have been reported for acetate including ion selective electrodes [5], colorimetric and fluorimetric probes [3, 6, 7]. The fluorimetric probes involve phenol based azo dyes and azo dyes with metal centre using the mechanism of proton removal and displacement of counter ions respectively, upon addition of acetate ion [6, 7]. Some of the other sensors report the use of Schiff base [3] that undergoes deprotonation in the presence of acetate.

Phosphorous is found in biological molecules like phospholipids, nucleic acids etc [8]. Phosphate is reported to play an important role in many basic processes like energy conversion and muscle contraction. It also finds use in the preparation of chemotherapy and antivirul drugs [9]. Phosphates can be inorganic or organic in nature and they are mainly classified as orthophosphates, polyphosphates and organic phosphates. Orthophosphates include H_3PO_4, $H_2PO_4^{2-}$, HPO_4^{2-}, PO_4^{3-} depending on the pH of water [10]. The use of synthetic detergents and fertilizers can cause excess phosphate in water resources [11]. The leaching of fertilizers and chemicals into water bodies eventually favour the growth of plankton making water unsuitable for drinking purposes. It also leads to abnormal algal blooming or eutrophication causing depletion of dissolved oxygen in water in turn harming aquatic life too [11].

The maximum permissible limit of phosphate in drinking water as set by the WHO is 1 ppm [11]. The most basic method for detection of orthophosphate involves the use of ammonium molybdate which forms a yellow coloured complex upon reaction with orthophosphate, but this method has low specificity [8]. The standard methods reported for phosphate detection are potentiometric methods and ion chromatography which are time consuming, tedious and expensive [11]. Many other detection techniques involve evanescent wave fiber optic sensor using ammonium molybdate [12], fluorescence based sensors using complexes of Zn [13] and Cu [9, 14], hydrogen bonding interaction of ferrocene amide [15] and morin dye-hydrotalcite complex used in hydrogel membranes

[16]. There are many sensors for the detection of fluoride and acetate [17, 18] as well as those that detect fluoride, acetate and phosphate [19-23]. The mechanisms used for detection mostly involve hydrogen bonding [19-23] and metal-ligand interaction [17, 18]

Many organo-metallic complexes find applications in medicine, catalysis, biological and analytical fields [24]. Dye metal complexes are extensively used in textile industry [25] and medicine [26]. They have also emerged as a versatile tool for sensing applications including sensing of biochemical species [27], chemical species [28]. These complexes are also known for their capability of array based sensing using a single dye with different metal centers or under different pH conditions [29]. The advantages of using dye metal complexes for sensing includes the generally different optical properties of dye-metal complexes in comparison to the dye alone, the high binding capacity of the metal with the dye as well as the analyte in aqueous or polar environment [29] and the electrostatic type of interaction of the metal centre [6]. Also, the metal-ligand interaction can be highly selective toward certain anions depending on the geometry [13]

A large number of metal complexes of Curcumin have been reported for a wide variety of applications as described in detail in the review by Wanninger et al [26]. Zinc-Curcumin complexes have been used for ZnO nanoparticle synthesis and Nickel complexes finds use in the modification of oxidation electrodes [26]. Gold-Curcumin complexes have been used as an anti-arthritic, whereas Curcumin complexes of Copper, Aluminium, Indium and Galium have been reported to possess anti-cancer properties [26, 30]. Antioxidant properties have been reported for Curcumin complexes of Manganese, Copper, Indium and Galium [26, 31]. The bio-imaging, antiviral and antimicrobial applications of Curcumin complexes have also been reported [24, 26]. There is a lot of ongoing research on the formation of Curcumin complex with certain metals that are associated with the onset of Alzheimers disease [26, 32]. Metal complexes of Curcumin have been reported to be comparatively more stable than the parent Curcumin molecule [33].

The chapter describes the use of Curcumin-Aluminium (Cur-Al) complexes for the detection of fluoride, phosphate and acetate. The non-hydrogen bonding nature of the interaction between the dye metal complex and the anions led to optical response even in mixture solvents containing high water content.

5.2 Experimental methods

The preparation of metal complexes of Curcumin generally involves the treatment of Curcumin with a strong base for deprotonation to take place and then a subsequent reaction with metal halide salts [26]. Curcumin-Aluminium complexes were prepared as reported in literature [32]. Curcumin (12 mM) (Acros Organic) and Aluminium chloride hexahydrate ($AlCl_3$.$6H_2O$, Sigma aldrich) were dissolved in methanol and water respectively. The solutions of Curcumin and varying concentrations of $AlCl_3$ were mixed in the volume ratio of 6:1 so that the resultant concentration of Curcumin and aluminium were in the molar ratio of 1:1, 1:2 and 1:4 (denoted as 1:1 Cur:Al, 1:2 Cur:Al and 1:4 Cur:Al respectively). These stock solutions of the complexes were then individually diluted using 50:50 v/v Methanol (MeOH): water (H_2O) mixture solvent and used for testing the response of anions.

The sodium salts of common anions like chloride (NaC, Merck), bromide (NaB, SRL chemicals Pvt. Ltd), nitrate (NaN, Merck), hydrogen sulphate (NaS, Nice chemicals), di-hydrogen phosphate (NaP, Merck), fluoride (NaF, Merck) and acetate (NaA, Fischer Scientific) were used to prepare anion stock solutions of required concentrations in de-ionised water. The absorption and fluorescence variation in the samples were studied using Jasco V-570 UV-Vis-NIR spectrophotometer and Varian (Cary Eclipse) fluorescence spectrophotometer respectively. The slit widths for excitation and emission of fluorescence were 5 nm and 10 nm respectively.

5.3 Results and discussion

5.3.1   Effect of anions on the optical properties of Curcumin

The normalized absorption and fluorescence response of Curcumin in 50:50 v/v MeOH:H_2O mixture solvent is as shown in Fig. 5.1a and its optical response in the presence of sodium salts of common anions is as shown in Fig. 5.1b. Curcumin has an absorption peak at 429 nm and fluorescence emission centered at 541 nm. It can be seen that in the presence of common anions there is no change in absorption or fluorescence of Curcumin. This could be owing to the presence of water which may lead to competitive binding between water molecules and anions [34].
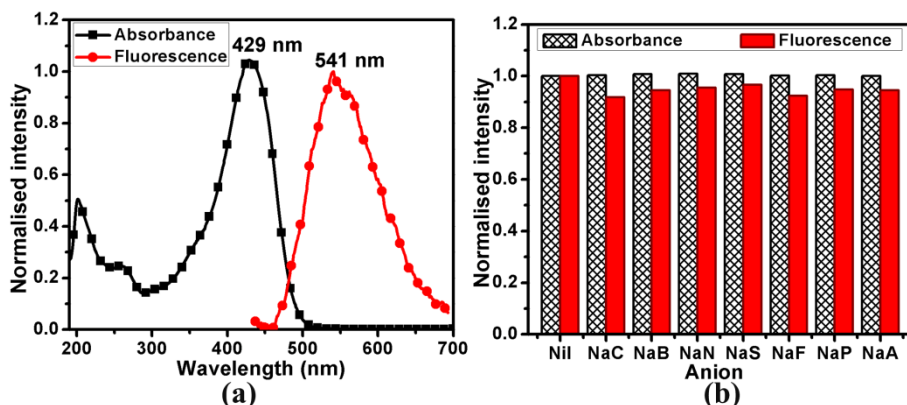
Figure 5.1 (a) Absorbance and fluorescence spectrum of Curcumin in 50:50 v/v MeOH:H_2O mixture solvent (b) Response of Curcumin towards common anions
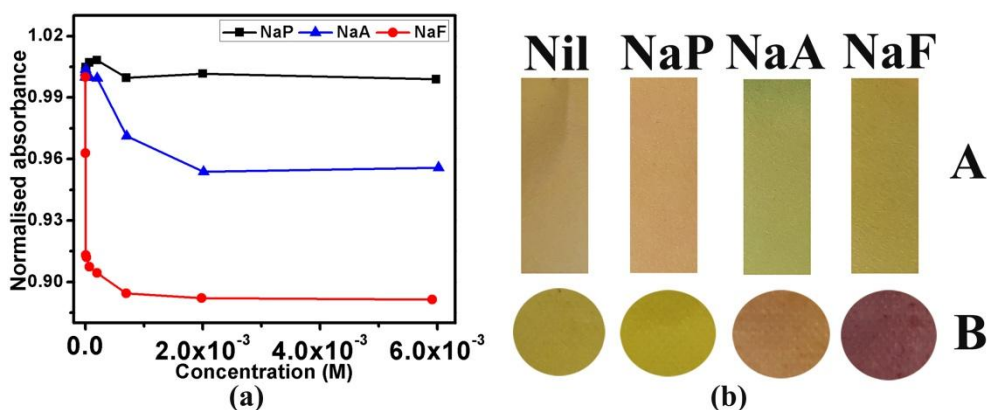
Figure 5.2 (a) Effect of addition of NaP, NaA and NaF on the absorbance of Curcumin in MeOH:H_2O mixture solvent (b) Colour changes of (A) standard pH paper and (B) Curcumin stained filter paper upon addition of 1 M NaP, NaA and NaF anions

The variation of normalized peak absorbance of Curcumin in mixture solvent upon addition of dihydrogen phosphate, acetate and fluoride is as shown in Fig. 5.2a. It can be seen that NaP exhibits no response in Curcumin whereas a decrease of 0.1 units was observed in the case of NaF. NaP, NaA and NaF are highly basic anions, and fluoride having the highest hydrogen bonding tendency [6, 23], it bonds with Curcumin at the phenolic OH site causing a decrease in absorbance. This was verified using standard pH paper and Curcumin stained filter paper as shown in Fig. 5.2b. Acetate shows a bluish green tinge in the pH paper indicating high basicity whereas fluoride has slightly less basicity. But in the case of Curcumin stained filter paper, fluoride showed dark purple colouration indicating the formation of a complex [34]. The pH of the solutions of 3×10^{-4} M

of NaP, NaF and NaA in de-ionised water were also measured using Lutron 206 pH meter and were found to be around 5.53, 6 and 6.5 respectively.

5.3.2 Cur-Al complexes

The formation of metal complexes depends on a variety of factors like concentration of reactants, solvent type and source of metal ion [33]. The formation and structural conformation of various Curcumin-Aluminium (Cur:Al) complexes have been described in detail by Jiang et al [32]. The absorption and fluorescence spectra of the prepared Cur:Al for different molar ratio of the precursors are as shown in Fig. 5.3. Curcumin has three OH sites which can be used for metal complexation, but the predominantly used site involves the OH of the β-diketone chain. Three types of complexes were reported to form at different molar ratios of Curcumin and Aluminium namely [Al(III)][curcumin]$_2$, [Al(III)]$_2$[curcumin]$_2$ and [Al(III)]$_2$[curcumin]. The complex of the type [Al(III)][curcumin]$_2$ was reported to be the dominant complex formed at lower molar ratio of Curcumin:Aluminium, whereas [Al(III)]$_2$[curcumin] was reported to be the most stable form of the complex at higher molar ratios [32].
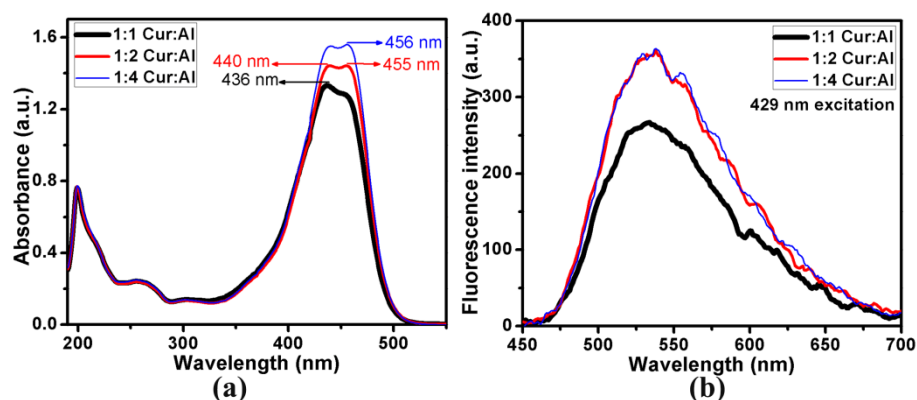
Figure 5.3 (a) Absorbance and (b) fluorescence of 1:1, 1:2 and 1:4 Cur:Al complexes in 50:50 v/v MeOH:H$_2$O mixture solvent

The peak absorption of 1:1 Cur:Al complex is at around 436 nm with a shoulder at 455 nm. The peaks at 440 nm and 455 nm are of approximately equal intensity for the 1:2 complex whereas the absorption peak of 1:4 complex is at around 456 nm. The increase in absorption with increase in molar ratio of Cur:Al is in accordance with literature [32]. Curcumin complexes have a shifted absorption spectrum (~1-8 nm) compared to Curcumin

alone [24, 32]. The peaks at 436 nm and 455 nm/456 nm can be attributed to the complexes of Curcumin with Aluminium [32]. The absorption peaks as well as the shoulders in absorption spectrum are expected to be different for different complexes depending on the metal ion [24]

5.3.3 Effect of anions on optical properties of Cur-Al complexes

The effect of different anions on the response of the prepared Cur:Al complexes is as shown in Fig. 5.4. It was observed that the anions NaP, NaA and NaF showed decrease in absorption and fluorescence intensity for all the complexes.
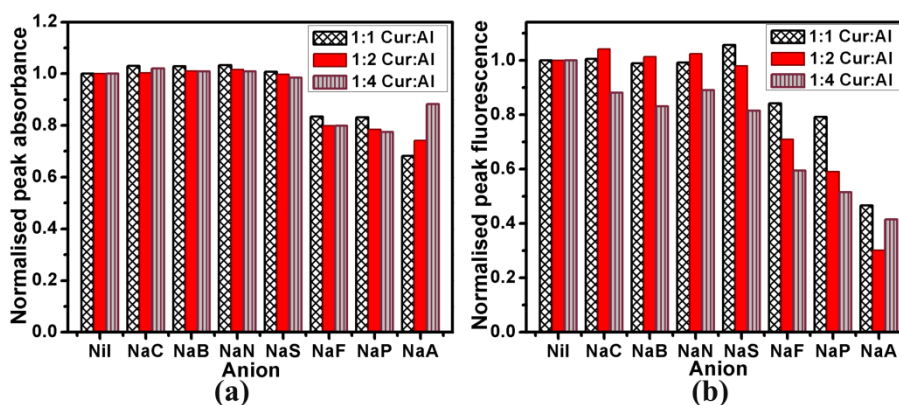
Figure 5.4 Normalised peak (a) absorbance and (b) fluorescence of 1:1, 1:2 and 1:4 Cur:Al complexes towards 2×10^{-4} M common anions

There was also blue shift in the absorption peaks of all the complexes towards the absorption peak of Curcumin alone (~429 nm) with increase in concentration of anions (Fig. 5.5). This indicates the conversion of Cur:Al complex to Curcumin via the displacement of Al cation from the complex. It is also possible that a sequential conversion of higher molar ratio Cur:Al complexes to lower ratio complexes could be taking place before the final conversion to Curcumin upon addition of higher concentration of anion. The complexes exhibit high selectivity towards NaP, NAF and NaA compared to other anions as can be seen from the peak absorption wavelength shift. Only NaP, NaF and NaA exhibit drastic shifts of wavelength towards the blue region of the spectrum. The other common anions evidently did not induce any change in the Cur:Al complexes.
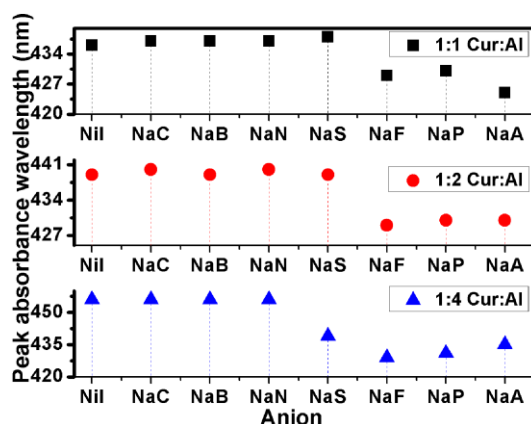
Figure 5.5 Shift in peak absorbance wavelength of the complexes in the presence of 2×10^{-4} M of common anions

5.3.4 Response of Cur-Al complexes to fluoride, phosphate and acetate

The effect of NaP, NaF and NaA addition to Cur-Al complexes were individually studied. Figures 5.6 and 5.7 show the decrease in absorption and fluorescence intensity of the 1:1 Cur:Al complex with increase in NaP.
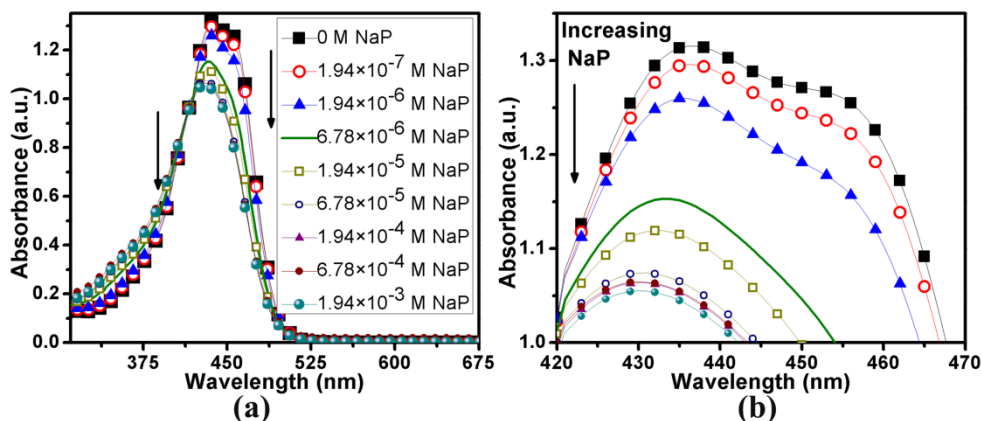
Figure 5.6 (a) Absorbance variation of 1:1 Cur:Al complex towards increasing NaP concentration (b) Expanded view of the peak absorbance showing blue shift in peak with increasing concentration

The blue shift in absorption peak is also very clear. The dihydrogen phosphate anion $H_2PO_4^-$ (NaP) has been reported to form complexes of the form $Al(H_2PO_4)_3$ via removal of Al from Al-morin complex [16, 35]. There are also reports of aluminium based compounds being used for removal of phosphate ions [36].

[127]
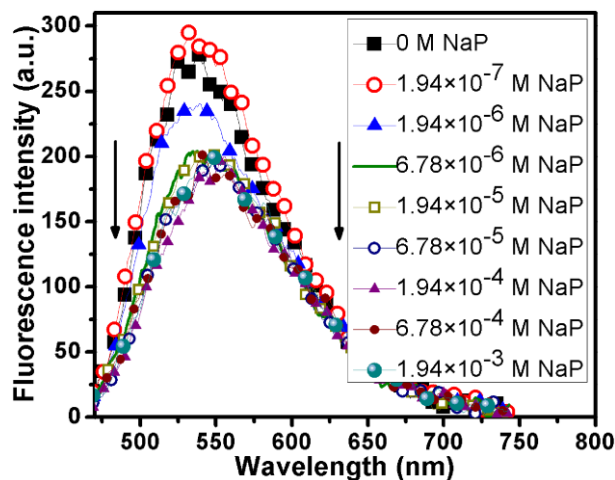
Figure 5.7 Fluorescence decrease of 1:1 Cur:Al complex in the presence of NaP (436 nm excitation wavelength)

The absorption and fluorescence variation of 1:1 Cur:Al complex upon NaF addition is as shown in figures 5.8 and 5.9. The curves in the case of NaF seemed very similar to the case of NaP addition. Fluoride ion has been reported to form stable complexes like AlF_2^+ [37] and AlF_3 [38] with aluminium. There are also multiple reports of sequential detection of fluoride after the formation of Al complex by different compounds [39-41].
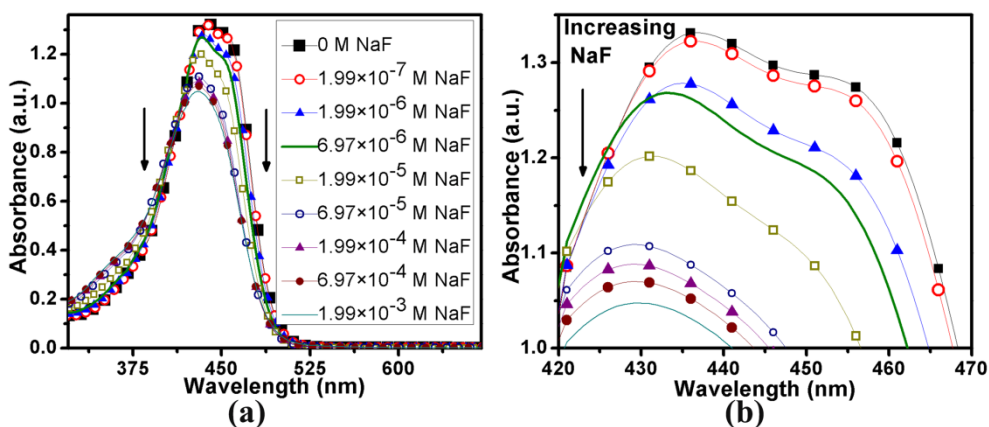
Figure 5.8 (a) Absorbance variation of 1:1 Cur:Al complex with increase in NaF concentration (b) Expanded view of the peak absorbance
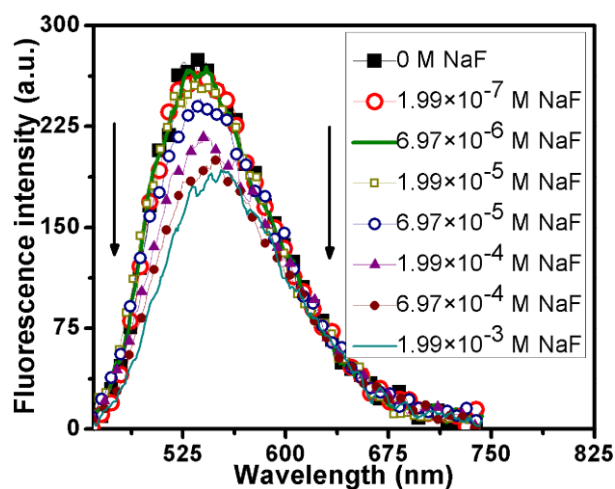
Figure 5.9 Fluorescence decrease of 1:1 Cur:Al complex in the presence of NaF (436 nm excitation wavelength)
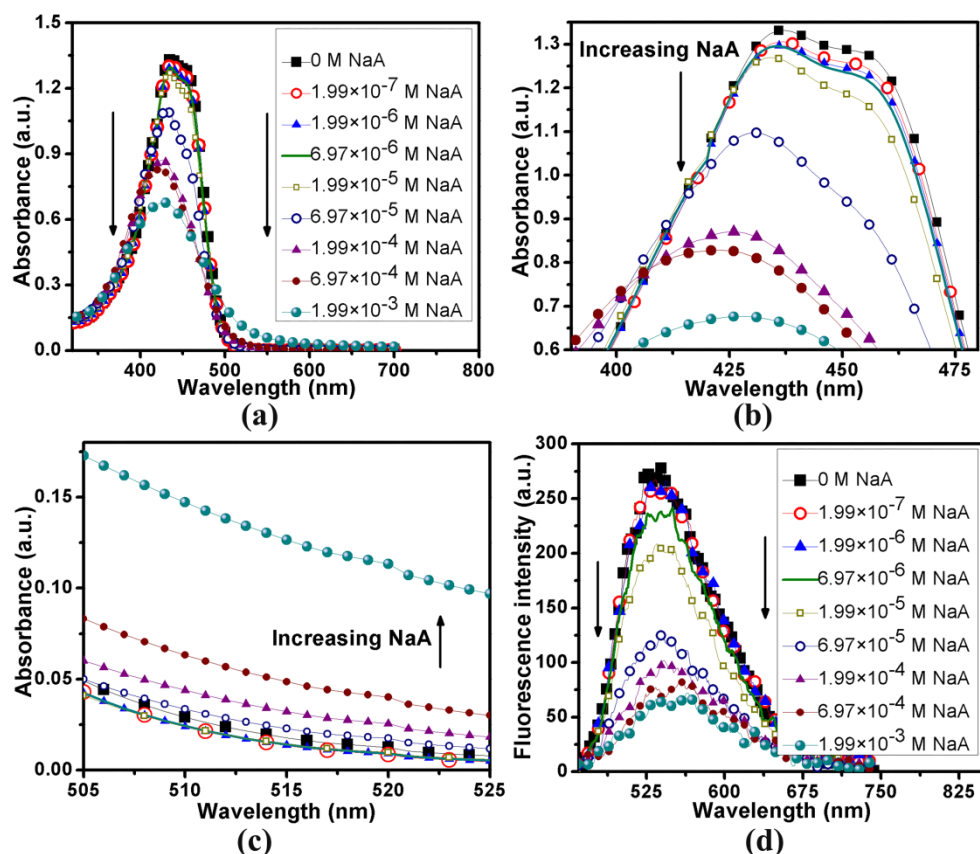
Figure 5.10 (a) Absorbance variation of 1:1 Cur:Al complex upon NaA addition (b) Expanded view of the absorption peaks (c) Expanded view of increase in the absorption intensity in the 500-525 nm wavelength range (d)Fluorescence decrease of 1:1 Cur:Al complex in the presence of NaA (436 nm excitation wavelength)

Figure 5.10 shows the variation in absorption and fluorescence intensity of 1:1 Cur:Al complex upon NaA addition. It can be seen that there is a huge decrease in absorption and fluorescence intensity especially at high concentration of NaA. The expanded region of the absorption spectrum above 500 nm shows an increase in absorption with increase in NaA. It was also observed that there was a tinge of brownish orange colour in the originally dark yellow colour of the solution at very high concentration of NaA.

Acetate has also been known to form complexes with Aluminium ion [17, 18]. The drastic changes in the absorption spectrum upon NaA addition can be attributed to not just disruption of Cur:Al complex (< 500 nm) but also to the increase in basicity of solvent environment with increase in NaA (> 500 nm) [6]. This could be causing deprotonation of Curcumin which can cause an increase in absorbance beyond 500 nm [34]. Sodium acetate finds use as a base to facilitate deprotonation of compounds to allow the complexation of the metal cation with the resultant anion of the compound [26].
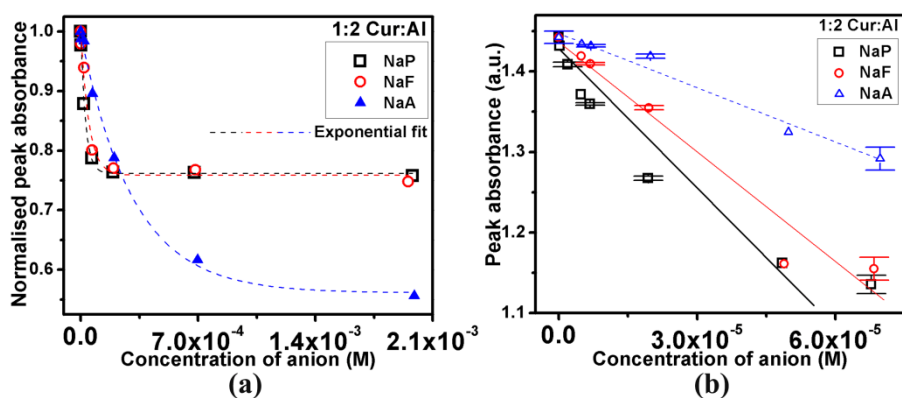
Figure 5.11 (a) Normalised peak absorbance values of 1:2 Cur:Al complex towards NaP, NaF and NaA (b) Variation in peak absorbance values at lower concentration of the anions

As described above NaP, NaF and NaA can all form complexes with aluminium. The normalized peak absorbance and variation of peak absorption of 1:2 Cur:Al complex in response to the anions are as shown in Fig. 5.11. Fig. 5.11b shows that there is a huge change in peak absorbance at lower concentration of NaP and NaF (steeper slope of linear fitted line) compared to that of NaA. This could be because of the formation of stable complexes of phosphate and fluoride with aluminium cation after its removal from the Cur-Al complex. Some reports suggest that acetate only forms a weak complex with

aluminium [42] and this could be the reason for a weaker response of the complex towards NaA at lower concentration of NaA.

Fig. 5.12 depicts the normalized change in peak fluorescence intensities as well as the variation in peak fluorescence intensities of 1:2 Cur:Al complex upon addition of NaP, NaF and NaA. The same trend was observed here too, with a faster decrease observed for NaP and NaF compared to that for NaA. The geometry of the anion concerned also contributes to the high sensitivity of the detection method or the sensing complex [23]
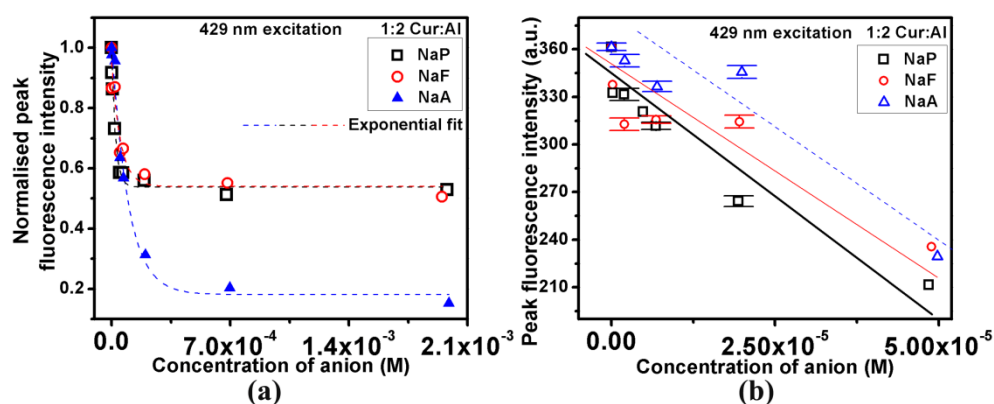
Figure 5.12 (a) Normalised peak fluorescence values of 1:2 Cur:Al complex towards NaP, NaF and NaA (b) Variation in peak fluorescence values at lower concentration of the anions
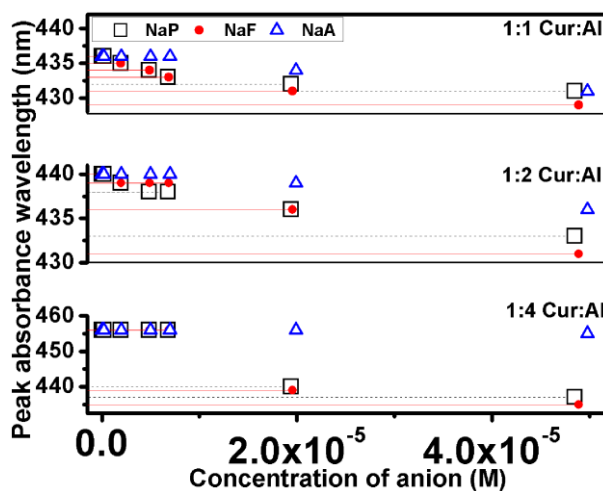
Figure 5.13 Shift in peak absorption wavelength of Cur:Al complexes upon addition of lower concentrations of NaP, NaF and NaA

The variation in peak absorption wavelengths of the three Cur:Al complexes upon addition of NaP, NaF and NaA are as shown in Fig. 5.13. The shifts observed for NaP and

NaF are almost similar in the case of 1:1 Cur:Al complex, whereas the shifts in the case of 1:2 Cur:Al complex are different for all three anions. The shifts in the case of NaA is significantly different from that of NaP and NaF in the case of 1:4 Cur:Al. Therefore, the shifts can also be used to selectively estimate the concentration of the three anions.

The peak absorbance values and the normalized values of peak absorbance for the complexes towards NaP are as shown in Fig. 5.14. It can be seen that the lower molar ratio (1:1) Cur:Al complex shows greater resolution between the peak absorbance values whereas the higher molar ratio (1:4) displays the capacity to detect higher NaP concentrations as inferred from the normalized spectrum.
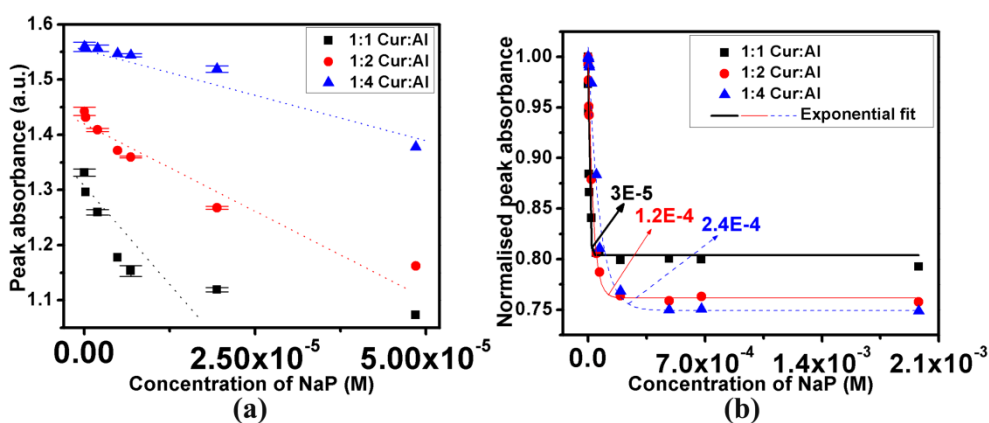
Figure 5.14 (a) Variation in peak absorbance values of varied molar ratio Cur:Al complexes towards NaP (b) Normalised values of decrease in peak absorbance of Cur:Al complexes in the presence of NaP
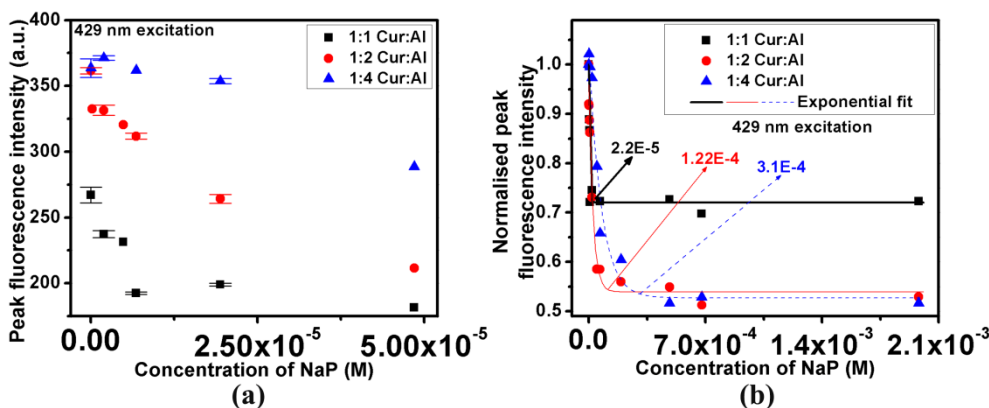
Figure 5.15 (a) Variation in peak fluorescence values of varied molar ratio Cur:Al complex towards NaP (b) Normalised values of decrease in peak fluorescence of Cur:Al complexes in the presence of NaP

The peak fluorescence values and the normalized values of peak fluorescence intensity of the complexes upon addition of NaP are as shown in Fig. 5.15. A similar trend was observed here as in the case of absorption. The changes in peak absorption wavelength shifts of the three complexes on NaP addition are as shown in Fig. 5.16. It can be seen from the expanded Fig. 5.16b that the three complexes display different shifts with change in concentration. Hence it is possible to detect concentration of a particular anion.
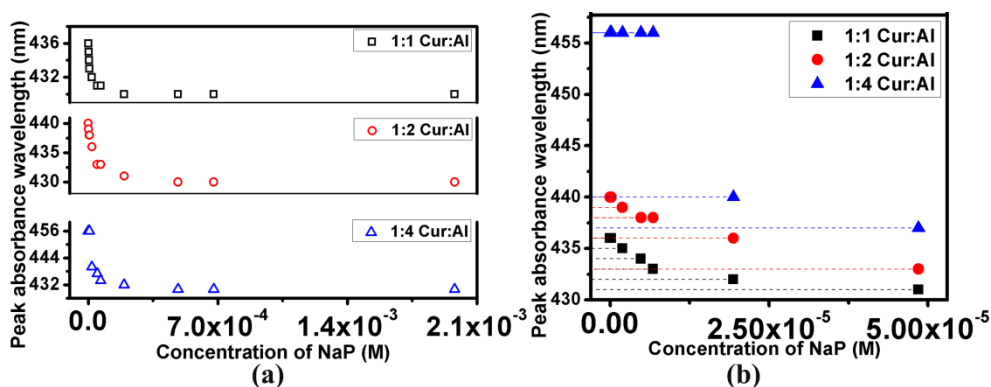
Figure 5.16 (a) Decrease in peak absorption wavelength of the different Cur:Al complexes with increasing NaP (b) Expanded view of the lower NaP concentration region
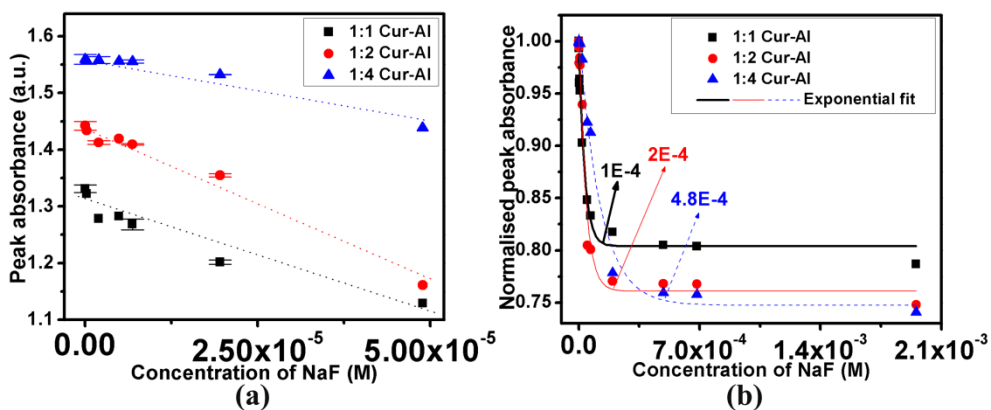
Figure 5.17 (a) Variation in peak absorbance values of Cur:Al complexes towards NaF (b) Normalised values of decrease in peak absorbance of the complexes in the presence of NaF

The peak absorbance values and the normalized values of peak absorbance for the complexes towards NaF are as shown in Fig. 5.17. The peak fluorescence values and the normalized values of fluorescence of the complexes upon addition of NaF are as shown in

Fig. 5.18. The changes in peak absorption wavelength shifts of the three complexes on NaF addition are as shown in Fig. 5.19.
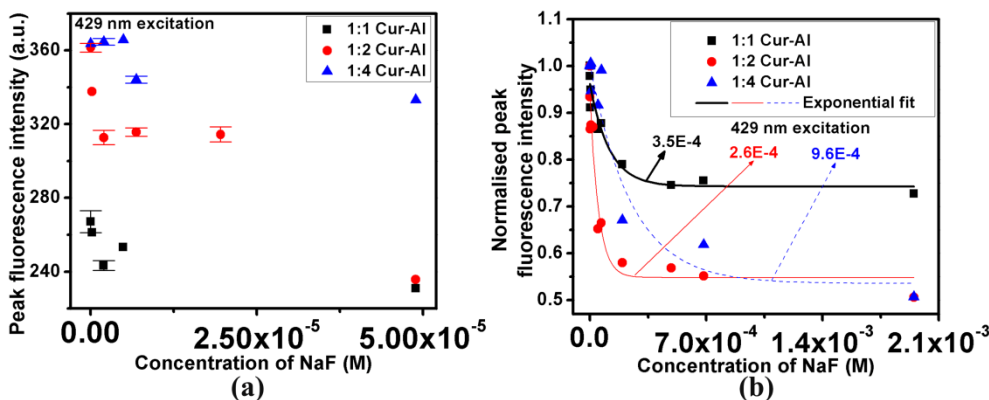
Figure 5.18 (a) Variation in peak fluorescence values of varied molar ratio Cur:Al complexes towards NaF (b) Normalised values of decrease in peak fluorescence of the complexes in the presence of NaF
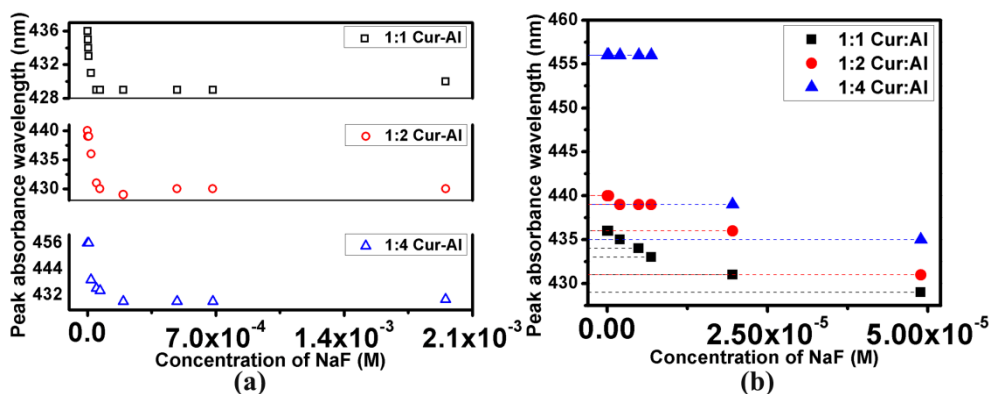
Figure 5.19 (a) Decrease in peak absorption wavelength of the different Cur:Al complexes with increasing NaF (b) Expanded view of the lower NaF concentration region

The peak absorbance values and the normalized values of absorbance for the complexes towards NaA are as shown in Fig. 5.20. The peak fluorescence values and the normalized values of peak fluorescence of the complexes upon addition of NaA are as shown in Fig. 5.21. The changes in peak absorption wavelength shifts of the three complexes on NaA addition are as shown in Fig. 5.22.
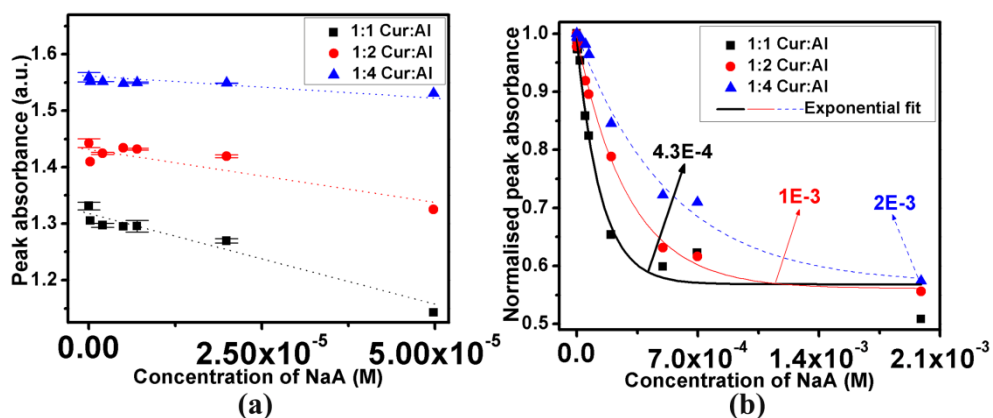
Figure 5.20 (a) Decrease in peak absorbance values of Cur:Al complexes towards NaA (b) Normalised values of decrease in peak absorbance of the complexes in the presence of NaA
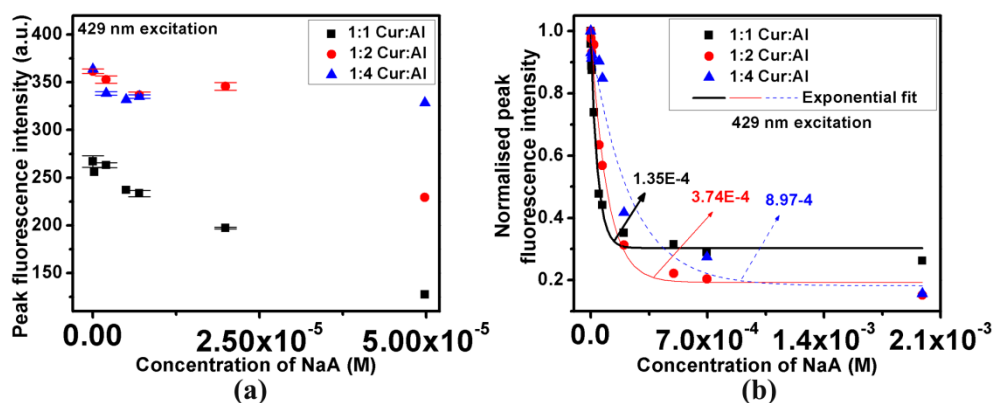
Figure 5.21 (a) Variation in peak fluorescence values of Cur:Al complexes towards NaA (b) Normalised values of decrease in peak fluorescence of the complexes in the presence of NaA
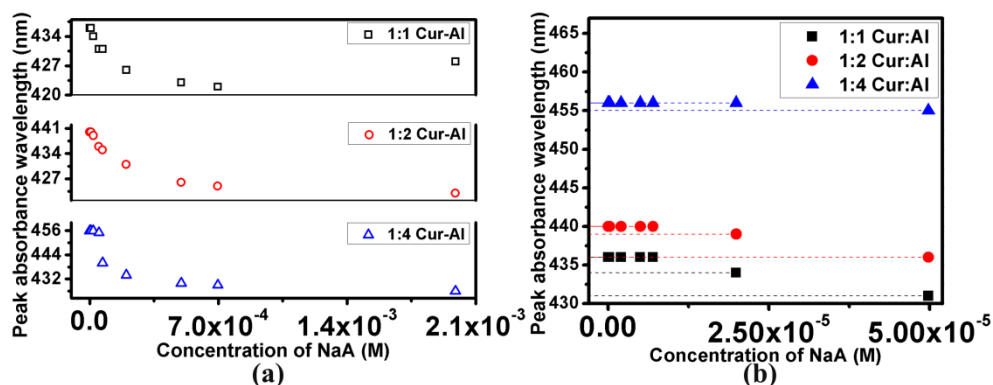
Figure 5.22 (a) Decrease in peak absorption wavelength of the different Cur:Al complexes with increasing NaA (b) Expanded view of the lower NaA concentration region

It can be seen that in the cases of NaF and NaA addition too, the lower molar ratio (1:1) Cur:Al complex shows greater resolution between the peak absorbance values whereas the higher molar ratio (1:4) displays a higher values for maximum measureable anion concentration as inferred from the normalized spectrum. This could be due to the higher number of Al sites available in higher molar ratio Cur-Al complexes for interaction with the anions.

The peak absorption wavelength shifts of Cur:Al complexes in the presence of some selected anion concentrations are as shown in Table 5.1. The blue shifting of absorption peaks can be attributed to the conversion of Cur-Al complexes to Curcumin via displacement of Al from the complex, as described in the earlier sections of the chapter. It can be seen that the peak absorption wavelength shifts can easily be used to infer the concentrations of anions either with the use of a single Cur:Al complex or multiple Cur:Al complexes (in some cases).

Table 5.1: Peak absorption wavelength shifts of Cur:Al complexes in the presence of NaP, NaF and NaA for some selected concentrations

Complex	Anion	Anion concentration			
		0	**1.62E-5**	**6.80E-5**	**6.96E-4**
		Peak absorption wavelength (nm)			
	NaP	436	434	431	430
1:1	NaF	436	435	429	429
	NaA	436	434	431	422
	NaP	440	438	433	430
1:2	NaF	440	440	430	430
	NaA	440	439	435	425
	NaP	456	440	434	430
1:4	NaF	456	455	434	429
	NaA	456	455	440	429

The maximum measurable concentration and limit of detection (LOD) of the different Cur:Al complexes towards NaP, NaF and NaA are summarized in Table 5.2. The LOD is estimated as that particular value of analyte (NaP, NaF, NaA) which when added to the sensing agent (Cur:Al complex) gives a signal (here, the peak absorbance) that is thrice the

value of the error (standard deviation) subtracted (or added) to the signal of blank sample [43]. The fluorescence values can also be used to calculate the LOD and dynamic range.

Table 5.2: Maximum measureable concentration and LOD of NaP, NaF and NaA using Cur:Al complexes

Complex	NaP		NaF		NaA	
	Maximum measureable concentration (M)	LOD (M)	Maximum measureable concentration (M)	LOD (M)	Maximum measureable concentration (M)	LOD (M)
1:1	3E-5	4E-7	1E-4	2E-6	4.3E-4	3E-6
1:2	1.2E-4	3E-6	2E-4	4E-6	1E-3	1.5E-5
1:4	2.4E-4	8E-6	4.8E-4	2E-5	2E-3	5E-5

It can be seen from the table that the lower molar ratio of Cur:Al complexes can be used to detect lower concentration of anions whereas the higher molar ratio complexes exhibited higher values for maximum measureable anion concentration. This is a very attractive feature of sensing with Cur:Al complexes in addition to the water based sensing capability. The different LOD and range of the Cur:Al complexes allows for tuning the sensitivity and range of detection of the complexes towards anions by simply tailoring the molar ratio of the precursors. The change in optical characteristics of Cur:Al complexes towards NaF was also studied in ethanol-water and acetonitrile-water mixture solvents. It was found that the method works in different mixture solvents and also exhibits sensitive response towards organic form of fluoride i.e TBAF. This could be owing to the non covalent electrostatic interaction between the anions and Al^{3+} cation [29].

5.4 Polymer optical fiber for sensing applications

Polymer fibers have generally been used in LAN interconnects and short distance communication [44]. Over the years it is extensively used in imaging [45], amplifier [46] and laser [47, 48] applications using dye doped polymer fibers. Polymer fibers find tremendous applications in sensing strain, pressure, humidity, liquid level, pH etc and hence are also used in structural health monitoring and medicine [44, 45, 49]. The ease of handling (large core diameters), low cost preparation [44], bio-compatibility [49] and low temperature processing of polymer fibers make it a desirable candidate for hosting sensing dyes which are prone to degradation at processing temperatures of silica fibers. The use of

polymer fiber to host Cur:Al complexes would further allow continuous monitoring and detection of anions in ground water resources.

5.4.1 Fabrication of polymer fiber preform

The poly-methylemethacrylate (PMMA) preform for fabricating PMMA polymer optical fiber (POF) was prepared by polymerising the monomer methylmethacrylate (MMA, Sigma Aldrich). Before it is polymerised, the MMA solution was washed repeatedly with equal volumes of 0.5 wt % sodium hydroxide (NaOH) solution so as to remove the inhibitors. The resultant MMA was then washed a number of times with equal volumes of water. A drying agent like Calcium chloride ($CaCl_2$) was then added to the washed MMA to remove water content. MMA was then filtered out and distilled under reduced pressure to get purified monomer [50].

To the monomer (30 ml) taken inside a test tube, 0.4 wt. % benzoyl peroxide (BPO), 0.1 wt. % n-butyl mercaptan and 1:2 Cur-Al complex dissolved in ethanol (~10^{-4} M dye) were added. BPO initiates the polymerization reaction and n-butyl mercaptan functions as the chain transfer agent that controls the rate of polymerization [47]. The mixture was stirred for a few minutes and placed in a temperature controlled oil bath for three days at 70°C.

5.4.2 Fiber drawing from preform

A dedicated fiber drawing station was used for drawing optical fibers from the prepared solid fiber preforms. The fiber drawing station has a heating furnace, a translational stage with a metallic slot for feeding the fixed fiber perform into the heating furnace and a section with two rollers for pulling the fiber at a regulated rate (Fig. 5.23). There is also a separate spool for collecting the fiber drawn.

The feed rate F_R, the draw rate D_R, the diameters of the preform D_P and fiber D_F are related by the equation [51]:

$$\frac{D_F}{D_P} = \left(\frac{F_R}{D_R}\right)^{\frac{1}{2}} \tag{5.1}$$

Hence for a given diameter of preform, optical fibers of different diameters can be drawn by adjusting the feed rate and the draw rate. The fiber preform was fixed in the preform holder and fibers of different diameters were drawn at a temperature of about 180° C. The fiber with approximately 400 μm diameter was used for the evanescent wave optical fiber sensor experiments.
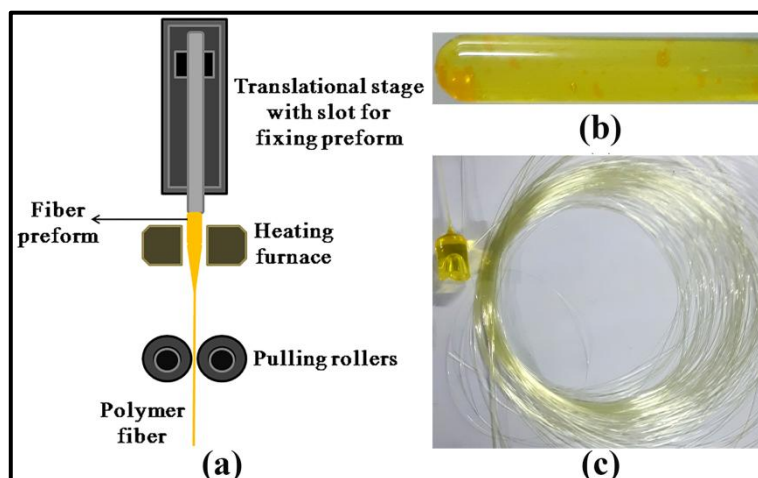
Figure 5.23 Schematic of the polymer optical fiber drawing station (b) Polymer fiber preform doped with 1:2 Cur:Al complex (c) Polymer optical fiber drawn from the doped preform

5.4.3 Experimental set up for evanescent wave straight fiber sensor using POF

The experimental set-up of the evanescent wave straight optical fiber sensor using Cur:Al doped polymer fiber is as shown in Fig. 5.24. About 12 cm of the Cur-Al doped fiber was fixed inside a cylindrical glass cell along its axis using epoxy glue. The cell has provisions for introducing the anion samples in water into the cell and also for the drainage of samples from the cell. A 403 nm laser was focused into one end of the polymer fiber using a convex lens having focal length 3.5 cm. The light output from the other end of the polymer fiber was collected using a fiber probe and was processed by a SpectraSuite HR 4000 Ocean Optics spectrometer. The cylindrical cell holding the fiber was flushed with water repeatedly in between each measurement.
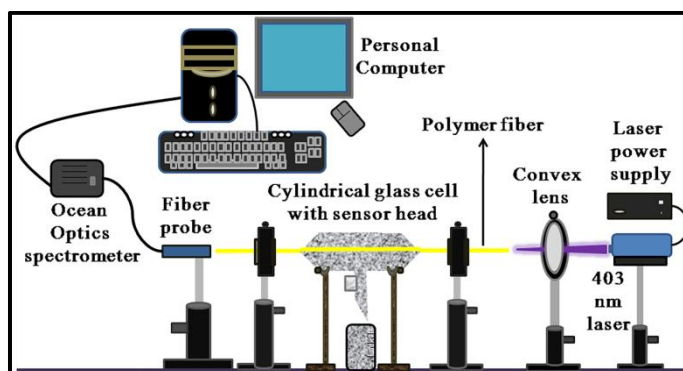
Figure 5.24 Schematic of the experimental set-up of the evanescent wave straight fiber sensor using Cur:Al complex doped PMMA polymer fiber

The light emission from the 1:2 Cur:Al complex doped fiber is as shown in Fig. 5.25a. The change in values of fluorescence recorded upon addition of water alone and anion samples in water with varying concentration of NaP, NaF and NaA is as shown in Fig. 5.25b. The fiber response shows similar trend of fluorescence decrease with increase in anion concentration as in the case of response of Cur:Al complex in $MeOH:H_2O$ mixture solvent. The 403 nm (incident light) wavelength region in the output spectrum did not show considerable change in intensity (~2-3 a.u.) when compared to the change in fluorescence signal values. The measurement of refractive index values of $2×10^{-6}$ M-$2×10^{-3}$ M NaF by Sipcon Abbe's refractometer showed no change in refractive index of the samples. Hence refractive index induced changes in transmission can be considered to be negligible.

The fluorescence decrease could possibly be due the partial bonding of anions at the exposed Al sites in the Cur:Al complex doped fiber. The intensity of fluorescence emission recorded depends on the length of the doped fiber since a longer length can cause attenuation in signal by scattering or re-absorption [52]. But in general, increase in length of fiber can provide better sensitivity for the fiber sensor [53]. Hence the accurate determination of optimum doped fiber length to get enhanced emission is necessary. This will further ensure better resolution between fluorescence intensities recorded from the fiber corresponding to different anion concentrations.
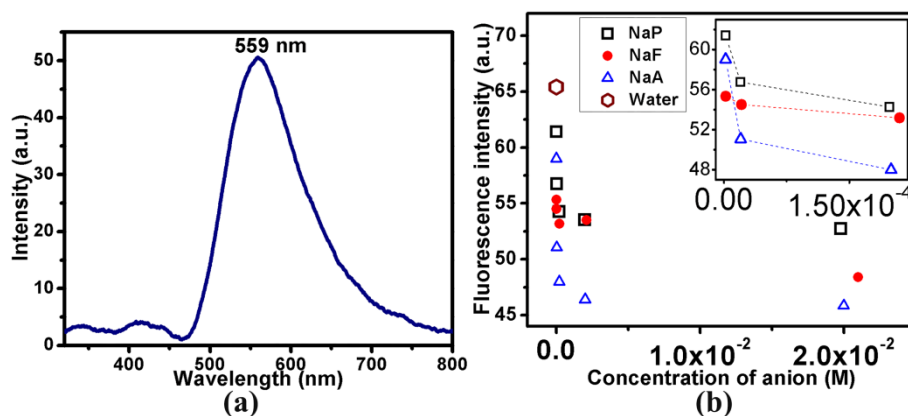
Figure 5.25 (a) Output spectrum of 1:2 Cur:Al doped polymer fiber (b) Fluorescence emission recorded from the polymer fiber sensor in response to NaP, NaF and NaA. Inset of figure 5.25b shows the expanded view of fluorescence values recorded from fiber corresponding to $2×10^{-6}$ M, $2×10^{-5}$ M and $2×10^{-4}$ M of NaP, NaF and NaA

5.5 Conclusions

Curcumin-Aluminium complexes with 1:1, 1:2 and 1:4 molar ratios were prepared using a simple direct reaction of Curcumin and metal halide salt. There was a blue shift in absorption peak along with a decrease in peak intensity for all the complexes upon addition of acetate, phosphate and fluoride anions owing to the removal of Al from the complexes. The 1:1 Cur:Al complex was found to exhibit very low limit of detection of 4×10^{-7} M, 2×10^{-6} M, 3×10^{-6} M towards phosphate, fluoride and acetate respectively. The 1:2 and 1:4 Cur:Al complexes, on the other hand, can be used to measure higher anion concentrations.

The peak absorbance, fluorescence intensity as well as peak absorption wavelength shift can be used to measure the concentration of anion. The Cur:Al complexes can respond to both inorganic and organic anion salts in solvent mixtures containing different water content owing to the non covalent interaction of the metal Al with the anions. An initial investigation into the use of 1:2 Cur:Al complex doped in PMMA polymer optical fiber as an evanescent wave straight optical fiber sensor was carried out. The polymer fiber sensor showed slight decrease in recorded fluorescence with increase in the concentration of anions.

5.6 References

[1] Sulaiman Ayoob and Ashok Kumar Gupta. "Fluoride in drinking water: a review on the status and stress effects." Critical Reviews in Environmental Science and Technology 36, no. 6 (2006): 433-487

[2] Lei Xiong, Jiao Feng, Rui Hu, Shuangqing Wang, Shayu Li, Yi Li, and Guoqiang Yang. "Sensing in 15 s for aqueous fluoride anion by water-insoluble fluorescent probe incorporating hydrogel." Analytical chemistry 85, no. 8 (2013): 4113-4119

[3] Shyamaprosad Goswami, Avijit Kumar Das, Krishnendu Aich, Abhishek Manna, Hoong-Kun Fun, and Ching Kheng Quah. "Single sensor for multiple analytes: fluorogenic detection of Al3+ in aqueous media and AcO− in organic media." Supramolecular Chemistry 26, no. 2 (2014): 94-104

[4] Xiaoliu Zhang, Revati Kumar, and Daniel G. Kuroda. "Acetate ion and its interesting solvation shell structure and dynamics." The Journal of Chemical Physics 148, no. 9 (2018): 094506.

[5] Shigeru Amemiya, Philippe Bühlmann, Yoshio Umezawa, Raymond C. Jagessar, and Dennis H. Burns. "An ion-selective electrode for acetate based on a urea-functionalized Porphyrin as a Hydrogen-Bonding Ionophore." Analytical chemistry 71, no. 5 (1999): 1049-1054.

[6] Divya Singhal, Neha Gupta, and Ashok Kumar Singh. "Selective colorimetric sensors for cyanide and acetate ion in partially aqueous medium." (2018). DOI:10.20944/preprints201803.0225.v1

[7] Kamalpreet Kaur, Ajnesh Singh, and Narinder Singh. "Azo dye coupled imine linked dipodal chemosensor: Anion recognition with counter anion displacement assay." Sensors and Actuators B: Chemical 191 (2014): 734-740.

[8] Matthew D. Patey, Micha JA Rijkenberg, Peter J. Statham, Mark C. Stinchcombe, Eric P. Achterberg, and Matthew Mowlem. "Determination of nitrate and phosphate in seawater at nanomolar concentrations." TrAC Trends in Analytical Chemistry 27, no. 2 (2008): 169-182.

[9] Karishma Tiwari, Sumit Kumar, Vipan Kumar, Jeevanjot Kaur, Saroj Arora, and Rakesh Kumar Mahajan. "An azine based sensor for selective detection of Cu2+ ions and its copper complex for sensing of phosphate ions in physiological conditions and in living cells." Spectrochimica Acta Part A: Molecular and Biomolecular Spectroscopy 191 (2018): 16-26.

[10] Christopher Warwick, Antonio Guerreiro, and Ana Soares. "Sensing and analysis of soluble phosphates in environmental samples: A review." Biosensors and Bioelectronics 41 (2013): 1-11.

[11] Samuel B. Adeloju, "Progress and recent advances in phosphate sensors: A review." Talanta 114 (2013): 191-203.

[12] Benjamin P. Varghese, Aji Balan Pillai, and Madhusoodanan Kottarathil Naduvil. "Fiber optic sensor for the detection of ammonia, phosphate and iron in water." Journal of Optics 42, no. 2 (2013): 78-82.

[13] Min Su Han, and Dong H. Kim. "Naked-eye detection of phosphate ions in water at physiological pH: a remarkably selective and easy-to-assemble colorimetric phosphate-sensing probe." Angewandte Chemie International Edition 41, no. 20 (2002): 3809-3811.

[14] Hossein Tavallali, Gohar Deilamy-Rad, Ali Moaddeli, and Khadijeh Asghari. "Indigo Carmine-Cu complex probe exhibiting dual colorimetric/fluorimetric sensing for selective determination of mono hydrogen phosphate ion and its logic behavior." Spectrochimica Acta Part A: Molecular and Biomolecular Spectroscopy 183 (2017): 319-331.

[15] Li-Jun Kuo, Jen-Hai Liao, Chao-Tsen Chen, Chien-Huang Huang, Chien-Sheng Chen, and Jim-Min Fang. "Two-arm ferrocene amide compounds: Synclinal conformations for selective sensing of dihydrogen phosphate ion." Organic letters 5, no. 11 (2003): 1821-1824.

[16] Hong Dinh Duong, and Rhee Jong Il. "Ratiometric fluorescence sensors for the detection of HPO_4^{2-} and $H_2PO_4^{-}$ using different responses of the morin-hydrotalcite complex." Sensors and Actuators B: Chemical 274 (2018): 66-77.

[17] Sai Sathish, Govindh Narayan, Nageswara Rao, and Chelli Janardhana. "A self-organized ensemble of fluorescent 3-hydroxyflavone-Al (III) complex as sensor for fluoride and acetate ions." Journal of fluorescence 17, no. 1 (2007): 1-5.

[18] Vinod Kumar Gupta, Naveen Mergu, Lokesh Kumar Kumawat, and Ashok Kumar Singh. "A reversible fluorescence "off–on–off" sensor for sequential detection of aluminum and acetate/fluoride ions." Talanta 144 (2015): 80-89.

[19] Kumaresh Ghosh, and Indrajit Saha. "Triphenylamine-based simple chemosensor for selective fluorometric detection of fluoride, acetate and dihydrogenphosphate ions in different solvents." Journal of Inclusion Phenomena and Macrocyclic Chemistry 70, no. 1-2 (2011): 97-107.

[20] Chaolong Yang, Jing Xu, Jingyuan Li, Mangeng Lu, Youbing Li, and Xuanlun Wang. "An efficiently colorimetric and fluorescent probe of fluoride, acetate and phosphate ions based on a novel trinuclear Eu-complex." Sensors and Actuators B: Chemical 196 (2014): 133-139.

[21] Ryuhei Nishiyabu, and Pavel Anzenbacher. "1, 3-Indane-based chromogenic calixpyrroles with push− pull chromophores: synthesis and anion sensing." Organic letters 8, no. 3 (2006): 359-362.

[22] Thorfinnur Gunnlaugsson, Paul E. Kruger, Paul Jensen, Juliann Tierney, Haslin Dato Paduka Ali, and Gillian M. Hussey. "Colorimetric "naked eye" sensing of anions in aqueous solution." The Journal of organic chemistry 70, no. 26 (2005): 10875-10878.

[23] Jianwei Li, Hai Lin, Zunsheng Cai, and Huakuan Lin. "A high selective anion colorimetric sensor based on salicylaldehyde for fluoride in aqueous media." Spectrochimica Acta Part A: Molecular and Biomolecular Spectroscopy 72, no. 5 (2009): 1062-1065.

[24] M. A. Subhan, K. Alam, M. S. Rahaman, M. A. Rahman, and R. Awal. "Synthesis and characterization of metal complexes containing curcumin (C 21 H 20 O 6) and study of their anti-microbial activities and DNA-binding properties." Journal of Scientific research 6, no. 1 (2014): 97-109.

[25] Ghulam Hussain, Nasir Abass, Ghulam Shabir, Makshoof Athar, Aamer Saeed, Rashid Saleem, Farman Ali, and Misbahul Ain Khan. "New acid dyes and their metal complexes based on substituted phenols for leather: Synthesis, characterization and optical studies." Journal of applied research and technology 15, no. 4 (2017): 346-355.

[26] Simon Wanninger, Volker Lorenz, Abdus Subhan, and Frank T. Edelmann. "Metal complexes of curcumin–synthetic strategies, structures and medicinal applications." Chemical Society Reviews 44, no. 15 (2015): 4986-5002.

[27] Friederike Zaubitzer, Thomas Riis-Johannessen, and Kay Severin. "Sensing of peptide hormones with dynamic combinatorial libraries of metal–dye complexes: the advantage of time-resolved measurements." Organic & biomolecular chemistry 7, no. 22 (2009): 4598-4603.

[28] Tatineni Balaji, and Hideyuki Matsunaga. "Naked-eye detection of fluoride using Zr (IV)-EDTA complex and pyrocatechol violet." Analytical sciences 21, no. 8 (2005): 973-977.

[29] Kay. Severin, "Pattern-based sensing with simple metal–dye complexes." Current opinion in chemical biology 14, no. 6 (2010): 737-742.

[30] Khaled Greish, Valeria Pittalà, Sebastien Taurin, Safa Taha, Fatemah Bahman, Aanchal Mathur, Anfal Jasim et al. "Curcumin–Copper Complex Nanoparticles for the Management of Triple-Negative Breast Cancer." Nanomaterials 8, no. 11 (2018): 884.

[31] Joseph Daisy. "Reactive centers of curcumin and the possible role of metal complexes of curcumin as antioxidants." Universal Journal of Physics and Application 9, no. 1 (2015): 6-16.

[32] Teng Jiang, Long Wang, Sui Zhang, Ping-Chuan Sun, Chuan-Fan Ding, Yan-Qiu Chu, and Ping Zhou. "Interaction of curcumin with Al (III) and its complex structures based on experiments and theoretical calculations." Journal of Molecular Structure 1004, no. 1-3 (2011): 163-173.

[33] Bachar Zebib, Zéphirin Mouloungui, and Virginie Noirot. "Stabilization of curcumin by complexation with divalent cations in glycerol/water system." Bioinorganic chemistry and applications 2010 (2010)

[34] Fang-Ying Wu, Mei-Zhen Sun, Yan-Ling Xiang, Yu-Mei Wu, and Du-Qiu Tong. "Curcumin as a colorimetric and fluorescent chemosensor for selective recognition of fluoride ion." Journal of Luminescence 130, no. 2 (2010): 304-308

[35] Amalina Ahmad, Norhadisah Mohd Zaini, Normazida Rozi, Nurul Huda Abd Karim, Siti Aishah Hasbullah, Lee Yook Heng, and Sharina Abu Hanifah. "A Fluorescence Phosphate Sensor Based On Poly (Glycidyl Methacrylate) Microspheres With Aluminium-Morin." Malaysian Journal of Analytical Sciences 20, no. 4 (2016): 704-712.

[36] Junling Wang, Jian Song, Jun Lu, and Xin Zhao. "Comparison of three aluminum coagulants for phosphorus removal." Journal of Water Resource and Protection 6, no. 10 (2014): 902.

[37] Phil. Jones, "Development of a high-sensitivity ion chromatography method for the determination of trace fluoride in water utilizing the formation of the AlF2+ species." Analytica chimica acta 258, no. 1 (1992): 123-127.

[38] Haiyang Liu, Bibo Zhang, Chunyan Tan, Feng Liu, Jiakun Cao, Ying Tan, and Yuyang Jiang. "Simultaneous bioimaging recognition of Al3+ and Cu2+ in living-cell, and further detection of F− and S2− by a simple fluorogenic benzimidazole-based chemosensor." Talanta 161 (2016): 309-319.

[39] Ankita Roy, Sudipto Dey, and Partha Roy. "A ratiometric chemosensor for Al3+ based on naphthalene-quinoline conjugate with the resultant complex as secondary sensor for F−:

Interpretation of molecular logic gates." Sensors and Actuators B: Chemical 237 (2016): 628-642.

[40] Rakesh Purkait, Chiranjit Patra, Ananya Das Mahapatra, Debprasad Chattopadhyay, and Chittaranjan Sinha. "A visible light excitable chromone appended hydrazide chemosensor for sequential sensing of Al+ 3 and F− in aqueous medium and in Vero cells." Sensors and Actuators B: Chemical 257 (2018): 545-552.

[41] Quanping Diao, Pinyi Ma, Linlin Lv, Tiechun Li, Ying Sun, Xinghua Wang, and Daqian Song. "A water-soluble and reversible fluorescent probe for Al3+ and F− in living cells." Sensors and Actuators B: Chemical 229 (2016): 138-144.

[42] Fabien Thomas, Armand Masion, Jean Yves Bottero, James Rouiller, Francine Genevrier, and Denis Boudot. "Aluminum (III) speciation with acetate and oxalate. A potentiometric and aluminum-27 NMR study." Environmental science & technology 25, no. 9 (1991): 1553-1559.

[43] J. Shi, C. Chan, Y. Pang, W. Ye, F. Tian, J. Lyu, Y. Zhang, and M. Yang, "A fluorescence resonance energy transfer (FRET) biosensor based on graphene quantum dots (GQDs) and gold nanoparticles (AuNPs) for the detection of mecA gene sequence of Staphylococcus aureus," Biosens. Bioelectron. 67, (2015): 595–600.

[44] Joseba Zubia, and Jon Arrue. "Plastic optical fibers: An introduction to their technological processes and applications." Optical Fiber Technology 7, no. 2 (2001): 101-140.

[45] Lúcia Bilro, Nélia Alberto, João L. Pinto, and Rogério Nogueira. "Optical sensors based on plastic fibers." Sensors 12, no. 9 (2012): 12184-12207.

[46] A. Tagaya, Yasuhiro Koike, Takeshi Kinoshita, Eisuke Nihei, T. Yamamoto, and K. Sasaki. "Polymer optical fiber amplifier." Applied physics letters 63, no. 7 (1993): 883-884.

[47] C. L. Linslal, S. Sebastian, S. Mathew, P. Radhakrishnan, V. P. N. Nampoori, C. P. Girijavallabhan, and M. Kailasnath. "Microring embedded hollow polymer fiber laser." Applied Physics Letters 106, no. 13 (2015): 131101.

[48] S. Sebastian, C. L. Linslal, C. P. G. Vallabhan, V. P. N. Nampoori, P. Radhakrishnan, and M. Kailasnath. "Random lasing with enhanced photostability of silver nanoparticle doped polymer optical fiber laser." Laser Physics Letters 11, no. 5 (2014): 055108.

[49] Kara Peters, "Polymer optical fiber sensors—a review." Smart materials and structures 20, no. 1 (2010): 013002.

[50] Mandamparambil Rajesh, Mavila Sheeba, Karinjamanna Geetha, Chakkalakkal PG Vallaban, Padmanabhan Radhakrishnan, and Vadakkedathu PN Nampoori. "Fabrication and characterization of dye-doped polymer optical fiber as a light amplifier." Applied optics 46, no. 1 (2007): 106-112.

[51] Changhong Jiang, Mark G. Kuzyk, Jow-Lian Ding, William E. Johns, and David J. Welker. "Fabrication and mechanical behavior of dye-doped polymer optical fiber." Journal of applied physics 92, no. 1 (2002): 4-12.

[52] M. Sheeba, M. Rajesh, S. Mathew, V. P. N. Nampoori, C. P. G. Vallabhan, and P. Radhakrishnan. "Side illumination fluorescence emission characteristics from a dye doped polymer optical fiber under two-photon excitation." Applied optics 47, no. 11 (2008): 1913-1921.

[53] B. D. Gupta, H. Dodeja, and A. K. Tomar. "Fibre-optic evanescent field absorption sensor based on a U-shaped probe." Optical and Quantum Electronics 28, no. 11 (1996): 1629-1639

Chapter 6

Conclusions and Future prospects

In this chapter, the general conclusions of the works presented in the thesis are summarized. A brief discussion on the possible future prospects of fluoride detection and measurement is also presented.

6.1 Conclusions

Fluoride is a highly reactive species which finds use in day to day life. But owing to the presence of even natural sources [1] that can contribute heavily to fluoride pollution in ground water resources and the resulting adverse effects in human health, fluoride sensing becomes an important challenge that needs urgent attention. Some synthetic, natural organic dyes and their derivatives were investigated for the development of optical sensing of both organic (TBAF) and inorganic (NaF) forms of fluoride in organic solvents and organo-aqueous medium. The results of the investigations towards the development of simple, sensitive and selective fluoride sensors are presented in the thesis.

Rh6G, a high quantum yield dye responds to fluoride sensitively in organic solvent acetonitrile via NH de-protonation and this is reflected in the fast decrease in absorption and fluorescence intensity values. The use of a FRET mechanism with the addition of C540A donor was studied and it allowed for the increase in the range of detection with comparable sensitivity to that of Rh6G alone. The increase in fluoride causes a reduction in FRET efficiency and a subsequent increase in C540A emission which can be helpful to quantify fluoride of high concentration. A hollow glass capillary externally coated with C540A doped in PMMA was also demonstrated for TBAF detection with the help of Rh6G. The concentration and thickness of the C540A coating was varied and the emission from capillary containing both C540A and Rh6G fluorescence components was used to estimate the concentration of fluoride. This non-FRET optical interaction of Rh6G and C540A seemed to show a similar trend in fluorescence emission recovery of C540A with increase in TBAF. The red shift of C540A fluorescence emission can be used along with the emission intensities for fluoride detection. A low cost UV LED source can also be used to excite fluorescence which further makes it an attractive, simple to use alternative to bulky spectrophotometers.

Curcumin, a non-toxic natural dye was used to detect fluoride in polar solvent acetonitrile and non-polar solvent anisole having different refractive indices. The OH de-protonation mechanism for optical response was confirmed using addition of protic solvents and studying the effect of pH on the shift of absorption spectrum of Curcumin. Simple evanescent wave absorption based straight and U shaped optical fiber sensors were fabricated. The fluoride concentration was quantified using the change in transmittance of the optical fiber sensor while immersed in Curcumin solution. Also, fiber probes consisting of combinations of chemically tapered and smaller length un-cladded sections were used to

collect the reduced fluorescence of Curcumin with increasing TBAF. The hybrid probes exhibited greater collection efficiency of Curcumin fluorescence and its decrease upon interaction with fluoride.

Both the above mentioned methods involve the use of organic solvents and are not effective in purely aqueous media owing to the hydrogen bonding nature of interaction. The use of natural dye Curcumin in aqueous medium would be immensely attractive owing to the low cost, non toxic nature of the dye. But Curcumin has very low solubility in water. This led us to consider the possibility of irradiation in mixture solvents as a technique for aqueous based sensing of fluoride. The irradiation of Curcumin in mixture solvents with different sources of light was demonstrated as a means to detect fluoride of both organic and inorganic forms. The addition of fluoride leads to changes in the basicity of the microenvironment of Curcumin in the mixture solvent leading to its accelerated degradation. This process leads to a decrease in absorption and fluorescence intensities of Curcumin accompanied by photo-fading. The degree of photo-degradation was found to increase with increase in fluoride concentration and was also found to be sensitive to the type of solvent used. Experimental set-ups were devised for studying the effect of solvent type and exposure time on Curcumin photo-degradation and the changes in optical properties of Curcumin upon irradiation in the presence of fluoride. The continuous monitoring of Curcumin fluorescence and transmittance of light was also carried out using low cost sources and detectors. The simple method of irradiation of filter paper strips stained with Curcumin was also demonstrated to detect NaF and slight colour changes of the strip were visible to the naked eye. But stark colour changes were observed in the cases of high fluoride concentration samples upon image subtraction with the use of simple image processing software.

Curcumin-aluminium complexes in the molar ratio of 1:1, 1:2 and 1:4 were prepared and the optical response (absorption, emission intensity and absorption wavelength) of the complexes towards phosphate, acetate and fluoride were studied. The blue shifted absorption peak of the complexes upon anion addition suggests the displacement or removal of Al from the complexes by the anions. The method can be used to detect both the inorganic and organic forms of anions in a wide range of mixture solvents owing to the non-covalent (non hydrogen bonding) nature of interaction with the Al metal. A preliminary investigation of PMMA based polymer fiber doped with 1:2 Cur:Al complex was carried out. The evanescent wave straight fiber sensor constructed using the polymer

optical fiber showed slight decrease in recorded fluorescence with increase in fluoride, phosphate and acetate.

6.2 Future prospects

The major challenges involving the development of optical sensors for fluoride involve the strong hydrogen bonding tendency of water molecules towards most sensing agents [2]. This is the reason for a large number of reports on fluoride detection in organic media or mixtures of organic solvents and water with water content in low proportions. Optical fiber sensors offer a lot of advantages including sensitivity, small size, lightweight, remote sensing capability and immunity to electromagnetic interference [3].

Tapered optical fibers offer efficient excitation and collection of fluorescence [4]. Different combinations of taper diameters and lengths can be used for increasing the efficiency of excitation and collection of fluorescence from Curcumin. In addition to the use of silica fibers, tapered polymer fibers with silica xerogel films doped with the sensing dyes like Rh6G and Curcumin can be used for the detection of fluoride. Hollow capillary based sensing requires very low volume of sample for interrogation and a low cost capillary element. The coating of Rh6G dye alone as well as the C540A-Rh6G FRET pair inside the capillary can be tried to directly detect samples of fluoride.

The use of paper based sensing mechanisms using low cost dyes like Curcumin is very attractive, but over time the paper based systems can get damaged due to environmental conditions. The incorporation of organic dyes in films is reported to increase photo-stability and Curcumin incorporated porous xerogel films are easy to handle and can be preserved for a long period of time. The use of free standing films and bio-compatible hydrogel films are also attractive to carry out the irradiation process with the added advantage of the option for continuous monitoring of the film absorption/fluorescence/transmittance.

The other interesting possibility towards sensing of fluoride can be the use of nanoparticles. Nanoparticles of different morphologies and sizes have different optical properties and are reported to have very high sensitive response to multiple parameters. There are only a few reports on the use of nanoparticles like Ag doped CdS/ZnS core-shell [5], gold [6], mesoporous silica [7] and carbon nanodots [8] for the detection of fluoride and the use of nanoparticles can allow the detection of fluoride in aqueous medium.

6.3 References

[1] Sulaiman Ayoob and Ashok Kumar Gupta. "Fluoride in drinking water: a review on the status and stress effects." Critical Reviews in Environmental Science and Technology 36, no. 6 (2006): 433-487.

[2] Soon Young Kim and Jong-In Hong. "Chromogenic and fluorescent chemodosimeter for detection of fluoride in aqueous solution." Organic letters 9, no. 16 (2007): 3109-3112

[3] K. T. V. Grattan, and T. Sun. "Fiber optic sensor technology: an overview." Sensors and Actuators A: Physical 82, no. 1-3 (2000): 40-61

[4] Joel P. Golden, George P. Anderson, S. Y. Rabbany, and F. S. Ligler. "An evanescent wave biosensor. II. Fluorescent signal acquisition from tapered fiber optic probes." IEEE Transactions on Biomedical Engineering 41, no. 6 (1994): 585-591.

[5] Siddhartha Sankar Boxi, and Santanu Paria. "Fluorometric selective detection of fluoride ions in aqueous media using Ag doped CdS/ZnS core/shell nanoparticles." Dalton Transactions 45, no. 2 (2016): 811-819.

[6] Anshu Kumar, Madhuri Bhatt, Gaurav Vyas, Shreya Bhatt, and Parimal Paul. "Sunlight induced preparation of functionalized gold nanoparticles as recyclable colorimetric dual sensor for aluminum and fluoride in water." ACS applied materials & interfaces 9, no. 20 (2017): 17359-17368

[7] Gaurav Jha, N. Anoop, Abdur Rahaman, and Moloy Sarkar. "Fluoride ion sensing in aqueous medium by employing nitrobenzoxadiazole-postgrafted mesoporous silica nanoparticles (MCM-41)." Physical Chemistry Chemical Physics 17, no. 5 (2015): 3525-3533

[8] Mojtaba Shamsipur, Afsaneh Safavi, Zahra Mohammadpour, and Amin Reza Zolghadr. "Fluorescent carbon nanodots for optical detection of fluoride ion in aqueous media." Sensors and Actuators B: Chemical 221 (2015): 1554-1560

Appendix.....

Publications

Chemically Tapered Multimode Optical Fiber Probe for Fluoride Detection Based on Fluorescence Quenching of Curcumin

Roopa Venkataraj, Vadakkedathu Parameswaran Narayana Nampoori,
Padmanabhan Radhakrishnan, and Madanan Kailasnath

Abstract—This paper reports a simple fluorescence-based tapered fiber optic probe for fluoride ion having a detection range of 2.08×10^{-6}–2.005×10^{-4} M. The performance of the tapered probe is evaluated with respect to the probes that consist of combinations of bare uncladded multimode optical fibers. The effect of fluorescence quenching of a natural dye curcumin in the presence of fluoride ion is used in the implementation of the probes. The probe effectively uses multiple mechanisms for the excitation and collection of fluorescence from the medium enabling higher sensitivity compared with conventional spectrophotometry especially at very low concentrations of fluoride.

Index Terms—Optical fiber sensors, evanescent wave fluorescence, tapered fiber, natural dye, curcumin.

I. INTRODUCTION

OPTICAL-TECHNOLOGIES have revolutionized the field of sensing and monitoring of hazardous species. They offer a spectrum of advantages including immunity to electrical interference, high sensitivity and cost effectiveness [1], [2]. In the class of optical sensing technologies, fiber optic sensors deserve special mention for their added positives including remote sensing, lower weight, compact nature etc [3]. Many groups have reported fiber optic sensors for different physical, chemical and biological parameters. Anion sensing is of utmost importance for present day water quality control in the light of many developing countries' heavy dependence on ground water resources and its considerable contamination from natural as well as industrial sources. Irrespective of the widely known attributes of the fiber optic sensor, there seems to be a deficit in fiber optic sensors for the detection of anions, specifically the fluoride ion.

Low concentrations (<1 ppm) of fluoride ion in drinking water resources are considered to be beneficial for the prevention of tooth decay, growth of bones etc. Beyond

this value, fluoride ion tends to increase the risk of dental and skeletal fluorosis in humans [4]. Different methods have been employed to sense the fluoride ion like ion selective electrodes, chromatography etc. [5], [6]. But in comparison to these bulky, high cost [7] methods many other relatively simpler works have also been carried out to enable colorimetric i.e. naked eye detection of fluoride ion in different solvents. But sometimes gradation of color may not be very effective in providing information about the exact amount of fluoride ion concentration in these solvents. Some of the reported studies that solve this problem involve simultaneous colorimetric and spectrophotometric response with the use of a wide range of sensing reagents like dyes, nanoparticles, classes of compounds like organogelators and boranes [8]–[12]. Even though these methods exhibit sufficient sensitivity and selectivity, the preparation of sensing reagents seems to be a tedious process requiring many steps. Moreover, it is interesting to note that most of the reported works on fluoride detection involve organic solvents [13], [14]. This is owing to the very large hydration energy of fluoride ion, which makes the operation of sensors in aqueous media difficult [15]. An interesting method to detect fluoride ion was reported by Wu *et al* using Curcumin as the sensing agent [16]. Curcumin responded to fluoride ion via the formation of a hydrogen bonded complex, which led to significant changes in its optical properties. Sometimes termed as the Indian solid gold [17], Curcumin is most researched for its medicinal properties and consequent applications in drug therapy for cancer and recently even in treatment of Alzheimer's [18]. Some work has also been published with reference to the application of Curcumin in the synthesis of nanoparticles and dye sensitized solar cells [19], [20]. The use of Curcumin for sensing is appealing because of its non-toxic nature and easy availability. There have been considerable efforts in the direction of solubilizing Curcumin as well as rendering it in a form suitable for drug delivery applications [21], [22]. It is in this context that a simple, easy to use fiber optic sensor for fluoride ion using Curcumin gains significant importance for replacing complex and costly sensors.

The intensity based fiber optic sensors are the simplest to implement [23], most of them being concentrated on absorption and fluorescence phenomena. Fluorescence based fiber optic sensors are highly sensitive and enable measure-

ment of very low value chemical specie concentrations [1]. Tapered fibers in general are reported to increase the coupling efficiency of the evanescent field to the surrounding medium as well as possess comparatively higher fluorescence coupling efficiency when compared to the bare fiber [24], [25]. Especially multimode fiber tapers are comparatively easier to handle when compared to the single mode fiber tapers [26]. Chemically tapered fibers are deemed to be more readily usable for capturing fluorescence owing to the absence of cladding in the taper structure [27]. Recently, there has been growing interest in the collection and quantification of intrinsic fluorescence signal in single as well as multimode fibers [28], [29]. A fiber optic sensor using the fluorescence phenomena of a natural dye like Curcumin for fluoride ions would enable huge cost reduction, meanwhile also enabling ease of use as compared to other existing techniques for fluoride ion sensing. An attempt in such a direction was carried out by our group, involving the excitation and collection of fluorescence from different combinations of tapered and simple un-clad multimode fiber pairs. In our work, we propose the use of multiple mechanisms for enhancing fluorescent signal generation and collection via the excitation and collection of fluorescence using evanescent wave and also axial excitation of fluorescence using bare unclad fibers. We observed that acetonitrile, an aprotic organic solvent, could easily dissolve Curcumin and that there was quite a strong fluorescence observable in this system, and hence acetonitrile was chosen as one of the solvents to test the performance of the fiber probes described in later sections of the paper.

It was found that considerable amount of fluorescence could be detected by all the combinations, particularly the probe consisting of optical fibers placed together that have dissimilar un-cladded lengths can function as a suitable substitute to the fragile tapered fibers. Since the refractive index of surrounding medium plays a major role in the coupling efficiency of the fiber probe, the probes were also tested with a solvent like anisole which has a higher refractive index than the core of the optical fiber. To the best of our knowledge, Curcumin has been used in the fluorescence based fiber sensing of an analyte for the first time. Even though there are numerous works on the use of tapered fibers for sensing a number of parameters, its use in the detection of fluoride ion has not yet been attempted. Also, the use of a hybrid system consisting of a short un-cladded length excitation fiber and a tapered fiber for fluorescence collection has not yet been studied. Moreover, the use of such a hybrid system for fluorescence signal acquisition from a higher refractive index medium has also not been investigated previously. The results indicate that with the proposed configurations, fluorescence can be detected even with solvents having higher refractive index than the core. Along with the use of a suitable sensing agent, the proposed tapered optical fiber fluorescence probe may also be extended for use in the detection of by-products of chemical reactions, irrespective of the refractive index of the solvents used. The probes in some cases seem to exhibit comparable, if not better resolution with respect to the conventional spectrophotometers in the range of interest, making it an attractive, highly sensitive, simple, low cost substitute for fluoride ion sensing.

II. THEORETICAL SECTION

In general, for an optical fiber of un-cladded length L, the breach of evanescent wave into the surrounding absorbing medium with concentration of absorbing species c is described by the expression [30]:

$$P = P_o e^{-\gamma cL} \qquad (1)$$

where P and P_o are respectively the power transmitted by the optical fiber with and without the presence of absorbing medium and γ is the evanescent absorption coefficient.

The depth of penetration of the evanescent wave for wavelength of light λ is given by the equation [24]:

$$d = \frac{\lambda}{2\pi \sqrt{n_{core}^2 sin^2\theta - n_{clad}^2}} \qquad (2)$$

where n_{core}, n_{clad} and θ are the refractive indices of the core, cladding of the fiber and incident ray angle normal to the interface respectively.

In the case of a multimode optical fiber, each propagating mode has a different penetration depth than any other, which in turn leads to an absorption profile consisting of a broad range of evanescent absorption coefficients associated with the large number of modes travelling along the optical fiber. So consequently in the case of a multimode optical fiber, the coupling of evanescent power to the surrounding medium leads to the supposed logarithmic nature of the detected transmitted power at the detector end [30]. Tapering a fiber increases the coupling of evanescent wave into the external media and hence increases the sensitivity. The smaller the diameter and larger the length of the taper, higher is the coupling efficiency [25].

The exposure of evanescent wave into the surrounding medium excites fluorescence from the dye molecules which is coupled back by guided modes of the core. Fluorescence collection efficiency depends on many factors like refractive indices of the core, cladding, sensing medium/layer, geometry of the probe [25]. The total number of modes propagating through a multimode optical fiber described by the V number is given by the equation [31]:

$$V = 2\pi r \frac{\sqrt{n_{core}^2 - n_{clad}^2}}{\lambda} \qquad (3)$$

where r is the radius of the core ($\approx$200 μm).

Theoretical investigations on the mode matching condition crucial to enable efficient fluorescence coupling back to guided modes in the core of the optical fiber lead to the concept of a matching radius which is given by the equation [24], [31]:

$$R_m = r \frac{\sqrt{n_{core}^2 - n_{clad}^2}}{\sqrt{n_{core}^2 - n_{med}^2}} \qquad (4)$$

where R_m is the matching radius, and n_{med} is the refractive index of the immersion medium respectively.

This formulation holds true for the case of a single tapered section in multimode optical fiber with the source and collection ends at two opposite extremities of the same optical fiber. But this would hold true also in the case of two multimode

optical fibers placed together to function as an evanescent wave fluorescence sensor. The matching radius in the case of 200/229 μm plastic clad silica (PCS) optical fiber with $n_{core} = 1.462$, $n_{clad} = 1.414$ and acetonitrile as the sensing medium ($n_{med} = 1.3431$) is calculated to be 129 μm. A core radius below the value of matching radius would curb the loss in fluorescent signal acquisition and hence chemically tapered multimode fibers are the easiest means to achieve the above mentioned criteria. For a medium with higher refractive index than the core of optical fiber like anisole ($n_{med} = 1.516$), it is not expected that there would be significant collection of excited fluorescence back into to the core of the optical fiber. It has been experimentally observed in an earlier study that the fluorescent signal collection approaches negligible value as the index of surrounding medium reaches a value above the core index value [32]. Moreover the right hand side (R.H.S) of Eq. 4 would possess a negative value and the concept of a matching radius seems obsolete in this case. But for the case of a higher index medium, whatever may be the mechanism of fluorescence signal generation, only those fluorescent rays that have angles between [0, θ_{cr}] can be coupled back into the fiber core of collection fiber. The critical angle θ_{cr} is given by the equation [25]:

$$\theta_{cr} = \sin^{-1}\frac{n_{core}}{n_{med}} \tag{5}$$

With $n_{core} = 1.462$ and $n_{med} = 1.516$, the value of θ_{cr} is calculated to be 0.42π radian = 74.7 degrees.

III. EXPERIMENTAL SECTION

Curcumin dye (Acros Organic) was at first dissolved in acetonitrile (and anisole) to get 1×10^{-5} M concentration dye solution. Aliquots of fluoride samples were prepared using specific volumes of tetrabutylammonium fluoride (TBAF, 75 % in water, Spectrochem Pvt Ltd, India) that were dissolved in the prepared stock solution to get a range of fluoride ion concentration in the solvents. Tapered sections in the 200/229 μm multimode plastic clad silica optical fibers (Polymicro Technologies) were formed by employing the chemical method using etchant HF in a similar fashion as reported in previous literature [27], [33]. About 2 cm from one end of about 60 cm length optical fiber was stripped off the buffer and immersed in acetone to remove the plastic cladding completely. The cleaved un-cladded end was then placed in a special cubical teflon chamber for carrying out the chemical tapering process. About 20 μL of 48 % HF was added to the chamber making sure that the drop of HF completely covers the un-cladded tip with the tip almost occupying the central position. The HF gradually moves along the un-cladded length of the fiber due to the Marangoni effect [33] and evaporates simultaneously as it moves. This creates a taper profile along the length of the optical fiber. The etchant exposure time for the formation of the tapered section in all the optical fibers was optimized to be 75 minutes. After the requisite amount of time the remnant acid was removed carefully and the whole chamber was rinsed with 5 N Sodium hydroxide solution so as to remove any unreacted acid leftover in the chamber, which could ruin the taper profile.
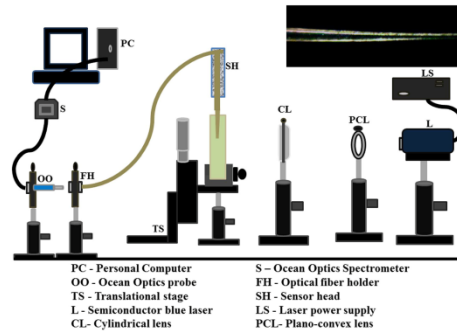
Fig. 1. Experimental set-up of the single chemically tapered multimode optical fiber for fluorescence measurement, (inset) CCD camera image of chemically tapered multimode optical fiber.

The tapered tips were then stored under 0.1 N NaOH solution until they were fixed for use in the optical fiber sensor. Many such tapered tips were prepared and examined under a GP-KR 222 CCD camera and were found to have an average taper length of 3.3 mm and diameter of 36 μm respectively. The chemically tapered multimode optical fiber as observed under the CCD camera is shown as an inset in Fig. 1.

A simple set up was assembled as shown in Fig. 1 to test the fluorescence of the samples using a single chemically tapered optical fiber. Light from a 100 mW Vortran Stradus semiconductor blue laser (403 nm) was converted to form a vertical strip of length approximately 2 cm using a combination of plano-convex lens and a cylindrical lens of focal length 50 cm. The bulk optics are adjusted and aligned in such a way that the laser light strip falls approximately close to the tapered optical fiber tip. This is done to ensure maximum fluorescence signal coupling to the optical fiber when it is immersed into the samples taken in a 1 cm quartz cuvette. A 3D translational stage is used to immerse the tapered tip into the samples.

The fluorescence signal collected by the tapered fiber is fed to a spectrometer (Ocean optics HR 4000, SpectraSuite) via the Ocean Optics (OO) probe. The OO probe is nothing but a connectorized jacketed step-index multimode optical fiber of similar core dimensions as the un-cladded optical fiber probe. Using the configuration of Fig. 1, considerably good fluorescence signal can be obtained. But so as to enable remote sensing capability of the optical fibers, it would be necessary to couple the excitation laser light to and fluorescence light from the optical fibers. Hence different combinations of un-cladded tapered and un-cladded optical fibers were attempted to test suitability of the same for onsite monitoring of fluoride ions in solution. To this end the different configurations were fixed on glass slides using epoxy glue as shown in Fig. 2.

Fig. 2a consists of a pair of fibers with 2 cm un-cladded from the edge, whereas Fig. 2b uses tapered fibers, in both cases with one optical fiber being used for excitation and other for collection of fluorescence from the medium. Figs. 2c and 2d both employ a small un-cladded length of about 0.7 cm for excitation of fluorescence. An un-cladded
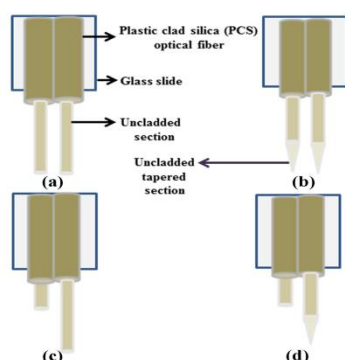
Fig. 2. Optical fiber probe combinations for fluorescence detection with (a) Two similar un-cladded multimode fibers, (b) two similar tapered multimode fibers, (c) dissimilar length un-cladded multimode fibers and (d) dissimilar length un-cladded-tapered multimode fiber pair.
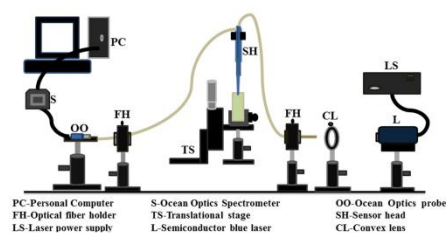
Fig. 3. Fluorescence measurement using combinations of tapered and un-cladded multimode optical fibers.

Fig. 4. Colour gradation of Curcumin dissolved in (a) acetonitrile and (b) anisole in the presence of (from left to right) 0, 2×10^{-6}, 7×10^{-6}, 2×10^{-5}, 7×10^{-5}, 2×10^{-4}, 7×10^{-4}, 2×10^{-3} M fluoride ion.

optical fiber and a tapered fiber respectively function as the collection fiber in the probes of Figs. 2c and 2d. The experimental set-up common to the probes of Figs. 2b, 2c and 2d is as shown in Fig. 3. A convex lens of focal length 3.5 cm was used to couple the laser light into the medium through the excitation fiber. This set-up did not require the use of couplers to segregate the incident light and the collected fluorescence light. The probe 2a was interrogated with direct laser light coupling into the excitation fiber.

IV. Results and Discussion

The color changes of the Curcumin in acetonitrile and anisole in the presence of fluoride ion are shown in Fig. 4. At particular concentrations of fluoride ion, the initial yellow
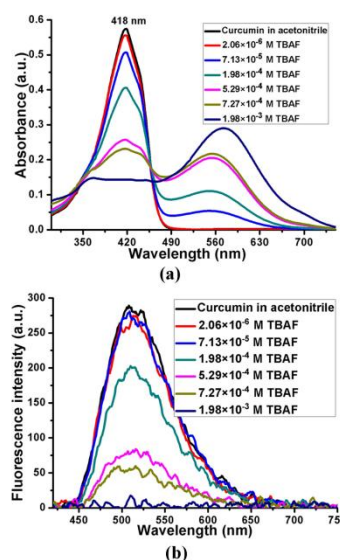
Fig. 5. (a) Absorption and (b) fluorescence spectrum of Curcumin (10^{-5}M) in the presence of fluoride ion in acetonitrile.

color solution of Curcumin transforms to purple and reddish brown color in acetonitrile and anisole respectively. The absorption and fluorescence spectra of the samples were recorded with a Jasco V 570 UV-Vis spectrophotometer and the Cary Eclipse (Varian) fluorescence spectrophotometer. The colorimetric response of Curcumin towards fluoride ion is also reflected in the optical spectra in the case of both the solvents as will be discussed in later sections.

The initial absorption peak of Curcumin in acetonitrile at 418 nm decreased continuously when carrying out absorption titration with fluoride ion. At a particular concentration (here 7×10^{-5} M TBAF) a new peak at 560 nm range emerged which increased in intensity with increase in fluoride ion concentration. Clearly formed isobestic points at 355 nm and 458 nm were also visible in the spectrum. These changes in the absorption behavior can be attributed to the effect of F$^-$ forming a complex with OH hydrogen of Curcumin [16]. This complex exists in equilibrium state with the deprotonated form of Curcumin, which is in turn formed in the presence of excess fluoride ion concentration. This leads to the colorimetric response of Curcumin in acetonitrile with a gradation of purple color from light to deep purple in the presence of increasing fluoride ion concentration. The fluorescence emission at 512 nm on the other hand, continuously decreases with increase in fluoride ion concentration as shown in Fig. 5(b). This particular result is ascribed to the energy transfer from Curcumin to the complex formed with fluoride ion [16].

The hydrogen bonding nature of the complex in acetonitrile was also verified by Wu *et al.* [16] using absorption titration with ethanol and also by our group with absorption titration

(a)

(b)
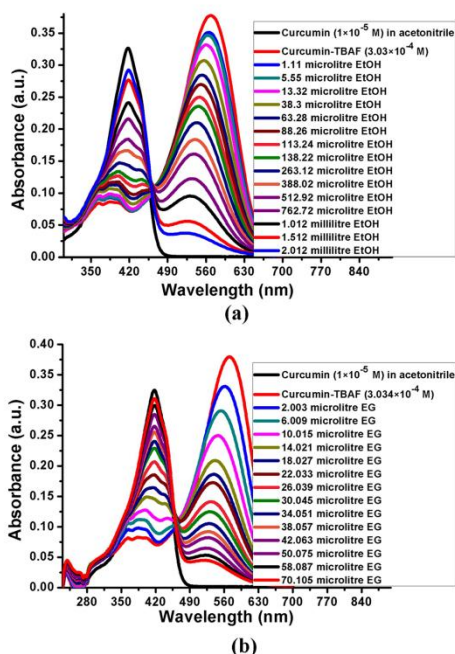
Fig. 6. Effect of protic solvents: (a) Ethanol (EtOH) and (b) Ethylene glycol (EG) on the interaction between Curcumin and tetrabutylammonium fluoride (TBAF) in acetonitrile.

(a)

(b)

Fig. 7. (a) Absorption and (b) fluorescence spectrum of Curcumin (10^{-5}M) in the presence of fluoride ion in anisole.

Fig. 8. Effect of Ethanol (EtOH) on the absorption spectrum of Curcumin in the presence of 2.2×10^{-4} M tetrabutylammonium fluoride.

with ethanol and ethylene glycol. We found that there was indeed a retrace of absorption curves as reported by the aforementioned group in the presence of protic solvents, especially a faster recovery in the case of the strongest protic solvent ethylene glycol as illustrated by the Fig. 6(b). It can be easily inferred from Fig. 6(b), that only a small volume of ethylene glycol was sufficient to facilitate the absorption spectrum retrace back to the spectrum of Curcumin in the absence of fluoride ion, when compared to that needed for ethanol. These results point to the fact that there is a marked sensitivity of the complex towards protic solvents making them difficult to be used in aqueous media.

Curcumin portrays an absorption maximum at 422 nm in anisole with isobestic points at 355 nm and 458 nm as depicted in the Fig. 7(a). Fluorescence emission in the range of about 482 nm-500 nm was observed (Fig. 7(b)). The response of Curcumin towards fluoride ion in anisole mimics that of its response in acetonitrile, with a similar complexation tendency, clearly inferred from the absorption spectrum. The higher concentrations above 2×10^{-4} M TBAF were excluded from the results as small amount of aggregates were formed owing to water insolubility of anisole and the presence of small amount of water in tetrabutylammonium fluoride (TBAF) solution. The effect of protic solvent ethanol on the complex formed between Curcumin and fluoride ion in anisole is as shown in Fig. 8. In this case also there is a recovery of

absorption spectrum of Curcumin [16] with increased addition of protic solvent ethanol (EtOH). This leads to the conclusion that hydrogen bonding does indeed play the major role in complex formation in anisole also.

Fig. 9 shows the response of the single tapered fiber of experimental set up of Fig. 1, for the solvents acetonitrile and anisole. The quantum yield of Curcumin in anisole was calculated using the comparative method, in comparison with the standard (for the blue region) C540a dissolved in ethanol [34], [35]. The quantum yield of Curcumin in anisole solvent was found to be about 1.3 times higher than that in acetonitrile. So it can be said that the lower fluorescence recorded in anisole may be due to the higher refractive index of anisole (=1.516 RIU) that prevents efficient coupling back into the core of the collection fiber.
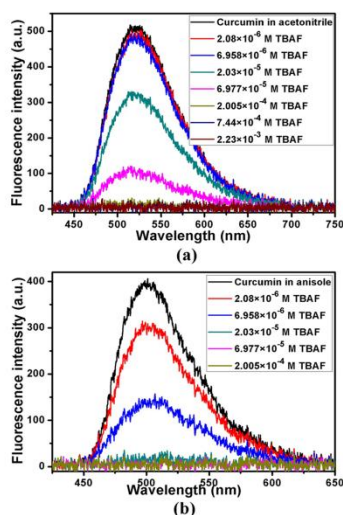
Fig. 9. Fluorescence response from the single tapered optical fiber probe set up with (a) acetonitrile and (b) anisole solvents.

Fig. 11. Incident 403 nm laser light path inside the solvents with (a) Curcumin in acetonitrile. (b) Curcumin in acetonitrile in the presence of fluoride ion. (c) Curcumin in anisole. (d) Curcumin in anisole in the presence of fluoride ion.

Fig. 10. Fluorescence of Curcumin in (a) acetonitrile and (b) anisole as recorded by probe 2a comprising of a pair of un-cladded optical fibers.

At first the optical fiber probe of Fig. 2a was tested for fluorescence in the solvents and the response is as shown in Fig. 10. It was observed that the fluorescence detected was feeble and there was especially not much resolution between the readings at lower concentration values. The noisy spectra observed here may be attributed to the intensity fluctuations of

the laser source. It was also noticed that the laser light through the Curcumin dissolved solvent using a un-cladded section of excitation fiber seemed to produce a cone of fluorescence light inside the medium. To make use of this fluorescence cone to increase the efficiency of the fiber probe, we constructed and tested the response of the fiber probes of figures 2(c) and 2(d). The path of light in both the solvents utilizing dissimilar lengths for excitation and collection fiber, with shorter length of un-clad section for coupling laser light into the media is as depicted in Fig. 11.

Both the solvents seem to produce the cone of fluorescence, but the refractive index of anisole being higher than the exposed core of the multimode silica optical fiber, a significantly divergent cone is observable in anisole. The light seems to reflect off the faces of the cuvette leading to a less intense, dispersed region of fluorescence inside anisole medium. As discussed in previous sections, tapered fibers can provide evanescent wave excitation of fluorescence as well as effectively couple it back into the core and hence the light is guided through the optical fiber [24]. An initial attempt of collecting fluorescence using a system of two tapered fibers like that of probe 2b was carried out by our group and reported in previous literature [36]. The fibers used were of higher taper diameter as compared to the ones used in the present work, and seemed to give a good response towards the detection of fluoride ion. Probe 2b in the present work serves to compare the response of a doubly tapered system with hybrid sensor heads proposed in this work. So as to further increase the fluorescence intensity a probe with a combination of unclad small length optical fiber for excitation and a tapered fiber for the collection of fluorescence was constructed as in Fig. 2(d). The response of the optical fiber probes of figures 2b, 2c and 2d in capturing the diminishing fluorescence of Curcumin in the presence of increasing fluoride ion concentration is as shown in the Fig. 12.

The detection limit for the optical fiber probes of Fig. 2 is 2.08×10^{-6} M, but there seemed to be considerable resolution between the readings of lower fluoride ion concentration in anisole. This marked shift in detected fluorescence level between fluoride concentrations in anisole may be due to the high quantum yield of Curcumin in anisole. Also it might
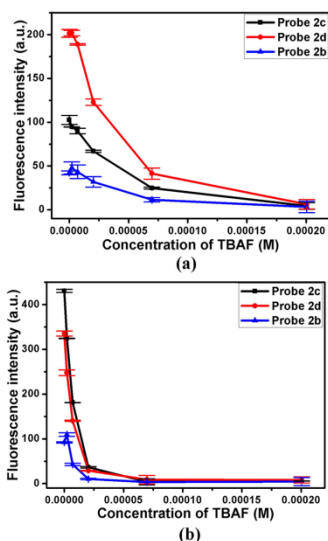
Fig. 12. Fluorescence based optical fiber probe response to fluoride ions using probes 2b, 2c and 2d in (a) acetonitrile and (b) anisole.

be expected that dissimilar absorption coefficients of different modes travelling along the fiber core [30] and also varied fluorescence collection efficiency of the guided modes in the multimode fiber would aid a higher resolution between fluorescence levels corresponding to varied fluoride concentrations. The fluorescence collection would also be dependent on the refractive index [32] of the surrounding medium which is higher than the fiber core in the case of anisole. Moreover, it was also observed that nil fluorescence was reached faster in anisole (6.977×10^{-5} M) than in acetonitrile (2.005×10^{-4} M). The negligible change in fluorescence intensity at higher fluoride concentrations may be attributed to 1:1 binding nature of Curcumin with fluoride ion [16].

The comparatively feeble value of fluorescence signals in the case of probes 2a and 2b may be due to the poor collection of fluorescence via the evanescent wave. In these cases major portion of fluorescent signal may have been coupled axially directly from the fluorescing medium. Whereas in the case of probes 2c and 2d which use axial along with evanescent wave excitation, fluorescence signal detected was considerably high. We propose that axial excitation through the end surface of the core of un-cladded multimode optical fiber lead to a fluorescence cone incident on the collection fiber covering a wide spectrum of angles for the same leading to major fraction of light satisfying critical angle condition and getting coupled into the fiber core as guided modes and reaching the detector. The fluorescence cone in close proximity to just a simple un-cladded fiber was able to give considerable resolution to fluoride ion sensing in a higher refractive index solvent like anisole as is evident in the Fig. 12(b). This is supported by the fact that in the higher index solvent anisole

with a dispersed fluorescence cone, the theoretically calculated critical angle being approximately 74 degrees, most of the fluorescent light was coupled back into the core. There was considerable collection of fluorescence in the case of probe 2d in the case of both the solvents which points to the use of such a hybrid system to detect low values of fluorescence consequently increasing the dynamic range of the fluorescence based fiber optic probe. The detection range spans a broad concentration of fluoride viz. 2.08×10^{-6} - 2.005×10^{-4} M (0.545-52.4 ppm) which is comparatively higher than that of previously reported fiber optic sensors for fluoride ion in literature [37], [38].

V. CONCLUSION

Fiber optic probes based on chemically tapered multimode fibers were constructed and their performances were evaluated with respect to probes constructed with just simple bare unclad optical fibers. Natural dye Curcumin is used as the sensing agent for fluoride ion in organic solvents acetonitrile and anisole which respectively possess lower and higher refractive index than the fiber core. The fluorescence of Curcumin was quenched in the presence of fluoride ion owing to the formation of hydrogen bond with it and subsequent de-protonation of Curcumin at higher concentration of fluoride ion. It was observed that comparatively higher fluorescence could be detected by the combination involving an unclad excitation fiber and tapered collection fiber. This is owing to the evanescent wave aided and axial excitation of fluorescence in the medium and its efficient collection by the probe. A considerably broad range of fluoride concentration from 2.08×10^{-6} - 2.005×10^{-4} M (0.545-52.4 ppm) could be measured by the probes described in the present work. These probes can very well be extended for use in measuring different chemical and biological species irrespective of the type of solvent used. The detection of fluoride in aqueous medium is a considerable challenge, but nonetheless a necessity. With this fact in view, aqueous medium based sensing of fluoride ion using Curcumin with the use of suitable buffer is currently being investigated by our group. This would enable an extremely simple, sensitive as well as low cost optical method for fluoride ion sensing in onsite applications.

REFERENCES

[1] W. R. Seitz, "Chemical sensors based on fiber optics," *Anal. Chem.*, vol. 56, no. 1, pp. 16A–34A, Jan. 1984.
[2] G. A. Ibañez and G. M. Escandar, "Fluorescence and phosphorescence chemical sensors applied to water samples," in *Smart Sensors for Real-Time Water Quality Monitoring*, vol. 4, S. C. Mukhopadhyay and A. Mason, Eds. Berlin, Germany: Springer-Verlag, 2013, pp. 45–64.
[3] E. Udd, "Overview of fiber optic sensors," in *Fiber Optic Sensors*, F. T. S. Yu and S. Yin, Eds. New York, NY, USA: Marcel Dekker, 2002, ch. 1, pp. 1–39.
[4] S. Ayoob and A. K. Gupta, "Fluoride in drinking water: A review on the status and stress effects," *Critical Rev. Environ. Sci. Technol.*, vol. 36, no. 6, pp. 433–487, 2006.

[5] A. B. M. Ismail, K. Furuichi, T. Yoshinobu, and H. Iwasaki, "Light-addressable potentiometric fluoride (F⁻) sensor," *Sens. Actuators B, Chem.*, vol. 86, no. 1, pp. 94–97, Aug. 2002.

[6] P. Jones, "Development of a high-sensitivity ion chromatography method for the determination of trace fluoride in water utilizing the formation of the AlF^{2+} species," *Anal. Chim. Acta*, vol. 258, no. 1, pp. 123–127, Mar. 1992.

[7] N. I. P. Valente, P. V. Muteto, A. S. F. Farinha, A. C. Tomé, J. A. B. P. Oliveira, and M. T. S. R. Gomes, "An acoustic wave sensor for the hydrophilic fluoride," *Sens. Actuators B, Chem.*, vol. 157, no. 2, pp. 594–599, Oct. 2011.

[8] J. Wang, Y. Hou, C. Li, B. Zhang, and X. Wang, "Selectivity tune of fluoride ion sensing for phenolic OH-containing BODIPY dyes," *Sens. Actuators B, Chem.*, vol. 157, no. 2, pp. 586–593, Oct. 2011.

[9] X. Zhuang, W. Liu, J. Wu, H. Zhang, and P. Wang, "A novel fluoride ion colorimetric chemosensor based on coumarin," *Spectrochim. Acta A, Mol. Spectrosc.*, vol. 79, no. 5, pp. 1352–1355, Sep. 2011.

[10] J.-A. Gu, Y.-J. Lin, Y.-M. Chia, H.-Y. Lin, and S.-T. Huang, "Colorimetric and bare-eye determination of fluoride using gold nanoparticle agglomeration probes," *Microchim. Acta*, vol. 180, nos. 9–10, pp. 801–806, Jul. 2013.

[11] Z.-Q. Liu *et al.*, "Highly selective two-photon chemosensors for fluoride derived from organic boranes," *Organic Lett.*, vol. 7, no. 24, pp. 5481–5484, Apr. 2005.

[12] L.-B. Xing *et al.*, "Reversible sol-to-gel transformation of uracil gelators: Specific colorimetric and fluorimetric sensor for fluoride ions," *Langmuir*, vol. 29, pp. 2843–2848, Feb. 2013.

[13] Y. Shiraishi, H. Maehara, T. Sugii, D. Wang, and T. Hirai, "A BODIPY–indole conjugate as a colorimetric and fluorometric probe for selective fluoride anion detection," *Tetrahedron Lett.*, vol. 50, pp. 4293–4296, Jul. 2009.

[14] A. K. Mahapatra, K. Maiti, P. Sahoo, and P. K. Nandi, "A new colorimetric and fluorescent bis(coumarin)methylene probe for fluoride ion detection based on the proton transfer signaling mode," *J. Lumin.*, vol. 143, pp. 349–354, Nov. 2013.

[15] M. H. Lee, T. Agou, J. Kobayashi, T. Kawashima, and F. P. Gabbaï, "Fluoride ion complexation by a cationic borane in aqueous solution," *Chem. Commun.*, no. 11, pp. 1133–1135, Feb. 2007.

[16] F.-Y. Wu, M.-Z. Sun, Y.-L. Xiang, Y.-M. Wu, and D.-Q. Tong, "Curcumin as a colorimetric and fluorescent chemosensor for selective recognition of fluoride ion," *J. Lumin.*, vol. 130, no. 2, pp. 304–308, Feb. 2010.

[17] B. B. Aggarwal, C. Sundaram, N. Malani, and H. Ichikawa, "Curcumin: The Indian solid gold," in *The Molecular Targets and Therapeutic Uses of Curcumin in Health and Disease*, vol. 595. Berlin, Germany: Springer-Verlag, 2007, pp. 1–75.

[18] T. W. Kee, R. Adhikary, P. J. Carlson, P. Mukherjee, and J. W. Petrich, "Femtosecond fluorescence upconversion investigations on the excited-state photophysics of curcumin," *Austral. J. Chem.*, vol. 64, no. 1, pp. 23–30, 2011.

[19] S. Kundu and U. Nithiyanantham, "*In situ* formation of curcumin stabilized shape-selective Ag nanostructures in aqueous solution and their pronounced SERS activity," *RSC Adv.*, vol. 3, no. 47, pp. 25278–25290, 2013.

[20] T. Ganesh *et al.*, "Photoactive curcumin-derived dyes with surface anchoring moieties used in ZnO nanoparticle-based dye-sensitized solar cells," *Mater. Chem. Phys.*, vol. 123, no. 1, pp. 62–66, Sep. 2010.

[21] D. P. Singh, C. Jayanthi, K. Joshi, G. Hanumanthachar, and G. Bharathi, "Enhancement of aqueous solubility of curcumin by solid dispersion technology," *World J. Pharmacy Pharmaceutical Sci.*, vol. 2, no. 5, pp. 4109–4120, 2013.

[22] A. Altunbas, S. J. Lee, S. A. Rajasekaran, J. P. Schneider, and D. J. Pochan, "Encapsulation of curcumin in self-assembling peptide hydrogels as injectable drug delivery vehicles," *Biomaterials*, vol. 32, no. 25, pp. 5906–5914, May 2011.

[23] T. G. Giallorenzi *et al.*, "Optical fiber sensor technology," *IEEE J. Quantum Electron.*, vol. 18, no. 4, pp. 472–511, Apr. 1982.

[24] J. P. Golden, G. P. Anderson, S. Y. Rabbany, and F. S. Ligler, "An evanescent wave biosensor. II. Fluorescent signal acquisition from tapered fiber optic probes," *IEEE Trans. Biomed. Eng.*, vol. 41, no. 6, pp. 585–591, Jun. 1994.

[25] Y. Yuan and L. Ding, "Theoretical investigation for excitation light and fluorescence signal of fiber optical sensor using tapered fiber tip," *Opt. Exp.*, vol. 19, no. 22, pp. 21515–21523, Oct. 2011.

[26] S. Guo and S. Albin, "Transmission property and evanescent wave absorption of cladded multimode fiber tapers," *Opt. Exp.*, vol. 11, no. 3, pp. 215–223, Feb. 2003.

[27] H. S. Haddock, P. M. Shankar, and R. Mutharasan, "Fabrication of biconical tapered optical fibers using hydrofluoric acid," *Mater. Sci. Eng. B*, vol. 97, no. 1, pp. 87–93, Jan. 2003.

[28] U. A. Gamm *et al.*, "Extraction of intrinsic fluorescence from single fiber fluorescence measurements on a turbid medium: Experimental validation," *Biomed. Opt. Exp.*, vol. 5, no. 6, pp. 1913–1925, Jun. 2014.

[29] T. H. Nguyen, S. A. Hardwick, T. Sun, and K. T. V. Grattan, "Intrinsic fluorescence-based optical fiber sensor for cocaine using a molecularly imprinted polymer as the recognition element," *IEEE Sensors J.*, vol. 12, no. 1, pp. 255–260, Jan. 2012.

[30] P. S. Kumar, S. T. Lee, C. P. G. Vallabhan, V. P. N. Nampoori, and P. Radhakrishnan, "Design and development of an LED based fiber optic evanescent wave sensor for simultaneous detection of chromium and nitrite traces in water," *Opt. Commun.*, vol. 214, nos. 1–6, pp. 25–30, Dec. 2002.

[31] G. P. Anderson, J. P. Golden, and F. S. Ligler, "An evanescent wave biosensor. I. Fluorescent signal acquisition from step-etched fiber optic probes," *IEEE Trans. Biomed. Eng.*, vol. 41, no. 6, pp. 578–584, Jun. 1994.

[32] E. Sinchenko, W. E. K. Gibbs, A. P. Mazzolini, and P. R. Stoddart, "The effect of the cladding refractive index on an optical fiber evanescent-wave sensor," *J. Lightw. Technol.*, vol. 31, no. 20, pp. 3251–3257, Oct. 15, 2013.

[33] E. J. Zhang, W. D. Sacher, and J. K. S. Poon, "Hydrofluoric acid flow etching of low-loss subwavelength-diameter biconical fiber tapers," *Opt. Exp.*, vol. 18, no. 21, pp. 22593–22598, Oct. 2010.

[34] A. M. Brouwer, "Standards for photoluminescence quantum yield measurements in solution (IUPAC technical report)," *Pure Appl. Chem.*, vol. 83, no. 12, pp. 2213–2228, 2011.

[35] C. Würth, M. Grabolle, J. Pauli, M. Spieles, and U. Resch-Genger, "Relative and absolute determination of fluorescence quantum yields of transparent samples," *Nature Protocols*, vol. 8, pp. 1535–1550, Jul. 2013.

[36] R. Venkataraj, V. P. N. Nampoori, P. Radhakrishnan, and M. Kailasnath, "A simple fluorescence based optical fiber sensor for fluoride ions," presented at the 12th Int. Conf. Fiber Opt. Photon., 2014, paper M4A.15.

[37] X. Yang, J. Wang, and L. Wang, "Sol–gel matrix modified microstructured optical fibre towards a fluoride sensitive optical probe," *Opt. Commun.*, vol. 282, no. 13, pp. 2502–2505, Jul. 2009.

[38] A. B. Pillai, B. Varghese, and K. N. Madhusoodanan, "Design and development of novel sensors for the determination of fluoride in water," *Environ. Sci. Technol.*, vol. 46, no. 1, pp. 404–409, 2012.

Roopa Venkataraj received the master's degree in physics from Mahatma Gandhi University, Kottayam, India, in 2010. She is currently pursuing the Ph.D. degree in fiber optic sensors with the International School of Photonics, Cochin University of Science and Technology, Kochi, India. Her research interests include fiber optic sensors, nanomaterials, and biomaterials for sensing applications.

V. P. N. Nampoori received the Ph.D. degree in physics from Maharaja Sayajirao University of Baroda, Baroda, India, in 1978. He is currently an Emeritus Professor of Photonics at the International School of Photonics, Cochin University of Science and Technology, Kochi. He has authored or co-authored over 300 research papers in peer-reviewed journals. His expertise and research interests include bio-photonics, nonlinear optics, and photonic materials.

P. Radhakrishnan received the Ph.D. degree in physics from CUSAT, Cochin, India, in 1986. He is currently an Emeritus Professor of Photonics at the International School of Photonics, Cochin University of Science and Technology, Kochi. His research interests and expertise include laser technology, laser spectroscopy, and fiber optic sensors. He has authored or co-authored over 200 research papers in peer-reviewed journals.

M. Kailasnath received the Ph.D. degree in photonics from the International School of Photonics (ISP), Cochin University of Science and Technology (CUSAT), Kochi, India, in 2011, and the Post-Doctoral degree from Texas University, USA, in 2014. He is currently the Director of ISP, CUSAT. He has authored or co-authored over 35 research papers in peer-reviewed journals. His research interests include speciality polymer optical fibers, fiber optic sensors, nanophotonics, and polymer fiber lasers.

[162]

CrossMark

Photochemical Degradation of Curcumin: a Mechanism for Aqueous Based Sensing of Fluoride

Roopa Venkataraj[1] · C. P. Girijavallabhan[1] · P. Radhakrishnan[1] · V. P. N. Nampoori[1] · M. Kailasnath[1]

Abstract The present work describes the enhanced photochemical degradation of natural dye Curcumin in acetonitrile–water mixture in the presence of fluoride upon irradiation with light. The strong basicity of fluoride modifies the solvent environment around Curcumin molecule leading to alkaline mediated degradation of Curcumin which is further accelerated by irradiation with light. The photochemical degradation of Curcumin is studied using absorption and fluorescence spectroscopy and verified using infrared spectroscopy and fluorescence lifetime studies. The results of the work indicate that the method of Curcumin irradiation can be used as a sensing technique for fluoride detection in a wide range.

Keywords Curcumin · Sensing · Irradiation · Degradation · Fluoride sensing

Introduction

Fluoride, an electronegative anion is added in small proportions to toothpastes, mouthwashes as well as drinking water in order to prevent dental caries and tooth decay [1, 2]. Owing to the industrial demand for fluoride based products and the availability of fluoride in soil, fluoride pollution via multiple pathways is a huge threat to the human population. Studies world over indicate that fluoride in excess of 1 ppm in water resources can lead to fluorosis, osteosarcoma etc [3, 4]. Organic dyes, triarylborane compounds and nanoparticles etc. have been used for the detection of fluoride ions in organic solvents, mixtures of organic-aqueous solvents and a few in aqueous medium [5–7]. While some methods are costly or involve complicated preparation methods, others exhibit higher fluoride detection limits [1, 7]. There is hence a need of simple techniques for fluoride detection with the help of low cost sensing agents with wide detection range.

Curcumin, frequently termed as the "Indian solid gold" [8] finds a plethora of interesting applications in a variety of fields like medicine, nanotechnology and gastronomy [9]. The optical properties of Curcumin and the excited state dynamics are also widely studied by different groups [10, 11]. The absorption and fluorescence characteristics of Curcumin are expected to vary in the presence of additives [12], temperature [13], polarity and pH of the solvent etc [10, 14]. Upon irradiation of solutions of Curcumin using wavelength of light λ > 400 nm, degradation products like vanilin, ferulic acid, ferulic aldehyde are reported to be formed [15]. The degradation of Curcumin is also reported to be sensitive to factors like presence of certain analytes and basicity of solutions [12, 14, 16]. Curcumin has very low solubility in water at room temperature [17] thereby limiting its use for room temperature aqueous media based studies. But the high sensitivity of Curcumin towards its solvent environment along with its easy availability in nature makes it an ideal candidate for sensing applications. In fact, Wu et al. [18] reported the use of Curcumin for fluoride sensing in pure organic solvent using the formation of a complex between Curcumin and fluoride. But as described by the same group, this complex is disrupted in the presence of even micro-liter volumes of protic solvents leading to a reversal of sensing response of Curcumin. The use of this non-toxic dye in an aqueous environment or even

✉ Roopa Venkataraj
  roopa.venkataraj@gmail.com

[1] International School of Photonics, Cochin University of Science & Technology, Kochi 682022, Kerala, India

✎ Springer

in one involving mixtures of organic and aqueous solvents would indeed be very attractive method for fluoride detection. Towards this end, we studied the degradation behavior of Curcumin in mixed organic-aqueous solvent in the presence of common anions upon irradiation of light. The results of our work point to the potential use of natural dye Curcumin towards the detection of fluoride in aqueous media with the help of simple irradiation technique.

Experimental Section

Preparation of Anion Samples

The stock solution of 10^{-5} M of Curcumin dye (Acros Organics, > 98% purity) was prepared in 9:1 *v/v* acetonitrile:water mixture solvent. AR grade acetonitrile and deionised water were purchased from Nice Chemicals Pvt. Ltd., Kerala and Spectrum Reagents and Chemicals Pvt. Ltd., Kerala respectively. Tetrabutylammonium fluoride (TBAF, Spectrochem Pvt. Ltd., Mumbai) was added to the stock solution to get fluoride samples of varying concentrations. Separate aliquots of stock solution of Curcumin were also prepared with addition of common tetrabutylammonium anions (Sigma Aldrich, Spectrochem India Pvt Ltd) of acetate (TBAA), dihydrogen phosphate (TBAP), hydrogen sulphate (TBAS), nitrate (TBAN), chloride (TBAC), bromide (TBAB) and iodide (TBAI).

Irradiation Using Different Light Sources

The samples (about 3.5 ml) were taken in a 1 cm × 1 cm quartz cuvette and irradiated with light from a 100 mW semiconductor laser (403 nm, Vortran Stradus) for different time durations using the experimental set-up shown in Fig. 1. The samples of about 10 ml in volume taken in glass bottles were also exposed to a 125 W mercury vapour lamp (GE) wavelengths (364, 403, 435, 545, 576 and 619 nm) and a 365 nm UV lamp by placing the sample bottles before the lamps directly. The variation in the optical characteristics of the samples, before and after irradiation was studied using Jasco V-570 absorption spectrophotometer and Varian (Cary Eclipse) fluorescence spectrophotometer. The excitation and emission slit widths for fluorescence measurements were 5 and 10 nm respectively. The fluorescence lifetime measurement of the samples was carried out using Horiba DeltaPro lifetime system coupled with a 370 nm ($\pm$ 10 nm) NanoLED as the pulsed excitation source and a picosecond photon detection module. Lifetime values ranging from 25 picoseconds to 1 s can be measured using this system. The analysis of fluorescence decay was carried out using Horiba DAS6 decay analysis software. The structural change in the Curcumin molecule upon photochemical degradation was studied using the Thermo Nicolet Avatar 370 FTIR spectrometer in the 400–4000 cm^{-1} range using the KBr pellet method for recording the spectrum.

Results and Discussion

Curcumin has an absorbance maximum of 421 nm and fluorescence maximum of 529 nm in acetonitrile–water mixture solvent when excited with the peak absorption wavelength. The presence of anions does not lead to any change in the optical characteristics of Curcumin as shown in Fig. 2.

The absence of variation in the absorbance and fluorescence spectra is attributed to the strong hydrogen bonding tendency of water molecules with Curcumin leading to the absence of any response of Curcumin in the presence of anions [18]. Consequently this leads to

Fig. 1 Experimental set-up for irradiation of samples with 403 nm semiconductor laser

TS – Translational stage
LS – Laser power supply
PCL – Plano–convex lens
L – 403 nm laser
CL – Cylindrical lens
C – Quartz cuvette

[164]
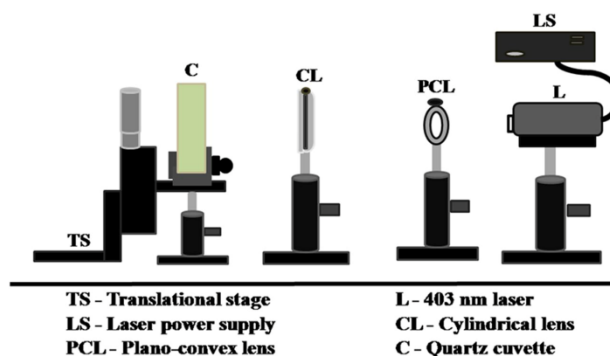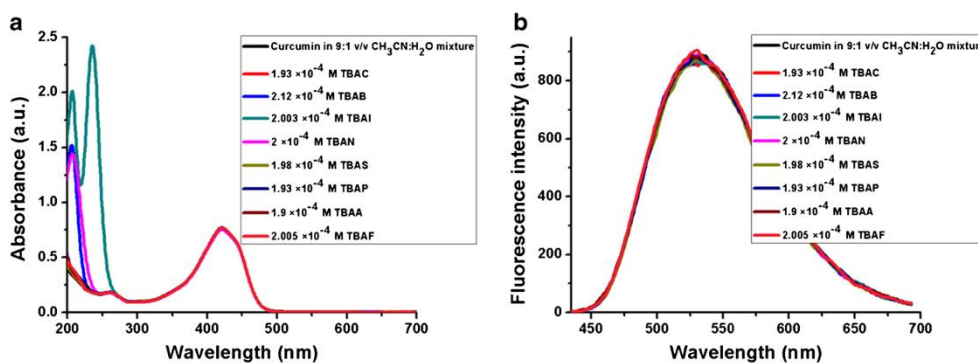
Fig. 2 **a** Absorption and **b** fluorescence spectra of 10^{-5} M Curcumin in 9:1 v/v $CH_3CN:H_2O$ solvent mixture in the presence of common anions

the absence of any colorimetric or optical changes in this case leading to the inference that Curcumin may not be suitable for aqueous based sensing of fluoride. But we believe that the photochemical degradation of Curcumin being very sensitive to the solution parameters may serve as an indicator of the amount of analyte present in the solution. We observed that on irradiation of the anion samples, there is a considerable decrease in the intensity of the initial yellow coloration of Curcumin and a change in absorption and fluorescence characteristics of Curcumin especially in the case of fluoride addition. The change in absorption and fluorescence of the anion samples on irradiation using the 403 nm laser is shown in Fig. 3.

From Fig. 3 it is clear that the presence of fluoride in the mixture solvent leads to maximum decrease in the intensity of the absorption and fluorescence peaks of Curcumin pointing to enhanced degradation of Curcumin. It was also observed that degradation of Curcumin in the presence of fluoride increased with increase in duration of exposure to different sources of light. This is evidenced from the increase in change in peak absorbance with time duration of exposure in the presence of fluoride as shown in the Fig. 4.

Figure 5 illustrates the changes in the absorption and fluorescence peaks of Curcumin under laser irradiation with varying fluoride concentration. There is a gradual decrease in peak absorbance at 421 nm along
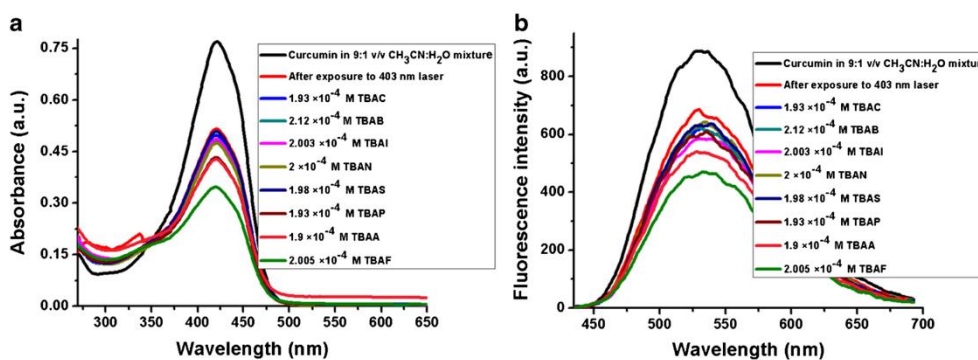
Fig. 3 **a** Absorption and **b** fluorescence spectra of 10^{-5} M Curcumin in 9:1 v/v $CH_3CN:H_2O$ solvent mixture in the presence of common anions after exposure to 45 min of 403 nm laser radiation
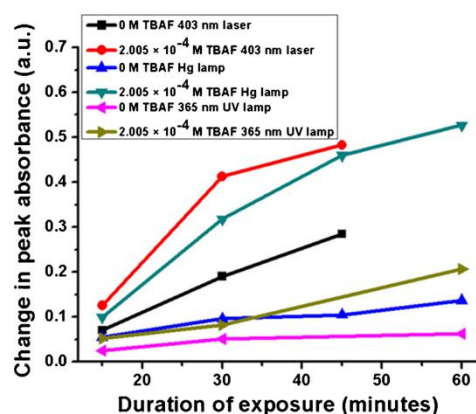
Fig. 4 Variation in peak absorbance of samples (with respect to un-irradiated Curcumin) with duration of exposure to radiation from different sources

with a slight increase in absorbance in the 250–350 nm as well as in the 480–600 nm region of the absorption spectrum. The expanded views of the two regions are as shown in Fig. 6. The presence of two isobestic points in the spectra around 349 and 495 nm along with the afore-mentioned changes in peak intensity about them, points to the degradation of Curcumin and subsequent forma-tion of its degradation products. Several alkaline degra-dation mechanisms of Curcumin have been described in detail in literature. Many reports suggested that the deg-radation products were formed via the deprotonation of phenolic OH group of Curcumin or the breakage in the

heptadienedione linkage [12, 15, 19]. Gordon et al. [20] reported auto-oxidation behavior of Curcumin at physi-ological pH to form bicyclopentadione as the major mechanism for degradation. The changes reflected in the absorption spectrum of Fig. 5 indicate photo-degra-dation of Curcumin via multiple mechanisms upon irra-diation in the mixture solvent. The increase in absorb-ance in the UV region may be ascribed to formation of lower molecular weight degradation products owing to breakage in the heptadienedione linkage of Curcumin [21]. The small increase in the absorbance region above 480 nm may be due to the deprotonation of the hydroxyl group [12]. There is also a huge decrease in fluores-cence of Curcumin upon irradiation in mixture solvent in presence of increasing fluoride indicating the conver-sion of fluorescent Curcumin to its degradation prod-ucts. We believe that the increase in basicity of the sol-vent environment of Curcumin with increase in fluoride concentration [22] leads to the enhanced degradation rate of Curcumin upon irradiation.

Figure 7 shows the comparison of peak absorbance and fluorescence intensity of Curcumin in mixture solvent in the presence of fluoride with and without irradiation. There is no change in the peak absorption and fluorescence inten-sities of un-irradiated Curcumin with increase in fluoride concentration whereas there is a huge decrease in the peak values in the case of irradiated samples. The plot of peak absorption and fluorescence intensities versus the logarithm of fluoride concentration as shown in the inset of Fig. 7 is approximately linear throughout the entire range of fluoride concentration studied in this work. Hence we believe there is a possibility of using the irradiation technique for direct readout of fluoride concentration in practical applications.
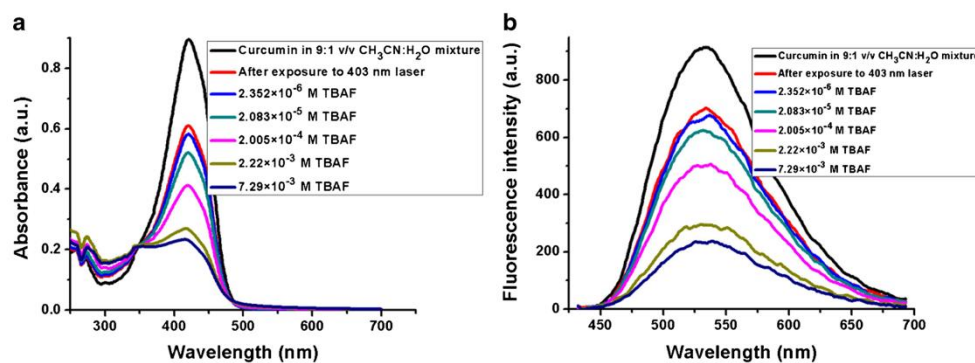
Fig. 5 **a** Absorption and **b** fluorescence change of 10^{-5} M Curcumin in 9:1 *v/v* CH$_3$CN:H$_2$O solvent mixture in the presence of varying fluoride concentration after exposure to radiation from 403 nm laser for 45 min

[166]
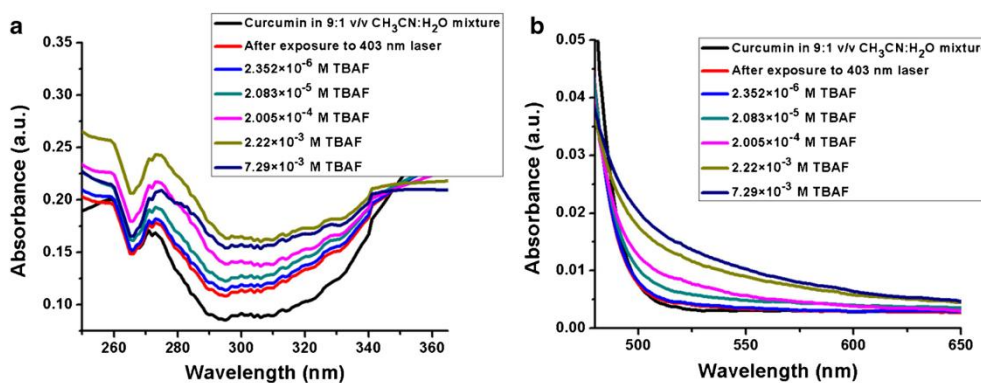
Fig. 6 Increase in absorbance of Curcumin in the (**a**) 250–350 nm and (**b**) 480–600 nm wavelength region with irradiation and in the presence of increasing fluoride concentration
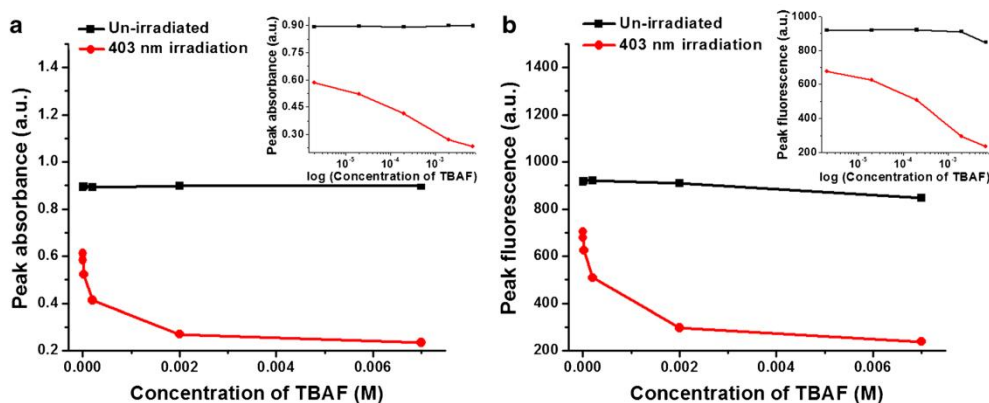
Fig. 7 Comparison of (**a**) peak absorbance and (**b**) peak fluorescence of un-irradiated and irradiated 10^{-5} M Curcumin in mixture solvent with fluoride concentration. Insets show the variation of peak absorbance and fluorescence with logarithm of fluoride concentration

The Fourier transform infrared (FTIR) spectrum of the samples is as shown in Fig. 8. The medium intensity band around 1640 cm^{-1} corresponds to the mixed C=O and C=C stretch in the benzene ring. There is a clear increase in the transmittance in this band region upon irradiation of Curcumin. The transmittance is still higher in the case of irradiation of Curcumin in the presence of fluoride. The weak band at 1423 cm^{-1} corresponds to the in plane bending of aromatic (CCC, CCH), enolic (COH), CH in plane bending due to CH$_2$ [23]. Here also a huge increase in transmittance is observed in the case of Curcumin irradiation with fluoride in mixture solvent. The results of the

FTIR analysis indicate a quantitative decrease in the Curcumin content as a result of irradiation in the presence of fluoride in mixture solvent pointing to the formation of degradation products of Curcumin.

The photochemical degradation of Curcumin in the presence of fluoride was also confirmed using the time correlated single photon counting (TCSPC) method for fluorescence lifetime determination. It was observed that there is a slight increase in average lifetime of irradiated Curcumin in mixture solvent in the presence of fluoride compared to the sample without fluoride. The change in the lifetime values
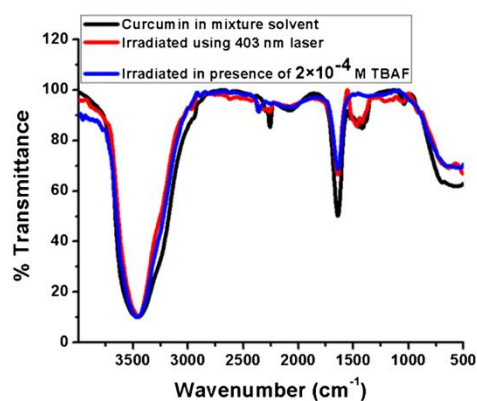
Fig. 8 Comparison of the FTIR spectrum of 10^{-5} M Curcumin in 9:1 *v/v* CH$_3$CN:H$_2$O solvent mixture in the absence and presence of fluoride under 403 nm laser irradiation

of the components of Curcumin in mixture solvent is as shown in Table 1.

The shorter fluorescence lifetime is the major component while the longer fluorescence lifetime is the minor component in all the samples as reported in literature [10]. But it was observed that there is considerable decrease in contribution of chemical species having shorter fluorescence lifetime and a corresponding increase in species having a longer fluorescence lifetime in the case of fluoride containing sample. This observation points to the enhanced photochemical degradation of Curcumin in mixture solvent in the presence of fluoride.

The detection of fluoride in both its organic (TBAF) and inorganic (NaF) form is very important for practical sensing applications. It was observed that the method of irradiation of Curcumin in mixture solvent can also be extended for the detection of inorganic NaF as depicted in Fig. 9.

Curcumin is expected to undergo photo-degradation in the presence of UV radiation too [16]. This prompted us to study the effect of irradiation using a low cost source like the 368 nm (3 W, FWHM ~ 14 nm) high power LED on fluoride containing samples of Curcumin in mixture solvent. It was found that high fluoride samples showed increased

Table 1 Fluorescence lifetime of Curcumin in 9:1 *v/v* CH$_3$CN:H$_2$O

Sample	Fluorescence lifetime		
	τ_1 (B$_1$) /ns	τ_2 (B$_2$) /ns	χ^2
Curcumin in 9:1 *v/v* CH$_3$CN:H$_2$O	0.175 (97.99%)	3.05 (2.01%)	1.329
403 nm irradiated Curcumin in 9:1 *v/v* CH$_3$CN:H$_2$O	0.163 (97.29%)	2.20 (2.71%)	1.299
403 nm irradiated Curcumin in 9:1 *v/v* CH$_3$CN:H$_2$O in the presence of 2×10^{-3} M TBAF	0.182 (91.82%)	2.86 (8.18%)	1.390

τ_1, τ_2 are the lifetime values of Curcumin

B$_1$, B$_2$ are the relative amplitudes
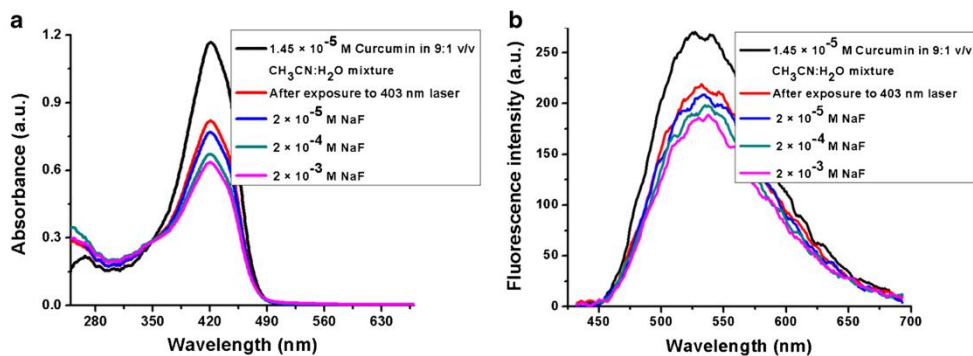
Fig. 9 **a** Absorption and **b** fluorescence spectra of Curcumin in 9:1 *v/v* CH$_3$CN:H$_2$O solvent mixture in the presence of inorganic fluoride (NaF) after exposure to 45 min of 403 nm laser radiation

[168]
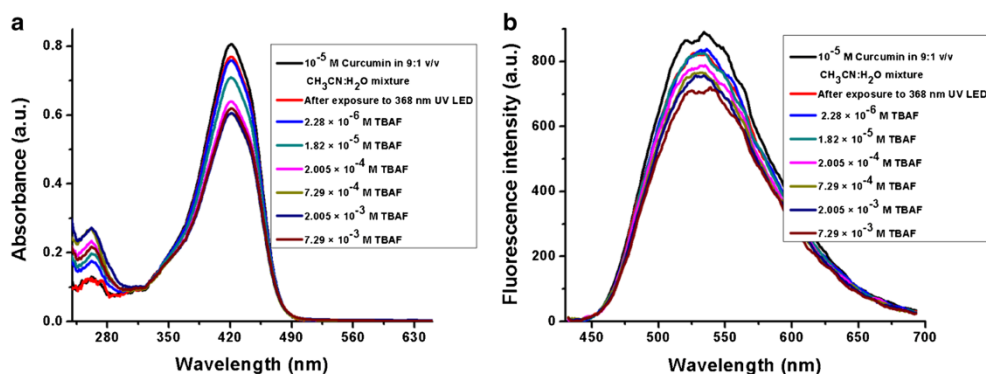
Fig. 10 **a** Absorption and **b** fluorescence spectra of Curcumin in 9:1 *v/v* $CH_3CN:H_2O$ solvent mixture in the presence of varying fluoride concentration after exposure to radiation from 368 nm UV LED for 45 min

change in absorbance upon irradiation with this source. Moreover there is also considerable resolution between acceptable and toxic levels of fluoride. The results depicted in Fig. 10 points to the potential of such a single LED source for fluoride detection using natural dye Curcumin in a very economical way.

Conclusion

The accelerated degradation of natural dye Curcumin in acetonitrile–water solvent with optical irradiation in the presence of fluoride and other common ions is studied in the present work. We believe that the dependence of the optical properties of Curcumin on the solution environment leads to decrease in absorption and fluorescence peaks of Curcumin upon irradiation in the presence of fluoride. The presence of anions in the solution introduces varying degrees of basicity in the vicinity of the Curcumin molecule inside the solution leading to preferential absorption and consequently enhanced degradation of Curcumin especially in the presence of fluoride samples. The results of the present work indicate that a large dynamic range of $2.3 \times 10^{-6} - 7.29 \times 10^{-3}$ M (0.62–579 ppm) can be detected using this irradiation method. We believe to the best of our knowledge that the method of Curcumin irradiation is one of the simplest, easy to implement and most economical for critical range fluoride detection (> 1 ppm) when compared to other works reported in the literature [24, 25].

References

1. Valente NIP, Muteto PV, Farinha ASF, Tomé AC, Oliveira JABP, Gomes MTSR (2011) An acoustic wave sensor for the hydrophilic fluoride. Sens Actuators B 157(2):594–599
2. Tang L, Wang N, Guo J (2012) Colorimetric and fluorescent recognition of fluoride by a binaphthol thioureido derivative. Bull Korean Chem Soc 33(7):2145–2148
3. Ayoob S, Gupta AK (2006) Fluoride in drinking water: a review on the status and stress effects. Crit Rev Environ Sci Technol 36(6):433–487
4. Cametti M, Rissanen K (2009) Recognition and sensing of fluoride anion. Chem Commun 20:2809–2829
5. Shiraishi Y, Maehara H, Sugii T, Wang D, Hirai T (2009) A BODIPY–indole conjugate as a colorimetric and fluorometric probe for selective fluoride anion detection. Tetrahedron Lett 50(29):4293–4296
6. Choi BH, Lee JH, Hwang H, Lee KM, Park MH (2016) Novel dimeric o-carboranyl triarylborane intriguing ratiometric color-tunable sensor via aggregation-induced emission by fluoride anions. Organometallics 35(11): 1771–1777
7. Watanabe S, Seguchi H, Yoshida K, Kifune K, Tadaki T, Shiozaki H (2005) Colorimetric detection of fluoride ion in an aqueous solution using a thioglucose-capped gold nanoparticle. Tetrahedron Lett 46(51): 8827–8829
8. Aggarwal BB, Sundaram C, Malani N, Ichikawa H (2007) Curcumin: the indian solid gold. Adv Exp Med Biol 595:1–75
9. Lee BH, Choi HA, Kim MR, Hong J (2013) Changes in chemical stability and bioactivities of curcumin by ultraviolet radiation. Food Sci Biotechnol 22(1): 279–282
10. Patra D, Barakat C (2011) Synchronous fluorescence spectroscopic study of solvatochromic curcumin dye. Spectrochim Acta A 79:1034–1041
11. Kee TW, Adhikary R, Carlson PJ, Mukherjee P, Petrich JW (2011) Femtosecond fluorescence upconversion investigations

on the excited-state photophysics of curcumin. Aust J Chem 64:23–30

12. Indira Priyadarsini K (2009) Photophysics, photochemistry and photobiology of curcumin: studies from organic solutions, bio-mimetics and living cells. J Photochem Photobiol C 10:81–95

13. Erez Y, Presiado I, Gepshtein R, Huppert D (2011) Temperature dependence of the fluorescence properties of curcumin. J Phys Chem A 115:10962–10971

14. Pill-Hoon B (2000) Spectral and photophysical behaviors of curcumin and curcuminoids. Bull Korean Chem Soc 21(1): 81–86

15. Tønnesen HH, Karlsen J, van Henegouwen GB (1986) Studies on curcumin and curcuminoids VIII. Photochemical stability of curcumin. Z Lebensm Unters Forsch 183(2): 116–122

16. Wang YJ, Pan MH, Cheng AL, Lin LI, Ho YS, Hsieh CY, Lin JK (1997) Stability of curcumin in buffer solutions and characterization of its degradation products. J Pharm Biomed Anal 15(12): 1867–1876

17. Jagannathan R, Abraham PM, Poddar P (2012) Temperature-dependent spectroscopic evidences of curcumin in aqueous medium: a mechanistic study of its solubility and stability. J Phys Chem B 116(50):14533–14540

18. Wu FY, Sun MZ, Xiang YL, Wu YM, Tong DQ (2010) Curcumin as a colorimetric and fluorescent chemosensor for selective recognition of fluoride ion. J Lumin 130(2):304–308

19. Kumavat SD, Chaudhari YS, Borole P, Mishra P, Shenghani K, Duvvuri P (2013) Degradation studies of curcumin. Int J Pharm Rev Res 3(2): 50–55

20. Gordon ON, Luis PB, Sintim HO, Schneider C (2015) Unraveling curcumin degradation-autoxidation proceeds through spiroepoxide and vinylether intermediates en route to the main bicyclopentadione. J Biol Chem 290(8):4817–4828

21. Liao JH, Huang YS, Lin YC, Huang FY, Wu SH, Wu TH (2016) Anticataractogenesis mechanisms of curcumin and a comparison of its degradation products: an in vitro study. J Agric Food Chem 64(10): 2080–2086

22. Yi Q, Qu S, Yang L, Hua J, Qu D (2012) A red-emission diketopyrrolopyrrole-based fluoride ion chemosensor with high contrast ratio working in a dual mode: solvent-dependent ratiometric and "turn on" pathways. Sens Actuators B 173:225–233

23. Mohan PRK, Sreelakshmi G, Muraleedharan CV, Joseph R (2012) Water soluble complexes of curcumin with cyclodextrins: characterization by FT-raman spectroscopy. Vib Spectrosc 62:77–84

24. Puneet P, Vedarajan R, Matsumi N (2016) Alternating poly (borosiloxane) for solid state ultrasensitivity toward fluoride ions in aqueous media. ACS Sensors 1(10): 1198–1202

25. Melo LB, Rodrigues JMM, Farinha ASF, Marques CA, Bilro L, Alberto N, Tomé JPC, Nogueira RN (2014) Concentration sensor based on a tilted fiber bragg grating for anions monitoring. Opt Fiber Technol 20(4): 422–427

[170]

Research Article

applied optics

Fluorescence resonance energy-transfer-based fluoride ion sensor

Roopa Venkataraj,* Arindam Sarkar, C. P. Girijavallabhan, P. Radhakrishnan, V. P. N. Nampoori, and M. Kailasnath

International School of Photonics, Cochin University of Science & Technology, Kochi-682022, Kerala, India
*Corresponding author: roopa.venkataraj@gmail.com

The present work describes an energy-transfer-based fluoride sensor using the highly photo-stable Coumarin 540a (C540a)–Rhodamine 6g (Rh6g) dye pair. Rh6g exhibits a decrease in fluorescence emission, whereas C540a shows no change in response to fluoride. The increase in fluoride concentration decreases the energy transfer efficiency between the C540a donor and Rh6g acceptor in acetonitrile, leading to a subsequent recovery of fluorescence emission from C540a molecules. The sensing mechanism using fluorescence resonance energy transfer is found to be highly specific towards fluoride detection when compared to the response towards other anions. The fluorescence emission of both dyes is monitored to enable fluoride detection within a broad range.   © 2018 Optical Society of America

1. INTRODUCTION

The detection of fluoride in drinking water resources is a challenging problem. The WHO permissible limit of fluoride in drinking water is about 1 ppm [1], while the actual concentration of fluoride in ground water resources in many regions around the world is reported to be 10 to 100 times higher than the permissible limit [2]. Hence, it is very important to sensitively detect fluoride over a broad concentration range. Ion selective electrodes are popular for the detection of fluoride ion because of their lower detection limits ($\sim 10^{-6}$ M), but they mostly offer a very limited detection range spanning 10^{-9}–10^{-6} M, which is extremely small compared to the fluoride concentration commonly found in ground water resources. Another disadvantage of ion selective electrodes involves the sensitivity to pH and consequently the stringent pH condition of around 5–6 for its accurate operation [1,3]. A vast amount of studies has been published illustrating the highly popular spectrophotometric detection of fluoride in organic as well as organic-aqueous media [4]. The use of a tilted fiber Bragg grating for anion monitoring was proposed by Melo *et al.* This involved the monitoring of the refractive index of the surrounding solution and demodulation of the signal based on a theoretical model [5]. Another interesting method involves the use of micro-structured fibers combined with spectrophotometry, operating in the range of 5–50 mM, but the sensor responds in the condition of acidic pH, which makes it difficult for practical use [6]. Both methods involve complex

preparation and treatment of specialized optical fibers and are therefore very costly. Fluorescence techniques are attributed with a wide array of advantages, including high specificity, high sensitivity, fast measurements, straightforward in nature, and also the possibility to study excitation-wavelength-based changes via changes in intensity and wavelength of emission [7,8]. But if only one fluorescence signal is monitored, there is considerable probability of instrument and environmental conditions affecting the recorded signal. Fluorescence resonance energy transfer (FRET), on the other hand, allows for the monitoring of intensities at two wavelengths, viz., that of the donor and the acceptor. It also facilitates ratio-metric sensing of analytes, increasing the accuracy of detection [7,9]. FRET has gained tremendous importance owing to its applications in lasing, fluorescence enhancement, sensing, and bio-imaging [7,10,11]. FRET phenomena in solutions and films, as well as in inorganic and polymeric hosts have been widely studied by many groups [12–15]. FRET depends on a variety of factors such as donor and acceptor concentrations, distance between them, their relative dipole angular orientations, the spectral overlap between the donor emission and acceptor absorption, and the refractive index of the solution [12]. The theoretical background for FRET has already been extensively described in literature [12,15,16]. Among the various materials exhibiting the energy transfer mechanism, the highly efficient energy transfer between the high-quantum-yield and photo-stable Rhodamine 6g (Rh6g) and Coumarin 540a (C540a) dyes deserves a special mention [17].

In the present work, we propose a simple, sensitive, and selective fluoride ion sensor based on the energy transfer between the C540a–Rh6g dye pair. It was found that there was a decrease in the efficiency of energy transfer between the donor C540a molecules and the acceptor Rh6g molecules with increase in fluoride, leading to a gradual recovery of fluorescence emission from C540a molecules. We could attain considerable range in the sensing of fluoride employing the energy transfer mechanism between Rh6g dye and C540a dye with only the former responding to fluoride. To the best of our knowledge, we believe that this is the first time the highly efficient energy transfer between the C540a–Rh6g dye pair has been demonstrated to be useful for sensing fluoride.

2. EXPERIMENTAL METHODS

The stock solutions of varied concentrations of C540a (Exciton) and Rh6g (Acros Organic) dyes in acetonitrile were first prepared, and specific volumes of tetrabutylammonium fluoride (TBAF) (Spectrochem India Pvt. Ltd, Mumbai) were introduced to prepare fluoride samples with concentrations ranging from 2.08×10^{-6} to 2.6×10^{-3} M. The energy transfer dye mixture system was also tested for its sensing response towards TBA salts of other common anions (Sigma Aldrich, Spectrochem India Pvt Ltd). The absorption and fluorescence spectra in this system of dyes were studied using the Jasco V-570 spectrophotometer and Cary Eclipse fluorimeter (Varian), respectively. The excitation and emission slit widths for the fluorescence measurements were 2.5 nm and 2.5 nm, respectively, unless explicitly mentioned otherwise. The fluorescence lifetime measurements were performed using the Horiba DeltaPro TCSPC lifetime measurement system with excitation using 370 nm NanoLED. A 500 nm long pass filter was used to separate the fluorescence emissions of both the individual dyes and that of the dye mixture system from the excitation wavelength. The decay curves were fitted, and the fluorescence lifetime values were calculated using the Horiba DAS6 decay analysis software. The FTIR spectrum in KBr was recorded in the range of 400–4000 cm^{-1} using a Jasco 4100 spectrometer with a resolution of 4 cm^{-1}.

3. RESULTS AND DISCUSSION

The absorption and fluorescence variation of C540a dye in the presence of varying fluoride concentrations are shown in Fig. 1. There is no change in the optical characteristics of the dye in the presence of fluoride owing to the specific chemical structure of the dye that does not allow bonding with fluoride.

On the other hand, the strong response of Rh6g dye towards fluoride was readily observed as a change in color of solution from bright pink to dull brownish orange and a marked decrease in observable fluorescence with increase in fluoride concentration. The changes in optical characteristics of Rh6g dye in the presence of fluoride ion are as shown in Fig. 2. It can be seen that there is a huge decrease in absorbance and fluorescence even at very low and permissible concentrations of fluoride. The absorption band was broadened, and there is a clear blue shift in the peak of Rh6g with increase in fluoride concentration. Fluoride is strongly basic in nature [18], but a
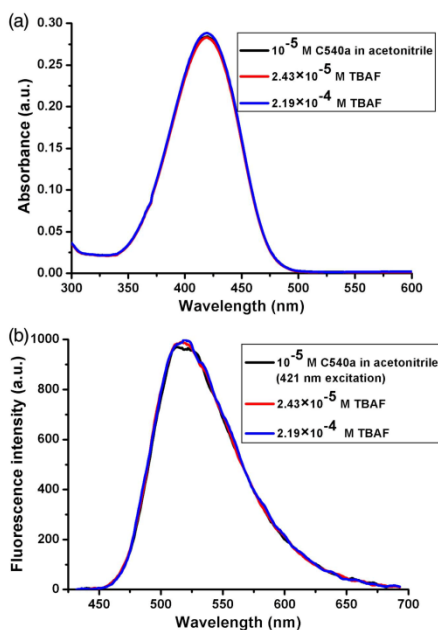
Fig. 1. (a) Absorption and (b) fluorescence response of 10^{-5} M C540a with varying fluoride concentrations (excitation-emission slit width = 2.5–5 nm).

change in pH of the solution is not expected to change the structure of esterified rhodamines such as Rh6g [19] into the zwitterionic form. The zwitterionic form, following deprotonation of the carboxylic group in the case of an unesterified dye leads to a 3–10 nm blue shift in the absorption and fluorescence spectra. Moreover, it is reported that the zwitterionic form also undergoes reversible changes to the lactone form in weakly polar solvents with an absorption peak only in the UV region [20,21]. The huge colorimetric and fluorescence changes in the behavior of Rh6g in this case could hence be attributed to the conversion of fluorescent amide form of the dye to the non-fluorescent deprotonated form.

The normalized peak absorbance and fluorescence intensity of Rh6g in acetonitrile in the presence of varying fluoride concentrations, as shown in Fig. 3, confirms the fast decrease of peak intensities with fluoride.

The hydrogen bonding nature of Rh6g with fluoride is verified by studying the variation of absorption and fluorescence intensity of Rh6g-TBAF in acetonitrile in the presence of a protic solvent such as water as reported in literature [22]. Figure 4 shows that the absorption and fluorescence peaks of Rh6g tend to return to their original values on addition of water owing to the disruption of the bond between Rh6g and fluoride. This tendency was observed in the case of the C540a–Rh6g dye mixture system too and hence is not included here.

The Fourier transform infrared (FTIR) spectrum of Rh6g in acetonitrile in the presence of fluoride is as shown in Fig. 5.
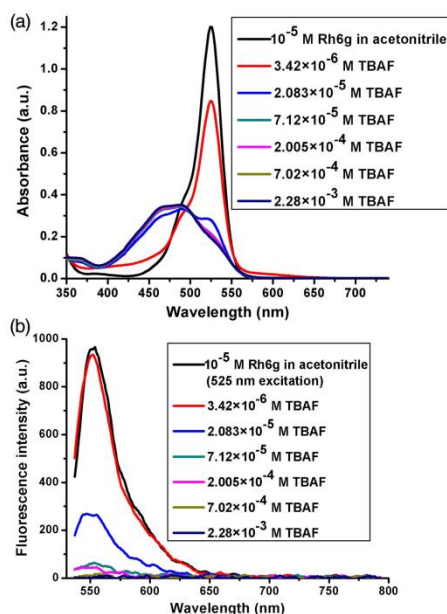
Fig. 2. Variation in (a) absorption and (b) fluorescence characteristics of 10^{-5} M Rh6g with varying fluoride concentrations.
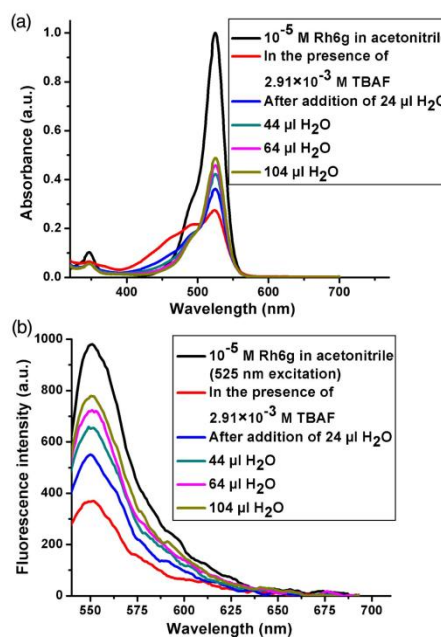
Fig. 4. (a) Absorption and (b) fluorescence characteristics of 10^{-5} M Rh6g in the presence of fluoride upon addition of water.
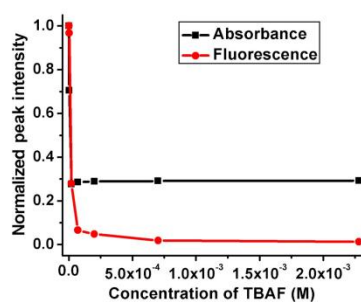
Fig. 3. Variation in normalized peak absorbance and fluorescence of 10^{-5} M Rh6g with increase in fluoride.
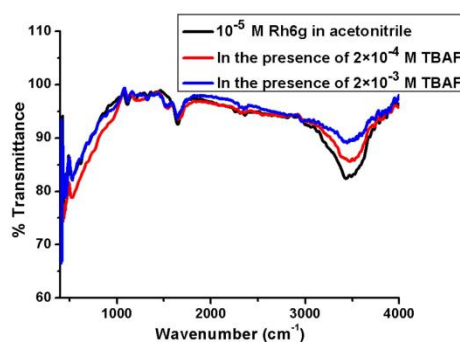
Fig. 5. FTIR spectral changes of Rh6g in the presence of fluoride.

There is an increase in transmittance of the band at 3431 cm^{-1}, which corresponds to the N–H stretching of Rh6g molecule. This increase in transmittance could be due to the quantitative conversion of the Rh6g molecule to the de-protonated form [23].

From Fig. 2, it is evident that owing to the strong change in absorption and fluorescence characteristics of Rh6g towards fluoride ion, it becomes difficult to distinguish higher concentrations of fluoride. This led us to the realization of a dye mixture system towards recognition of fluoride involving the optical interaction of two highly photo-stable fluorescent dyes,

one of which does not respond and the other exhibiting a strong response towards fluoride. The FRET from C540a dye excited at wavelength 421 nm to Rh6g dye absorbing at 525 nm in acetonitrile is illustrated in Fig. 6(a). There is a huge overlap between the fluorescence curve of C540a and absorption curve of Rh6g. The increase in fluorescence of Rh6g dye in the presence of C540a dye is as shown in Fig. 6(b). It is very clear from this figure that the acceptor Rh6g does not have considerable fluorescence emission when excited with the donor

Fig. 7. Samples of (a) 10^{-5} M Rh6g and (b) 10^{-5} M C540a-10^{-5} M Rh6g in the presence of (from left to right) 0, 2×10^{-5} M, 2×10^{-4} M, and 2×10^{-3} M TBAF in acetonitrile.

Fig. 6. (a) Normalized absorption/fluorescence spectra of 10^{-5} M C540a and Rh6g dyes in acetonitrile. (b) Increase in the fluorescence of Rh6g dye in the presence of C540a dye under 421 nm excitation.

Fig. 8. (a) Absorption and (b) fluorescence variation in the 10^{-5} M C540a-10^{-5} M Rh6g dye mixture system with increase in fluoride (excitation-emission slit width = 2.5–5 nm).

absorption wavelength. Moreover, the emission of the donor C540a molecule decreased considerably in the presence of the Rh6g molecule, pointing to the efficient energy transfer between the two dyes. The efficiency of FRET (E) is given by the equation [16]

$$E = 1 - \frac{F_{da}}{F_d}, \qquad (1)$$

where F_{da} and F_d are the donor emission intensity in the presence and absence of the acceptor, respectively. The value of E for 10^{-5} M of C540a and Rh6g dyes in acetonitrile was calculated to be 0.52.

The color changes in the solution of Rh6g alone and that with the dye mixture of C540a–Rh6g in the presence of varying fluoride is as shown in Fig. 7. The absorption and fluorescence response of the dye mixture system towards varying fluoride content is as shown in Fig. 8. It was observed that there is a blue shift for the absorption peak of Rh6g along with a decrease in intensity. The transfer of fluorescence energy from C540a to Rh6g decreases with increase in fluoride due to the decreasing spectral overlap between the absorption of the Rh6g acceptor with the emission of the C540a donor. This gradual decrease in the efficiency of fluorescence energy transfer between C540a and Rh6g dyes in the presence of increasing fluoride leads to a clear increase in the fluorescence from donor C540a molecules. There is consequently an observable increase in resolution between different fluoride concentrations as well as

increase in the range of detection with the use of a dye mixture system for fluoride sensing.

The variation of peak fluorescence intensity of Rh6g as well as the C540a–Rh6g dye mixture with low fluoride concentration is as shown in Fig. 9. The limit of detection (LOD) can be estimated as that concentration of TBAF whose signal is the signal of the blank sample (0 M TBAF) added to thrice the noise signal (standard deviation) as reported in literature [24]. From the plot of Fig. 9(b), the limit of detection of
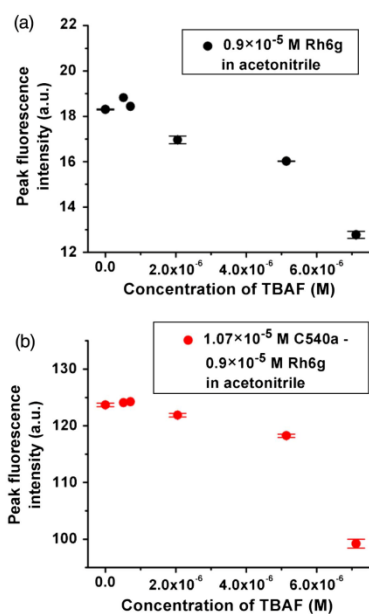
Fig. 9.   (a) Variation of peak fluorescence intensity of (a) Rh6g alone and (b) C540a–Rh6g dye mixture in acetonitrile with increase in fluoride (0–7 × 10⁻⁶ M TBAF).

Fig. 10.   Normalized plot of peak fluorescence intensity of Rh6g and C540a-Rh6g dye mixture in the lower TBAF concentration range.

Fig. 11.   (a) Fluorescence decay curves for Rh6g acceptor (A), C540a donor-Rh6g acceptor (B), and C540a donor-Rh6g acceptor pair in the presence of TBAF (C). (b) Expanded views of the peaks.

the dye mixture system can be approximated to 3×10^{-6} M (∼0.78 ppm), which is comparable to the LOD of Rh6g alone.

The normalized plot of the peak fluorescence intensities in both cases along with the standard deviation from average is shown in Fig. 10. From the normalized plot of peak fluorescence intensity, it is clear that Rh6g alone as well as the C540a–Rh6g dye mixture respond approximately linearly in this range of fluoride concentration. From the slopes of the linear portion of the normalized plot, sensitivity may be calculated. It was found that Rh6g alone had a higher sensitivity compared to the dye mixture system. But the rapid decrease in intensity with fluoride leads to almost nil fluorescence at higher concentrations, which is not desirable for practical purposes.

We also studied the lifetimes of the donor, acceptor, and the donor–acceptor combination using the time-correlated single-photon counting (TCSPC) system. The characterization of multiple lifetimes is possible with this system. The fluorescence decay curves for the acceptor Rh6g and the C540a–Rh6g dye mixture system are as shown in Fig. 11(a). The lifetime of the donor molecules is expected to decrease, whereas the apparent fluorescence lifetime of the sensitized emission of the acceptor would increase in the case of FRET phenomena [25]. C540a dye exhibits a single exponential decay in acetonitrile with a lifetime of 5.68 ns, as reported in literature [26]. The value of the lifetime of Rh6g dye in acetonitrile as estimated from the single exponential decay was found to be 5.36 ± 0.01 ns. The absorption and emission spectral overlap of the C540a

donor is very low compared to the spectral overlap of C540a emission and Rh6g absorption, and hence the donor–donor interaction-mediated excitation energy transfer [27] is not expected to take place in this case. Moreover, it is also reported that even in the case of highly efficient FRET systems, the quenching of donor fluorescence is not reflected accurately as a reduction of donor lifetime. This is owing to the larger lifetime of the unquenched donor emission, which does not take part in the

FRET process [28]. Also, the Rh6g acceptor has very low fluorescence emission when excited with 370 nm wavelength, and hence direct excitation of the acceptor in the presence of the donor can be considered as negligible. Considering these factors and that the fluorescence lifetimes of the dyes are comparable, the time-resolved fluorescence decay of the dye mixture could be easily fitted with that of a bi-exponential decay. In the case of the C540a–Rh6g dye mixture in acetonitrile, the bi-exponential decay indicates the presence of two lifetime components having values 3.28 ± 0.04 ns and 6.17 ± 0.02 ns with negative $(-0.13 \times 10^{-2}$, -1.39 relative amplitude) and positive $(4.9 \times 10^{-2}$, 101.39 relative amplitude) pre-exponential factors, respectively. The shorter component with a negative pre-exponential factor can be attributed to the energy transfer process [28,29]. On addition of a high concentration of fluoride to the dye mixture system, the shorter and longer lifetime components were found to be 4.88 ± 0.29 ns and 6.18 ± 0.12 ns with corresponding positive pre-exponential factors of 2.85×10^{-2} (50.66 relative amplitude) and 2.19×10^{-2} (49.34 relative amplitude), respectively. The absence of a lifetime component with a negative pre-exponential factor indicates the absence of a rise time associated with FRET, and this could be due to the reduced or even disappearance of FRET with high fluoride concentration.

The energy transfer process between the dyes was found to be very sensitive and selective with respect to the determination of fluoride. This was evident from the negligible change in optical characteristics of the dye mixture system in the case of other common anions, as shown in Fig. 12.

The FRET efficiency E is very sensitive to changes in concentration of the donor and acceptor, as described in literature [12,16]. The efficiency of energy transfer between the C540a–Rh6g dye system as well as their combined response towards fluoride were studied by varying the concentration of C540a and Rh6g dyes. The fluoride response of the dye mixture in acetonitrile with C540a:Rh6g concentration of 10^{-4} M:10^{-5} M and 10^{-5} M:10^{-5} M are presented here. A 10^{-4} M solution of C540a in acetonitrile exhibits a peak wavelength of absorption and fluorescence of 417 nm and 516 nm, respectively. The variation of absorption and fluorescence peak intensity of the dye mixture system with varying fluoride, at the wavelengths of peak absorbance and fluorescence of the individual donor and acceptor dyes, are as shown in Figs. 13 and 14, respectively. The wavelength of excitation is chosen to be 421 nm in all the cases. It was observed that there was almost comparable but small increase in absorbance values with changes in fluoride concentration at donor absorption wavelength for both dye mixture systems [Fig. 13(a)]. This could be attributed to the overlap of the absorption spectrum of C540a with that of the blue-shifted absorption spectrum of Rh6g in the presence of high fluoride concentration. A slightly higher fluorescence peak intensity was observed in the case of the C540a–Rh6g dye mixture with a
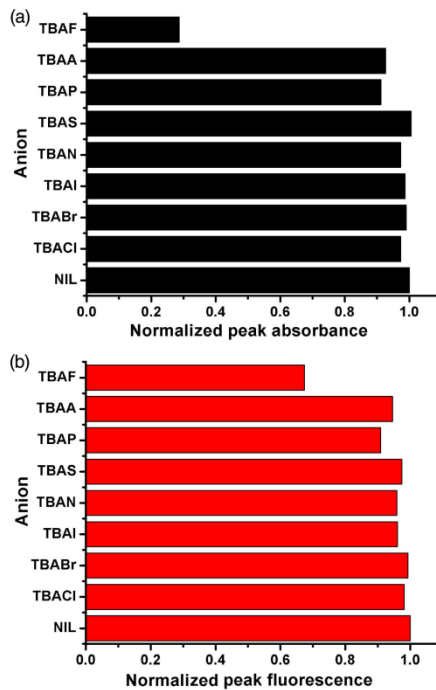
Fig. 12. Normalized (a) peak absorbance and (b) peak fluorescence of C540a–Rh6g (10^{-5} M) energy transfer pair in the presence of 2×10^{-4} M of common anions (Cl-Chloride, Br-Bromide, I-Iodide, N-Nitrate, S-Hydrogen Sulphate, P-Dihydrogen Phosphate, A-Acetate).
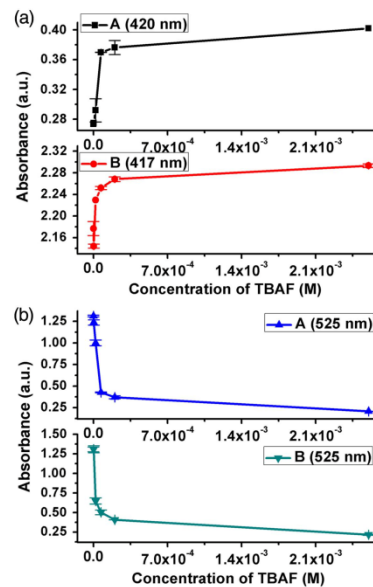
Fig. 13. Variation in absorption peak intensity of different concentration ratio C540a–Rh6g dye mixtures in the presence of fluoride at (a) C540a donor and (b) Rh6g acceptor absorption wavelengths for A-10^{-5} M C540a-10^{-5} M Rh6g and B-10^{-4} M C540a-10^{-5} M Rh6g.
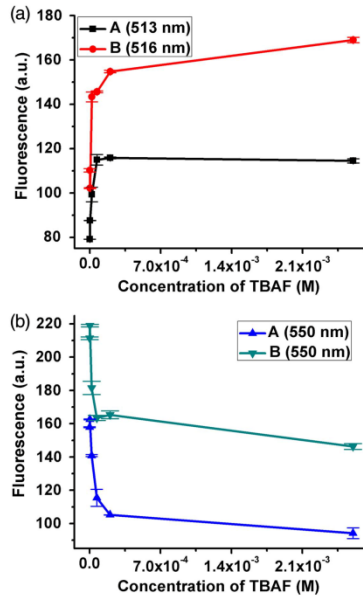
Fig. 14. Variation in fluorescence peak intensity of different concentration ratio C540a–Rh6g dye mixtures in the presence of fluoride at (a) C540a donor and (b) Rh6g acceptor emission wavelengths for A-10^{-5} M C540a-10^{-5} M Rh6g and B-10^{-4} M C540a-10^{-5} M Rh6g.

Fig. 15. (a) Peak absorbance and (b) peak fluorescence wavelength variation of the donor with increase in fluoride concentration for A-10^{-5} M C540a-10^{-5} M Rh6g and B-10^{-4} M C540a-10^{-5}M Rh6g.

concentration ratio of 10^{-4} M:10^{-5} M as shown in Fig. 14, owing to higher fluorescence intensity of C540a dye molecules.

The variation in the peak absorbance and fluorescence wavelength in the region of donor absorption and emission in the case of both dye mixture systems is as shown in Fig. 15. There is a considerable overlap of the absorption spectrum of Rh6g associated with high concentration fluoride with the absorption band of C540a, as already shown in Fig. 8(a). This leads to a bathochromic shift in peak absorbance wavelength values of the 10^{-5} M C540a:10^{-5} M Rh6g dye mixture ratio with increasing fluoride concentration. The 10^{-4} M C540a:10^{-5} M Rh6g mixture system was not affected by this blue shift in Rh6g peak owing to the higher absorption of the C540a dye molecules themselves in the region. The red shift in fluorescence peak wavelength can be attributed to the recovery of the broad fluorescence spectrum of C540a dye molecules on dissociating from the energy transfer mechanism with Rh6g in the presence of increasing fluoride concentration.

The advantage of highly sensitive ratio-metric FRET sensing in most cases can be offset by the crosstalk of donor emission in the acceptor channel. The change in acceptor fluorescence emission is hence not always reliable, as there could be considerable overlap of donor fluorescence in the acceptor emission band. Therefore, monitoring the donor fluorescence and the shift in donor emission peak wavelength could provide a better indicator of change in FRET efficiency with respect to fluoride concentration. The variations in FRET efficiency would cause

consequent variations in the donor emission. Hence, the FRET efficiency E calculated as the result of donor quenching [Eq. (1)] can serve as a useful indicator [25] in studying the sensing response, especially at higher fluoride concentrations.

The variation in FRET efficiency with fluoride concentration is as shown in Fig. 16. It can be observed that the dye mixture pair with a higher concentration of donor molecules (10^{-4} M) has a lower value of E. This could be due to the imbalance in the donor acceptor ratio. A higher donor-to-acceptor ratio can improve FRET efficiency, provided the donor decay time is higher than that of the acceptor. Also, this condition can lead to very sensitive sensitized emission measurements. But, a higher value of donor concentration could also lead to competition of multiple donors to transfer energy to the lower number of acceptors. This can lead to donor fluorescence emission along with FRET, thereby reducing the value of E [25,30].

A minor change in the donor and acceptor concentrations can lead to significant changes in the FRET efficiency, as mentioned in earlier sections [12]. To confirm the sensitivity of the FRET pair at a lower concentration of fluoride, we carried out the experiment with slightly modified donor and acceptor concentrations. The variation of peak fluorescence intensity of the dye pair with respect to changes in fluoride concentration when the acceptor is excited directly with its excitation wavelength (525 nm) is as shown in Fig. 17(a). The variation of FRET efficiency of the same dye pair in the presence of fluoride is shown in Fig. 17(b). It can be observed from the figure that
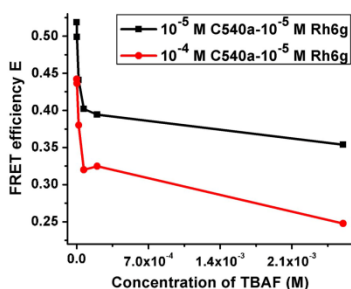
Fig. 16. Variation of FRET efficiency with increase in fluoride.
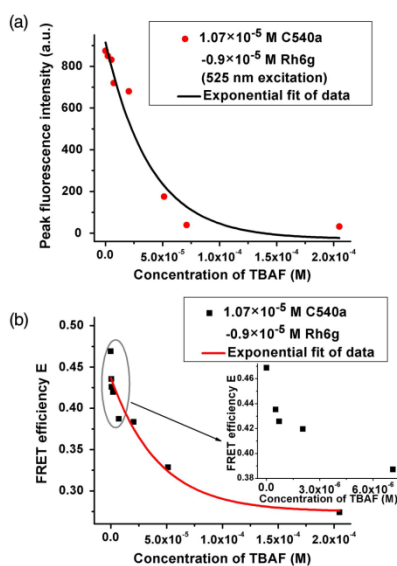
Fig. 17. Variation of (a) peak fluorescence intensity and (b) FRET efficiency of C540a–Rh6g dye pair with change in fluoride concentration. Inset of (b) shows the expanded view of $0\text{-}7 \times 10^{-6}$ M fluoride concentration range.

only FRET efficiency can be used to directly read out a higher fluoride concentration at the higher range, whereas both direct excitation of acceptor and FRET efficiency can be used for lower fluoride concentration.

The above results indicate that with the proposed mechanism of sensing using a combination of dyes exhibiting energy transfer phenomena, it is possible to detect and measure the acceptable concentrations of fluoride from reported toxic values using FRET efficiencies. It is also possible to monitor the concentration of fluoride using the absorption and/or fluorescence

peak intensity or shift in peak wavelength values of both the donor and acceptor (direct excitation) entities of the dye mixture system, enabling multiple paths towards accurate determination of fluoride in the medium.

4. CONCLUSION

The present work reports a simple, sensitive, and selective fluoride ion sensor in organic media implemented using the phenomena of FRET between high-quantum-yield and photostable C540a and Rh6g laser dyes. The increase in fluoride concentration led to a decrease in efficiency of fluorescence resonance energy transfer between the two dyes, leading to a recovery in fluorescence of C540a molecules, even at a high fluoride concentration. It was found that optical interaction between the two dyes enabled selective measurement of fluoride ion covering a broad range of $2.08 \times 10^{-6}\text{–}2.6 \times 10^{-3}$ M (0.54–680 ppm TBAF) more efficiently than with the use of a single dye or its derivative [31–33]. The C540a–Rh6g FRET pair displays good sensitivity towards a broad range of fluoride concentrations with an LOD of 3×10^{-6} M (0.78 ppm). Aqueous-based sensing of fluoride is a considerable challenge, and the use of a fluorescence energy transfer mechanism for sensing can prove to be an efficient mechanism towards its realization.

REFERENCES

1. N. I. P. Valente, P. V. Muteto, A. S. F. Farinha, A. C. Tomé, J. A. B. P. Oliveira, and M. T. S. R. Gomes, "An acoustic wave sensor for the hydrophilic fluoride," Sens. Actuators B **157**, 594–599 (2011).
2. S. Ayoob and A. K. Gupta, "Fluoride in drinking water: a review on the status and stress effects," Crit. Rev. Environ. Sci. Technol. **36**, 433–487 (2006).
3. E. Bakker, P. Bühlmann, and E. Pretsch, "Carrier-based ion-selective electrodes and bulk optodes. 1. General characteristics," Chem. Rev. **97**, 3083–3132 (1997).
4. Y. Zhou, J. F. Zhang, and J. Yoon, "Fluorescence and colorimetric chemosensors for fluoride-ion detection," Chem. Rev. **114**, 5511–5571 (2014).
5. L. B. Melo, J. M. M. Rodrigues, A. S. F. Farinha, C. A. Marques, L. Bilro, N. Alberto, J. P. C. Tomé, and R. N. Nogueira, "Concentration sensor based on a tilted fiber Bragg grating for anions monitoring," Opt. Fiber Technol. **20**, 422–427 (2014).
6. X. Yang, J. Wang, and L. Wang, "Sol-gel matrix modified microstructured optical fibre towards a fluoride sensitive optical probe," Opt. Commun. **282**, 2502–2505 (2009).
7. X. Zhang, Y. Xiao, and X. Qian, "A ratiometric fluorescent probe based on FRET for imaging Hg^{2+} ions in living cells," Angew. Chem. **47**, 8025–8029 (2008).
8. S. Kumar, V. Luxami, and A. Kumar, "Chromofluorescent probes for selective detection of fluoride and acetate ions," Org. Lett. **10**, 5549–5552 (2008).
9. Y. Liu, Z. M. Zhao, J. Y. Miao, and B. X. Zhao, "A ratiometric fluorescent probe based on boron dipyrromethene and rhodamine Förster resonance energy transfer platform for hypochlorous acid and its application in living cells," Anal. Chim. Acta **921**, 77–83 (2016).

[178]

10. L. Cerdán, E. Enciso, V. Martín, J. Bañuelos, I. López-Arbeloa, A. Costela, and I. García-Moreno, "FRET-assisted laser emission in colloidal suspensions of dye-doped latex nanoparticles," Nat. Photonics **6**, 621–626 (2012).

11. J. S. Kang, G. Piszczek, and J. R. Lakowicz, "Enhanced emission induced by FRET from a long-lifetime, low quantum yield donor to a long-wavelength, high quantum yield acceptor," J. Fluoresc. **12**, 97–103 (2002).

12. J. Saha, A. D. Roy, D. Dey, S. Chakraborty, D. Bhattacharjee, P. K. Paul, and S. A. Hussain, "Investigation of fluorescence resonance energy transfer between fluorescein and rhodamine 6G," Spectrochim. Acta A **149**, 143–149 (2015).

13. A. K. Sheridan, A. R. Buckley, A. M. Fox, A. Bacher, D. D. C. Bradley, and I. D. W. Samuel, "Efficient energy transfer in organic thin films—implications for organic lasers," J. Appl. Phys. **92**, 6367–6371 (2002).

14. B.-J. Kim and K.-S. Kang, "Fluorescence resonance energy transfer of sulforhodamine B attached on silica spheres," Mater. Chem. Phys. **148**, 964–967 (2014).

15. M. Kailasnath, P. R. John, P. Radhakrishnan, V. P. N. Nampoori, and C. P. G. Vallabhan, "A comparative study of energy transfer in dye mixtures in monomer and polymer matrices under pulsed laser excitation," J. Photochem. Photobiol. A **195**, 135–143 (2008).

16. C. Berney and G. Danuser, "FRET or no FRET: a quantitative comparison," Biophys. J. **84**, 3992–4010 (2003).

17. C. Banerjee, N. Kundu, S. Ghosh, S. Mandal, J. Kuchlyan, and N. Sarkar, "Fluorescence resonance energy transfer in microemulsions composed of tripled-chain surface active ionic liquids, RTILs, and biological solvent: an excitation wavelength dependence study," J. Phys. Chem. B **117**, 9508–9517 (2013).

18. S. Watanabe, H. Seguchi, K. Yoshida, K. Kifune, T. Tadaki, and H. Shiozaki, "Colorimetric detection of fluoride ion in an aqueous solution using a thioglucose-capped gold nanoparticle," Tetrahedron Lett. **46**, 8827–8829 (2005).

19. D. A. Hinckley, P. G. Seybold, and D. P. Borris, "Solvatochromism and thermochromism of rhodamine solutions," Spectrochim. Acta A **42**, 741–746 (1986).

20. M. Beija, C. A. M. Afonso, and J. M. G. Martinho, "Synthesis and applications of rhodamine derivatives as fluorescent probes," Chem. Soc. Rev. **38**, 2410–2433 (2009).

21. K. H. Drexhage, "Fluorescence efficiency of laser dyes," J. Res. Natl. Bur. Stand.A **80A**, 421–428 (1976).

22. R. B. P. Elmes and T. Gunnlaugsson, "Luminescence anion sensing via modulation of MLCT emission from a naphthalimide–Ru(II)–polypyridyl complex," Tetrahedron Lett. **51**, 4082–4087 (2010).

23. M. Majoube and M. Henry, "Fourier transform Raman and infrared and surface-enhanced Raman spectra for rhodamine 6G," Spectrochim. Acta A **47**, 1459–1466 (1991).

24. J. Shi, C. Chan, Y. Pang, W. Ye, F. Tian, J. Lyu, Y. Zhang, and M. Yang, "A fluorescence resonance energy transfer (FRET) biosensor based on graphene quantum dots (GQDs) and gold nanoparticles (AuNPs) for the detection of mecA gene sequence of Staphylococcus aureus," Biosens. Bioelectron. **67**, 595–600 (2015).

25. F. S. Wouters, "Förster resonance energy transfer and fluorescence lifetime imaging," in *Fluorescence Microscopy: From Principles to Biological Applications*, U. Kubitscheck, ed., 2nd ed. (Wiley-Blackwell, 2017), pp. 430–444.

26. P. Verma and H. Pal, "Aggregation studies of dipolar coumarin-153 dye in polar solvents: a photophysical study," J. Phys. Chem. A **118**, 6950–6964 (2014).

27. U. Tripathy, P. B. Bisht, and K. K. Pandey, "Study of excitation energy migration and transfer in 3,3'-dimethyloxacarbocyanine iodide (DMOCI) and o-(6-diethylamino-3-diethylimino-3H-xanthen-9-yl) benzoic acid (RB) in thin films of polyvinyl alcohol," Chem. Phys. **299**, 105–112 (2004).

28. A. Roy, N. Kundu, D. Banik, and N. Sarkar, "Comparative fluorescence resonance energy-transfer study in pluronic triblock copolymer micelle and niosome composed of biological component cholesterol: an investigation of effect of cholesterol and sucrose on the FRET parameters," J. Phys. Chem. B **120**, 131–142 (2015).

29. A. Ghosh, C. K. De, T. Chatterjee, and P. K. Mandal, "What type of nanoscopic environment does a cationic fluorophore experience in room temperature ionic liquids," Phys. Chem. Chem. Phys. **17**, 16587–16593 (2015).

30. O. A. Goryacheva, N. V. Beloglazova, A. M. Vostrikova, M. V. Pozharov, A. M. Sobolev, and I. Y. Goryacheva, "Lanthanide-to-quantum dot Förster resonance energy transfer (FRET): application for immunoassay," Talanta **164**, 377–385 (2017).

31. X. Zhuang, W. Liu, J. Wu, H. Zhang, and P. Wang, "A novel fluoride ion colorimetric chemosensor based on coumarin," Spectrochim. Acta A **79**, 1352–1355 (2011).

32. Y. Qu, J. Hua, and H. Tian, "Colorimetric and ratiometric red fluorescent chemosensor for fluoride ion based on diketopyrrolopyrrole," Org. Lett. **12**, 3320–3323 (2010).

33. S. S. Razi, P. Srivastava, R. Ali, R. C. Gupta, S. K. Dwivedi, and A. Misra, "A coumarin-derived useful scaffold exhibiting Cu^{2+} induced fluorescence quenching and fluoride sensing (On–Off–On) via copper displacement approach," Sens. Actuators B **209**, 162–171 (2015).